UNIVERSITÉ DU QUÉBEC À TROIS-RIVIÈRES

DÉMÊLER L'INTERACTION COMPLEXE ENTRE LE VIH-1, L'ENVELOPPE NUCLÉAIRE ET L'IMMUNITÉ INNÉE: PERSPECTIVES DES ÉTUDES GS-CA1 ET INTERFÉRON-B

UNRAVELING THE COMPLEX INTERPLAY BETWEEN HIV-1, NUCLEAR ENVELOPE, AND INNATE IMMUNITY: INSIGHTS FROM GS-CA1 AND INTERFERON-B STUDIES

THÈSE PRÉSENTÉE

COMME EXIGENCE PARTIELLE DU

DOCTORAT EN BIOLOGIE CELLULAIRE ET MOLÉCULAIRE

PAR

AMITA SINGH

DECEMBRE 2025

UNIVERSITÉ DU QUÉBEC À TROIS-RIVIÈRES

BIOLOGIE CELLULAIRE ET MOLÉCULAIRE (DOCTORAT)

Direction de recherche :

Lionel Berthoux	Directeur de recherche

Jury d'évaluation

Lionel Berthoux	Directeur de recherche
Tagnon Missihoun	Président du jury
Hugo Germain	Évaluateur interne
Andrew J. Mouland	Évaluateur externe

Acknowledgement

This thesis represents not only my efforts but also the incredible contributions, support, and inspiration provided by so many remarkable people throughout my academic journey. I am deeply grateful to everyone who has played a part in this accomplishment.

First and foremost, I would like to express my sincerest gratitude to my supervisor, Dr. Lionel Berthoux, for his unwavering support, guidance, and encouragement during this journey. I am also deeply thankful to Professor Hugo Germain for his mentorship and insightful advice, as well as Marc Germain for his guidance and inspiration.

I extend my heartfelt thanks to Victor Fourcassié, Karen Cristine Goncalves Dos Santos, Hocine Chelbi, and Natacha Mérindol for their contributions to the research and collaboration efforts that enriched this thesis. I am also grateful to Arnaud Droit for his expertise and support in the proteomics platform of the CHU de Québec, Québec. My profound thanks go to the teams at the Department of Medical Biology and the Department of Chemistry, Biochemistry, and Physics at UQTR for their assistance and facilities that enabled this research.

To Natacha, you were a constant source of support and patience, and without your guidance in the lab, I wouldn't have been able to learn and navigate the challenges. My gratitude also goes to Melodie, Soumeya, Nour, and Kevin, whose assistance was invaluable to my progress.

Priya, your positivity and encouragement were a steady light throughout my journey. Your faith in me gave me the strength to persevere during difficult times. Hema, your kindness and dedication were a great source of comfort and motivation, and I am forever grateful for your friendship. Priyanka, I deeply appreciate your camaraderie and thoughtful insights that supported me immensely along the way.

I am blessed with friends who have been my anchors and cheerleaders. Shweta, Kiran, Rinki, Ram Shiromani, Atul, Kunal, and Barkha, thank you for your unwavering companionship.

To my cherished family-Mummy, Papa, my sisters Uma, Namrata, and Ankita, and my brother Vivek, I owe everything to your love and encouragement. Your belief in me was my driving force, and I am eternally thankful. My nephews- Advik and Yatharth and my niece Vedita, thank you for bringing joy and giggles in my life. I love you so much, guys.

I am profoundly indebted to my academic mentors, including my master's professor, Harsh Chauhan, and my graduate professor, Pragya Mam, whose inspiration shaped my academic path. I also extend my gratitude to my previous lab members, Reeku Mam and Parul Mam, for their guidance during my earlier research endeavors.

Lastly, I want to acknowledge everyone else whose contributions and support have made this achievement possible; thank you for being an integral part of my journey.

Summary

This study investigates the complex interactions between Human Immunodeficiency Virus type 1 (HIV-1), the host cell's nuclear envelope, and the innate immune response, focusing on interferon-beta (IFN-β) and the interferon-stimulated gene (ISG, genes activated by interferons that help establish an antiviral state in cells), myxovirus resistance protein 2 (MX2). The research examines the effects of GS-CA1, a novel HIV-1 capsid inhibitor, on early HIV-1 infection stages at the nuclear envelope. The study revealed that both HIV-1 infection and IFN-β treatment modulate the abundance levels of nuclear envelope proteins. ISGs such as TRIM22 (tripartite motif containing 22), TRIM14 (tripartite motif containing 14), and MX2 were upregulated at the nuclear envelope by IFN-β. The Nup (nucleoporin; proteins that make up the nuclear pore complex, regulating transport between nucleus and cytoplasm) TPR (translocated promoter region), known to facilitate HIV-1 complementary DNA (cDNA; DNA synthesized from an RNA template, such as HIV-1 reverse-transcribed genome) integration into the host cell genome, was selectively upregulated upon HIV-1 infection, while the nuclear pore-associated protein vimentin was downregulated. A key finding was that IFN-β treatment enhanced the accumulation of HIV-1 proteins at the nuclear envelope.

This led to the hypothesis that MX2, known to interact with HIV-1 capsid near the nuclear pore complex, might be responsible for this accumulation. However, experiments using MX2 knockdown cells challenged this hypothesis. While HIV-1 peptides were more abundant in IFN-β-treated samples, there was no significant difference in peptide accumulation between MX2 knockdown cells and control cells. These findings indicate that MX2 not alone but along with other ISGs might be responsible for HIV-1 peptide accumulation at the nuclear envelope-enriched fractions during IFN-β treatment. The research findings suggest that HIV-1 infection dampens the effect of IFN-β on certain ISGs, supporting previous findings that HIV-1 can partially evade or suppress the innate immune response. This research advances our understanding of HIV-1 interactions with the nuclear envelope and the host cell's innate immune response. The findings

suggest that HIV-1 nuclear entry mechanisms and the host cell's attempts to block this entry are more complex than previously thought, involving multiple proteins and pathways.

We then utilized GS-CA1, an inhibitor that prevents capsid formation, to study the impact of HIV-1 infection, GS-CA1 treatment, and beta interferon (IFN-β) treatment on the nuclear envelope, as well as the localization of HIV-1 capsid cores at the nuclear envelope and nuclear pores. Mass spectrometry experiments revealed that GS-CA1 treatment combined with HIV-1 infection significantly altered protein levels in nuclear envelope-enriched fractions, including proteasomal components. Immunofluorescence microscopy experiments showed that GS-CA1 induced a small but significant accumulation of HIV-1 capsid cores at nuclear pores, while IFN-β caused a strong accumulation at the nuclear envelope, but not specifically at nuclear pores. These observations suggest that GS-CA1 inhibits the nuclear translocation of HIV-1 capsid cores through nuclear pores. The study's results have important implications for HIV-1 research and potential therapeutic strategies. By identifying proteins modulated during HIV-1 infection and IFN-β treatment, the research provides potential new targets for antiviral therapies.

The unexpected findings regarding MX2 highlight the need for further investigation into other ISGs and cellular mechanisms involved in restricting HIV-1 infection at the nuclear envelope. Future research directions include investigating the specific functions of newly identified modulated proteins in HIV-1 infection and interferon response, exploring mechanisms by which IFN-β compensates for MX2 knockdown, and identifying other factors responsible for HIV-1 peptide accumulation at the nuclear envelope. Additionally, the identified proteins could be studied as potential biomarkers for HIV-1 infection or interferon response, and their roles in other viral infections could be investigated to determine if the observed effects are HIV-1 specific or part of a broader antiviral response.

Résumé

Cette étude les interactions complexes entre le VIH-1, l'enveloppe nucléaire de la cellule hôte et la réponse immunitaire innée, en se concentrant sur l'interféron bêta (IFN-β) et le gène MX2 stimulé par l'interféron. Cette recherche examine les effets de GS-CA1, un nouvel inhibiteur de la capside du VIH-1, sur les premiers stades de l'infection par le VIH-1 au niveau de l'enveloppe nucléaire. L'étude a révélé que l'infection par le VIH-1 et le traitement par l'IFN-β modulent les niveaux d'abondance des protéines de l'enveloppe nucléaire. Les protéines codées par les gènes stimulés par l'interféron (ISG) tels que TRIM22, TRIM14 et MX2 ont été régulés à la hausse à l'enveloppe nucléaire par l'IFN-β. La nucléoporine TPR, connue pour faciliter l'intégration de l'ADNc du VIH-1 dans le génome de la cellule hôte, a été sélectivement régulée à la hausse lors de l'infection par le VIH-1, tandis que la vimentine, une protéine associée aux pores nucléaires, a été régulée à la baisse. L'une des principales conclusions est que le traitement par l'IFN-β augmente l'accumulation des protéines du VIH-1 au niveau de l'enveloppe nucléaire.

Cela a conduit à l'hypothèse que MX2, connu pour interagir avec la capside du VIH-1 près du complexe de pores nucléaires, pourrait être responsable de cette accumulation. Cependant, des expériences utilisant des cellules knockdown MX2 ont remis en question cette hypothèse. Bien que les peptides du VIH-1 soient plus abondants dans les échantillons traités à l'IFN-β, il n'y avait pas de différence significative dans l'accumulation de peptides entre les cellules knockdown MX2 et les cellules témoins. Ces résultats indiquent que MX2, non seulement mais avec d'autres ISG, pourrait être responsable de l'accumulation de peptides du VIH-1 dans les fractions enrichies en enveloppe nucléaire pendant le traitement par IFN-β. L'étude a également observé que l'infection par le VIH-1 semblait atténuer l'effet de l'IFN-β sur certains ISG, confirmant ainsi les résultats antérieurs selon lesquels le VIH-1 peut partiellement échapper ou supprimer la réponse immunitaire innée. Cette recherche fait progresser notre compréhension des interactions du VIH-

1 avec l'enveloppe nucléaire et la réponse immunitaire innée de la cellule hôte. Les résultats suggèrent que les mécanismes d'entrée nucléaire du VIH-1 et les tentatives de la cellule hôte pour bloquer cette entrée sont plus complexes qu'on ne le pensait auparavant, impliquant plusieurs protéines et voies.

Nous avons ensuite utilisé le GS-CA1, un inhibiteur qui empêche la formation de capside, pour étudier l'impact de l'infection par le VIH-1, du traitement par le GS-CA1 et du traitement par l'interféron bêta (IFN-β) sur l'enveloppe nucléaire, ainsi que la localisation des capside du VIH-1 au niveau de l'enveloppe nucléaire et des pores nucléaires. Des expériences de spectrométrie de masse ont révélé que le traitement par GS-CA1 combiné à l'infection par le VIH-1 modifiait significativement les niveaux de protéines dans les fractions enrichies en enveloppe nucléaire, y compris les composants protéasomaux. Des expériences de microscopie par immunofluorescence ont montré que GS-CA1 induisait une accumulation faible mais significative de noyaux de capside du VIH-1 au niveau des pores nucléaires, tandis que l'IFN-β provoquait une forte accumulation au niveau de l'enveloppe nucléaire, mais pas spécifiquement au niveau des pores nucléaires. Ces observations suggèrent que GS-CA1 inhibe la translocation nucléaire des noyaux de capside du VIH-1 à travers les pores nucléaires. Les résultats de l'étude ont des implications importantes pour la recherche sur le VIH-1 et les stratégies thérapeutiques potentielles. En identifiant les protéines modulées pendant l'infection par le VIH-1 et le traitement par l'IFN-β, la recherche fournit de nouvelles cibles potentielles pour les thérapies antivirales.

Les résultats inattendus concernant MX2 soulignent la nécessité d'approfondir les recherches sur d'autres ISG et mécanismes cellulaires impliqués dans la limitation de l'infection par le VIH-1 à l'enveloppe nucléaire. Les orientations de recherche futures comprennent l'étude des fonctions spécifiques des protéines modulées nouvellement identifiées dans l'infection par le VIH-1 et la réponse à l'interféron, l'exploration des mécanismes par lesquels l'IFN-β compense l'inactivation de MX2 et l'identification d'autres facteurs responsables de l'accumulation de peptides du VIH-1 dans l'enveloppe nucléaire. De plus, les protéines identifiées pourraient être étudiées en tant que biomarqueurs potentiels de l'infection par le VIH-1 ou de la réponse à l'interféron, et leur rôle

dans d’autres infections virales pourrait être étudié pour déterminer si les effets observés sont spécifiques du VIH-1 ou s’ils font partie d’une réponse antivirale plus large.

Abbreviations

AGC	Automatic gain control
APOBEC3G	Apolipoprotein B mRNA Editing Enzyme, Catalytic Polypeptide-Like 3G
ATL	Adult T-cell leukemia/lymphoma
AZT	Azidothymidine (also known as zidovudine)
BDCRB	5-bromo-5,6-dichloro-1-β-D-ribofuranosyl benzimidazole (BDCRB)
BIV	Bovine Immunodeficiency Virus
cGAS	Cyclic GMP-AMP Synthase
CPSF6	Cleavage and Polyadenylation Specificity Factor 6
CRFK	Crandell Rees feline kidney (cells)
CTL	Cytotoxic T lymphocyte
CyPA	Cyclophilin A
DMEM	Dulbecco's Modified Eagle Medium
dsDNA	Double-stranded DNA
FACS	Fluorescence-activated cell sorting
FBS	Fetal bovine serum
FDR	False discovery rate
FIV	Feline Immunodeficiency Virus
GAPDH	Glyceraldehyde 3-phosphate dehydrogenase
GFP	Green fluorescent protein
HAART	Highly active antiretroviral therapy
HAM/TSP	HTLV-1-associated myelopathy/tropical spastic paraparesis
HCMV	Human cytomegalovirus
HEK293T	Human embryonic kidney 293T (cells)
HPLC	High-performance liquid chromatography

HRP	Horseradish peroxidase
IFN	Interferon
ISG	Interferon-stimulated gene
LFQ	Label-free quantification
LTR	long terminal repeat
MOI	Multiplicity of infection
MX2	Myxovirus resistance protein 2
NNRTIs	Non-nucleoside reverse transcriptase inhibitors
NPC	Nuclear pore complex
NRTIs	Nucleoside reverse transcriptase inhibitors
Nup	Nucleoporin
PC1 & PC2	Principal component 1 and Principal component 2
PCA	Principal component analysis
PEI	Polyethyleneimine
PIs	Protease inhibitors (PIs)
PrEP	Pre-exposure prophylaxis
PVDF	Polyvinylidene fluoride
Rig-I	Retinoic Acid-Inducible Gene I
RPMI	Roswell Park Memorial Institute (medium)
SCID	Severe combined immunodeficiency
SDG	Sustainable development goals
SDS	Sodium dodecyl sulfate
SIV	Simian Immunodeficiency Virus
TAR	trans-activating response element
TPR	Nucleoporin TPR (Translocated Promoter Region)
TRIM14	Tripartite Motif-containing Protein 14

TRIM22	Tripartite Motif-containing Protein 22
TRIM5α	Tripartite Motif-containing Protein 5 alpha
UNG2	Uracil-DNA Glycosylase 2

Table of contents

List of Figures

List of Tables

Chapter 1

Introduction

1.1 Viruses

Viruses are small, obligate intracellular parasites that contain either DNA or RNA as their genetic material, enclosed within a protein capsid (1). These organisms have long posed a threat to various species, including humans, nonhuman primates, and plants (2). Throughout history, viruses have caused widespread pandemics, such as the Spanish flu (3), the 2009 H1N1 influenza pandemic (formerly known as swine flu) (4), and most recently, COVID-19 (5). According to the World Health Organization (WHO), HIV is currently a pandemic (6). Since the identification of AIDS in 1981 (7) and its causative agent, HIV, in 1983-4 (8, 9), there has been ongoing research into the HIV life cycle and anti-HIV drugs. HIV is a lentivirus from the retroviridae family, and one of its unique features is that it can reverse transcribe its RNA genome into dsDNA, integrating it into the host (10, 11). This thesis investigates HIV-1–host interactions at the nuclear envelope, focusing on innate immune responses during HIV-1 nuclear entry and their impact on nuclear envelope proteins.

1.1.1 HIV types and classification of HIV-1

HIV remains a major global public health issue, having claimed 40.4 million [32.9–51.3 million] lives so far with ongoing transmission in all countries globally; with some countries reporting increasing trends in new infections when previously on the decline. There were an estimated 39.0 million [33.1–45.7 million] people living with HIV at the end of 2022, two-thirds of whom (25.6 million) are in the African Region according to WHO data. In 2022, around 630,000 [480 000–880, 000] people died from HIV-related causes and 1.3 million [1.0–1.7 million] people acquired HIV. There is no cure for HIV infection. However, with access to effective HIV prevention, diagnosis, treatment, and care, including for opportunistic infections, HIV infection has become a manageable chronic health condition, enabling people living with HIV to lead long and healthy lives. WHO, the Global Fund, and UNAIDS all have global HIV strategies that are aligned with sustainable development goals (SDG) target 3.3 of ending the HIV epidemic by 2030.

HIV-1, or Human Immunodeficiency Virus Type 1, is a lentivirus that infects humans and is responsible for causing acquired immunodeficiency syndrome (AIDS). It is a member of the Retroviridae family, which is further classified into the subfamily Orthoretrovirinae. HIV-1

primarily targets and infects immune cells called CD4+ T lymphocytes, compromising the host's immune system over time. HIV-1 was first identified in the early 1980s at the onset of the HIV pandemic. The virus was initially isolated from individuals with AIDS-related symptoms and named LAV (Lymphadenopathy-Associated Virus) by researchers in France and HTLV-III (Human T-cell Lymphotropic Virus Type III) by researchers in the United States.

In 1986, a consensus was reached, and the virus was officially named HIV (Human Immunodeficiency Virus) (8, 9). Further research led to the classification of two main types of HIV: HIV-1 and HIV-2, with HIV-1 being more widespread and pathogenic. Like other lentiviruses, HIV-1 can infect both dividing and non-dividing cells, making it more efficient in replication and integration into the host genome, especially in terminal differentiated cells such as neural cells and macrophages. Other retroviruses, such as murine leukemia virus (MLV) require the nuclear membrane to rupture in order to access the host genome (12). With this unique feature, HIV-1 can manipulate many cellular proteins to complete its life cycle, as discussed later in this chapter.

Among two types of HIV, HIV-1 is the most prevalent around the world and it causes AIDS (advanced type) (13). Whereas HIV-2 is predominantly found in western Africa. This study will focus on HIV-1. Before going into details of HIV-1, let’s look at the classification of HIV-1 according to the International Committee on Taxonomy of Viruses (ICTV) (14). Figure 1.1 presents the classification of HIV-1 into distinct subtypes and sub-subtypes based on genetic sequence variations

Realm: *Riboviria*
Kingdom: *Pararnavirae*
Phylum: *Artververiricota*
Class: *Revtraviricetes*
Order: *Ortervirales*
Family: *Retroviridae*
Subfamily: *Orthoretrovirinae*
Genus: *Lentivirus*
Species: *Human immunodeficiency virus 1*

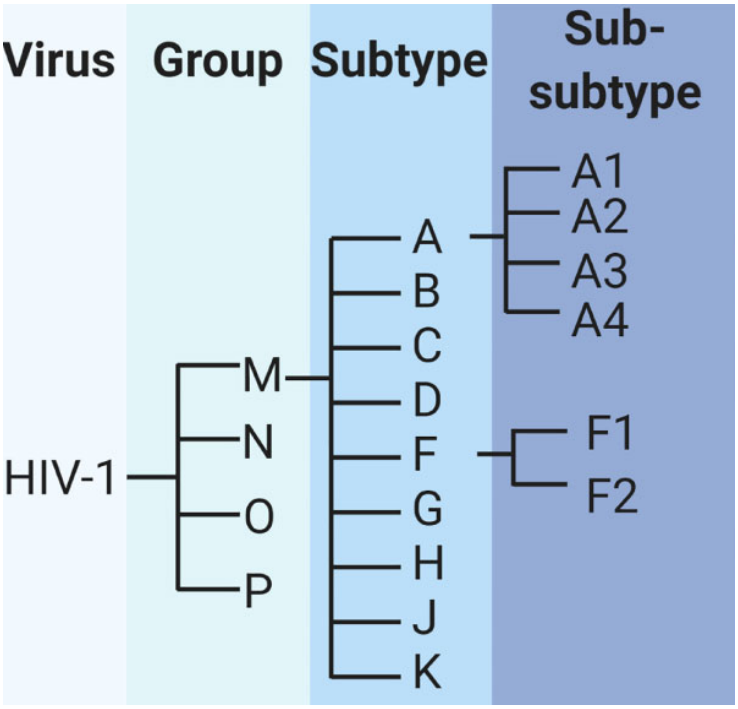

Figure 1.1: Classification of HIV-1 (Adapted From (15)) Classification of HIV-1 subtypes and sub-subtypes

Since the discovery of HIV-1 as the causative agent of AIDS in the early 1980s, remarkable progress has been made in both understanding the virus and developing effective treatments. The introduction of zidovudine (AZT) in 1987 marked the first breakthrough in antiretroviral therapy (16), followed by the advent of protease inhibitors and the era of highly active antiretroviral therapy (HAART) in the mid-1990s. More recently, advances such as integrase inhibitors (17)and the capsid inhibitor lenacapavir (18) have further expanded the therapeutic landscape.

Figure 1.2 summarizes these key milestones in HIV-1 research and treatment.

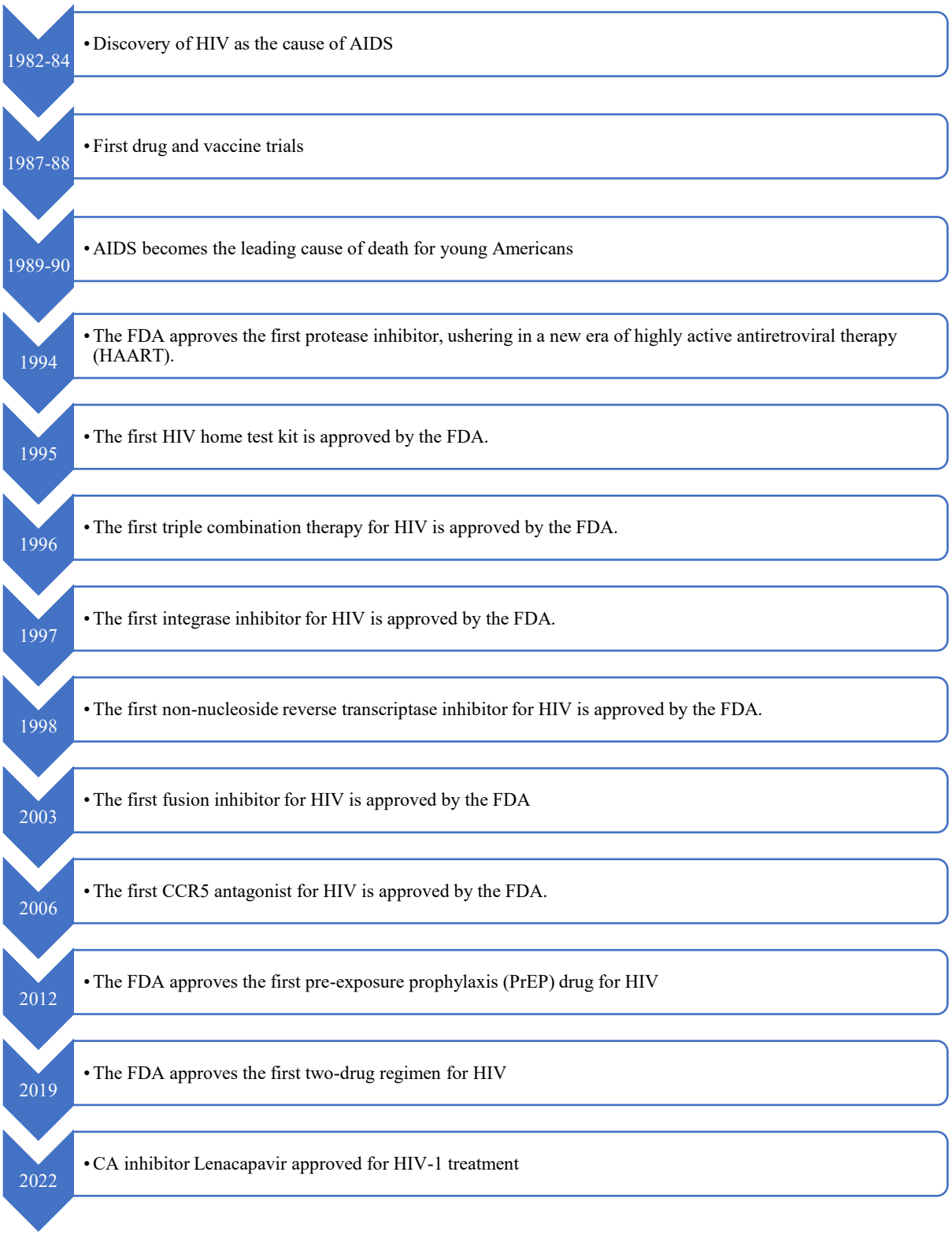

Figure 1.2: Important events in the HIV-1 Discovery and hunt for the Treatments. The figure provides a timeline that outlines key milestones in HIV/AIDS research and treatment, spanning from 1982 to 2022. It begins with the discovery of HIV as the cause of AIDS in the early 1980s and includes major advancements such as the approval of the first antiretroviral therapies, groundbreaking drug classes like integrase inhibitors and CCR5 antagonists, and innovations like the first home test kit and pre-exposure prophylaxis (PrEP). The timeline culminates in 2022 with the approval of a new treatment, Lenacapavir, for HIV-1.

1.1.3 HIV-1 virus structure and HIV-1 genome

HIV-1 is a retrovirus with a spherical structure approximately 100-120 nm in diameter (19, 20). Its outer layer consists of a lipid bilayer membrane derived from the host cell, embedded with viral envelope glycoproteins gp120 and gp41 ((20)(see **Figure 1.3)**. Beneath the membrane lies a matrix composed of p17 proteins. The viral core, or capsid, is conical-shaped and made up of p24 proteins. Inside the capsid are two identical single-stranded RNA genomes, along with essential viral enzymes such as reverse transcriptase, integrase, and protease. The RNA is bound to nucleocapsid proteins. This comsplex structure enables HIV-1 to infect host cells, primarily CD4+ T lymphocytes and macrophages, by binding to CD4 receptors and co-receptors on the cell surface, initiating the viral replication cycle (20).

The full-length transcript of HIV contains numerous 5' and 3' splice sites (21) (see **Figure 1.3)**. During the early stages of infection, multiple spliced mRNAs produce the regulatory proteins Tat and Rev, along with the accessory protein Nef (22). These mRNAs are abundant at this point due to Tat's stimulation of transcription. However, as Rev protein accumulates, it triggers a shift in mRNA patterns, resulting in a temporal change in viral gene expression. Rev, an RNA binding protein, identifies a specific sequence within the env region of the elongated transcript known as the Rev-responsive element (RRE) (22). This protein facilitates the nuclear export of any RNA containing the RRE. As Rev levels increase, unspliced or singly spliced transcripts with the RRE are transported out of the nucleus. This process promotes the production of viral structural proteins (Gag, Env) and enzymes (Pol) while ensuring full-length genomic RNA is available for incorporation into new virus particles. In the later stages of infection, singly spliced mRNAs dependent on Rev for cytoplasmic export produce the accessory proteins Vif, Vpr, and Vpu (in HIV-1) or Vif, Vpr, and Vpx (in HIV-2) (22).

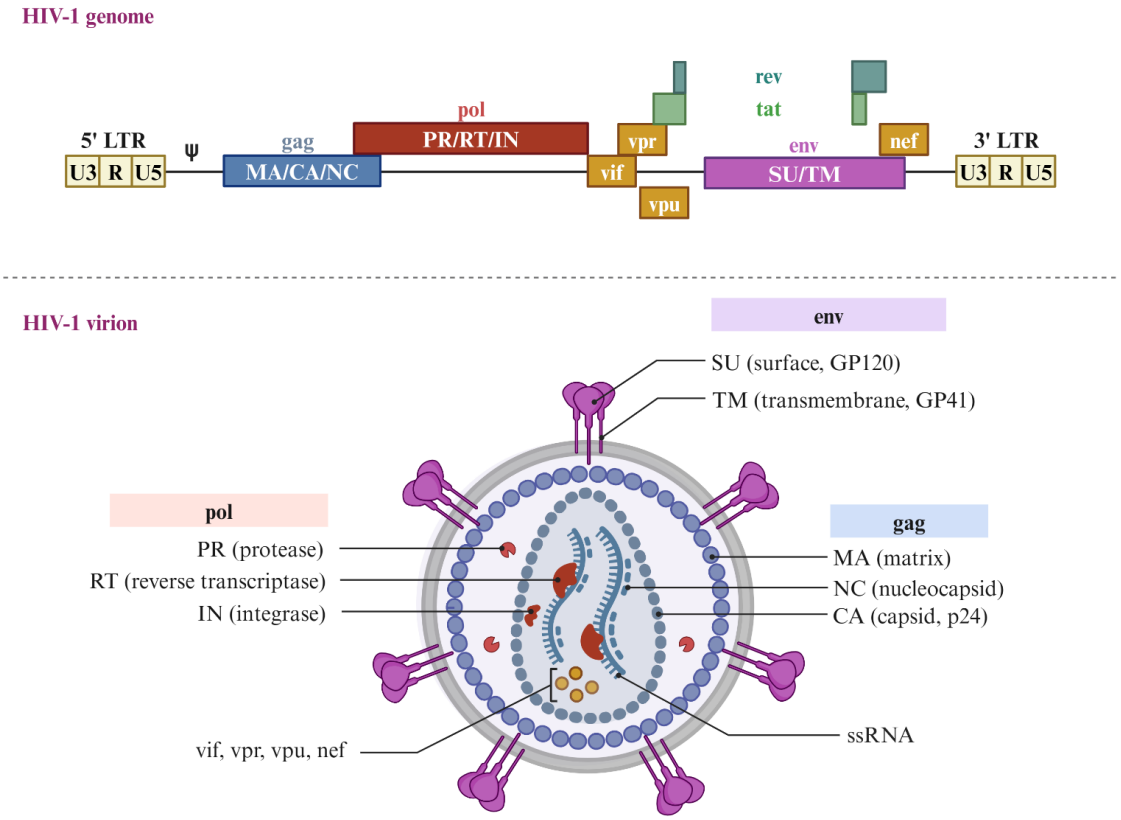

Figure 1.3: A general depiction of the HIV-1 genome (upper part) and HIV-1 virus structure (lower part). (created with biorender.com) Schematic representation of the HIV-1 genome and its encoded proteins. The genome consists of structural, enzymatic, and regulatory genes. The gag gene encodes matrix protein (MA), capsid protein (CA), nucleocapsid protein (NC), and p6. The pol gene encodes protease (PR), reverse transcriptase (RT), and integrase (IN). The env gene encodes surface glycoprotein (SU/gp120) and transmembrane glycoprotein (TM/gp41). Accessory proteins include trans-activator of transcription (Tat), regulator of viral expression (Rev), viral infectivity factor (Vif), viral protein R (Vpr), and viral protein U (Vpu). Schematic representation of HIV-1 virus structure showing the envelope, core, and genetic material. Single-stranded RNA (ssRNA).

A) Tat: Tat functions as a transcriptional activator that enhances productive transcription during HIV infection (23). The viral long terminal repeat governs the expression of integrated HIV DNA by interacting with cellular transcriptional machinery (23). While the HIV LTR serves as a promoter in diverse cell types, its baseline activity is comparatively low. The LTR contains an enhancer sequence that interacts with cell-specific transcriptional activators, including Nf-kB (23). This interaction may explain the necessity of T-cell activation for HIV replication. The trans-

activating response element (TAR), a distinctive viral regulatory sequence, is located downstream of the transcription initiation site in the HIV LTR (23). TAR RNA adopts a stable bulged stem-loop configuration that binds to Tat and various host proteins. Tat enhances transcriptional processivity and facilitates viral RNA elongation (23). Infected cells release Tat, which can affect other cells by acting as a chemoattractant for monocytes, basophils, and mast cells. Upon entering cells, Tat can trigger the production of crucial proteins that significantly impact virus dissemination and immune cell functionality. For instance, in transient-expression assays, Tat can upregulate genes encoding the CXCr4 and CCr5 coreceptors in target cells and boost the production of several chemokines (24). The Tat protein exhibits cytotoxicity in certain cultured cells and demonstrates neurotoxicity when injected intracerebrally into mice (25).

B) Rev: Rev is a 19 kD phosphoprotein of HIV-1 and acts as a regulatory factor mainly found in the nucleus/nucleolus. It is functionally conserved in lentiviruses and shuttles between the nucleus and cytoplasm (26). Rev binds to the rev responsive element (RRE) of viral pre-mRNA and later to XPO1 to facilitate viral pre-mRNA export (27). In the early infection when Rev is not synthesized, spliced viral mRNA is exported to the cytoplasm and is translated to many regulatory viral proteins including Rev. Then Rev translocates to the nucleus and starts the cycles for export of viral pre-mRNA (28, 29). Hence Rev regulates the other viral protein expression.

C) Vif: Vif is a protein found in infected cells that is necessary for virus assembly and acts as an RNA-binding protein. The absence of the vif gene in virus particles leads to a significant reduction in infectivity. Virus particles lacking Vif can initiate reverse transcription but do not complete it, indicating that Vif is essential for reverse transcription completion. Vif is required for infectivity in certain cell types, and experiments with cell fusion suggest that nonpermissive cells dominate (30). The infectivity of virus particles is enhanced in the presence of Vif, suggesting that Vif may suppress a host cell function that would otherwise inhibit viral infectivity. Vif forms a complex with other cellular proteins to target and degrade APOBEC3G (3F,3H, 3DE) a cellular protein that inhibits virus reproduction in various ways, including binding to viral RNA. Vif prevents the incorporation of APOBEC3G into virus particles by binding to it and inducing its proteasomal degradation (31, 32). In the absence of Vif, APOBEC3G is incorporated into the viral particles.

Then APOBEC3G inhibits the viral DNA synthesis and may induce the mutagenesis for hyper G→A transitions (33).

D) Vpr: Vpr, a viral protein weighing 15 kDa and also known as R, causes the rapid destruction of T cells in HIV-1 infections. It binds to the Gag polyprotein of viral particles and also the host's protein uracil -DNA glycosylase 2 (UNG2). It also functions as an adapter protein in an E3-ligase (34, 35). Vpr facilitates the recruitment of the cellular Slx4 structure-specific endonuclease regulator and triggers G2/M arrest and apoptosis in response to Vpr (34). Preventing infected cells from entering mitosis seems to have no obvious advantage, especially since the need for Vpr's function is most evident in HIV infection of nondiving cells, macrophages (34). Vpr enhances virus production by increasing the activity of LTR promoters during the G2 phase of the cell cycle (34, 35). In addition to cell cycle arrest and apoptosis, Vpr modulates the transcription of host and viral genes, maintains reverse transcriptase fidelity, recruits UNG2, and facilitates the nuclear import of preintegration complexes in non-dividing cells (34). By binding to nuclear pore proteins hCG1 (NupL2, NupL1/2), Vpr may also play a role in the docking of the HIV-1 preintegration complex at the nuclear pore for import (36).

E) Vpu: The Vpu protein is a 16-kDa viral protein HIV-1. It is not present in HIV-2. It has an N-terminal membrane-spanning domain and two alpha-helices in its cytoplasmic domain. Vpu is an integral membrane protein that forms oligomers through self-association (37). It is found on all membranes of intracellular organelles of infected cells, including in the endoplasmic reticulum (ER), trans-Golgi network, and endosomes. Vpu is crucial for proper maturation and targeting of progeny virus particles and their efficient release (38). Without Vpu, particles with multiple cores are produced, and budding is directed to multivesicular bodies instead of the plasma membrane (39). Vpu reduces viral cytopathogenicity by limiting the accumulation of envelope (Env) glycoproteins at the host cell surface, thereby inhibiting Env-mediated cell-cell fusion and syncytium formation (40, 41).

Tetherin is a membrane protein with a cytoplasmic tail, a transmembrane region, and a glycophosphatidyl inositol membrane anchor (39). It inhibits the spread of the virus by capturing the progeny at the plasma membrane (37). Vpu interacts with tetherin in the trans-Golgi network

and inhibits its transport to the plasma membrane hence facilitating the release of viruses (42). It also traps the CD4 at the ER, facilitating the degradation of CD4 (43). This reduces the quantity of CD4 at the cell surface, limits superinfection by HIV-1, and enhances the production of infectious particles (44). Vpu also forms an ion-conducting channel known as a viroporin, similar to that of the influenza A virus protein M2. It is noteworthy that HIV-1 is the only virus that has Vpu, which is a tetherin antagonist. This is likely due to different retroviral proteins assuming this function during evolution, such as the envelope protein of HIV-2 and the Nef proteins of several primate viruses, which act as tetherin antagonists in their host species.

F) Nef: Most laboratory strains of HIV-1 have been modified to grow well in T cell lines and often contain deletions or other mutations in the nef gene. The restoration of nef reduces the efficiency of virus reproduction in these cells, leading to the name "negative factor" (45). Nef (27-32KD) is produced from multiply spliced early mRNA transcripts (45). The size of these proteins can differ due to posttranslational modifications. Nef is incorporated into virus particles by interacting with Gag polyproteins. Nef plays a role in capsid disassembly following infection. Nef undergoes post-translational modification via N-terminal myristoylation, which facilitates its anchoring to the inner leaflet of the plasma membrane. (46). It includes a protein-protein interaction domain (SH3) that binds to components of intracellular signaling pathways, eliciting a program of gene expression similar to that observed after T-cell activation (47, 48). Nef is a well-studied HIV-1 accessory protein that downregulates the surface expression of CD4 and MHC class I molecules (49, 50). By connecting the cytoplasmic domain of MHC class I molecules with the clathrin adapter protein complex (AP-1) in the trans-Golgi network, Nef facilitates their delivery to lysosomes for degradation, thereby inhibiting cytotoxic T lymphocyte (CTL) recognition and enhancing HIV-1 pathogenesis.

G) CA (capsid): The HIV-1 capsid (CA) protein plays crucial roles in viral particle assembly and early infection stages. CA forms the conical core shell of mature virions, encapsulating the viral genome and associated proteins (51).

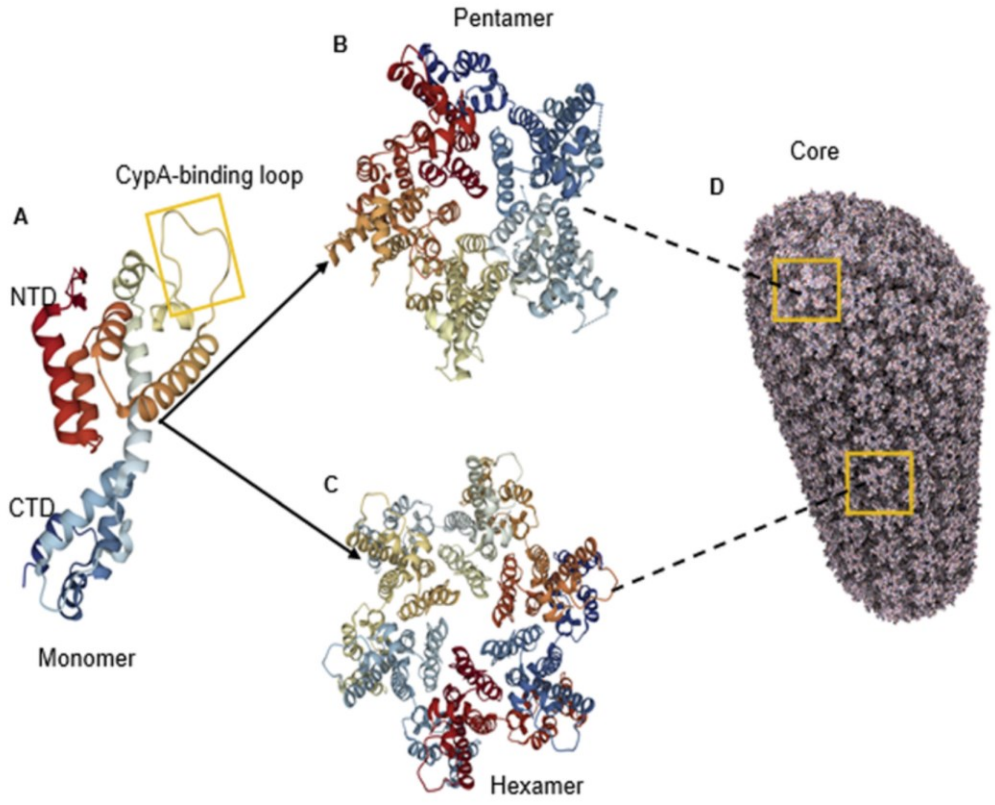

Figure 1.4: Structure of HIV-1 capsid (A) The structure of the CA monomer showing the N-terminal domain (NTD), the C-terminal domain, and the CypA-binding loop (highlighted) (PDB 4XFY). (B) The structure of pentameric HIV-1 CA (PDB 3P05). (C) The structure of hexameric HIV-1 CA (PDB 4XFY). (D) The hexameric and pentameric subunits assemble into a fullerene conical capsid core (PDB 3J3Y). In this model, the core is composed of 186 hexamers and 12 pentamers (from (52)).

The HIV-1 capsid (CA) protein (see **Figure 1.4)** consists of two predominantly α-helical domains, the N-terminal domain (CA-NTD) and the C-terminal domain (CA-CTD), connected by a flexible linker (51, 53). The NTD is essential for mature core formation and interacts with cyclophilin A (CyPA), facilitating its incorporation into virions and enhancing infectivity (54-56). The CTD mediates CA dimerization, which is critical for both immature particle assembly and viral replication (51, 57). During maturation, proteolytic cleavage at the CA-p2 junction acts as a molecular switch, enabling the transition from spherical to conical core structures (58, 59). In vitro, CA can self-assemble into tubes resembling those seen in mature virions, with hexameric rings

formed by NTDs and inward-projecting CTDs (60, 61). This flexible architecture supports the fullerene cone model, where the HIV-1 core consists of a hexagonal lattice closed by 12 pentameric defects, determining core geometry (59, 62, 63). The relatively open structure may allow nucleotide entry for reverse transcription within the intact core (61).

H) Pol (polymerase): POL region of HIV-1 genome encodes produced as a Gag-Pol precursor polyprotein. This polyprotein is further cleaved into viral enzymes polymerase (PR), reverse transcriptase (RT), and integrase (IN) (65). These enzymes are crucial to complete the viral life cycle as they help in reverse transcription and integration into the host genome.

I) Env (envelop protein): It includes viral glycoproteins; gp160 precursor, processed to gp120 and gp41, which form trimers on the cell surface and contain binding sites for CD4 and co-receptors CCR5 or CXCR4 (66). This finding initiates the fusion of HIV-1 to the host cell membrane.

1.1.4 HIV-1 Replication cycle

HIV-1 primarily targets and infects CD4+ T lymphocytes, compromising the host's immune system over time (67). This section will delve into the stages of the HIV-1 life cycle, including attachment, fusion, reverse transcription, integration, transcription and translation of viral genes, assembly, budding, and maturation.

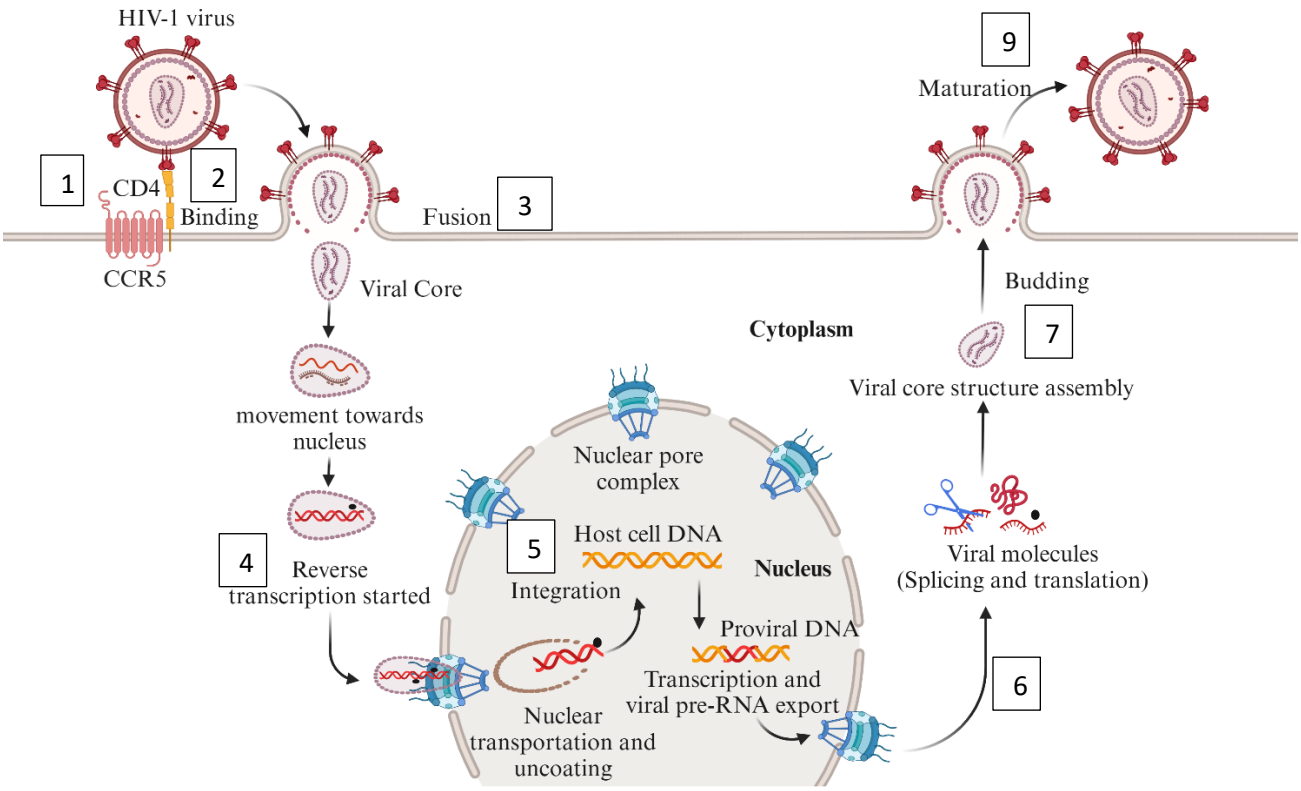

Figure 1.5: HIV-1 life cycle. Created with biorender.com, inspired by (68). Schematic representation of the different stages of the HIV-1 life cycle, beginning with attachment to the host cell and concluding with the budding of new virions. The process involves the interaction of a cluster of differentiation 4 (CD4) receptors and C-C chemokine receptor type 5 (CCR5) co-receptors on the host cell surface with the viral envelope glycoproteins.

Stage 1- Attachment: The first step in the HIV-1 life cycle involves the attachment of the virus to CD4 receptors on the surface of host immune cells, particularly CD4+ T lymphocytes (see **Figure 1.5)**. This initial attachment is mediated by the viral envelope glycoprotein gp120 binding to CD4 receptors (9).

Stage 2- Co-receptor binding: Following attachment, HIV-1 binds to co-receptors on the host cell surface (see **Figure 1.5)**. The two major coreceptors for HIV-1 are CXCr4 and CCr5 (69). strains of HIV that bind to CXCr4 or CCr5 are referred to as X4 and R5 strains, respectively (70, 71). R5 viruses are typically transmitted during early-stage infection, while X4 viruses are mostly transmitted in the late stages (72, 73). These receptors are critical for HIV-1 infection, and certain mutations, particularly in CCR5, can contribute to HIV-1 resistance. For instance, individuals

homozygous for the CCR5-Δ32 mutation are highly resistant to HIV-1 infection, while heterozygous individuals may experience slower disease progression if infected (74). Cell lineages with CD4 receptors and chemokine receptors (especially CCR5 and CXCR4) are the main targets of HIV-1 and they also produce most viral particles (75, 76). Several additional chemokine receptors have been identified as coreceptors for HIV in cell culture experiments, but their roles in natural infection remain unclear (69). These additional coreceptors may allow the virus to enter a broader range of cells than initially thought. They are found in cells such as those in the thymus gland and brain and could play a role in infection during infancy or in cells of the central nervous system (77). It has been suggested that binding to these additional coreceptors may trigger signals that affect virus reproduction in target cells or harm nonpermissive cells, leading to a "bystander" effect (78, 79). This binding event triggers a conformational change in the viral envelope glycoprotein gp41, leading to the fusion of viral and cellular membranes. It also requires a coreceptor to trigger the fusion of the viral and cellular membranes and gain entry into the cytoplasm (80, 81).

Stage 3- Fusion and entry: The process of merging viral and host cell membranes facilitates the entry of the viral core into the host cell's cytoplasm. The unbroken core, which encircles the viral RNA genome and accompanying proteins, is then propelled towards the nuclear membrane by myosin and actin (82). Previously, it was believed that the virus's capsid disassembles near the nuclear pore in the cytoplasm, but recent research has revealed that the capsid remains intact during entry into the nuclear pore and also might act as an opportunistic nuclear import receptor (83). However, additional capsid residues are detected within the nucleus, though they may not always be in their original, unbroken state (see **Figure 1.5)**.

Stage 4- Reverse transcription: Upon entering the host cell, the viral RNA genome is converted into a DNA copy by the viral enzyme reverse transcriptase (9). This process leads to the formation of a double-stranded viral DNA molecule referred to as the provirus. The completion of reverse transcription has been the subject of debate regarding its location and timing. However, recent research indicates that reverse transcription commences in the cytoplasm but concludes near the integration site in the nucleus (84).

Stage 5- Integration: The processes of transporting the HIV-1 core to the nucleus and integrating viral DNA into the host genome are interconnected (85). The provirus is transported to the host cell nucleus, where it integrates with the help of the viral integrase enzyme into the host cell's genomic DNA, becoming a permanent part of the cell's DNA (9).

Stage 6 - Transcription and translation: The integrated provirus can potentially be transcribed by the host cell's RNA polymerase, resulting in the production of viral RNA and messenger RNA (mRNA). These mRNA molecules are subsequently translated by the host cell's ribosomes, ultimately synthesizing viral proteins, such as structural and regulatory proteins.

Stage 7- Assembly and budding: The formation of newly synthesized viral components, including viral RNA, proteins, and enzymes, occurs at the host cell's plasma membrane. These viral proteins and RNA are subsequently packaged into new virions, which bud from the host cell's membrane and acquire an envelope composed of host cell membrane components.

Stage 8-Maturation and release: The maturation of viral protease involves cleaving precursor proteins into functional forms, resulting in the release of mature virions from the host cell. These mature virions can then infect other CD4+ T lymphocytes, perpetuating the cycle (see **Figure 1.5)**.

The HIV-1 life cycle is a complex and tightly regulated process that ultimately results in the production of new viral particles and the depletion of host CD4+ T cells, contributing to the progressive immunodeficiency observed in AIDS patients. This process is further complicated by the ability of HIV-1 to infect and replicate within CD4+ T cells, leading to the destruction of these cells and the subsequent loss of immune function. Additionally, HIV-1 has the ability to evade the host immune response through the use of various mechanisms, such as the production of viral variants with mutations that prevent recognition by the immune system (86).

1.1.5 HIV-1 and the nuclear envelope

As mentioned earlier the HIV-1 life cycle is incomplete without the integration of the viral genome in the host genome. This process involves the nuclear envelope. The nuclear envelope plays a crucial role in the HIV-1 life cycle, serving as both a barrier and a gateway for viral components. As HIV-1 replicates, it must overcome the challenge of transporting its genetic material and associated proteins across this double-membrane structure to access the host cell's nucleus. The nuclear pore complexes (NPCs) embedded in the nuclear envelope are essential for

this process, allowing the viral pre-integration complex to enter the nucleus and integrate the viral DNA into the host genome. NPCs are large protein assemblies embedded in the nuclear envelope that regulates transport between the nucleus and cytoplasm. They are composed of multiple nucleoporins (Nups), which are specialized proteins that form the structural scaffold and mediate the selective passage of macromolecules. Additionally, the nuclear envelope facilitates the export of viral RNA back into the cytoplasm for protein translation and virion assembly. Understanding the interactions between HIV-1 and the nuclear envelope is crucial for developing targeted antiviral therapies and elucidating the mechanisms of viral persistence and replication.

Several key Nups have been identified as important for HIV-1 docking, translocation, and integration (87). Nup358/RanBP2, located on the cytoplasmic filaments of the NPC, is involved in docking HIV-1 cores through interactions with its cyclophilin-homology domain (87) (88). Nup153, positioned on the nucleoplasmic side, is critical for HIV-1 translocation through the nuclear pore (83, 87). Mutations in CA can alter the virus's dependence on specific Nups and host factors like TNPO3 (89). The central polypurine tract-central termination sequence (cPPT-CTS) in the viral DNA also affects the kinetics of nuclear entry, although it is not required (83, 90). This process is critical for HIV-1 replication in non-dividing cells and represents a potential target for antiviral strategies (91).

1.2 Nucleopore and nucleoporins

Gene expression, cell growth, and cell division in eukaryotic cells rely on the continuous transport of molecules and macromolecules between the nucleus and cytoplasm (92). This transport occurs through nuclear pore complexes (NPCs). Nucleoporins (Nups) are the building blocks of the NPCs, around 30 different Nups assemble and create NPCs of around 120 MDa (see **Figure 1.6** (93, 94). These Nups are generally conserved across eukaryotes, but there is no unifying scheme specifying their functional homologs across the Tree of Life. In this thesis, human Nup nomenclature is used consistently, and yeast (*Saccharomyces cerevisiae*) Nup names are mentioned only when directly relevant to specific experimental contexts discussed. The structure of NPCs, which integrates approximately 500-1000 Nups, is generally conserved (93, 94). The primary structural components of the NPC are the inner pore ring, which connects the inner and outer nuclear membranes, the nuclear and cytoplasmic rings anchored by the inner pore ring, the

nuclear basket, and the cytoplasmic filaments extending from the nuclear and cytoplasmic rings (93, 94) (see **Figure 1.6)**. The cytoplasmic filaments may not be true filaments as they lack typical properties such as oligomerization from monomers and persistence length. They are best described as disordered domains (95). It is unclear whether filament-like structures observed in traditional electron microscopy are components of NPCs. Nups are organized into stable subcomplexes, which serve as building blocks for the NPC. The most studied module is the conserved Y-complex, but other modules include the Nup214 complex, the Nup62 complex, and the inner ring complex (96, 97) (98).

In addition to its well-known role in nucleocytoplasmic transport, the NPC has several other functions (see **Figure 1.7)**. These include the spatial organization of other complexes closely associated with the nuclear periphery, such as the transcription export (TREX) complexes that help assemble and monitor messenger ribonucleoproteins (mRNPs) before export (99). Other functions include regulation of transcription, transcriptional memory, and chromatin organization (100-102). Research on Nup post-translational modifications, NPC segregation during mitosis, mechanical links between the NPC and cytoskeleton, and NPC biogenesis are also active and closely related fields of study. These insights have revealed fascinating details about how Nups and NPC modules are arranged and connected within the NPC scaffold (103). This knowledge also helps us understand how diseases caused by NPC mutations or misexpression in cancer cells could be linked to NPC dysfunction and pathologic phenotypes. Structural studies allow us to better understand how alterations to the NPC structure and/or assembly might affect transport pathways, leading to impaired nucleocytoplasmic shuttling of signaling proteins that regulate cell proliferation, differentiation, and organism development.

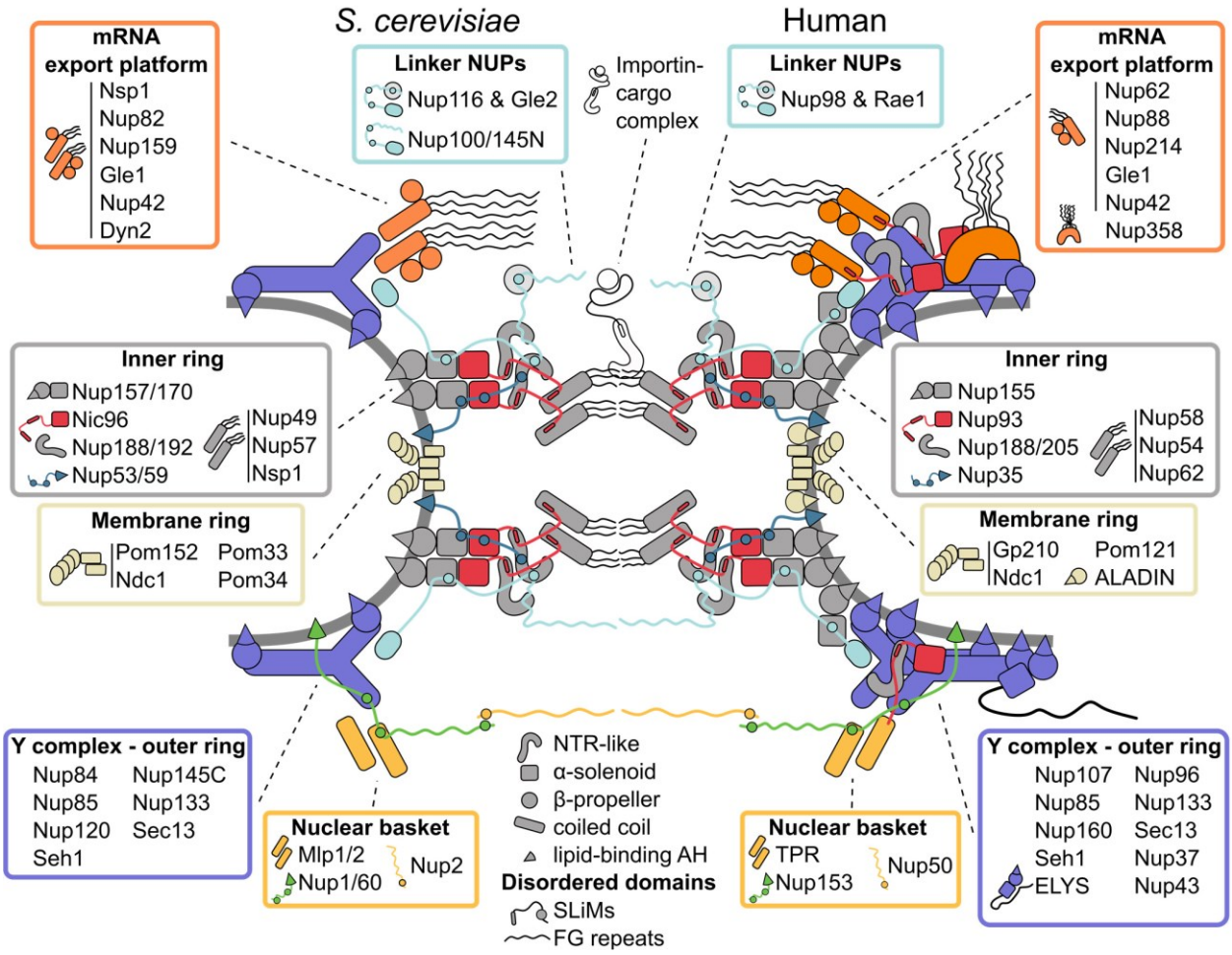

Figure 1.6: Structure of human nucleopore in comparison to yeast nucleopore, adapted From (93) The structural organization of conserved Nups from yeast and humans within the human NPC framework is depicted, with Nups arranged in subcomplexes represented by color-coded boxes superimposed on the general NPC architecture. These subcomplexes include Y-complexes (blue), inner ring complex (grey), transmembrane Nups (faded yellow), Nup62 complex (grey; Nsp1 complex in yeast), mRNA export platform or cytoplasmic complexes (bright orange), and nuclear basket complexes (yellow). GP210, glycoprotein 210; mRNA, messenger RNA; Mlp, myosin-like protein; NDC1, nuclear division cycle 1; POM, pore membrane protein; rRNA ribosomal RNA; TPR, translocated promoter region.

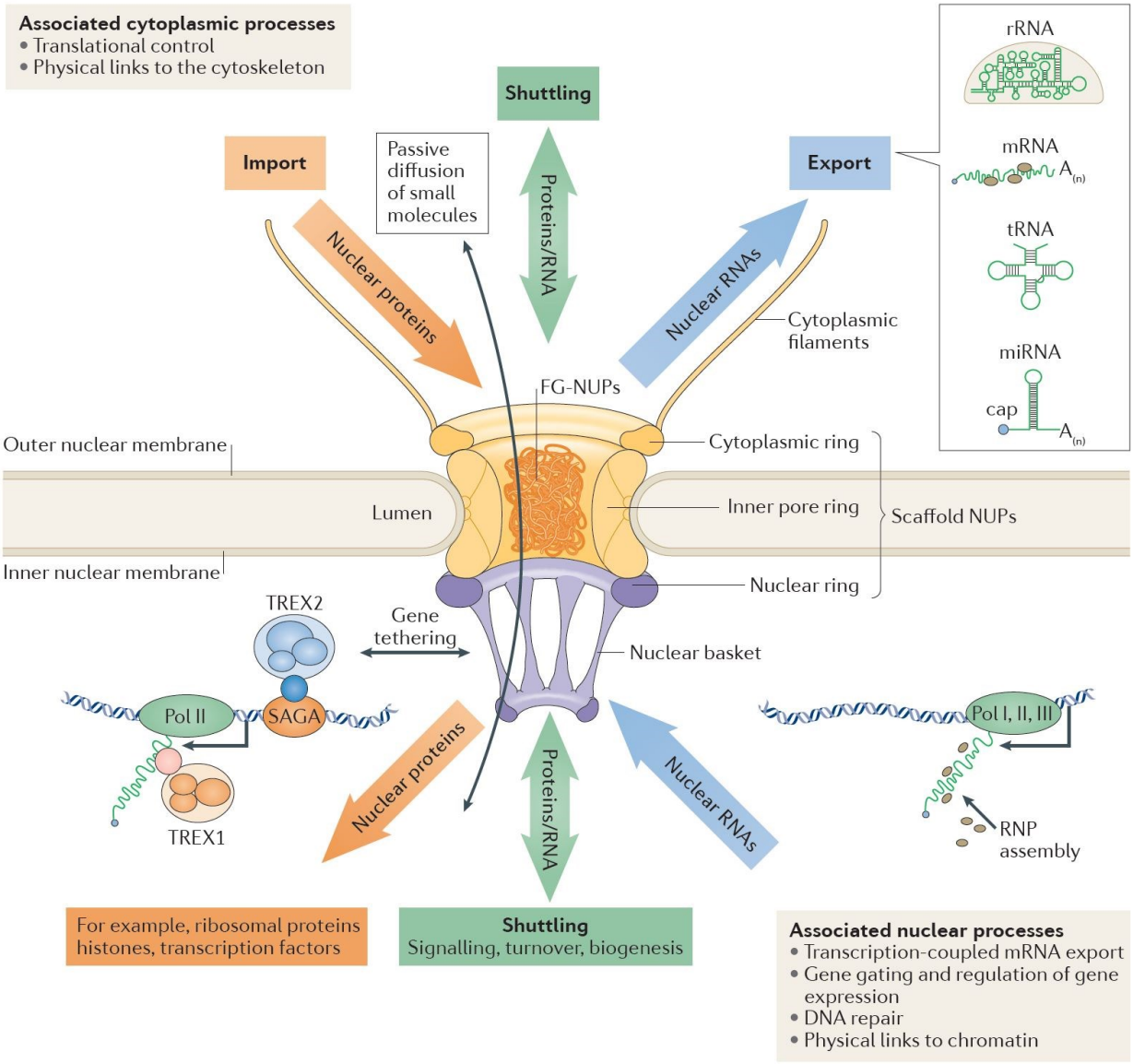

Figure 1.7: Nucleopore functions adapted from (104) The nuclear pore complex (NPC), a structure embedded in the nuclear envelope, consists of nucleoporins (NUPs). Its primary structural components include the cytoplasmic, inner pore, and nuclear rings, along with peripheral elements such as the nuclear basket and cytoplasmic filaments. The NPC's central channel is lined with NUPs containing Phe and Gly-rich repeats (FG-NUPs). This complex enables bidirectional nucleocytoplasmic transport, allowing small molecules to diffuse freely and facilitating major active transport pathways. These pathways include protein import into the nucleus, RNA and ribonucleoprotein (RNP) export, and the bidirectional movement of molecules involved in various cellular processes such as signaling, biogenesis, and turnover. Examples include SMAD signaling proteins, p53, and spliceosomal small nuclear RNP particles (snRNPs), which rely on transport-receptor-mediated import and export routes. The NPC also serves non-canonical functions, including transcription-coupled mRNA export linked to mRNP assembly, gene tethering to the

nuclear envelope via transcription export (TREX) complexes, and processes related to chromatin biology. These subcomplexes include Y-complexes (red), inner ring complex (blue), transmembrane NUPs (yellow), NUP62 complex (orange; NSP1 complex in yeast), cytoplasmic complexes (green), and nuclear basket complexes (purple). miRNA, micro RNA; rRNA, ribosomal RNA; tRNA, transfer RNA.

1.2.1 Roles of structural NUPs

Nups are categorized into scaffold Nups, FG-Nups and linker Nups (105, 106). Scaffold Nups comprise folded protein domains with structural functions, whereas FG-Nups, characterized by FG-repeats and intrinsically disordered domains, interact with the nucleocytoplasmic transport machinery (105). Linker Nups connect scaffold Nups with FG-Nups, maintaining the overall structure and function of the NPC (106). FG-Nups primarily constitute the permeability barrier within the central transport channel but also extend into the nucleoplasm and cytoplasm (107). FG-Nups contribute to scaffolding functions due to their structured domains and interaction motifs, indicating an overlap between scaffold Nups and FG-Nups (108).

A) FG-Nups and their function:

Nuclear transport receptors (NTRs), including importins and exportins of the karyopherin family, small GTPase RAN, and recycling elements NTF2 and CAS (109), are essential for active, energy-dependent transport (110). The classical import pathway exemplifies active nucleocytoplasmic transport, wherein importin-α and importin-β bind to the nuclear localization signals of cargo proteins, facilitating their passage through the NPC's central channel (110). RAN-GTP releases the cargo into the nucleoplasm, and the resulting complexes are exported and disassembled in the cytoplasm (111, 112). NTF2 re-imports RAN-GDP into the nucleoplasm. Similarly, exportin 1 (XPO1) mediates nuclear export by binding to cargo in a RAN-GTP-dependent manner and releasing it in the cytoplasm upon GTP hydrolysis (110, 113).

The NPC's central channel, bordered by FG-NUPs, facilitates bidirectional transport between the nucleus and cytoplasm (114). Recent studies demonstrate that FG-repeats of the NUP62 complex (NUP62, NUP58, NUP54) and NUP98 are located at the central channel's inner ring plane. The precise locations of other FG-NUPs are less well-defined; however, FG-NUPs' repeat domains transiently bind to NTRs, enabling passage through the NPC (114, 115). Small proteins (<30 kDa) diffuse freely through the channel, whereas larger proteins require NTRs, forming the basis of the gating function or permeability barrier of NPCs (see Figure 9).

B) Scaffold Nups:

The elucidation of the architecture of the NPC was a significant challenge for structural biologists due to its size and location within the double membrane of the nuclear envelope. However, it was soon discovered that the NPC is composed of smaller subcomplexes. Early biochemical research identified two such subcomplexes, the Y-complex and the inner ring complex, which are major components of the NPC scaffold (116). The Y-complex consists of seven conserved members, including Nup96, NUup160, Nup133, Nup85, Nup107, SEC13 homologue 1 (SEH1), and SEC13, which form a Y-shaped arrangement (117). In vertebrates, Nup43 and Nup37 also bind to the Y-complex, with Nup37 and ELYS occurring in *Schizosaccharomyces pombe* (118). The inner ring complex includes the scaffold Nups Nup205, Nup188, Nup155, Nup93, and Nup35, which bind to transmembrane proteins such as NDC1 and Nup98. The three members of the Nup62 complex, which are also classified as FG-Nups, contain a coiled-coil domain at their carboxyl termini that serves additional scaffolding functions (119). The core of the inner ring complex is iso-stoichiometric *in situ*, similar to the Y-complex (116). Although there are elevated levels of Nup155, Nup98, Nup62, and Nup93, these are because of the binding of additional copies of these proteins to the outer rings and connectors, highlighting the promiscuity of Nups with respect to their subcomplex association (120, 121).

C) Linker Nups:

Linker Nups are crucial in connecting modules within the NPC in human cells, contributing to its structure and function. These linker Nups have short sequences that facilitate supercomplex formation between NPC modules (122).

The versatile linker Nup in human cells is the conserved Nup98-96, the human homolog of yeast Nup145N. Nup98-96 has multiple binding sites for interacting with various NPC subcomplexes, including those with Nup205 (human homolog of yeast Nup192), Nup155 (human homolog of yeast Nup170), and Nup88 (human homolog of yeast Nup82). This enables Nup98-96 to connect multiple subcomplexes within the human NPC, serving as a key connector in NPC protomer assembly (122). The ability of linker Nups to bind multiple components highlights their importance in maintaining the structural integrity of human NPC.

Interestingly, NPC composition can vary among human cell types and tissues, suggesting different combinations of Nups, including linker Nups, to assemble NPCs with distinct properties and functions (123). This heterogeneity could contribute to tissue-specific roles in human organs and explain why mutations in certain Nups result in tissue-specific diseases.

In summary, linker Nups are essential connectors within the human NPC, facilitating super complex formation between modules. Their versatile binding capabilities, exemplified by Nup98-96, allow complex NPC assembly in human cells. The variability in linker Nups composition across human cell types may contribute to specialized NPC functions in tissues and organs, influencing cellular processes and disease susceptibility.

1.2.2 NPC functions

NPCs are essential multiprotein channels that span the nuclear envelope, regulating macromolecular traffic between the nucleus and cytoplasm (124, 125). While their primary function is nucleocytoplasmic transport, NPCs have been shown to play critical roles in chromatin organization, gene regulation, and DNA repair (104, 125, 126). These large macromolecular assemblies are composed of multiple copies of approximately 30 different proteins called Nups (104, 124). Interestingly, recent evidence suggests that NPC composition may vary among cell types and tissues, challenging the traditional view of NPCs as structures with ubiquitous composition (123). This heterogeneity in NPC composition could allow cells to assemble pores with specialized functions. Additionally, the central channel of NPCs exhibits significant structural diversity, supporting the idea that the cohesiveness of intrinsically disordered FG-Nups facilitates collective rearrangements with minimal energy cost (127). In conclusion, NPCs are dynamic hubs that integrate gene regulation and nuclear transport processes (125). Their functions extend beyond nuclear gatekeeping, influencing various aspects of nuclear organization and cellular physiology. The complex interplay between NPC structure, composition, and function highlights the need for further research to fully understand their roles in health and disease (96, 128). NPCs interact with chromatin and transcription factors, influencing gene expression patterns. Certain nucleoporins (e.g., NUP98) shuttle between the NPC and nucleoplasm to modulate transcriptional activity (129).

1.3 HIV-1 infection and host response

The host response to viral infections, particularly HIV-1, heavily relies on the type I interferon (IFN) system, which plays a crucial role in initiating and coordinating antiviral defenses (130, 131). Upon viral detection, cells produce IFNs that trigger a signaling cascade leading to the expression of hundreds of Interferons stimulated genes (ISGs) (see **Figure 1.8)**, which collectively establish an antiviral state (132). ISGs are a diverse group of genes induced by IFN signaling, encoding proteins with various antiviral functions. In the context of HIV-1 infection, several ISGs have been identified as key players in restricting viral replication. These include APOBEC3G, tetherin, SAMHD1, MX2, GBP5, and SLFN11 (133). Interestingly, the effectiveness of the IFN response against HIV-1 is not straightforward, as studies in animal models have shown both beneficial and detrimental effects of IFN signaling on viral replication and pathogenesis (133). Among the ISGs involved in HIV-1 restriction, MX2 (MX dynamin-like GTPase 2) has emerged as an important factor. MX2 has been shown to inhibit HIV-1 replication by targeting the early stages of the viral life cycle, specifically interfering with the nuclear import of the viral pre-integration complex (133-135). This highlights the significance of nuclear envelope-associated factors in the antiviral response. HIV-1, however, has evolved mechanisms to counteract the host's IFN response. The virus can downregulate certain ISGs to evade immune detection and promote its replication. One notable example is the viral protein Vpu, which antagonizes the antiviral activity of tetherin, an ISG that prevents viral particle release from infected cells (136, 137). Additionally, HIV-1 has been observed to manipulate nuclear envelope components, potentially interfering with the function of NPC-associated ISGs, although specific details on this mechanism are not very well studied (138) (139)In conclusion, the interplay between HIV-1 and the host IFN response, mediated by ISGs, is complex and multifaceted. While many ISGs exhibit potent antiviral activities, HIV-1 has developed countermeasures to subvert these defenses, highlighting the ongoing evolutionary arms race between host and pathogen.

1.3.1 Innate immune response

The early stage of HIV-1 infection is characterized by explosive viral replication, followed by a decline in viremia as innate immune responses, including type I interferons and NK cells, contribute to initial control before adaptive immunity is fully established (140)-. Dendritic cells'

recognition of viral components initiates the release of IFN-I and TNF-α, leading to the robust induction of additional cytokines and the inhibition of virus reproduction in infected cells (see **Figure 1.8)**. An array of immune cells, including phagocytes like macrophages and cytolytic cells like NK cells, respond to this cytokine cascade and participate in the destruction of infected cells and the capture of viral antigens for presentation to the adaptive immune system. The production of higher levels of IFNs by female dendritic cells may partly explain why women often have a lower viral set point than men. A strong cytotoxic T lymphocyte (CTL) response is associated with a low virus reactive response and a milder disease course, while end-stage disease is characterized by a rapid decline in anti-HIV-1 CTLs (141). Studies with SCID mice that have been reconstituted with human lymphoid cells suggest that adoptive transfer of human anti-HIV-1 CTLs can provide some protection against subsequent virus challenges. Collectively, these findings highlight the crucial role of CTLs in combating HIV-1 infection. Innate immunity is further discussed in the later sections.

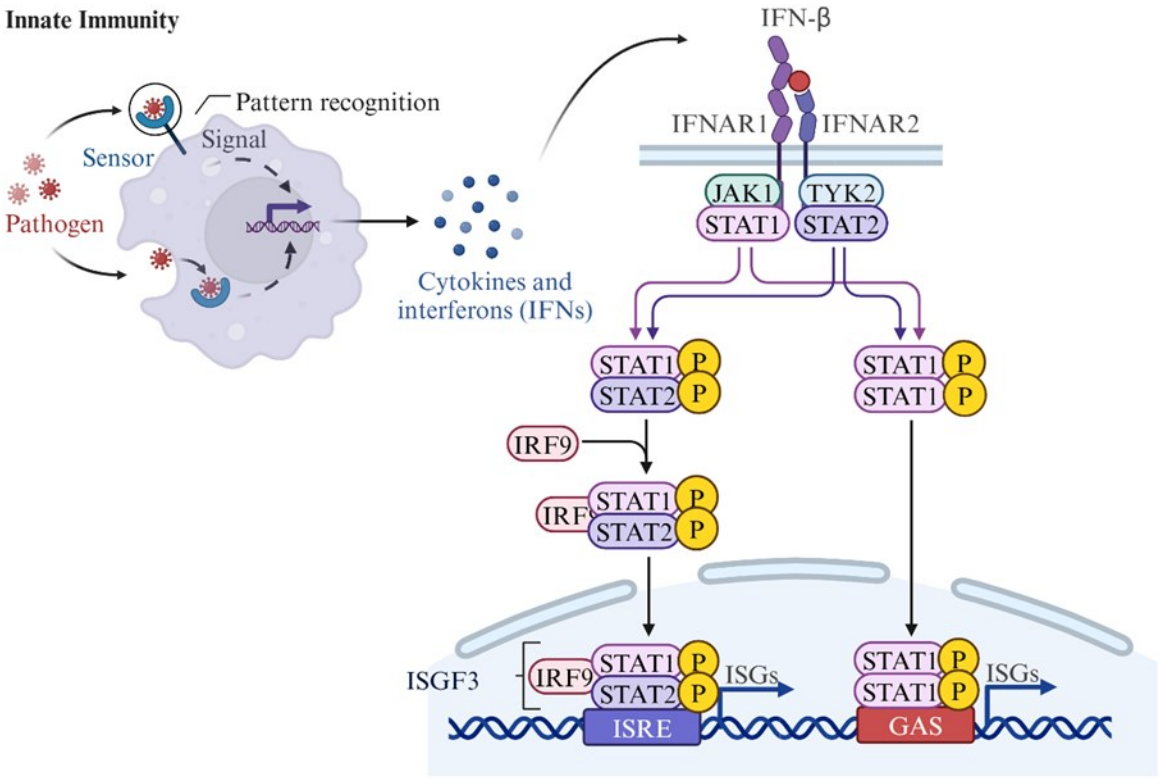

Figure 1.8: Innate immune response on viral infection and IFN-β stimulated gene expression. (created using biorender.com, inspired from (128)) Schematic representation of type I interferon (IFN-I, specifically IFN-β) stimulation and the production of interferon-stimulated genes (ISGs). The pathway involves the activation of Janus kinase 1 (JAK1) and the formation of the interferon-stimulated gene factor 3 (ISGF3) complex, comprising signal transducer and activator of transcription 1 (STAT1), STAT2, and interferon regulatory factor 9 (IRF9). The interaction of interferon-alpha/beta receptor subunits 1 and 2 (IFNAR1 and IFNAR2) with IFN-β initiates the signaling cascade. The ISGF3 complex binds to interferon-stimulated response elements (ISREs) in the genome, leading to ISG transcription. Additionally, gamma-activated sequence (GAS) elements are targeted by STAT1 homodimers.

The two human genes, MXA(MX1) and MXB (MX2) are also induced by IFN. Mx proteins reside in the cytoplasm, with MxA but not MxB blocking the reproduction of the influenza virus. MXA inhibits influenza virus and prevents the reproduction of vesicular stomatitis virus (VSV), measles virus, and other negative-strand RNA viruses. These human Mx proteins are related to the dynamin superfamily of GTPases, which regulate endocytosis and vesicle transport, but the connection between this property and their antiviral activities remains unknown.

1.3.2 Interferon stimulate gene (ISG)-MX2

MX2 is an innate immune protein that plays a crucial role in the host response to viral infections, including HIV-1. This section will explore the interaction between HIV-1 and MX2 and the potential use of MX2-based therapies for HIV-1 treatment.

MX2 structure:

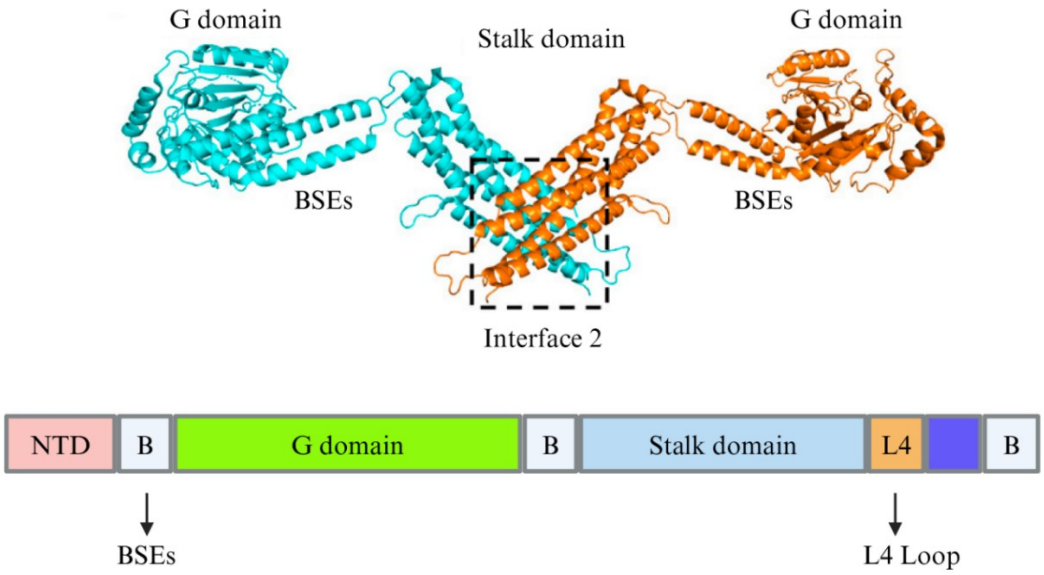

Figure 1.9: MX2 protein structure (adapted from (142) created with biorender.com) Crystal structure of the hMX2 monomer from (143) (PDB entry 4WHJ), in cartoon representation with one monomer in cyan and the other in orange. The dimerization interface (interface II) is highlighted (PDB entry 4WHJ). The lower part of this figure shows MX2 domain organization, indicating the amino-terminal domain (NTD), bundle signaling elements (B or BSEs), GTPase domain (G domain), stalk domain, and the L4 loop (L4) (142).

MX2, also known as MXB, is an essential interferon-induced GTPase that helps in curbing human immunodeficiency virus-1 (HIV-1) infection (144, 145). It operates after reverse transcription, particularly at the viral DNA nuclear import and/or integration stage into the host cell genome (144, 145). The HIV-1 capsid (CA) is a critical determinant of MX2 sensitivity, with complex interactions occurring between MX2, CA, Nups, and cyclophilin A (CypA) that influence viral infection outcomes. Direct interactions between CA and CypA impact MX2's antiviral activity and specificity. For instance, when CA-CypA interactions are abolished, such as through cyclosporine A treatment, MX2's antiviral effect is heightened (146). MX2's GTP hydrolysis plays a role in its antiviral activity, and abrogating this activity enhances antiviral activity when CA-CypA interactions are disrupted (146).

The antiviral activity of MX2 is dependent on its N-terminal region, particularly a triple arginine motif at residues 11-13 (144) (see **Figure 1.9)**. MX2 interacts with components of the NPC and nuclear import machinery, including NUP214 and transportin-1, which help position it at the nuclear envelope to restrict HIV-1 (144). MX2's antiviral activity involves other cellular factors

and mechanisms: 1. The N-terminal domain of MX2 is crucial for its anti-HIV-1 activity, with a single residue near the N-terminus capable of determining antiviral specificity (147). This domain likely interacts with the viral capsid or cellular cofactors. 2. MX2 appears to work in conjunction with other cellular factors, including members of the polymerase-associated factor 1 (PAF1) complex, the human silencing hub (HUSH) complex, and the regulation of nuclear pre-mRNA domain containing 2 (RPRD2) protein (148). These factors may cooperate with MX2 to impede viral replication. 3. Cyclophilins, particularly cyclophilin A (CypA), play a role in modulating MX2's antiviral activity. While CypA itself is not directly involved in MX2-mediated restriction, other Cyclosporine A-sensitive cyclophilins contribute to IFN-α-induced blocks that include MX2 (149).

Interestingly, while MX2 is effective against HIV-1, its closely related protein MX1 (MxA), which is known to inhibit various RNA/DNA viruses including the influenza A virus, does not affect HIV-1 (145). This distinction highlights the specific anti-HIV-1 activity of MX2. The antiviral activity of MX2 is dependent on its N-terminus, as demonstrated by the fact that adding the MX2 N-terminus to MX1 confers anti-HIV-1 activity to the chimeric protein (150). In terms of the relationship between MX2 and interferon-beta (IFN-β), it's important to note that MX2 is an ISG. While previous studies mentioned that MX2 inhibits the nuclear accumulation of viral cDNAs (145) there are no studies on the impact of MX2 on NPC, nuclear envelope, and HIV-1 capsid proteins at the nuclear envelope. This suggests that MX2 may interact with or affect the NPC in some way to prevent HIV-1 genetic material from entering the nucleus. Further research would be needed to elucidate the exact mechanism of this interaction. In conclusion, MX2 is an important ISG that specifically inhibits HIV-1 through interactions with the viral capsid and nuclear import machinery. However, its precise mechanism of action and relative contribution to overall interferon-mediated restriction of HIV-1 remain subjects of ongoing research and debate.

1.3.3 TRIM5α

TRIM5α is a potent antiviral protein that restricts infection by HIV-1 and other retroviruses (151). It acts early after viral entry, preventing the accumulation of reverse transcription products (152). TRIM5α recognizes and binds to the HIV-1 capsid, leading to premature disassembly of viral cores and blocking infection before reverse transcription can occur (153). It recognizes the

retrovirus capsid lattice through its B30.2 (PRY/SPRY) domain, inducing premature disassembly of the viral capsid and activating innate immune responses (151, 154). TRIM5α acts as a pattern recognition receptor specific for retroviral capsids and promotes innate immune signaling (154).

Interestingly, the restriction mechanism of TRIM5α involves multiple pathways. While proteasome inhibition allows reverse transcription to proceed, it does not fully rescue viral infectivity, suggesting that TRIM5α restricts HIV-1 through both proteasome-dependent and independent mechanisms (155, 156). Additionally, TRIM5α is degraded via autophagy in the absence of restriction-sensitive virus, but autophagic machinery is not required for its antiviral activity (156). In conclusion, TRIM5α plays a crucial role in innate immunity against HIV-1 by targeting the viral capsid and inducing its premature disassembly. The restriction process involves complex interactions with cellular pathways, including the proteasome and autophagy systems. Understanding these mechanisms could lead to novel therapeutic strategies for HIV/AIDS treatment and prevention (157).

1.4 HIV-1 capsid interaction with cellular proteins

HIV-1 proteins interact with the host nuclear envelope and NPC to facilitate viral entry into the nucleus. While various viral elements have been implicated in this process, recent evidence highlights the critical role of the HIV-1 capsid in mediating nuclear import (158). The capsid, composed of approximately 1,200 copies of the capsid protein, encases the viral genome and essential enzymes (159). The HIV-1 capsid interacts with numerous host factors to navigate the cytoplasm, traverse the NPC, and reach chromosomal integration sites (159). Notably, the capsid can bind to NPC proteins like Nup153 and Nup358, as well as other host factors such as transportin 3 and CPSF6, through a conserved Phe-Gly (FG) motif (158, 160). These interactions are crucial for productive infection, allowing the virus to overcome the size constraints of the NPC central channel, which is much smaller than the intact capsid (161, 162). Recent studies suggest that the HIV-1 capsid may remain largely intact during nuclear import, challenging the long-held view that uncoating precedes nuclear transport (159, 163). The capsid's elasticity appears to be a fundamental property enabling its passage through the NPC, with mutant capsids exhibiting reduced elasticity showing impaired nuclear entry (164). The exact mechanism of capsid translocation through the NPC remains under investigation, with some models proposing that the

capsid mimics cellular karyopherins to penetrate FG- Nup condensates (161). The capsid-host interactions during HIV-1 trafficking across cellular compartments are crucial for establishing productive infection (160). By maintaining its integrity until reaching the nuclear pore or even entering the nucleus, the capsid protects the viral genome from cytoplasmic defense mechanisms and ensures proper movement to the nucleus (163). Given the capsid's central role in multiple stages of HIV-1 replication, including nuclear entry and integration, it has emerged as a promising target for antiviral therapies. The recent approval of lenacapavir, a long-acting capsid-targeting inhibitor, underscores the clinical relevance of targeting the HIV-1 capsid (159, 165). Compared to conventional antiretroviral therapies that primarily target HIV-1 enzymes, capsid-centric approaches offer the potential to disrupt multiple stages of the viral life cycle, making them an attractive option for future drug development (165).

1.5 HIV-1 transmission and type of infection

1.5.1 HIV-1 Transmission

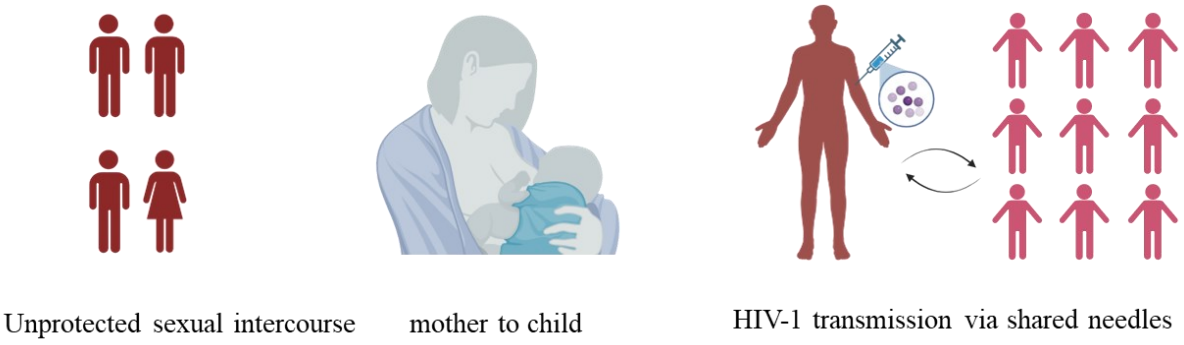

Figure 1.10: Routes of HIV-1 transmission among humans (created By Biorender.com) The figure illustrates main distinct modes of transmission: first is sexual intercourse, highlighting the exchange of bodily fluids (highest risk of infection); second is vertical transmission during labor, or breastfeeding; third is HIV-1 transmitted through shared needles among injection drug users as it facilitate blood to blood transmission. Each mode is depicted with corresponding visual representations.

Routes of transmission

HIV-1 is transmitted primarily through exposure to infected body fluids (**Figure 1.10)**. Unprotected sexual contact is the most common global route, with anal and vaginal intercourse posing the greatest risk due to mucosal vulnerability, while oral sex carries lower but measurable risk (166). Parenteral transmission occurs via sharing contaminated needles among people who inject drugs, unsafe medical injections, or transfusion of unscreened blood products (167). Transmission from mother to child can occur during delivery, or through breastfeeding (168), see **Figure 1.10**. Occupational exposure, particularly needlestick injuries among healthcare workers, represents another route (169), (170). Rarely, transfusions or transplants during the seronegative "window period" have transmitted HIV-1 (171). Other routes of transmission, such as non-sexual physical contact, exposure to saliva (unless there are cuts in the mouth) or urine, and exposure to blood-sucking insects, are relatively unimportant or non-existent. Fortunately, HIV-1 infectivity can be reduced by air-drying, heating, exposure to germicides, or exposure to pH extremes, which have helped to establish safety regulations to prevent transmission in public and healthcare settings based on epidemiological studies.

1.5.2 The course of infection

A) The acute phase

In the initial stage of infection, the activated lymphocytes produce a large number of virus particles, which can cause lymph nodes to swell and result in flu-like symptoms. These particles are released into the bloodstream and can be detected through cell culture infectivity or by screening for viral RNA or proteins. At this stage, there can be around 5 to 10^3 infectious particles or 1 to 10^7 viral RNA molecules per milliliter of plasma (172, 173). During this time many CD4+ T cells in the gut are destroyed, leading to the translocation of viral products into the blood that affects metabolic and digestive functions. A percentage of quiescent memory T cells in the gut-associated lymphoid tissue (GALT) can survive because replication-competent proviruses cannot be transcribed in these cells (174). These cells form a long-lived, latent viral reservoir. This reservoir can be activated by interaction with cognate antigens, leading to the transcription of the latent provirus (175). In the absence of antiviral treatments, progeny particles generated by these cells can start a new cycle of infection. Within a few weeks of infection, the peak of viremia is greatly reduced as the susceptible T cell population is depleted, and a cell-mediated immune

response is mounted (176). The number of CTLs increases before neutralizing antibodies can be detected, and the inflammatory response that occurs during primary infection stimulates the production of additional CD4+ T cells, helping to stem the depletion of this population. Consequently, the CD4+ T cell count returns to near normal levels, but these cells represent a new source of susceptible targets and their infection produces chronic immune stimulation.

B) The asymptomatic phase

By 3 to 4 months after infection, viremia typically decreases to low levels, with occasional virus particle bursts. This stage of infection, known as the virologic set point, predicts the rate of disease progression in an individual. The higher the set point, the faster the progression (177). During this period, CD4 T cell numbers decrease at a slow rate (178). Cytopathogenicity induced by the virus and apoptosis due to immune stimulation and inappropriate cytokine production appear to be the underlying reasons. In the protracted asymptomatic period, which can last for years, the CTL count remains slightly elevated, while virus reproduction continues at a low rate, mainly in the lymph nodes. In this phase of persistent infection, also known as clinical latency, only some infected cells in the lymph nodes may release virus particles. It is believed that antiviral CTLs suppress virus propagation during this stage, similar to acute infection. The number of these specific lymphocytes decreases as the stage progresses. During the asymptomatic phase, viral genetic diversity increases due to continuous, positive selection for mutants that can evade the host's immune responses.

C) The symptomatic phase and AIDS

The late stage of AIDS, when the infected individual experiences symptoms, is characterized by an increase in the number of virus particles and a decrease in CD4+ T cell count. Additionally, the total CTL count decreases, possibly due to a decline in specific HIV-targeting cells (179). In the lymph nodes, virus reproduction increases, leading to the destruction of lymphoid cells and normal lymphoid tissue architecture. The cause of this lymph node degeneration is unclear, but it may result from virus reproduction, chronic immune stimulation, or both. It is suggested that rapid lymphocyte population turnover and differentiation, induced by chronic antigenic stimulation, eventually leads to the loss of regenerative potential. In this stage, the virus population becomes relatively homogeneous and specific to the CXCr4 receptor, with properties associated with increased virulence, such as an expanded cellular host range, the ability to form syncytia, rapid

reproduction kinetics, and CD4+ T cell cytopathogenicity. Late-emerging viruses also appear to be less sensitive to neutralizing antibodies and more readily recognized by antibodies that enhance infectivity. In some cases, strains with enhanced neurotropism or increased pathogenicity for other organ systems emerge. These changes have sometimes been linked to specific mutations, such as in the viral envelope gene or a regulatory gene (e.g., tat).

1.6 HIV-1 drug targets and drugs

HIV treatment strategies have primarily targeted viral enzymes, with current antiretroviral therapies focusing on inhibiting reverse transcriptase, protease, and integrase (165) (see **Table 1.1)**. However, the emergence of drug-resistant viral strains has necessitated the development of new inhibitor classes, with the HIV capsid emerging as a particularly promising target (180). Capsid targeting is important because the capsid plays multiple critical roles throughout the viral life cycle, including intracellular trafficking, nuclear import, and integration site selection (165, 180). The capsid's interactions with host factors make it an attractive target for disrupting viral replication at multiple stages. Several capsid-targeting compounds have been developed, with lenacapavir (LEN, formerly GS-6207) and GS-CA1 being the most notable (180, 181). Lenacapavir has shown exceptional clinical success, becoming the first capsid inhibitor approved for medical use (182). GS-CA1, a precursor to lenacapavir, demonstrated remarkable potency and long-acting potential in animal models (181, 183). Both lenacapavir and GS-CA1 bind at the interface between capsid protein subunits, interfering with capsid nuclear import, HIV particle assembly, and ordered assembly (165). They exhibit picomolar antiviral potency against a broad array of HIV strains, including those resistant to existing antiretrovirals (181, 183).

Table 2.1: FDA-approved HIV medicines (184) (154): FDA-approved HIV medicines **(184, 185)**:

Drug Class	Generic Name (Other names and acronyms)	FDA Approval Date
Nucleoside Reverse Transcriptase Inhibitors (NRTIs): NRTIs block	abacavir (abacavir sulfate, ABC)	December 17, 1998
	emtricitabine (FTC)	July 2, 2003

reverse transcriptase, an enzyme HIV needs to make copies of itself.	lamivudine (3TC)	November 17, 1995
	tenofovir disoproxil fumarate (tenofovir DF, TDF)	October 26, 2001
	zidovudine (azidothymidine, AZT, ZDV)	March 19, 1987
Non-Nucleoside Reverse Transcriptase Inhibitors (NNRTIs): NNRTIs bind to and later alter reverse transcriptase, an enzyme HIV needs to make copies of itself.	doravirine (DOR)	August 30, 2018
	efavirenz (EFV)	September 17, 1998
	etravirine (ETR)	January 18, 2008
	Nevirapine	June 21, 1996
	(extended-release nevirapine, NVP)	March 25, 2011
	rilpivirine (rilpivirine hydrochloride, RPV)	May 20, 2011
Protease Inhibitors (PIs): PIs block HIV protease, an enzyme HIV needs to make copies of itself.	atazanavir (atazanavir sulfate, ATV)	June 20, 2003
	darunavir (darunavir ethanolate, DRV)	June 23, 2006
	fosamprenavir (fosamprenavir calcium, FOS-APV, FPV)	October 20, 2003
	Ritonavir	March 1, 1996
	tipranavir (TPV)	June 22, 2005
Fusion Inhibitors: Fusion inhibitors block HIV from entering the CD4 T lymphocytes (CD4 cells) of the immune system.	enfuvirtide (T-20)	March 13, 2003
CCR5 Antagonists: CCR5 antagonists block CCR5 coreceptors on the surface of certain immune cells that HIV needs to enter the cells.	Maraviroc	August 6, 2007
Integrase Strand Transfer Inhibitors (INSTIs): Integrase inhibitors block HIV integrase, an	cabotegravir (cabotegravir sodium, CAB)	January 22, 2021
	dolutegravir (dolutegravir sodium, DTG)	August 12, 2013 June 12, 2020

enzyme HIV needs to make copies of itself.	raltegravir (raltegravir potassium, RAL)	October 12, 2007, May 26, 2017
Attachment Inhibitors: Attachment inhibitors bind to the gp120 protein on the outer surface of HIV, preventing HIV from entering CD4 cells.	fostemsavir (fostemsavir tromethamine, FTR)	July 2, 2020
Post-Attachment Inhibitors: Post-attachment inhibitors block CD4 receptors on the surface of certain immune cells that HIV needs to enter the cells.	ibalizumab-uiyk (Hu5A8, IBA, Ibalizumab, TMB-355, TNX-355)	March 6, 2018
Capsid Inhibitors: Capsid inhibitors interfere with the HIV capsid, a protein shell that protects HIV's genetic material and enzymes needed for replication.	lenacapavir (GS-6207, GS-HIV, GS-CA2, GS-CA1)	December 22, 2022
Pharmacokinetic Enhancers: Pharmacokinetic enhancers are used in HIV treatment to increase the effectiveness of an HIV medicine included in an HIV treatment regimen.	cobicistat (COBI, c)	September 24, 2014
Combination HIV Medicines: Combination HIV medicines contain two or more HIV medicines from one or more drug classes.	abacavir and lamivudine (abacavir sulfate / lamivudine, ABC / 3TC)	August 2, 2004
	abacavir, dolutegravir, and lamivudine (abacavir sulfate / dolutegravir sodium / lamivudine, ABC / DTG / 3TC)	August 22, 2014, March 30, 2022
	abacavir, lamivudine, and zidovudine (abacavir sulfate / lamivudine / zidovudine, ABC / 3TC / ZDV)	November 14, 2000

	atazanavir and cobicistat (atazanavir sulfate / cobicistat, ATV / COBI)	January 29, 2015
	bictegravir, emtricitabine, and tenofovir alafenamide (bictegravir sodium / emtricitabine / tenofovir alafenamide fumarate, BIC / FTC / TAF)	February 7, 2018
	cabotegravir and rilpivirine (CAB and RPV, CAB plus RPV, Cabenuva kit, cabotegravir extended-release injectable suspension and rilpivirine extended-release injectable suspension)	January 22, 2021
	darunavir and cobicistat (darunavir ethanolate/cobicistat, DRV / COBI)	January 29, 2015
	darunavir, cobicistat, emtricitabine, and tenofovir alafenamide (darunavir ethanolate / cobicistat / emtricitabine / tenofovir AF, darunavir ethanolate / cobicistat / emtricitabine / tenofovir alafenamide, darunavir / cobicistat / emtricitabine / tenofovir AF, darunavir / cobicistat / emtricitabine / tenofovir alafenamide fumarate, DRV / COBI / FTC / TAF)	July 17, 2018
	dolutegravir and lamivudine (dolutegravir sodium / lamivudine, DTG / 3TC)	April 8, 2019
	dolutegravir and rilpivirine (dolutegravir sodium / rilpivirine hydrochloride, DTG / RPV)	November 21, 2017
	doravirine, lamivudine, and tenofovir disoproxil fumarate (doravirine / lamivudine / TDF, doravirine / lamivudine / tenofovir DF, DOR / 3TC / TDF)	August 30, 2018
	efavirenz, emtricitabine, and tenofovir disoproxil fumarate (efavirenz / emtricitabine / tenofovir DF, EFV / FTC / TDF)	July 12, 2006
	efavirenz, lamivudine, and tenofovir disoproxil fumarate (EFV / 3TC / TDF)	March 22, 2018
	efavirenz, lamivudine, and tenofovir disoproxil fumarate (EFV / 3TC / TDF)	February 5, 2018
	elvitegravir, cobicistat, emtricitabine, and tenofovir alafenamide (elvitegravir / cobicistat / emtricitabine /	November 5, 2015

	tenofovir alafenamide fumarate, EVG / COBI / FTC / TAF)	
	elvitegravir, cobicistat, emtricitabine, and tenofovir disoproxil fumarate (QUAD, EVG / COBI / FTC / TDF)	August 27, 2012
	emtricitabine, rilpivirine, and tenofovir alafenamide (emtricitabine / rilpivirine / tenofovir AF, emtricitabine / rilpivirine / tenofovir alafenamide fumarate, emtricitabine / rilpivirine hydrochloride / tenofovir AF, emtricitabine / rilpivirine hydrochloride / tenofovir alafenamide, emtricitabine / rilpivirine hydrochloride / tenofovir alafenamide fumarate, FTC / RPV / TAF)	March 1, 2016
	emtricitabine, rilpivirine, and tenofovir disoproxil fumarate (emtricitabine / rilpivirine hydrochloride / tenofovir disoproxil fumarate, emtricitabine / rilpivirine / tenofovir, FTC / RPV / TDF)	August 10, 2011
	emtricitabine and tenofovir alafenamide (emtricitabine / tenofovir AF, emtricitabine / tenofovir alafenamide fumarate, FTC / TAF)	April 4, 2016
	emtricitabine and tenofovir disoproxil fumarate (emtricitabine / tenofovir DF, FTC / TDF)	August 2, 2004
	lamivudine and tenofovir disoproxil fumarate (3TC / TDF)	February 28, 2018
	lamivudine and zidovudine (3TC / ZDV)	September 27, 1997
	lopinavir and ritonavir (ritonavir-boosted lopinavir, LPV/r, LPV / RTV)	September 15, 2000

Following the discovery of HIV-1 in 1983, the first anti-HIV-1 drug, ZDV, was developed in 1987, followed by the development of approximately 30 additional drugs over the next thirty years. These drugs have been classified into different categories according to their target (see **Figure 1.11 and Table 3.1)**:

1. Nucleoside Reverse Transcriptase Inhibitors (NRTIs): NRTIs block reverse transcriptase, the viral enzyme that copies the viral RNA into DNA.
2. Non-Nucleoside Reverse Transcriptase Inhibitors (NNRTIs): NNRTIs bind to and later alter reverse transcriptase.
3. Protease Inhibitors (PIs): PIs block HIV protease, the viral enzyme that processes viral polyproteins to mature products
4. Fusion Inhibitors: Fusion inhibitors block HIV from entering the CD4 T lymphocytes (CD4 cells) of the immune system.
5. Integrase Strand Transfer Inhibitors (INSTIs): Integrase inhibitors block HIV integrase, the enzyme that integrates HIV DNA into host DNA.
6. Attachment Inhibitors: Attachment inhibitors bind to the gp120 protein on the outer surface of HIV, preventing HIV from entering CD4 cells.
7. Capsid Inhibitors: Capsid inhibitors interfere with the HIV capsid, a protein shell that protects HIV's genetic material and enzymes needed for replication.

Despite continuous medication, patients infected with HIV-1 cannot be fully cured and must take medication for the rest of their lives. This leads to a situation in which HIV-1 is constantly exposed to drugs and develops resistance mutations to escape inhibition (186, 187). Consequently, new strains of the virus that are resistant to drugs emerge (187, 188). To combat HIV-1's resistance, researchers have developed various therapeutic targets and drugs since the development of NRTIs. In the mid-1990s, PIs such as atazanavir and NNRTIs such as nevirapine were developed to inhibit viral mutation and overcome the high frequency of resistance development and cross-resistance of NRTIs (189, 190). With more than two types of therapeutic targets developed, cART, which prescribes more than three types of drugs targeting different aspects of the virus, has become the standard treatment for HIV/AIDS (191). However, the virus still poses a problem due to continuous drug exposure, leading to the development of multiple drug resistance. In the 2000s, researchers have been working to find new therapeutic targets to overcome multi-drug resistance. Enfuvirtide and maraviroc, developed in 2003 and 2007 respectively, target different stages of the HIV-1 life cycle (192-194). However, these drugs have also induced resistance, driving the need for more potent anti-HIV-1 therapies. The integrase enzyme, which incorporates viral nucleic acid

into the host chromosome, has emerged as a promising therapeutic target (195). Raltegravir (RAL) was the first integrase inhibitor to be developed, paving the way for subsequent agents such as dolutegravir (DTG), elvitegravir (EVG), bictegravir (BIC), and cabotegravir (CAB), which serve as advanced therapeutic options (196, 197). The development of long-term integrase inhibitor-based drugs has reduced the burden of daily drug administration. Additionally, the humanized antibody IBA was successfully developed, offering a new type of therapeutic option (198). Although antiretroviral drugs have been continuously developed, eradicating the latent viral reservoir is essential for a cure. A latent viral reservoir is a group of long-living cells, mainly resting memory $CD4^+$ T cells, that contain HIV-1 DNA in a silent state. These cells do not normally produce the virus but can become active again and start making the virus. This makes it hard to completely get rid of HIV-1, even with strong antiretroviral treatment. However, specific markers for latent viral reservoirs have not yet been identified, and the development of new drug-resistant strains remains a concern. Therefore, new therapeutic targets and complete cure technologies are needed to address these challenges and ultimately defeat HIV-1.

1.6.1 Challenges in HIV-1 treatment

Persistence and Latency

Eradicating HIV from an infected individual is a complex challenge. The reservoir of long-lived, latently infected cells is established early in the infection and can be replenished during short bursts of viremia (199). In some cases, these cells can also be expanded by provirus-induced cell proliferation. Despite early attempts to eliminate the reservoir by intensifying drug therapy, some of these cells may reside in drug-inaccessible sanctuaries, such as the brain. Latently infected cells are derived from infected quiescent CD4+ memory or activated T cells that survive infection long enough to revert to the resting memory state (199). A variety of mechanisms that inhibit proviral gene transcription in such cells have been described, including epigenetic suppression and deficiency of essential host transcriptional regulators, such as nuclear Nf-κB (199, 200). The "shock and kill" treatment strategy aims to induce provirus expression in latently infected cells while preventing virus infection of new cells with antiviral drugs and/or neutralizing antibodies (201). Although some increase in virus production could be detected after treatment, the size of the latent reservoir did not decrease (200, 202). Research in this area continues with the expectation

that a better understanding of the cell types that comprise the latent reservoir and more detailed knowledge of their biology will lead to more effective methods for their activation and elimination. Recently developed drugs: 1) Doravirine (DOR) is a next-generation NNRTI approved by the US FDA in August 2018 for treating multi-drug-resistant HIV-1 with 3TC and TDF (Delstrigo) (203, 204). It rarely interacts with other anti-HIV-1 drugs, has lower LDL levels and minimal CNS side effects. FDA approval is monitored based on an ongoing study. 2) Fostemsavir (FTR) metabolizes to temsavir (TMR), binding to gp120 of HIV-1 and blocking virus: receptor CCR5 or CXCR4 (205). Approved by the US FDA in March 2018 for treating multi-drug-resistant HIV-1, it's administered intravenously every 14 days (206). 3) Islatravir is being developed as a nucleoside reverse transcriptase translocation inhibitor for HIV-1 prevention with multiple mechanisms. It has high potency, long plasma half-life, and is in phase 3 trials for HIV-1 treatment and Pre-Exposure Prophylaxis (PrEP) using a two-drug fixed-dose combination of DOR and islatravir (207). PrEP is a preventive medical strategy involving the use of antiretroviral drugs by HIV-negative individuals to reduce their risk of acquiring HIV infection 4) Lenacapavir (GS-6207) interferes with HIV-1 capsid protein by binding to a conserved interface between capsid monomers, blocking interaction with cofactors like Nup153 and CPSF6 necessary for viral replication (208). CPSF6 is a host RNA-processing protein that also binds to the HIV-1 capsid, influencing nuclear import and integration site selection (209). Research continues to discover novel substances by screening compound libraries, while pharmaceuticalization studies aim to develop these into antiretroviral drugs.

Amongst the recently developed drugs, GS-CA1 is the drug of our interest. The following section will discuss the GS-CA1 drug’s mode of action and its limitations.

1.6.2 GS-CA1 and other drugs

Capsid inhibitors are a promising class of antiviral agents that target the HIV-1 capsid protein, such as PF74. PF74 is a small-molecule capsid inhibitor that binds the HIV-1 capsid, disrupting nuclear entry and uncoating (210). It targets host factor interfaces (binds to the same pocket in the capsid as cleavage and polyadenylation specificity factor 6 (CPSF6)), making it a valuable tool for mechanistic and therapeutic studies. This section will delve into the mechanism of action of GS-CA1, including its effects on HIV-1 replication and potential targets for antiviral therapy.

Mechanism of action of GS-CA1:

GS-CA1 and Lenacapavir (GS-6207) represent a novel class of antiviral drugs that target the HIV-1 capsid and were discovered by Gilead Sciences (211, 212) (see **Figure 1.11, Figure 1.12)**. GS-CA1 and Lenacapavir have antiviral activity at nanomolar and picomolar ranges, respectively ((213, 214). Structurally, GS-CA1 is an analog of Lenacapavir and both share a polyphenyl core and a linker region similar to PF74, a well-known capsid binder (213, 214) see **Figure 1.13**. By binding to a conserved interface on the HIV-1 capsid protein, GS-CA1 seems to inhibits several critical steps in the viral life cycle, including capsid assembly, nuclear entry, and virus assembly and release (211, 213-215). In preclinical studies, GS-CA1 demonstrated high efficacy in humanized mouse models of HIV-1 infection (183). Similarly, Lenacapavir has shown promising results against multidrug-resistant HIV strains and offers a long-acting formulation that allows for subcutaneous administration every six months (212, 214, 216).

Both GS-CA1 and PF74 bind to overlapping amino acids on the HIV-1 capsid (211). However, their mechanisms of action diverge significantly. PF74 accelerates the uncoating of the HIV-1 core, mimicking the activity of rhesus TRIM5α, and inhibits nuclear entry (217). In contrast, GS-CA1 seems to stabilizes the viral core during infection, allowing normal nuclear entry and reverse transcription to proceed. This stabilization suggests GS-CA1 induces a conformational change in the capsid that prevents premature uncoating(218).

GS-CA1 and PF74 inhibit HIV-1 infection in primary CD4+ T cells even in the absence of CPSF6. They both block the interaction between CPSF6 and the HIV-1 core. However, their mechanisms are different: PF74's antiviral activity is influenced by its ability to compete with CPSF6 for capsid binding and can disrupt CPSF6 complexes in nuclear speckles. In contrast, GS-CA1 act independently of CPSF6 and does not disaggregate preformed CPSF6 complexes, indicating a distinct mechanism of action.

Lenacapavir, while structurally related to GS-CA1, exhibits a slightly different binding profile. It overlaps with the benzyl group of F321 in CPSF6 and F1417 in Nup153, disrupting interactions critical for viral uncoating and nuclear import (219, 220). Crystal structures reveal that six

Lenacapavir molecules bind to each capsid hexamer, forming extensive hydrophobic, cation-π, and hydrogen bond interactions (220).

GS-CA1 and Lenacapavir both primarily act by hyperstabilizing the capsid lattice, leading to a loss of dissemble of core, a key step in HIV replication. Lenacapavir's activity remains unaffected by Gag cleavage site mutations or resistance to other antiretroviral classes, and it also alters intracellular trafficking and HIV DNA integration patterns (213)

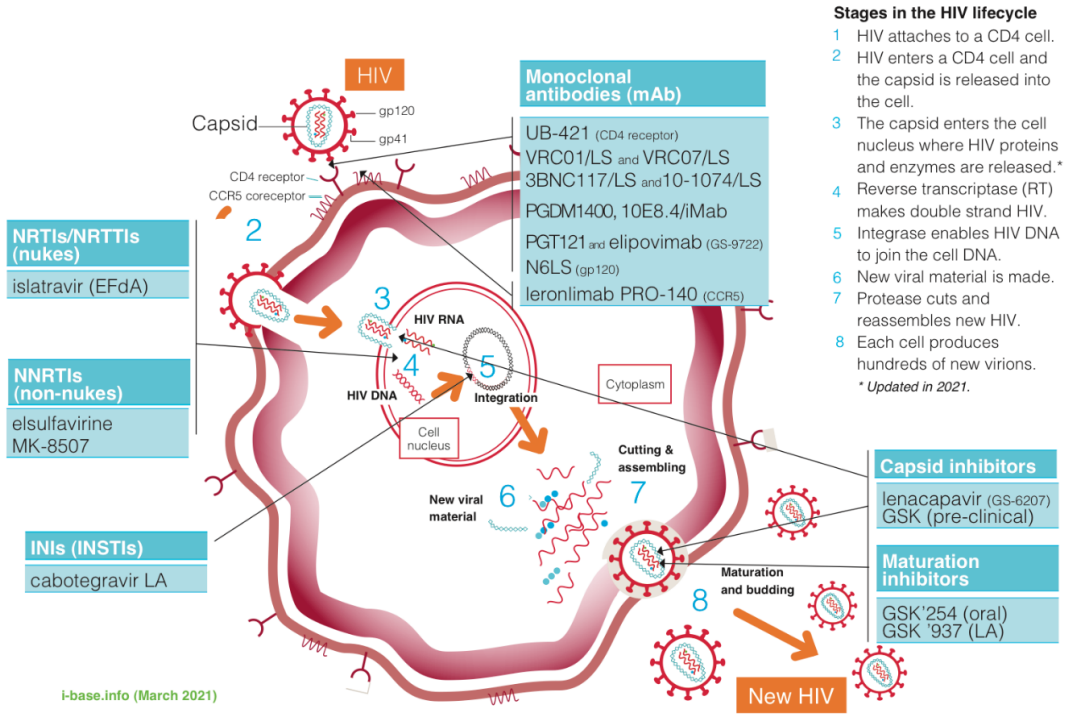

Figure 1.11: Prominent classes of HIV-1 drugs. Different antiviral drugs and along with their mechanisms of action For example Cabotegravir LA is an integration inhibitor (INI), and lenacapavir is a capsid inhibitor. Key: INSTI: integrase strand transfer inhibitor; LA: long-acting; mAb: monoclonal antibody; NRTI: nucleoside/tide reverse transcriptase inhibitor; NNRTI: non-nucleoside reverse transcriptase inhibitor. Adapted from (221, 222)

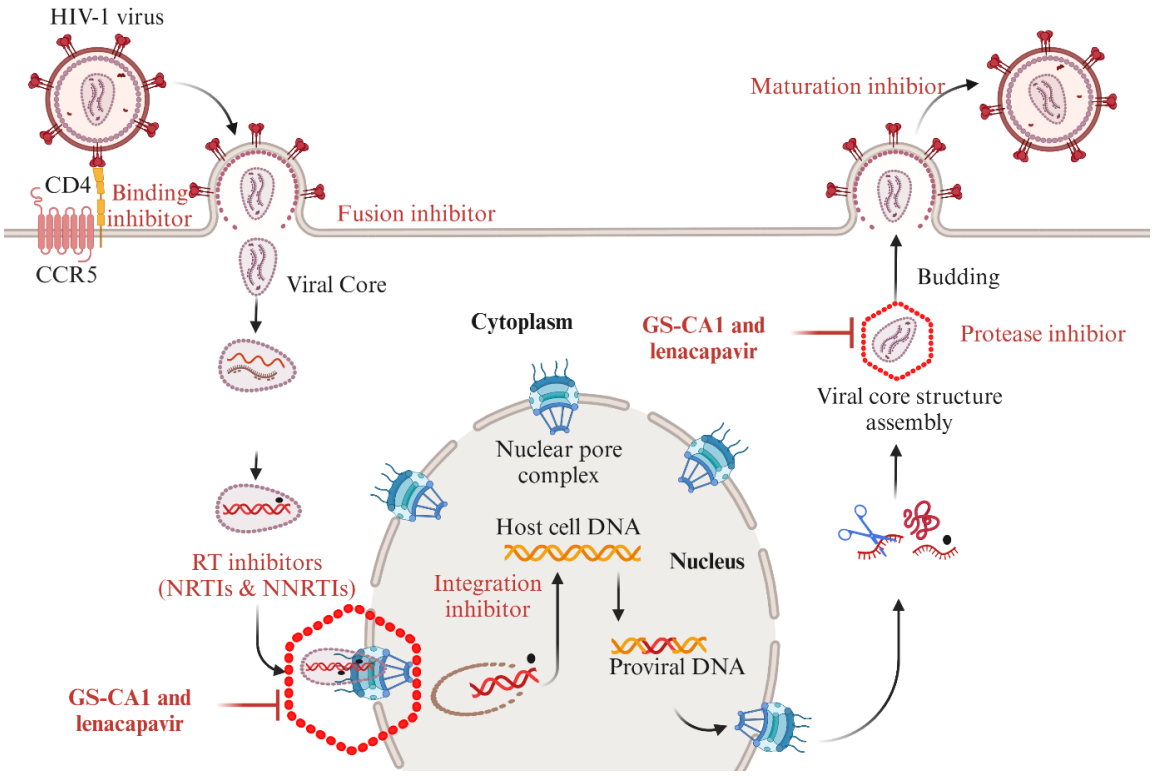

Figure 1.12: GS-CA1 mechanism of action. (created with BioRender.com) Schematic representation of the mechanism of action of the capsid inhibitor GS-CA1. The figure highlights the HIV-1 core at the nuclear pore, marked within a red hexagon, demonstrating how GS-CA1 inhibits core nuclear transport (inspired by (223)).

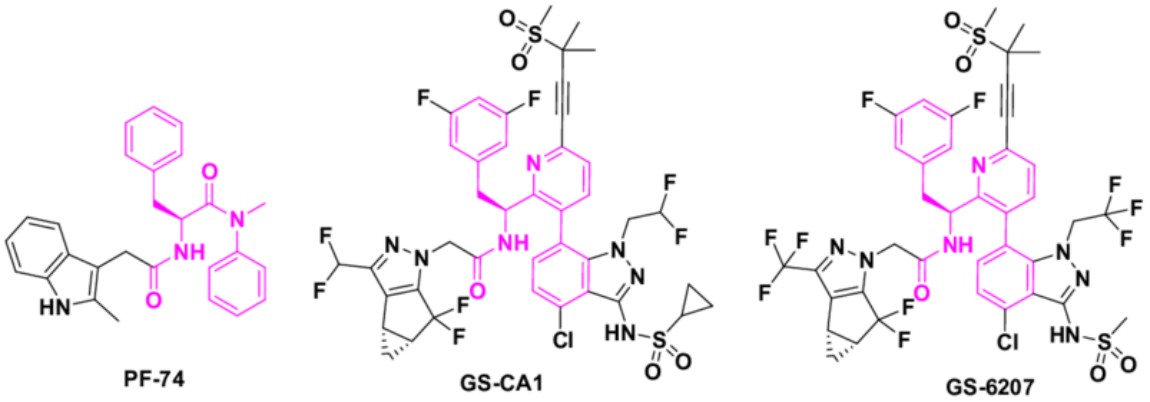

Figure 1.13: Chemical structure of capsid inhibitors. Chemical structures of reported representative HIV-1 CA inhibitors. Polyphenyl core moieties in structures of PF74, GS-CA1 and GS-6207 compounds are shown in magenta (224).

This mechanism aligns closely with GS-CA1, challenging earlier views that the two act through distinct pathways. Lenacapavir's formulation allows for oral administration daily or weekly, and subcutaneous dosing every six months (214), offering a significant advantage over conventional daily regimens (226). Its biannual subcutaneous schedule is a notable therapeutic innovation (212).

Given the mechanistic overlap, our study investigates GS-CA1's impact on early HIV-1 replication, particularly nuclear entry. By examining its interaction with nuclear envelope proteins and viral components, we aim to clarify GS-CA1's inhibitory role and provide new insights into capsid-targeting strategies.

The precise mechanisms by which these drugs affect nuclear envelope interactions and NPC traversal are not fully understood. Recent research has shown that the HIV-1 core enters the nucleus prior to capsid disassembly, challenging previous assumptions about uncoating (159, 164). The elasticity of the HIV-1 core appears to be crucial for nuclear entry, with capsid-targeting compounds like lenacapavir reducing core elasticity and blocking HIV-1 nuclear entry at concentrations that preserve interactions between the viral core and the nuclear envelope (164). Studying the effects of GS-CA1 and lenacapavir on HIV-1 interaction with nuclear envelopes/NPCs interactions is important to elucidate their full antiviral mechanisms and potentially inform the development of even more effective capsid inhibitors. Additionally, investigating the interplay between these drugs and host factors like interferon (IFN) could provide insights into how the immune response might modulate the efficacy of capsid-targeting therapies in vivo.

1.7 Problem statement

HIV-1 nuclear entry is a critical step in the viral life cycle, enabling integration of the viral genome into host chromatin. This process requires traversal of the nuclear pore complex (NPC), yet the molecular mechanisms regulating capsid transit through the NPC remain poorly understood. While antiretroviral therapy (ART) has significantly improved patient outcomes, it

does not target early nuclear events and cannot eradicate latent reservoirs. Thus, understanding the earliest stages of HIV-1 infection, particularly nuclear entry, may reveal new therapeutic opportunities.

Recent evidence challenges the long-standing assumption that HIV-1 uncoating precedes nuclear import. Instead, intact viral cores have been observed inside the nucleus, suggesting that capsid elasticity is essential for NPC traversal (159, 163). Capsid-targeting drugs such as GS-CA1 and lenacapavir reduce core flexibility and block nuclear entry, even at concentrations that preserve capsid–nuclear envelope interactions. However, the precise mechanisms by which these compounds interfere with HIV-1 passage through the NPC remain unclear.

In parallel, host immune responses, especially interferon-β (IFN-β), activate interferon-stimulated genes (ISGs) that may restrict HIV-1 at the nuclear envelope. MX2, a key ISG, has been implicated in capsid retention at the NPC, but its spatial and mechanistic role remains unresolved. Whether host-induced restriction and drug-induced inhibition converge at the NPC is a major unanswered question.

This thesis investigates how HIV-1 capsid localization at the nuclear periphery is modulated by host immune factors and capsid inhibitors. By focusing on nuclear membrane-enriched fractions, we aim to determine whether the NPC serves as a regulatory checkpoint for both innate restriction and pharmacological blockade.

1.8 Hypothesis

Recent findings suggest that the nuclear pore complex (NPC) is not merely a passive conduit for HIV-1 nuclear entry but may also serve as a regulatory site where host immune factors and pharmacologic agents exert antiviral effects (164). The intact HIV-1 core can traverse the NPC prior to uncoating, and capsid elasticity appears to be essential for this process. Host responses such as interferon-β (IFN-β) and capsid-targeting drugs like GS-CA1 may act directly at the NPC to restrict viral entry. For this, we hypothesize that:

1. IFN-β blocks HIV-1 nuclear entry by promoting capsid retention at the NPC via activation of interferon-stimulated genes (ISGs), particularly MX2.

2. The capsid inhibitor GS-CA1 prevents HIV-1 nuclear entry by stabilizing the capsid and interfering with NPC traversal.

These hypotheses aim to test whether the NPC functions as a dual interface, facilitating viral nuclear import while simultaneously serving as a platform for host-mediated restriction and drug action.

Objectives

HIV-1 entry triggers the intrinsic innate response through the upregulation of IFN-β, which activates downstream genes known as ISGs. Previous studies suggest that ISGs play a role in limiting further infection. However, it remains unclear whether ISGs target the NPC to block HIV-1 nuclear entry (**Hypothesis 1**). To investigate this, the following objectives were proposed for Chapter 2:

1) Investigate the impact of IFN-β on HIV-1 capsid peptide distribution at nuclear membranes
2) Analyze the role of MX2, in HIV-1 capsid peptide accumulation at nuclear membranes

GS-CA1 is a drug that binds to the HIV-1 capsid core, preventing its uncoating and the release of the HIV-1 genome. However, it remains unclear whether GS-CA1 targets the HIV-1 capsid at the NPC (**Hypothesis 2**). Additionally, it is unknown whether the host's natural response via IFN-β differs from the synthetic drug GS-CA1 in blocking HIV-1 nuclear entry. To explore this, the following objectives were outlined for Chapter 3:

1) Investigate the effect of GS-CA1 on HIV-1 capsid accumulation in nuclear membrane-enriched samples.
2) Compare the mechanisms of action of IFN-β and GS-CA1 on the HIV-1 capsid at the NPC.

Thus, this thesis aims to provide a comprehensive understanding of HIV-1, focusing on the early stages of its life cycle and the mechanisms by which both host immune responses and synthetic drugs interact with the NPC. Together, these objectives aim to elucidate the NPC's dual role as both a gateway for HIV-1 nuclear entry and a platform for host-mediated antiviral defense. This mechanistic insight may inform the development of synergistic strategies to block HIV-1 at the earliest stages of infection. The insights gained from this research may pave the way for developing synergistic treatment strategies to more effectively combat HIV-1 infection.

Chapter 2
Manuscript Project-1

We hypothesized that NPCs play a role in the innate immune response to HIV-1 infection and/or that HIV-1 modulates nuclear pore composition.

To investigate these hypotheses, we employed an unbiased proteomic approach to assess nuclear pore composition during the early stages of HIV-1 infection and following IFN-β treatment. For this, we have 2 objectives:

1) Investigate the impact of IFN-β on HIV-1 capsid peptide distribution in nuclear membrane-enriched samples.
2) Analyze the role of MX2, an ISG, in HIV-1 capsid peptide accumulation in nuclear membrane-enriched samples.

MX2 knockdown in the context of TRIM5α: To specifically assess MX2's role in HIV-1 nuclear restriction, we performed siRNA-mediated knockdown of both MX2 and TRIM5α. TRIM5α is a well-characterized capsid-targeting restriction factor that acts upstream of MX2, interfering with core stability in the cytoplasm. Its presence could confound the interpretation of MX2-dependent effects at the nuclear envelope. By depleting TRIM5α, we ensured that observed capsid retention at the NPC could be attributed to MX2 activity.

Elevated expression of both TRIM5α and MX2 has been reported in elite controllers, individuals who naturally suppress HIV-1 without therapy, suggesting their complementary roles in viral restriction (227).

Methodology

Cell culture. THP-1 monocytic cells, shMX2shTRIM5a THP-1 and shLuc shTRIM5 THP-1 double knockdown were cultured in Roswell Park Memorial Institute (RPMI) 1640 medium (HyClone, Thermo Scientific, USA) with 10% fetal bovine serum (FBS, HyClone) and antibiotics (penicillin and streptomycin, HyClone). Crandell-Rees Feline Kidney (CRFK) cells and Human embryonic kidney cells 293T (HEK293T) were maintained in Dulbecco's Modified Eagle Medium (DMEM) (HyClone) supplemented with10%FBS and penicillin/streptomycin (HyClone). Double knockdown cells were generated by transducing THP-1 cells with lentiviral vectors encoding

shMX2, shTRIM5α, and control shLUC constructs. The shMX2 and shTRIM5α plasmids were previously described in (227). site the paper describing the plasmids)Cells transduced with shMX2 and shLUC (hygromycin-resistant) were selected using hygromycin at 200 µg/ml, while those expressing shTRIM5α and shLUC (puromycin-resistant) were selected with puromycin at 1 µg/ml.

HIV-1 vector production and titration. To produce the GFP-expressing HIV-1 vector $NL43_{GFP}$, HEK293T cells were transfected with 10 µg of $pNL43_{GFPDEnvDNef}$ and 5 µg of pMD2G using polyethylenimine (PEI, polysciences, Niles, IL) for 16 h, after which supernatants were replaced with fresh medium (228). Similarly, 293T cells were transfected with pAHMshMX2 along with deltaR8.9 and pMD2G to produce a shMX2 viral vector (similar to shLUc and shTRIM5a). Supernatants were collected 24 h and 48 h later. Cell debris were removed by low-speed centrifugation (3,000 rpm, 10 min at room temperature) followed by filtration through 0.45 µm filters (MilliporeSigma Durapore PVDF, Thermo Fisher Scientific). Virus titrations were performed by infecting CRFK cells with serial dilutions of vector preparations. CRFK cells were then fixed in PBS containing 4% formaldehyde and the percentage of infected cells was assessed by flow cytometry using a Beckman Coulter FC500 instrument. Viral titers were determined following analysis using the FCS Express 6 software (De Novo software).

Infections and nuclear envelope purification. 13-20 $x10^6$ THP-1 cells and knockdown cells (shMX2 shTRIM5a, shLUC shTRIM5a) cultured in flasks were treated or not with IFN-b (10 ng/ml; PeproTech, Rocky Hill, NJ) for 12 h and then infected or not with $NL43_{GFP}$ (MOI = 1) for 12 h. Nuclear envelopes were extracted using the Minute™ Nuclear Envelope Protein Extraction Kit (Invent Biotechnologies, Plymouth, MN). Whole-cell lysates, cytoplasmic extracts and nuclear extracts prepared using the same kit were also included in purification validation experiments.

Western blotting. Protein concentration in the nuclear envelope extracts was determined using the Bio-Rad Protein Assay kit prior to SDS-SDS-polyacrylamide gel electrophoresis and transfer to polyvinylidene difluoride (PVDF) or nitrocellulose membranes. Blotted proteins were analysed using the MAb414 mouse monoclonal antibody (BioLegend, San Diego, CA), which recognizes phenylalanine-glycine (FG) repeats in some NPC proteins (1:2,000 dilution) followed by hybridization with an HRP-conjugated anti-mouse secondary antibody (Cell Signaling

Technology, Whitby, Ontario). Detection of glyceraldehyde phosphate dehydrogenase (GAPDH) with the 9484-mouse monoclonal antibody (Abcam, Toronto, ON) was used as a marker for cytosolic proteins (229, 230). Blots were revealed using the Thermo Scientific SuperSignal West Femto substrate, and images were recorded using the Bio-Rad ImageLab system. MX2 knockdown samples were analysed using anti-MX2 (MX2 Antibody, Novus biologicals, NBP1-81018, 1:500 dilution) and HRP Anti-beta Actin antibody [mAbcam 8226 at 1:50000 dilution as a control protein. Anti-Rabbit antibody (Molecular Probes) at 1:2000 dilution was used to detect MX2 bands. Among the replicates of knockdown cell's nuclear envelope enriched extracts, lamin B1 (ab133741) Anti-Lamin B1 antibody, dilution 1:5000) was used as a control. Blots were revealed using the Clarity Western ECL Substrate, Bio-Rad, and images were recorded using the Bio-Rad ImageLab system.

Mass spectrometry: Nuclear envelope extracts were subjected to label-free mass spectrometry. Samples were analysed following trypsinization by nano-LC/MSMS using a Dionex UltiMate 3000 nanoRSLC chromatography system (Thermo Fisher Scientific) attached to a nanoelectrospray ion source containing an Orbitrap Fusion mass spectrometer (Thermo Fisher Scientific, San Jose, CA, USA). Fragmented peptides were collected in loading solvent (2% acetonitrile, 0.05% TFA) on a 5 mm x 300 μm C18 pepmap cartridge pre-column (Thermo Fisher Scientific) at the rate of 20 uL/min for 5 min. The pre-column was replaced with the Pepmap Acclaim column (ThermoFisher). Peptides from this column were eluted in 90 min at 300 nL/min with a 5-40% linear gradient solvent B (A: 0.1% formic acid, B: 80% acetonitrile, 0.1% formic acid) by high-performance liquid chromatography (HPLC). Mass spectra for the peptides were obtained in data-dependent acquisition mode using Thermo XCalibur software version 4.1.50. Full scan mass spectra (350 to 1800 m/z, 120,000 resolution) were obtained from Orbitrap using an AGC target of 4e5 with 50 ms of maximum injection time. Internal Calibration was done using lock mass on the m/z = 445.12003 siloxane ion. Fragmentation MS/MS spectra were obtained in a top-speed mode for a total cycle time of 3 sec for the most intense ions. The quadrupole analyser was used to isolate selected ions in a window of 1.6 m/z. Isolated ions were further fragmented into smaller peptide ions by Higher energy Collision-induced Dissociation (HCD) with 35% of collision energy. The resulting fragments were detected by the linear ion trap at a rapid scan rate

with an AGC target of 1e4 and a maximum injection time of 50 ms. Dynamic exclusion of previously fragmented peptides was set for a period of 30 sec and a tolerance of 10 ppm.

For knockdown samples: 10 µg of protein from nuclear envelope-enriched fractions were reduced using 0.2 mM dithiothreitol, alkylated using 0.8 mM iodoacetamide and digested with 0.2 µg of trypsin (sequencing grade, Promega, Madison, WI). Samples were analysed by nano-LC/MSMS using a Dionex UltiMate 3000 nanoRSLC chromatography system (Thermo Fisher Scientific) interfaced to an Orbitrap Fusion mass spectrometer (Thermo Fisher Scientific, San Jose, CA, USA) equipped with a nanoelectrospray ion source. 1 µg of peptides were separated on a C18 Pepmap Acclaim column (50 cm length, 75 µm internal diameter) using a 90 min linear gradient at 300 nL/min with 5-40% solvent B (A: 0.1% formic acid, B: 80% acetonitrile, 0.1% formic acid). Mass spectra were obtained with a data-dependent acquisition method using the Thermo XCalibur software version 4.1.50. Full scan mass spectra (350–1800 m/z, 120,000 resolution) were acquired from Orbitrap using an AGC target of 4e5 with a maximum injection time of 50 ms. Precursors were filtered in the quadrupole analyzer with 1.6 m/z isolation windows and fragmented by higher-energy Collision-induced Dissociation (HCD) with 35% collision energy. The resulting fragments were detected using the linear ion trap at a rapid scan rate with an AGC target of 1e4 and a maximum injection time of 50 ms.

Data analysis: The acquired spectra were processed using the Minora feature detector algorithm in Proteome Discoverer 2.3 (Thermo Fisher Scientific). The resulting data were submitted to MASCOT searches against the UniProt Homo sapiens protein database (downloaded on 2019-02-12). The following parameters were set as dynamic modifications: two missed cleavage sites by trypsin, deamidation of asparagine or glutamine, oxidation of methionine; and carbamidomethylation of cysteine was set as a static modification. We also set mass search tolerance of 10 ppm and 0.6 Da for MS and MS/MS, respectively. For protein validation, a false discovery rate of ≤ 0.01 was allowed at peptide and protein levels based on a target/decoy search. Unique and razor peptides were considered for protein quantification and normalisation was performed based on the summed abundance of peptides. Data were normalised using the intensity normalisation factor which was calculated by dividing the median intensity for each sample by the median intensity for all samples combined.

Results were exported to an excel file. Samples were compared to each other using Z-score values and proteins with absolute log_2-transformed Z-score ratios >1.96 and adjusted p-Value (Benjamini Hochberg correction) < 0.01.

For the MX2 knockdown cell experiment, the acquired spectra were processed using the Minora feature detector algorithm in Proteome Discoverer 2.3 (Thermo Fisher Scientific). The resulting data were subjected to MASCOT searches against the UniProt Homo sapiens protein database (reference proteome UP000005640 with 74485 entries, downloaded on 2019-02-12) considering trypsin digestion. For protein validation, a false discovery rate (FDR) of ≤ 0.01 was allowed at peptide and protein levels based on a target/decoy search. Unique and razor peptides were considered for protein quantification, and normalization was performed based on the summed abundance of the peptides. The data were normalized using the intensity normalization factor, which was calculated by dividing the median intensity for each sample by the median intensity for all samples combined. The results were exported to an Excel file where samples were compared to each other using absolute Z-score > 1.96, q-value < 0.05 and log2 ratio between the two conditions > 0, in order to determine the statistical significance of the observed variations. For the GS-CA1 experiments, spectra were analyzed in Maxquant using the Andromeda search engine (version 2.0.2.0) against a UniProt Homo sapiens protein database (reference proteome UP000005640 with 97094 entries, downloaded on 2020-09-24). Trypsin was set as the digestion parameter and a maximum FDR of 1% was set both at the peptide and protein level. The proteinGroups.txt output file was imported into R software and the LFQ normalized intensities were used to compare the groups considering the same z-score and q-value thresholds as above.

Results

1. Nuclear envelope protein composition is altered by HIV-1 infection and IFN-β treatment

Firstly, we evaluated the purity of nuclear envelope-enriched fractions prepared from THP-1 cells by performing western blot (WB) analysis using the MAb414 antibody, which detects FG-repeat motifs, a characteristic feature of multiple Nups (231, 232). Additionally, GAPDH levels were analyzed to assess potential cytosolic contamination in the nuclear envelope fractions (230). The presence of several FG motif-containing proteins, along with the absence of GAPDH, confirmed that the nuclear envelope fraction was successfully enriched for nuclear envelope

proteins (Figure 2.1A, B). Next, we examined the effect of IFN-β treatment on nuclear envelope protein purification by treating THP-1 cells with IFN-β for 12 hours prior to fractionation, and subsequent analysis revealed that IFN-β treatment did not interfere with the purification process. However, some FG-repeat-containing proteins exhibited differential expression, with certain proteins being upregulated or downregulated in the nuclear envelope fraction following IFN-β treatment (Figure 2.1A, B).

Further, the changes in the nuclear envelope proteome were assessed by performing label-free quantitative mass spectrometry analysis on nuclear envelope-enriched fractions from HIV-1-infected and IFN-β-treated THP-1 cells. THP-1 cells were either pre-treated with IFN-β for 12 hours or left untreated (control), followed by infection with the NL43GFP HIV-1 vector for an additional 12 hours. As expected, IFN-β treatment significantly reduced HIV-1 infection rates from 16.2% to 0.8%, confirming its antiviral efficacy (Figure 2.3). Western blot analysis of nuclear envelope fractions using the MAb414 antibody revealed similar overall protein profiles; however, specific FG-repeat-containing Nups displayed differential expression depending on the presence of HIV-1 and/or IFN-β (Figure 2.4).

Label-free mass spectrometry enables relative quantification of protein abundance across samples without isotopic labeling, relying on spectral counting and ion intensity measurements to detect changes with high sensitivity and throughput. To ensure data robustness, MS/MS spectra were normalized as detailed in the methods section (Figure 2.5). Principal component analysis (PCA) was performed to assess replicate consistency and visualize global proteomic changes. PC1 and PC2 accounted for 35.4% and 15% of the variance, respectively (Figure 2.6). Samples from control, IFN-β-treated, and co-treated (IFN-β + HIV-1) conditions exhibited low cross-replicate variability, indicating high consistency within these groups. In contrast, samples from cells infected with NL43GFP alone displayed greater variability, suggesting a broader impact on the nuclear envelope proteome (Figure 2.6). A total of 6,033 proteins were detected across all experimental groups (orange bars, Figure 2.7). Proteins consistently identified across all replicates within a given group were considered quantifiable (green bars, Figure 2.7), and those with at least two unique peptides were subjected to further analysis (blue bars, Figure 2.7). Differential expression analysis revealed that IFN-β treatment altered the abundance of 121 proteins, HIV-1

infection modulated 99 proteins, and the combination of both conditions affected 145 proteins compared to the control (Figure 2.2). While both IFN-β treatment and HIV-1 infection resulted in protein upregulation and downregulation, upregulation events were more prevalent across conditions, suggesting a more pronounced host response activation upon infection and immune stimulation.

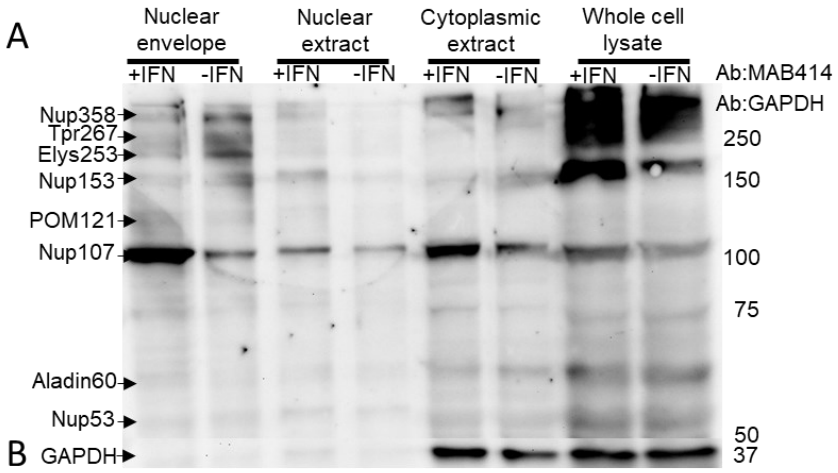

Figure 2.1: Purified nuclear membrane extracts displaying differences in the FG-repeat following IFN treatment. A) Western blot analysis using the Mab414 antibody specific for FG repeats. THP-1 cells treated with IFN (+IFN) and without (-IFN) for 12 hours before purification, lysed and different cellular fractions were purified and loaded. Probable corresponding Nups are represented here according to their molecular weight. B) Western blot analysis using the GAPDH antibody as a cytosolic marker

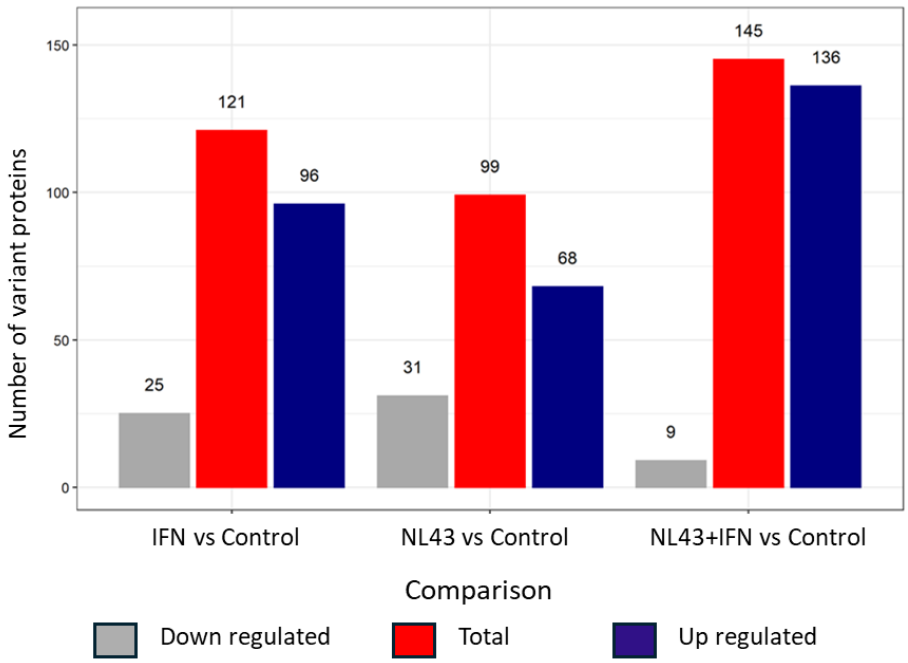

Figure 2.2: Quantitative mass spectrometry data showing differential protein modulation in response to IFN-β treatment and HIV-1 infection. A) Total modulated proteins are shown in red, up-regulated proteins are shown in blue and down-regulated in grey. (THP-1 wild type non-treated and uninfected cells= Control; IFN is IFN-β treated THP-1 wild type (12 h prior to infection; 10 ng/ml); NL43 is NL43GFP infected (12 h; MOI=1) THP-1 wild type cells; IFN+NL43 is IFN-β treated and NL43GFP infected THP-1 cells.

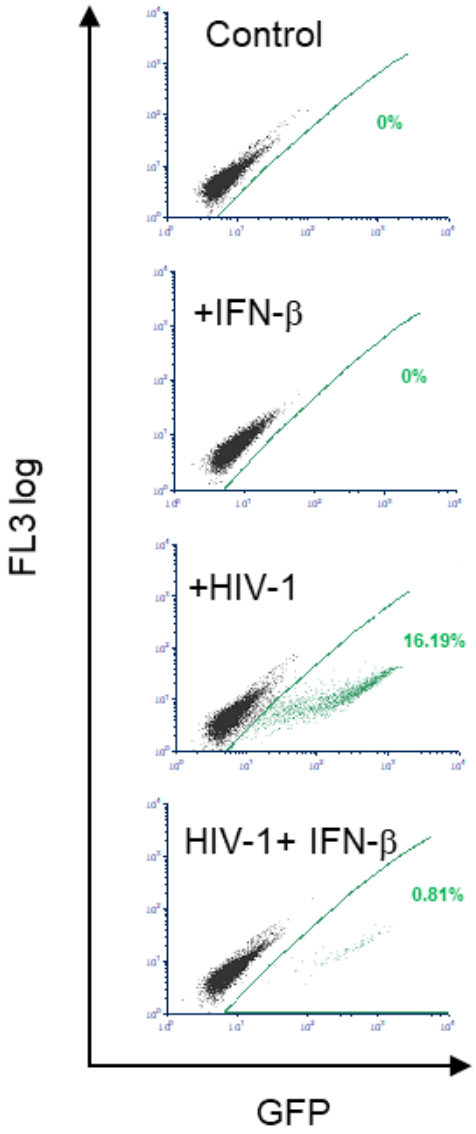

Figure 2.3 FACS analysis showing infection following IFN-β pre-treatment. THP-1 wild-type cells were fixed in 4% formaldehyde after 48 h infection with NL43GFP. Cells were subjected to flow cytometry to obtain %GFP positive cells (shown in colour dot blot). Control= nontreated and uninfected THP-1 cells; + IFN-β = THP-1 cells treated with IFN-β (12 h prior to infection, 10ng/mL); +HIV-1= THP-1 cells infected with NL43GFP (MOI=1); HIV-1+IFN-β = THP-1 cells treated with IFN-β and infected with $NL43_{GFP}$

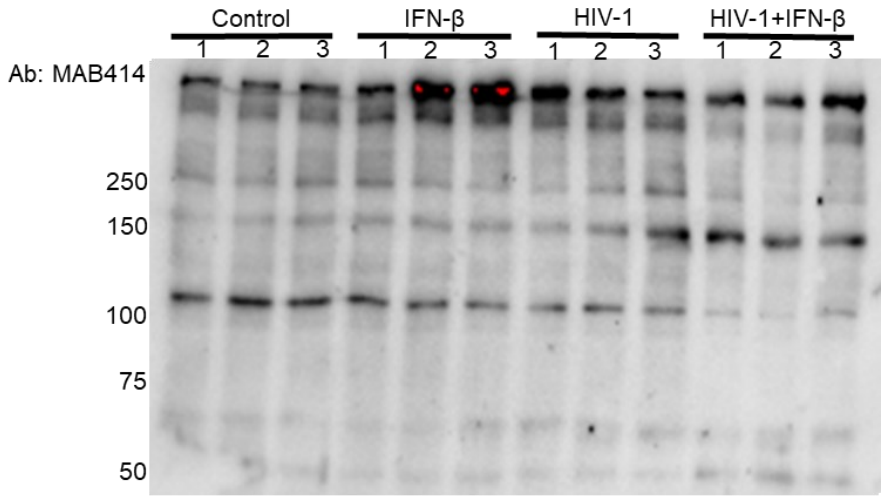

Figure 2.4 Nuclear envelope extracts from THP-1 wild-type cells following HIV-1 infection and IFN-β treatment: Membrane was tagged with Mab414 antibody. (THP-1 wild type non treated and uninfected cells= CTRL_1, CTRL_2 and CTRL_3; IFN_1, IFN_2 and IFN_3 are IFN-β treated THP-1 wild type cells (12 h prior to infection; 10 ng/mL); NL43_1, NL43_2 and NL43_3 are NL43GFP infected (12 h; MOI=1) THP-1 wild type cells; IFN+NL43_1, IFN+NL43_2 and IFN+NL43_3 is IFN-β treated and NL43GFP infected THP-1 cells.

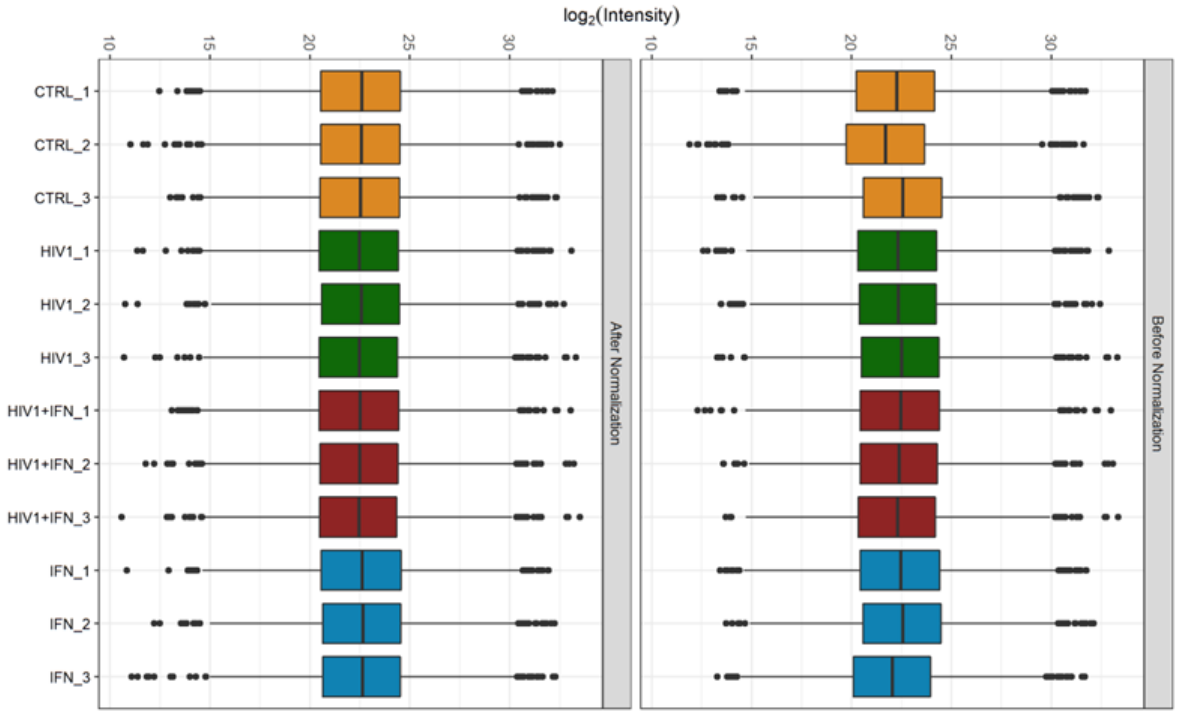

Figure 2.5 Normalized sample intensity for data analysis. Sample intensity was normalized to ensure comparability across different experimental conditions. A box plot was generated to represent protein intensities before and after normalization. For each sample, the median intensity

was calculated, and the normalization factor was obtained by dividing the median intensity of the sample by the median intensity of all samples. Finally, the intensity of each protein in each sample was normalized by dividing it by the corresponding normalization factor. The experimental groups included: CTRL_1, CTRL_2, CTRL_3: Untreated and uninfected THP-1 wild-type cells. IFN_1, IFN_2, IFN_3: THP-1 wild-type cells treated with IFN-β (10 ng/mL) for 12 hours prior to infection. NL43_1, NL43_2, NL43_3: THP-1 wild-type cells infected with NL43GFP (MOI = 1) for 12 hours. IFN+NL43_1, IFN+NL43_2, IFN+NL43_3: THP-1 cells pre-treated with IFN-β (10 ng/mL, 12 hours) and subsequently infected with NL43GFP (MOI = 1).

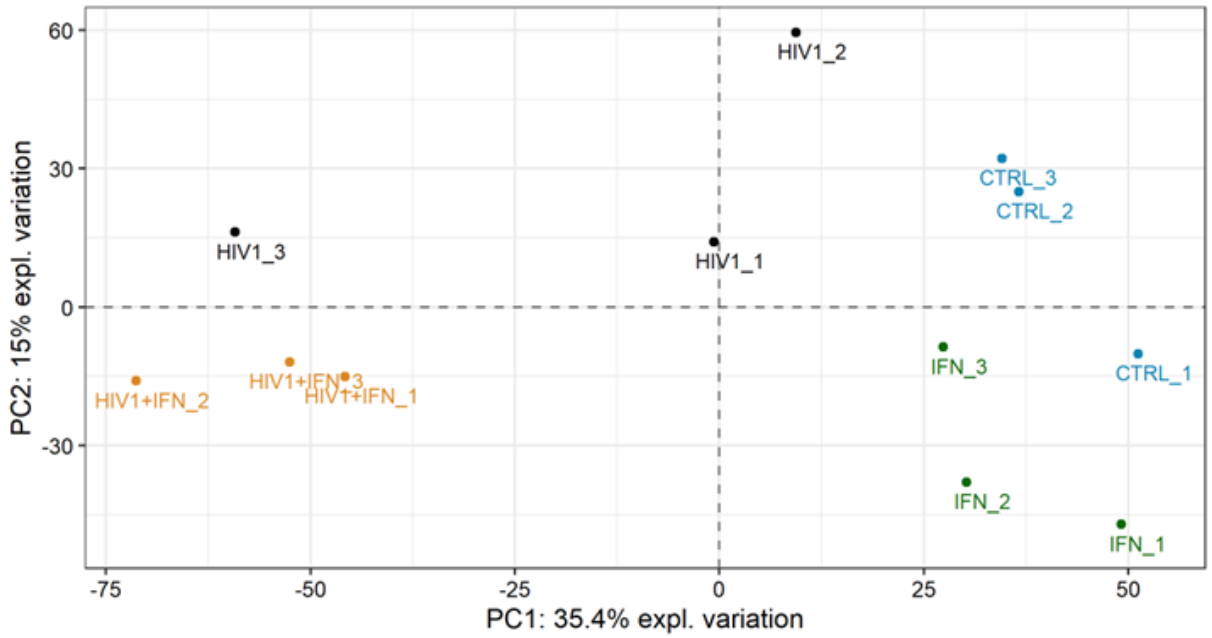

Figure 2.6 Variation in protein expression across experimental conditions based on principal component analysis: Principal component analysis was calculated with the z-Score of all proteins in all samples. Distance between dots indicate level of dissimilarity between the replicates. X-axis is representing (PC1) 34.5% of dissimilarity between the samples and Y- axis (PC2) is representing 15% of dissimilarity. Blue: control (non treated and uninfected sample); green: IFN-βtreated samples- dark green; black: NL43GFP infected cells; orange: NL43GFP infection in the presence of IFN-β. ($-1.96 \leq |z\ Score| \geq 1.96$)

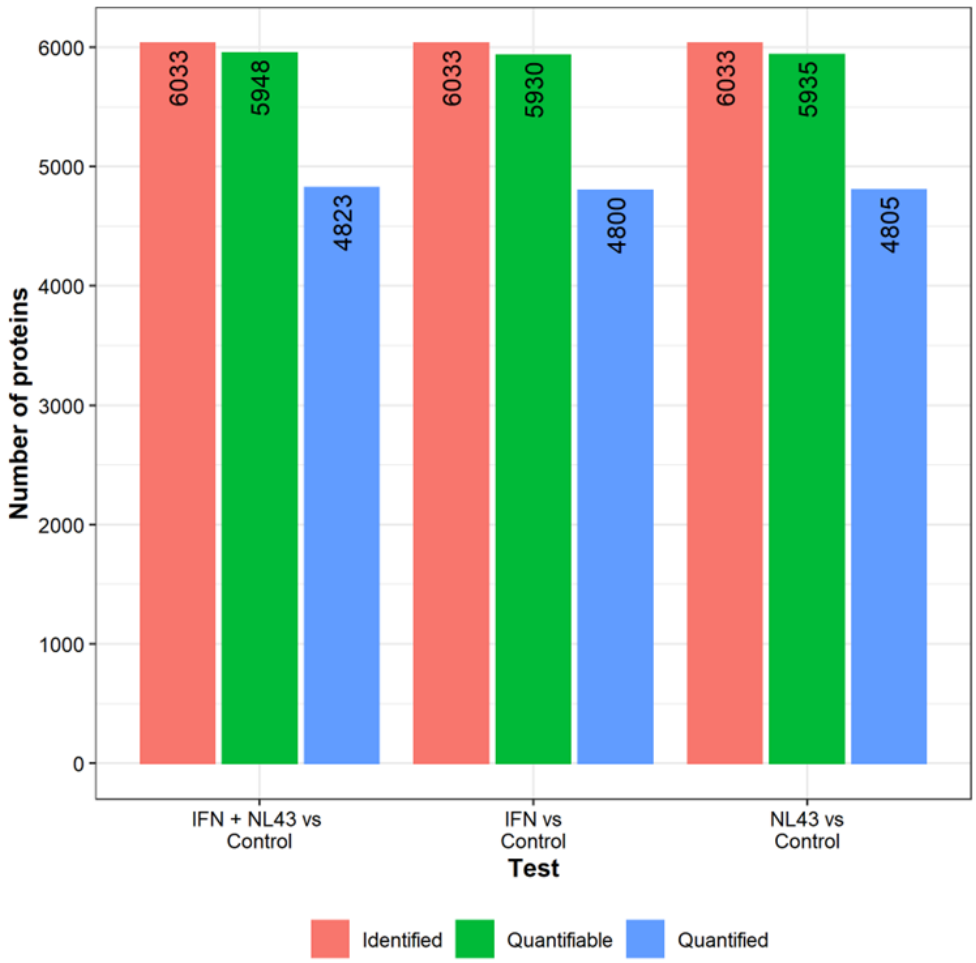

Figure 2.7 Breakdown of protein identification and quantification across experimental groups. Identified Proteins (red) - total proteins identified in this analysis; quantifiable proteins (green) – proteins identified in all replicates of at least one of the two groups (4612 proteins were quantifiable on average for the whole analysis); quantified proteins (blue) - quantifiable proteins with at least 2 peptides. Control nontreated and uninfected THP-1 cells; + IFN-β= THP-1 cells treated with IFN-β (12 h prior to infection, 10ng/mL); +HIV-1= THP-1 cells infected with NL43GFP (MOI=1); HIV-1+IFN-β= THP-1 cells treated with IFN-βand infected with NL43GFP.

2. Modulation of the cellular proteome by IFN-β treatment and NL43GFP infection: Insights into antiviral responses

To examine the impact of IFN-β treatment and NL43GFP infection on the cellular proteome, we identified and clustered proteins modulated by these treatments. A heatmap of protein expression was generated to visualize the relative abundance of modulated proteins across conditions (Figure 2.8). The clustering of proteins showed distinct groups affected by NL43GFP

infection, IFN-β treatment, and their combination, highlighting the unique effect of each condition on the proteome. Notably, NL43GFP-infected samples exhibited greater variation between replicates, resulting in a slightly different heatmap pattern, which was also evident in the principal component analysis (PCA) (Figure 2.6). The dendrogram to the left of the heatmap illustrates the clustering of proteins exhibiting similar modulation across conditions.

To further evaluate protein modulation, we compared fold changes between conditions and visualized the data using volcano plots, which display the -log10 (q-values) versus log2 (Z-score ratios). These plots enabled the identification of the most significantly modulated proteins. IFN-β treatment downregulated several proteins, such as ribosomal protein L36A (RPL36A) (interacts with pr55 HIV-1 protein), and cyclase-associated actin cytoskeleton regulatory protein 1 (CAP1). On the other hand, proteins such as MX2, ISG15, transporter 1 (TAP1), poly (ADP-ribose) polymerase family member 9 (PARP9, which interacts with HIV-1 Tat protein) were upregulated in IFN-β-treated samples (Figure 2.9A).

In contrast, NL43GFP infection resulted in the downregulation of proteins such as block of proliferation 1 protein (BOP1) that interact with Tat HIV-1 protein, and Fas-associated factor 1 (FAF1) (Figure 2.9B). Meanwhile, proteins like H1.2 linker histone, cluster member (HIST1H1C, interacts with Pr55 and Tat proteins), thyroid hormone receptor-associated protein 3 (THRAP3, interacts with Pr55, IN), G protein pathway suppressor 2 (GPS2, interacts with Vif protein), and TPR were significantly upregulated in NL43GFP-infected cells, specifically with TPR showing a 2.12-fold increase. The significant upregulation of TPR, a nuclear basket Nup (is implicated in genome organization and viral replication) may enhance HIV-1 integration and replication (233). To explore the effect of IFN-β treatment on NL43GFP infection, we compared NL43GFP infection in IFN-β-treated cells with various control conditions (Figure 2.10). During NL43GFP infection in the presence of IFN-β, proteins such as aryl hydrocarbon receptor nuclear translocator (ARNT), which is reported to interact with the HIV-1 MA protein, were modulated (241). Previously noted ISGs continued to show elevated expression under these conditions. Additionally, IFN-β pre-treatment reduced the expression of the translocase of outer mitochondrial membrane 20 (TOMM20) (which interacts with gp120 HIV-1 protein) and RPL36A.

We further assessed whether HIV-1 infection dampened the expression of ISGs. NL43GFP infection with IFN-β pre-treatment to controls showed that HIV-1 infection reduced the effect of IFN-β on ISG expression (Figure 2.11). Volcano plots revealed significant reductions in the expression of ISG15, MX2, and TAPBPL, while RPL36A expression was enhanced in the presence of HIV-1 infection (Fig 2.9 and 2.10), suggesting viral activity.

These findings provide insights into the proteins modulated by IFN-β treatment and NL43GFP infection and highlight potential antiviral factors and pathways that may play a role in the cellular response to HIV-1 infection. Altogether, the data suggests that HIV-1 infection upregulates Nup proteins like TPR, facilitating viral replication and IFN-β treatment is capable of inducing a strong antiviral response by upregulation multiple ISGs, including MX2, ISG15, and TRIM22, which are known to restrict HIV-1 replication. MX2, a well-characterized HIV-1 restriction factor, was highly enriched at the nuclear envelope, suggesting a potential role in blocking nuclear import.

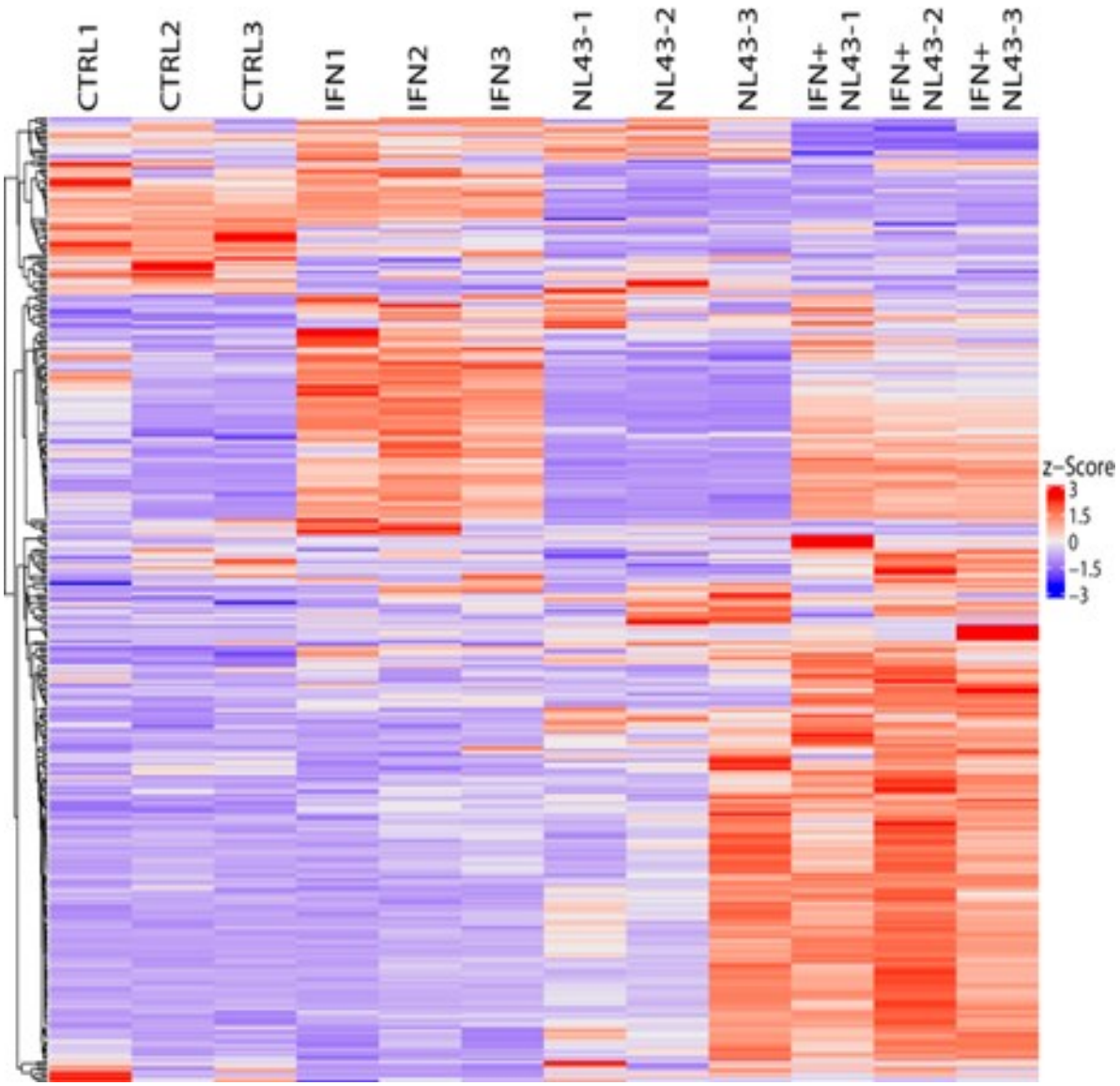

Figure 2.8: Proteins deregulated by IFN-β, HIV-1, or both strongly cluster into distinct groups based on their expression levels: The heatmap displays the relative expression of deregulated proteins, with colors indicating the protein expression in each sample (red: positive z-score, stronger than average expression; blue: negative z-score, weaker than average expression). The dendrogram on the left shows the clustering of proteins with similar deregulation patterns. THP-1 cells were plated and treated or left untreated with IFN-β (10 ng/mL) for 12 hours before infection with NL43GFP or not. CTRL_1, CTRL_2, and CTRL_3 represent the replicates of the control (wild-type cells without infection or IFN-β treatment). IFN_1, IFN_2, and IFN_3 represent IFN-β-treated cells; NL43_1, NL43_2, and NL43_3 are NL43GFP-infected (12 h, MOI=1) cells; IFN+NL43_1, IFN+NL43_2, and IFN+NL43_3 are IFN-β-treated and NL43GFP-infected cells. ($1.96 \leq |\text{z-score}| \leq -1.96$).

A

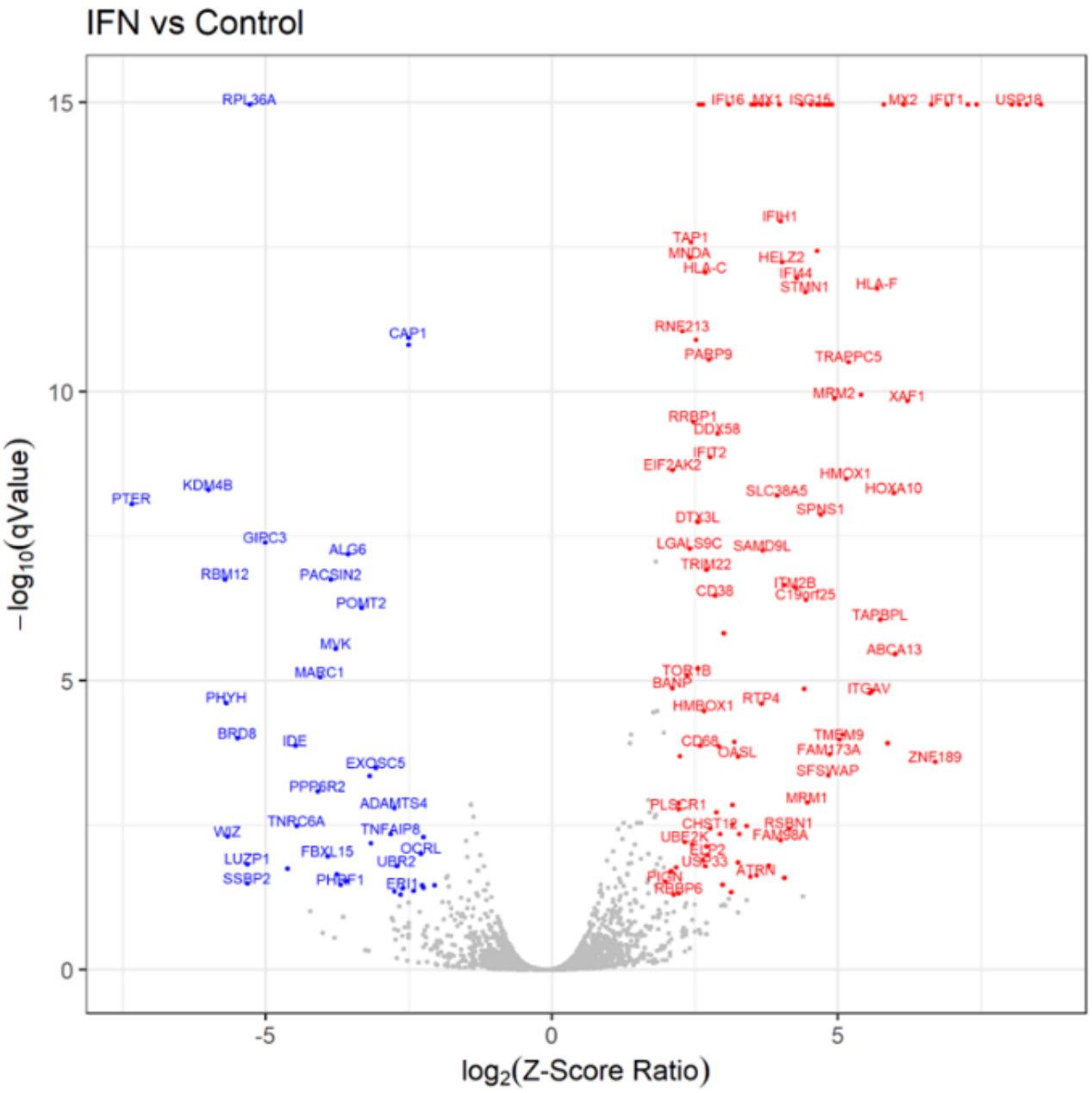
IFN vs Control
15
10
5
0
−log10(qValue)
-5
0
5
log2(Z-Score Ratio)
RPL36A
CAP1
KDM4B
PTER
GIPC3
ALG6
RBM12
PACSIN2
POMT2
MVK
MARC1
PHYH
BRD8
IDE
EXOSC5
PPP6R2
ADAMTS4
TNRC6A
WIZ
TNFAIP8
OCRL
FBXL15
LUZP1
UBR2
SSBP2
PHF1
EBI1
IFI6
MX1
ISG15
MX2
IFIT1
USP18
IFIH1
TAP1
MNDA
HELZ2
HLA-C
IFI44
STMN1
HLA-F
RNF213
PABPC9
TRAPPC5
MRM2
XAF1
RRBP1
DDX58
IFIT2
EIF2AK2
HMOX1
SLC38A5
HOXA10
SPATS1
DTX3L
LGALS9C
SAMD9L
TRIM22
CD38
ITM2B
C19orf25
TAPBPL
ABCA13
TOR1B
BANP
ITGAV
HMBOX1
RTP4
CD68
OASL
TMEM9
FAM173A
ZNF189
SFSWAP
PLSCR1
MRM1
CHST12
RSBN1
UBE2K
FAM98A
EIF2
USP33
ATRN
PIGN
RRBP6

B

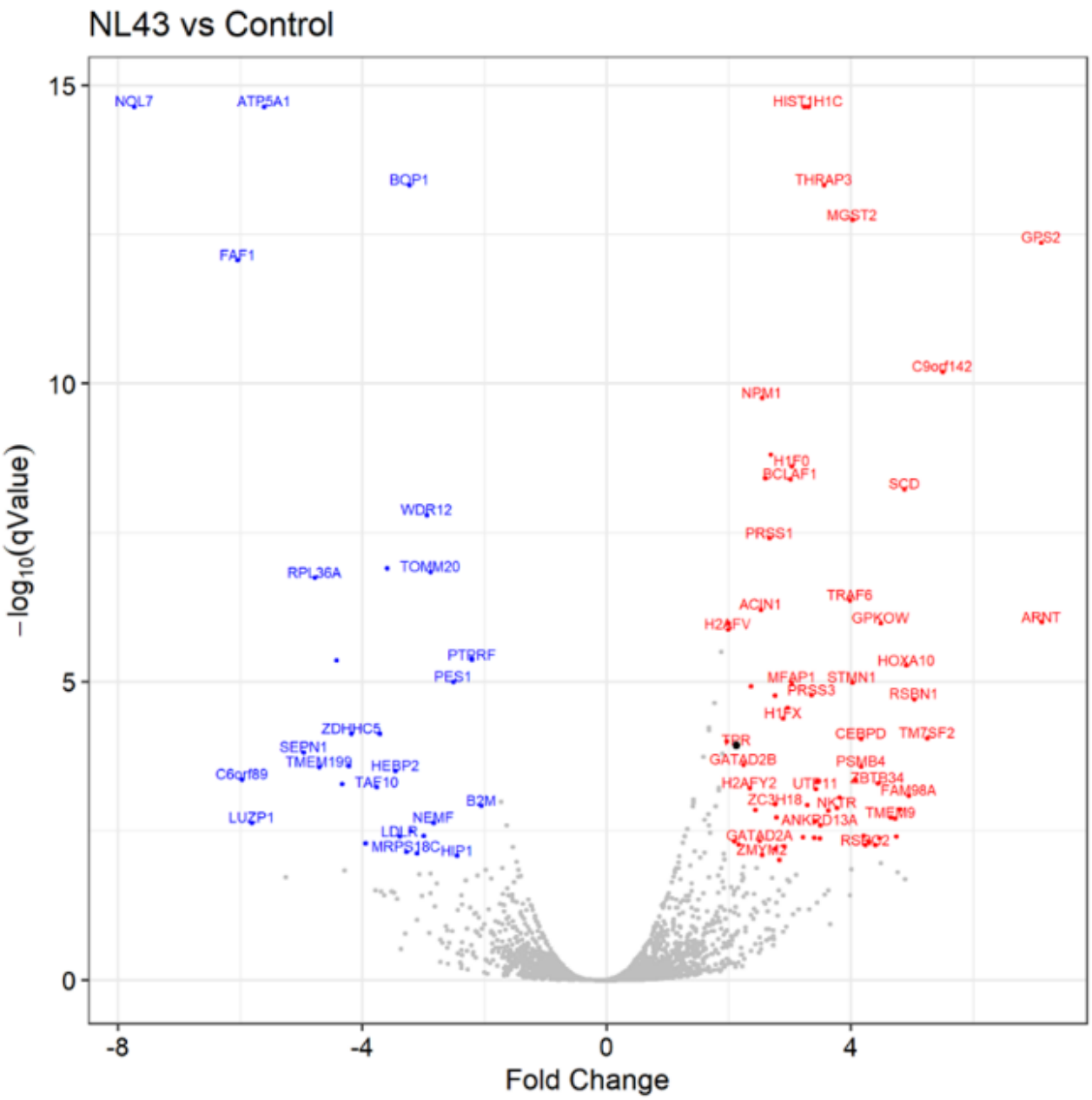

Figure 2.9: Effect of IFN-β and NL43GFP on protein expression in nuclear membrane extracts. Volcano plots of nuclear membrane extracts from uninfected THP-1 cells pre-treated with A) IFN-β (IFN) or without (Control), and B) NL43GFP-infected THP-1 cells. A) Volcano plots show the deregulation of proteins following IFN-β treatment (top) and B) NL43GFP infection (bottom), compared to control (uninfected, non-treated cells). Colored dots represent up-regulated proteins (red) and down-regulated proteins (blue), while grey dots indicate non-deregulated proteins. The black dot represents the Nup TPR. Criteria for deregulation include a fold change or Log2 (Z-Score Ratio) greater than 1.96 or less than -1.96, with an FDR < 0.01 and -log10 (q value) ≥ 2.

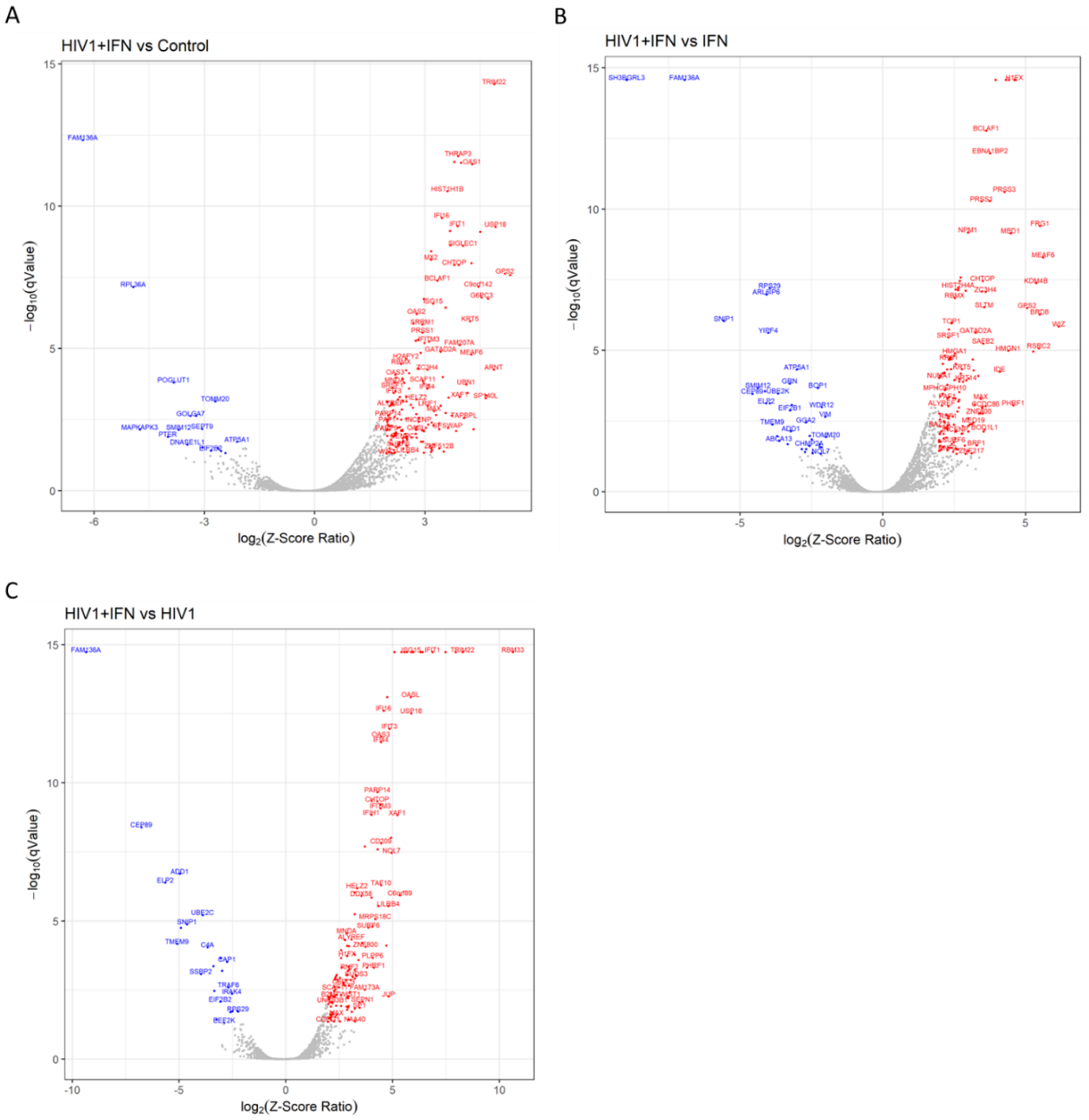

Figure 2.10: Volcano plots comparing HIV+IFN-β to control and HIV+IFN-β to IFN-β revealed consistent protein modulation patterns across conditions A) Volcano plot showing deregulated proteins by HIV+IFN-β treatment compared to control, **B)** HIV+IFN-β treatment compared to IFN, and **C)** HIV+IFN-β treatment compared to HIV1. Colored dots indicate proteins up-regulated (red) or down-regulated (blue). Grey dots indicate non-deregulated proteins. (Fold change or Log2 (Z-Score Ratio) more than 1.96 or less than -1.96; FDR< 0.01; -log10 (q value) ≥ 2)

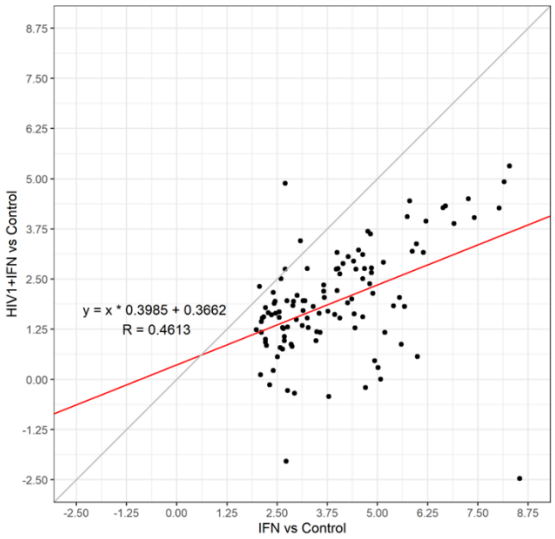

Figure 2.11: Impact of HIV-1 on IFN-treated samples. Proteins are plotted based on their fold change (log2-transformed z-score ratio) in the comparison of IFN-β vs Control (x-axis) and their fold change in HIV-1 infection with IFN-β compared to Control (y-axis). The grey line represents the expected relationship if the fold changes in both comparisons were the same. The red line indicates the linear regression formula.

3. HIV-1 infection alters host protein interactions and promotes viral protein accumulation at the nuclear envelope in IFN-β-treated cells

Next, we performed an *insilico* analysis to explore the interaction between cellular proteins modulated by HIV-1 infection and viral proteins. By searching for interactions in the HIV-1 Interactions Database (NCBI - NIH), we generated an interaction map (Figure 2.12), revealing several key interactions between HIV-1 proteins (e.g., Rev, Gag, Vpr, Tat, Capsid) and modulated cellular proteins. For instance, the viral protein gp120 interacts with the downregulated protein TAPBPL and the upregulated TPR, while the Tat protein interacts with downregulated GATA zinc finger domain-containing 2A (GATAD2A), HIST1H1B and upregulated BOP1, while TRAF6 interacts with Tat protein (234-237). Notably, vimentin and NPC-associated proteins were identified as having antiviral activity, suggesting their role in inhibiting HIV-1 infection. These results highlight how HIV-1 proteins impact the cellular proteome and interact with host factors to influence viral replication.

Furthermore, we assessed the abundance of HIV-1 proteins in infected cells with or without IFN-β pre-treatment. Mass spectrometry analysis revealed that HIV-1 peptides were present only

in infected samples and not in the controls. Remarkably, 47 HIV-1 peptides were detected when IFN-β treatment preceded infection, almost twice the number detected when HIV-1 infection occurred without IFN-β pre-treatment (Figure 2.13). This suggests that IFN-β treatment results in the accumulation of HIV-1 proteins at the nuclear pore complex (NPC), potentially trapping them and altering viral replication. While this accumulation may reflect IFN-induced restriction, it is also possible that viral proteins themselves contribute to sequestering host defense factors at the NPC (86). Overall, these findings provide valuable insights into the interactions between HIV-1 proteins and host cellular proteins, as well as how IFN-β treatment influences the abundance and localization of HIV-1 proteins at NPC, which may play a role in modulating HIV-1 replication and antiviral responses, potentially by preventing nuclear entry.

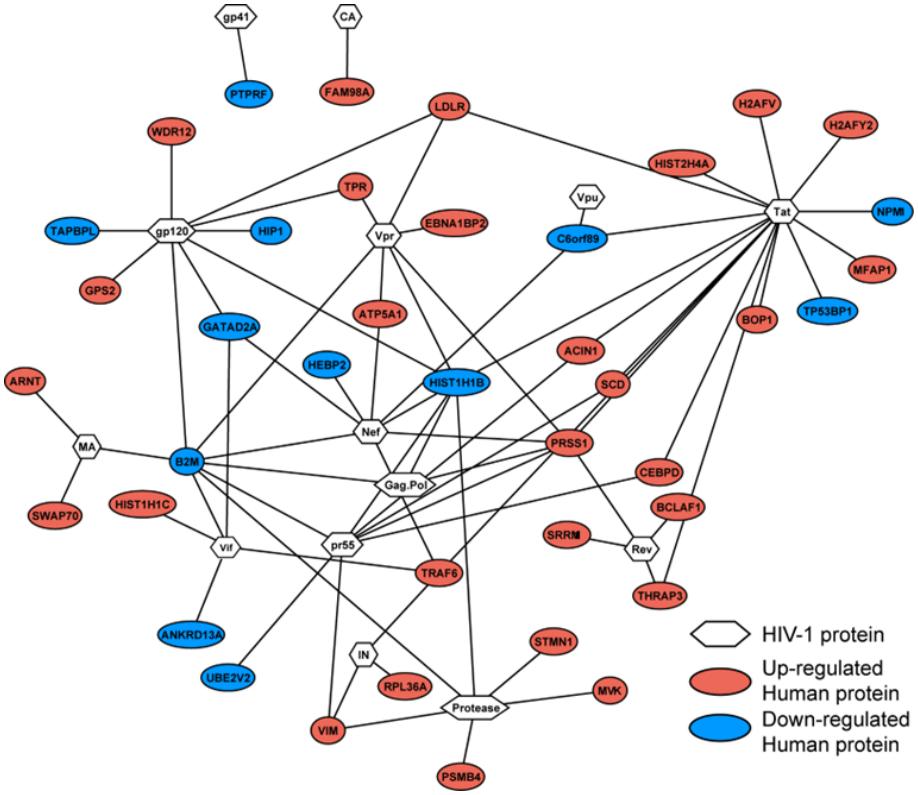

Figure 2.12: Interactome map between viral and host cell proteins. The figure was generated using Cytoscape 3.8. Interaction between the proteins was searched in the NCBI database "Human Immunodeficiency Virus Type 1 (HIV-1), Human Interaction Database". Colored oval nodes indicate up-regulated (red) and down-regulated (blue) cellular proteins observed following HIV or

IFN treatment. In the nuclear envelope-enriched fractions of THP-1 cells following MS, white hexagonal nodes indicate viral proteins.

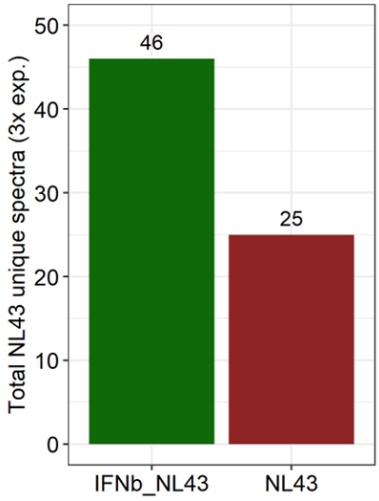

Figure 2.13: Graph of HIV-1 proteins total spectral count detected following HIV-1 infection with and without IFN-β treatment. Bars indicate the numbers of HIV-1 peptides quantified by mass spectrometry. The green bar indicates the NL43GFP peptides in the cells without IFN-β treatment and the red bar shows the NL43GFP peptides in the cells treated with IFN-β (maximum FDR 1%; P<0.01; 1.96>|zScore|>1.96).

4.MX2 knockdown alters nuclear envelope protein modulation and impairs IFN-β-mediated antiviral response against HIV-1.

MX2 is an interferon-induced inhibitor of HIV-1 infection (134). The GTPase domain of MX2 interacts with the HIV-1 capsid, enabling its short isoform to moderate antiviral restriction (238). To further investigate the cause of higher HIV-1 peptide levels at the nuclear envelope, we knocked down MX2 along with TRIM5α to assess its role. MX2 knockdown was performed using shMX2shTRIM5α cells, with shLUCshTRIM5α serving as a control (Figure 2.14A). Following IFN-β treatment, MX2 expression was strongly induced in control cells (shLUCshTRIM5α), while only a faint signal was detected in MX2-knockdown cells, confirming effective suppression. The antiviral activity of knockdown cells lacking MX2 (shMX2shTRIM5α) was significantly impaired compared to cells in which MX2 was present (shLUCshTRIM5α). When these knockdown cells were treated with IFN-β, shLUCshTRIM5α exhibited greater antiviral activity compared to shMX2shTRIM5α (+IFN-β) (Figure 2.14A, lower section).

We further isolated nuclear envelope-enriched fractions from these cells after 12 hours of IFN-β treatment, 12 hours of HIV-1 infection, both conditions combined, or without IFN-β treatment or HIV-1 infection (Figure 2.14B). Nups were detected using the Mab414 antibody, and Lamin B1 was used as a nuclear envelope loading control (244). Samples were analyzed via label-free quantitative mass spectrometry. As expected, we observed various proteins being modulated in different conditions of knockdown cells (Figure 2.14C). A total of 11 proteins were modulated in shMX2shTRIM5α vs. shLUCshTRIM5α in the presence of HIV-1 infection and IFN-β treatment, while 118 proteins were modulated in untreated knockdown cells. shLUCshTRIM5α was used as the control condition. 75 proteins were modulated in shMX2shTRIM5α in the presence vs. absence of IFN-β treatment. 65 proteins were modulated in shLUCshTRIM5α in the presence vs. absence of IFN-β treatment. Only two proteins were modulated in shLUCshTRIM5α untreated vs. IFN-β-untreated HIV-1-infected samples. Additionally, shMX2shTRIM5α HIV-1 vs shLUC hsTRIM5α HIV-1+IFN-β, shMX2 shTRIM5α HIV-1 vs shLUCshTRIM5α, shMX2 shTRIM5α HIV-1+IFN-β vs shLUCshTRIM5α HIV-1 and shLUCshTRIM5α HIV-1+IFN-β vs shLUCshTRIM5α have 112, 50, 81 and 75 proteins modulated respectively (see Figure 2.14C). Altogether, our findings indicated that the absence of MX2 significantly alters protein modulation at the nuclear envelope. The observed changes in protein expression further suggest that MX2, in conjunction with TRIM5α, may be playing a pivotal role in antiviral defense, particularly upon IFN-β treatment. They may have implications for developing novel antiviral strategies targeting nuclear envelope-associated processes.

As observed in the earlier experiment (Figure 2.2), HIV-1 infection combined with IFN-β treatment also led to increased expression of numerous ISG proteins, including MX2, ISG15, TRIM14, OAS1, OAS2, and IFITM3 (239) in the shLUCshTRIM5α control cell line, as shown in Figure 2.15 A. Additionally, other proteins such as AXL, CD209, IFI27, IFI44, IFI44L, IFIT1, IFIT3, LGALS3BP, PARP14, SIGLEC1, SP110, USP18, and XAF1 also exhibited upregulation, aligning with the previous experiment's findings when comparing IFN to Control conditions (Figure 2.15 A). Similarly, in shMX2shTRIM5α cells infected with HIV-1 in the presence of IFN-β, many ISGs were modulated (Figure 2.15B). While several ISGs overlapped with the shLUCshTRIM5α condition (such as ISG15 and TRIM14), additional proteins were exclusively

modulated in MX2 knockdown cells, including DDX60, TRIM21, and TNFSF10. Many of these proteins have previously been demonstrated to function as ISGs, antiviral factors, or both directly or indirectly

A

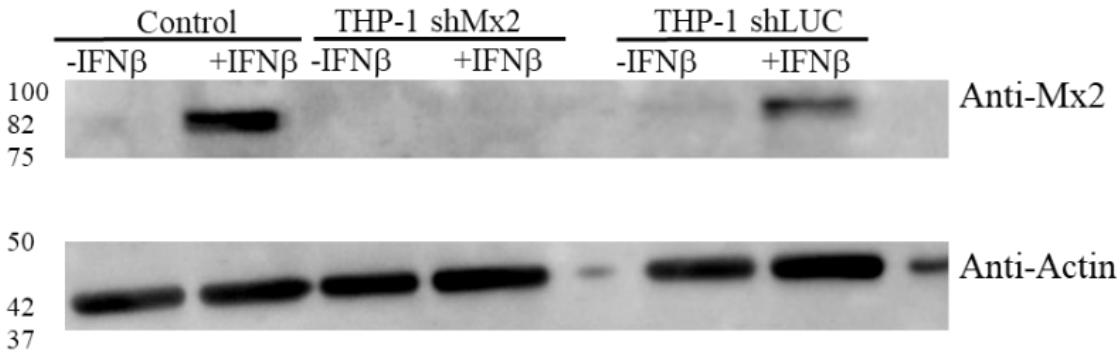

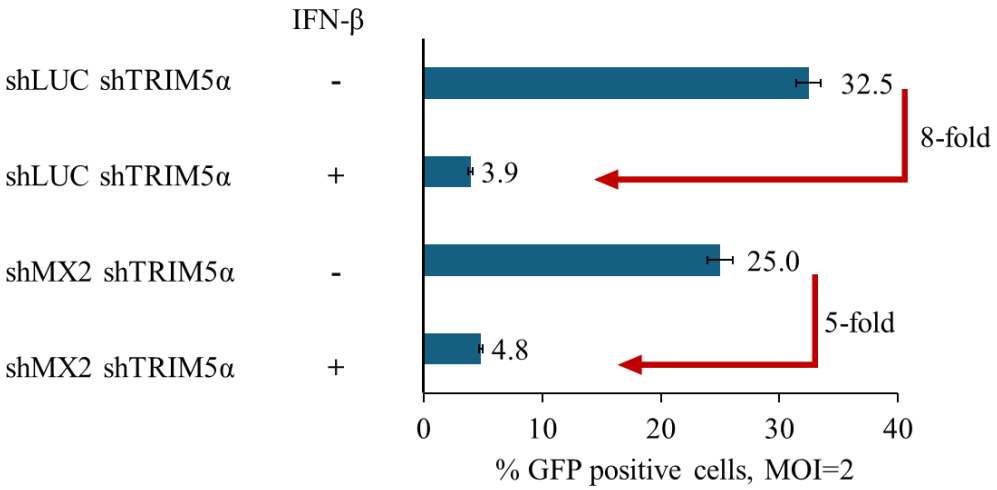

B

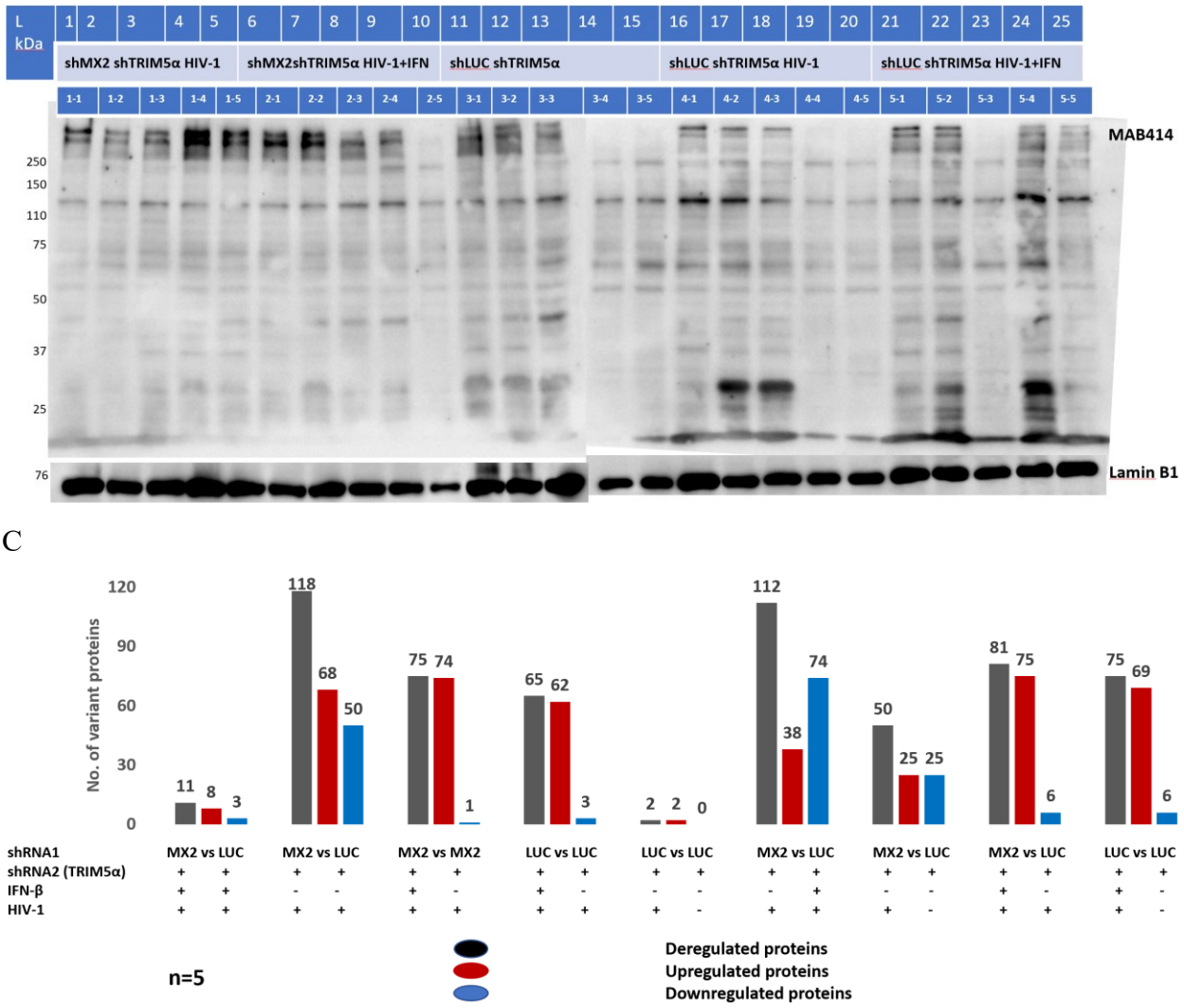

Figure 2.14: MX2 knockdown alters the proteins at the nuclear envelope. A) (upper)Western blot analysis using the MX2 antibody and actin antibody (as a control) to confirm MX2 knockdown and (lower part) MX2 knockdown cells antiviral activity: knockdown cells fixed in 4% formaldehyde after 48 h infection with NL43GFP. Cells were subjected to flow cytometry to obtain %GFP positive cells (shown in blue bar graph in figure 2.14A). ShLUCshTRIM5α with IFN-β (12 h prior to infection, 10ng/mL); +HIV-1, shLUCshTRIM5α +HIV-1, shMX2shTRIM5α with IFN-β (12 h prior to infection, 10ng/mL); +HIV-1 and shMX2shTRIM5α +HIV-1 (MOI=2, n=5) B) MX2 knockdown cells nuclear envelope enriched samples were analysed using Mab41 and LaminB1 (as a control). C) Total modulated proteins are shown in dark grey, up-regulated proteins are shown in red and down-regulated in blue. THP-1 shLUC shTRIM5α non treated and uninfected cells= Control, IFN-β treatment-12 h prior to infection; 10 ng/mL; other conditions shMX2shTRIM5α, shLUC shTRIM5α were infected for 12 h; MOI=2, n=5. Proteins with absolute $-1.96 \geq |\text{z-score}| \geq 1.96$ and adjusted p-value ≤ 0.01 were considered significantly modulated.

A) ShLUCshTRIM5α HIV-1 + IFN-β vs shLUCshTRIM5α HIV-1

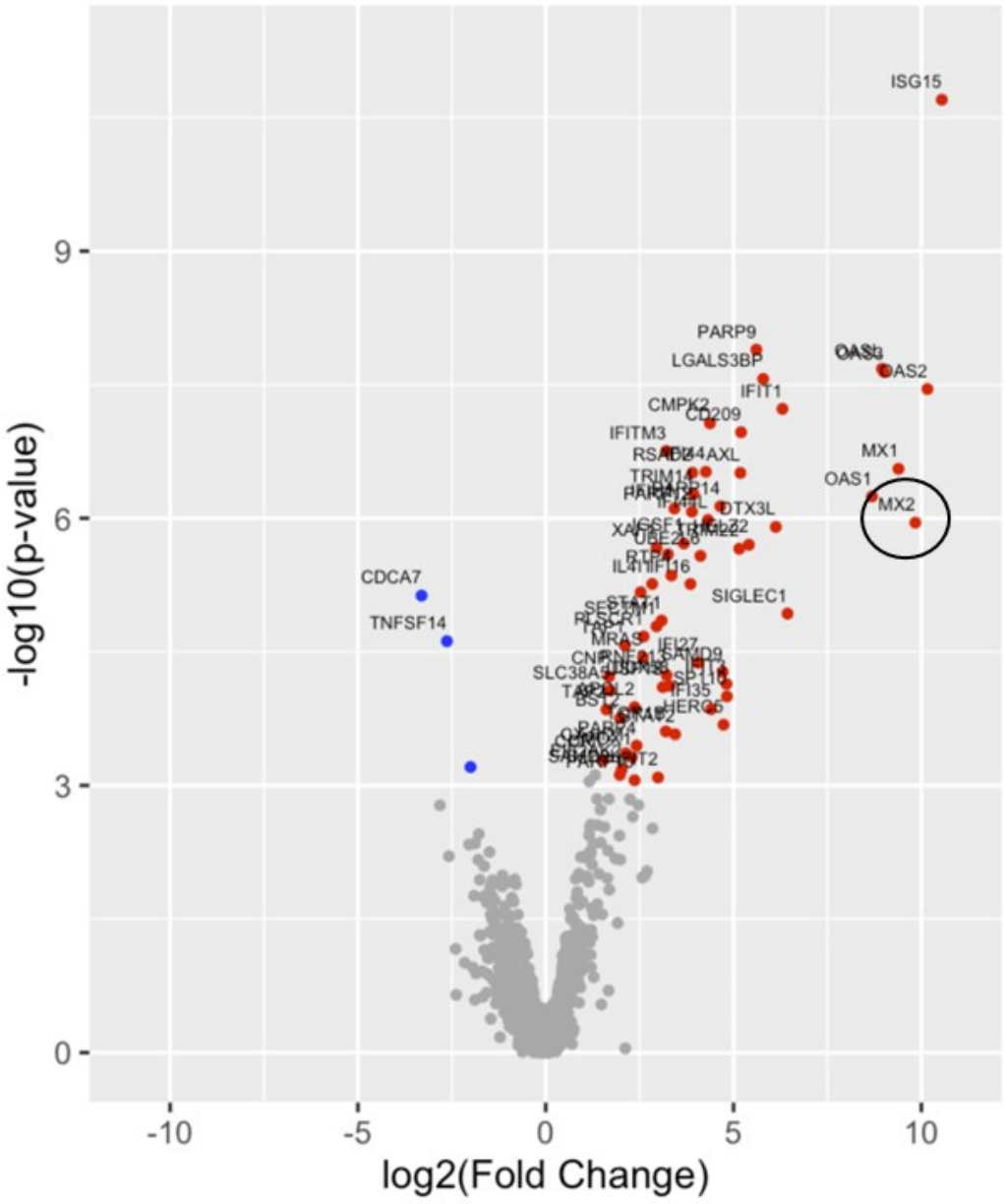

B) shMX2shTRIM5α HIV-1 + IFN-β vs shMX2shTRIM5α HIV-1

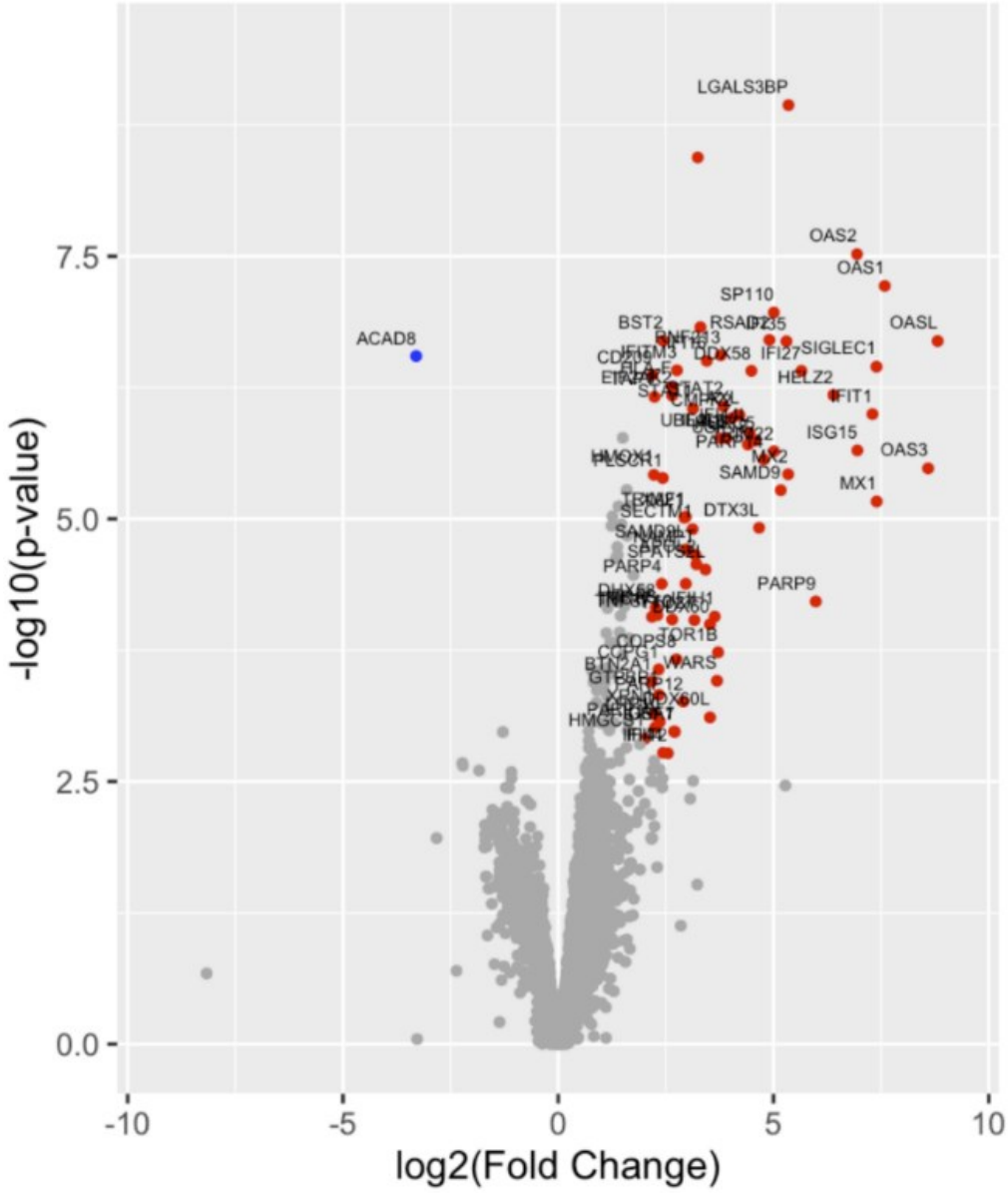

Figure 2.15: Modulation of proteins in nuclear envelope-enriched fractions by HIV-1 infection and IFN-β treatment in MX2 knockdown cells. shMX2shTRIM5α THP-1 and shLUCshTRIM5α THP-1 cells were infected or not with NL43GFP (CRFK MOI = 2) and treated or not with 10ng/ml IFN-β for 12 before infection. Infections were done in quintuplicates (N=5). 12 h later, cells were processed for MS. Volcano plots show dysregulated proteins for 8 **A)** ShLUCshTRIM5α HIV-1 + IFN-β vs shLUCshTRIM5α HIV-1, 8 **B)** shMX2shTRIM5α HIV-1 + IFN-β vs shMX2shTRIM5α HIV-1. Colored dots indicate proteins upregulated (red) or downregulated (blue). Grey dots indicate non-dysregulated proteins.

We then compared the proteins modulated in shMX2shTRIM5α HIV-1 vs. shLUCshTRIM5α+HIV-1 (Figure 2.16A) to shMX2shTRIM5α HIV-1+IFN-β vs. shLUCshTRIM5α HIV-1+IFN-β (Figure 2.16B) to assess the effect of MX2 knockdown in the presence of IFN-β treatment. Among the 118 modulated proteins, 68 were upregulated, and 50 were downregulated in the absence of IFN-β. However, when IFN-β was introduced, only 11 proteins remained significantly modulated in the shMX2shTRIM5α HIV-1 vs. shLUCshTRIM5α+HIV-1 comparison. Among these proteins, WLS, FCGR2C, CD209, and LGALS3BP were upregulated in both conditions, while DACH1 and SLC12A7 were consistently downregulated. Notably, MYOF, DNASE2, HLA-F, and MX2 were detected exclusively in IFN-β-treated cells, supporting their previously established role as IFN-β-regulated proteins (240-242). In total, 114 proteins were differentially accumulated in shMX2shTRIM5α HIV-1 vs. shLUCshTRIM5α+HIV-1, with 107 proteins uniquely deregulated under this condition (Figure 2.16A; see Table 1 for a complete list). In contrast, shMX2shTRIM5α HIV-1+IFN-β vs. shLUCshTRIM5α HIV-1+IFN-β (Figure 2.16B) revealed only two uniquely upregulated proteins, DNASE2 and GRP124 (Table 1, second row). Similarly, shMX2shTRIM5α HIV-1+IFN-β vs. shMX2shTRIM5α HIV-1 (Figure 2.15B) exhibited 11 unique differentially expressed proteins, while shLUCshTRIM5α HIV-1+IFN-β vs. shLUCshTRIM5α HIV-1 (Figure 8A) displayed four unique modulated proteins. Additionally, 50 proteins were deregulated in shLUCshTRIM5α HIV-1+IFN-β vs. shLUCshTRIM5α (Figure 2.16C), with an equal distribution of 25 upregulated and 25 downregulated proteins. Notably, several ISGs, including MX2, ISG15, and MX1, were upregulated (Figure 2.16C). Interestingly, 11 proteins were uniquely modulated in this condition. Among them, BAG4, SLC8A1, and PHF3 were significantly downregulated (blue in the volcano plot, Figure 2.16C), while ISG20, ICAM1, PSMB9, VPS37A, ENDOD1, GBP1, and GAS6 were upregulated (red in Figure 2.16C). These findings highlight the complex regulatory role of MX2 in the IFN-β-mediated antiviral response, further emphasizing its impact on nuclear envelope-associated protein modulation.

A) shMX2 shTRIM5α HIV-1 vs shLUC shTRIM5α HIV-1

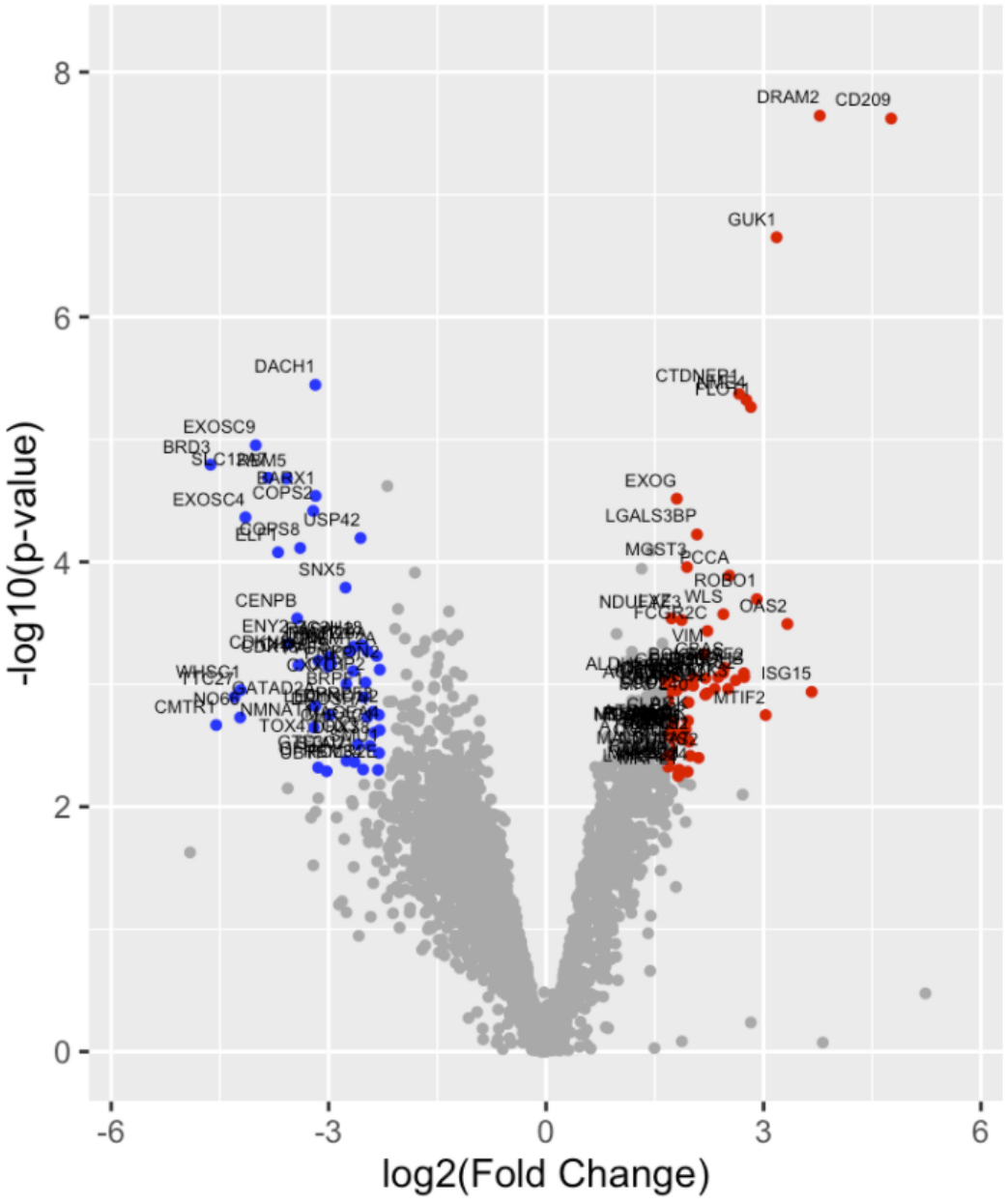

B) shMX2shTRIM5a HIV-1+IFN-β vs shLUC shTRIM5α HIV-1 +IFN-β

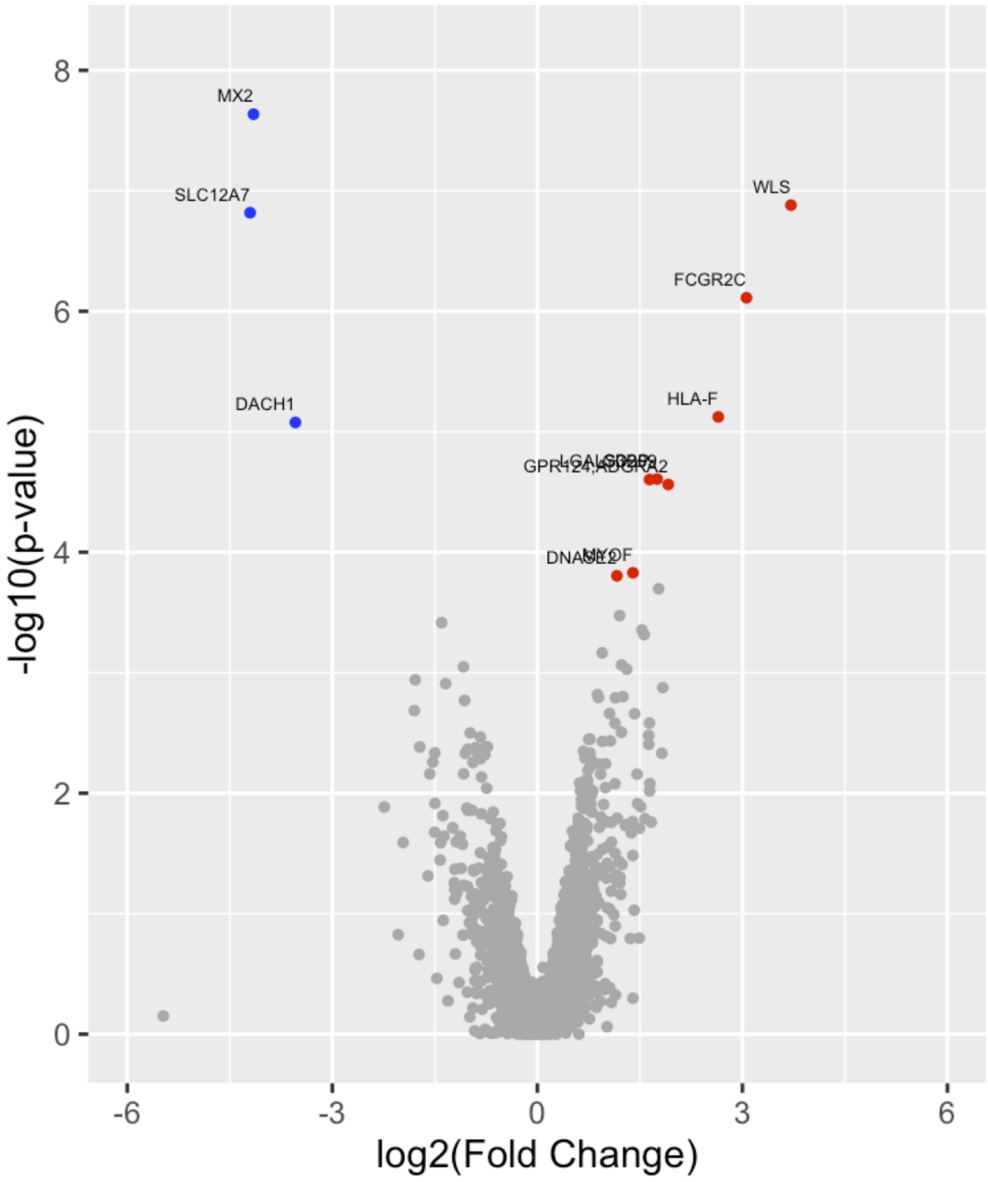

9 C) shLUCshTRIM5α HIV+IFN-β vs shLUCshTRIM5α

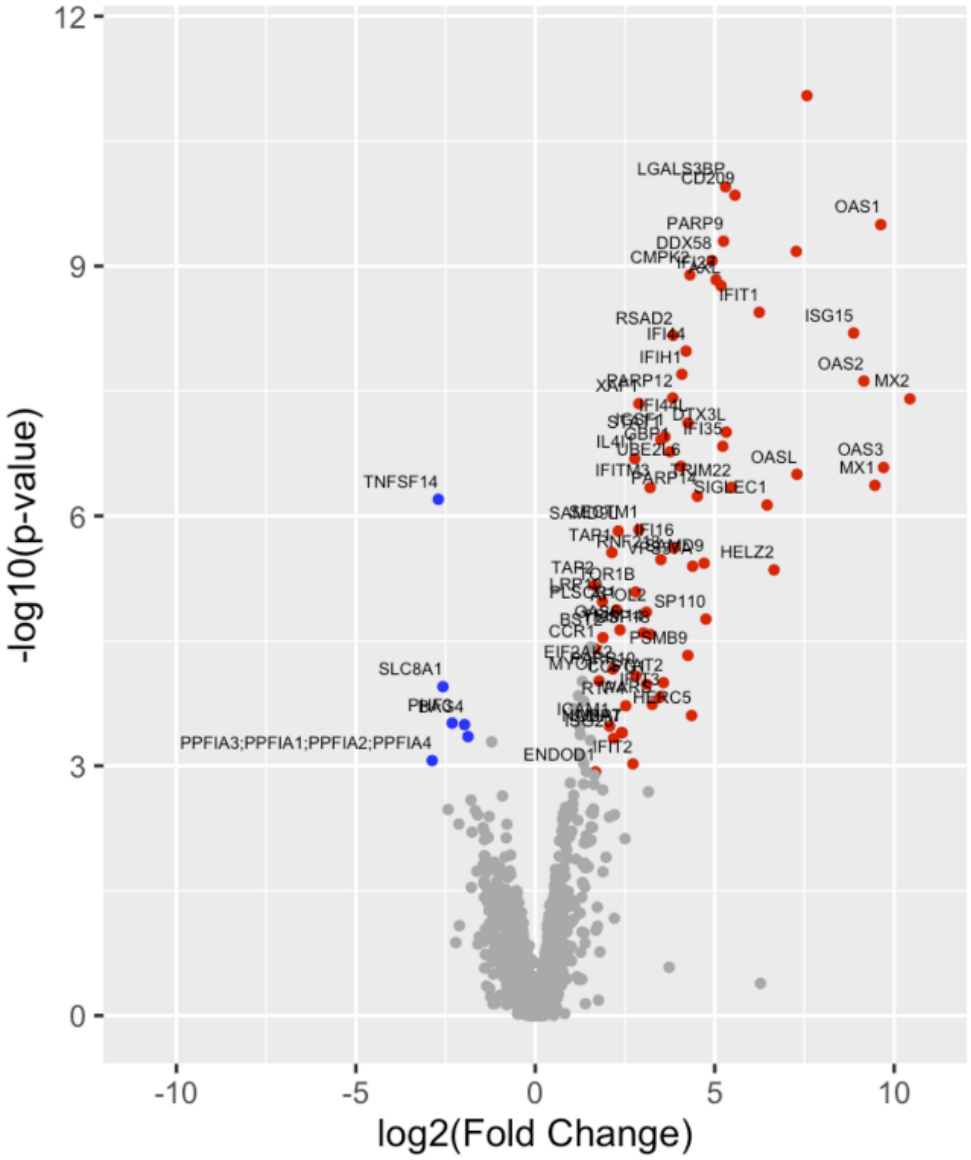

Figure 2.16: Modulation of proteins in nuclear envelope-enriched fractions by HIV-1 infection and IFN-β treatment in MX2 knockdown cells. shMX2shTRIM5α THP-1 and shLUCshTRIM5α THP-1 cells were infected or not with NL43GFP (CRFK MOI = 2) and treated or not with 10ng/ml IFN-β for 12 before infection. Infections were done in quintuplicates (N=5). 12 h later, cells were processed for MS. Volcano plots show dysregulated proteins for A) shMX2 shTRIM5α HIV-1 vs shLUC shTRIM5α HIV-1, 9 B) shMX2shTRIM5α HIV-1+IFN-β vs shLUC

shTRIM5α HIV-1 +IFN-β, 9 C) shLUCshTRIM5α HIV+IFN-β vs shLUCshTRIM5α (LMIX CTRL). Colored dots indicate proteins upregulated (red) or downregulated (blue). Grey dots indicate non-dysregulated proteins.

Table 2.1: List of modulated proteins

Conditions	Modulated Proteins
shMX2 shTRIM5α + HIV-1 vs shLUCshTRIM5α+HIV-1	PON2, UBTF, CDK13, USP42, gPRPF3, ENY2, ZC3H18, WHSC1 , RBM34, MAGEA4, CTBP2, CENPB, CHAF1B, SMU1, STAU1, PAF1, GTF3C2, LEO1, DHX38, PNKP GFI1, FAM129A, ADNP NO66, NMNAT1, CHRAC1, DROSHA, CDKN2AIP, RASAL2, POLR2E, ELF1, BRPF1 CXXC1, COPS2, EXOSC9, TOX4;TOX3 RBM5, KMT2A, DYNC1I2, BRD3, SNX5 GATAD2A, CMTR1, PATZ1, BARX1, EXOSC4, IFI30, ROBO1, ALDH5A1, TXNRD2, AGK, PCCB BCKDHA, GRSF1, MRPL34, SCO2, CTNND1, GBAS, CLPX, NDUFA7, GOT2, LMNA, OAT, MGST3, FH, VIM, DBT, MTHFD2, FLOT1, BCKDHB, MUT, FECH, DTYMK, PYCR1, ACADSB, MTIF2, IDH3G, LYZ, ECH1, CLPP, PITRM1, ADCK3, NIPSNAP1, RARS2, MECR, MRPL1, NDUFAF3, PLGRKT, MRPL40, WARS2, MRPS33, NME4, ATPAF1, GUK1, ACSF2, CTDNEP1, PCCA, MRPS11, SURF1, EARS2, LYPLAL1, DRAM2, CCBL2, ATPAF2, MALSU1, MRPS24, EXOG
shMX2shTRIM5α+HIV-1+IFN-β vs shLUCshTRIM5α+HIV-1+IFN-β	DNASE2 , GPR124; ADGRA2
shMX2shTRIM5α+HIV-1+IFN-β vs shMX2shTRIM5α+HIV-1	SPATS2L, GTPBP1, TRIM21, TNFSF10, DDX60L, HMGCS1, BTN2A1, DDX60, XRN1, DHX58, TTC17

shLUC2shTRIM5α+HIV-1+IFN-β vs shLUC2shTRIM5α+HIV-1	CDCA7, CNP, SLC38A5, CXorf21
shLUC2shTRIM5α+HIV-1+IFN-β vs shLUC2shTRIM5α	BAG4, PPFIA3;PPFIA1;PPFIA2;PPFIA4, SLC8A1, PHF3, ISG20, ICAM1, PSMB9, VPS37A, ENDOD1, GBP1, GAS6

5. MX2 is not the sole ISG regulating HIV-1 peptide accumulation at the nuclear envelope.

In our previous experiment, we observed an increased presence of HIV-1 peptides in nuclear envelope-enriched fractions when cells were infected with HIV-1 in the presence of IFN-β treatment (Figure 2.13). Given that MX2 is a known ISG that interacts with the HIV-1 capsid near the NPC, we hypothesized that MX2 might play a key role in this accumulation, and its absence could lead to increased viral entry or altered processing at the nuclear envelope. To test this, we quantified HIV-1 peptides in MX2-knockdown cells and compared them to control knockdown cells under different conditions of infection and IFN-β treatment. For this analysis, shLUCshTRIM5α without infection and IFN-β treatment was used as the control. HIV-1 peptides were detected at approximately fourfold higher levels in shLUCshTRIM5α upon IFN-β treatment (Figure 2.17). Interestingly, in shMX2shTRIM5α cells, HIV-1 peptide accumulation in the presence of IFN-β showed only a threefold increase compared to the control condition (Figure 2.17). Contrary to our expectations, the difference between MX2-knockdown and control cells was not statistically significant. However, this result provides valuable insights into MX2's role in antiviral defense, suggesting that additional antiviral factors may compensate for the loss of MX2, highlighting the robustness of the interferon-mediated defense mechanism. Since our data has already shown that IFN-β treatment modulates other antiviral factors, these factors may mitigate the impact of MX2 depletion. This compensatory effect might explain why the difference in HIV-1 peptide accumulation between MX2-knockdown and control cells was not as pronounced as expected.

Rather than acting alone, MX2 may function in coordination with other ISGs or host factors to regulate HIV-1 peptide accumulation at the nuclear envelope. This finding points to a broader,

more intricate antiviral response mediated by IFN-β. Future studies focused on identifying additional ISGs involved in this process could provide deeper insights into host defense mechanisms and open new avenues for antiviral therapeutic strategies. In summary, while MX2 plays a significant role in restricting HIV-1 nuclear entry, its knockdown does not completely abolish IFN-β-mediated antiviral effects, indicating that a broader network of ISGs contributes to HIV-1 regulation.

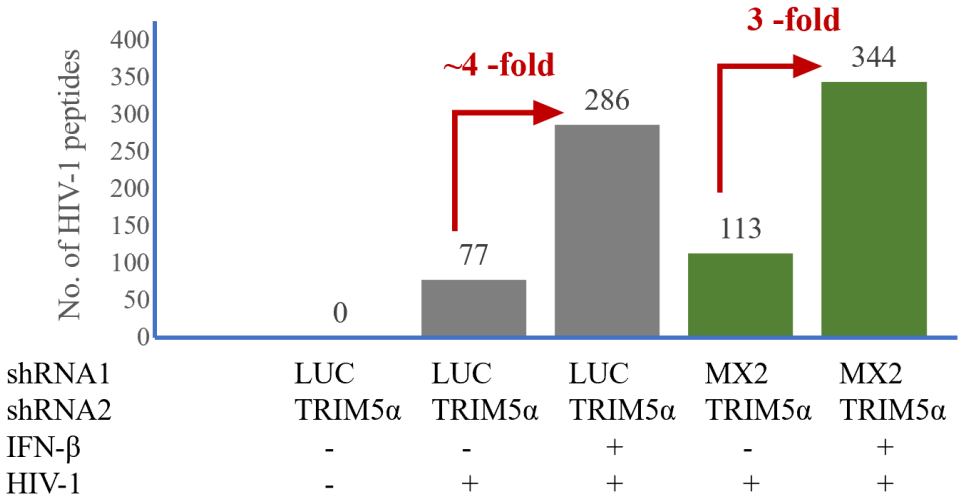

Figure 2.17: Graph of HIV-1 proteins total spectral count detected following HIV-1 infection with and without IFN-β treatment in knockdown cells. Bars indicate the numbers of HIV-1 peptides quantified by mass spectrometry. ShLUC shTRIM5α without infection and IFN-β treatment, shLUCshTRIM5α infection with HIV-1 with and without IFN-β treatment and shMX2TRIM5α infection with HIV-1 with and without IFN-β treatment. (maximum FDR 1%; P<0.01; 1.96>|zScore|>1.96).)

Discussion

HIV-1 infection leads to AIDS, severely compromising immune function and reducing life expectancy (243, 244). Despite the effectiveness of cART in managing HIV-1 infection, drug resistance remains a major concern (229, 245). Therefore, identifying ideal drug targets for HIV-1 remains a key focus in HIV-1 drug research. This study investigates the impact of the innate immune response, specifically IFN-β, and HIV-1 infection on nuclear envelope proteins and their associated interactions. Since innate immunity is triggered by viral infections, we pretreated cells with IFN-β to evaluate its effects on the nuclear envelope. We employed label-free quantitative

mass spectrometry to quantify the relative abundance of proteins in nuclear envelope-enriched fractions from NL43GFP-infected and/or IFN-β-treated cells, compared to uninfected and non-treated controls. Our results show that both HIV-1 infection and innate immune response (via IFN-β treatment) significantly modulate the protein levels in the nuclear envelope extracts, confirming our hypothesis. Out of 4849 quantified proteins, 365 (121 with IFN-β treatment, 99 with NL43GFP infection, and 145 with both NL43GFP infection and IFN-β pre-treatment) proteins showed statistically significant variation compared to the control, indicating that both factors impact the nuclear envelope protein composition.

1. **Alteration in nuclear envelope protein composition by HIV-1 infection and IFN-β treatment**

IFN-β, known for its antiviral activity, was used to pre-treat cells before isolating the nuclear envelope extracts. Flow cytometry results demonstrated that IFN-β pretreatment reduced NL43GFP infection by 20-fold compared to cells infected with NL43GFP without IFN-β treatment (see Figure 2.3) (228). IFN-β induces the expression of ISGs, establishing an antiviral state in cells (246). Western blot analysis of nuclear envelope fractions showed modulation in the protein levels of FG-repeat-containing proteins in response to IFN-β and NL43GFP infection (see Figure 2.4), motivating us to further quantify total nuclear envelope proteins and assess their modulation by IFN-β, NL43GFP infection, and their combination.

Label-free quantitative mass spectrometry revealed that several ISGs known for their antiviral properties, such as MX2 and TRIM22, were modulated in response to IFN-β treatment (Dataset MSV000086616) (Figure 2.9A). MX2 inhibits HIV-1 by interacting with the CA protein during the early stages of the HIV-1 life cycle (134), while TRIM22 interferes with HIV-1 replication by targeting the Tat protein (247). Additionally, TAP-binding protein-like (TAPBPL), involved in antigen processing and presentation, was modulated by IFN-β treatment (Figure 2.9A). We also observed that RPL36A, which interacts with gp160 and Pr55 (Figure 2.9A) (248, 249), was modulated by IFN-β, further supporting its antiviral activity (Figure 2.3).

2. **Key antiviral factors identified by IFN-β treatment and NL43GFP infection.**

NL43GFP infection deregulated numerous proteins (Figure 2.9). For instance, the HIV-1 Tat protein has been reported to downregulate the ribosome biogenesis protein, BOP1, in Jurkat cells,

which was confirmed by our data (Figure 2.9A). We also found that Aryl hydrocarbon receptor nuclear translocator (ARNT) was 14.66 times more abundant compared to the control, contrary to previous reports where ARNT was downregulated upon HIV-1 matrix protein p17 exposure (250). Interestingly, Histone H1.2 (HIST1H1B) was upregulated upon NL43GFP infection, and it interacts with Nup and TPR, proteins that play a positive role in HIV-1 genome integration.

We also observed that the nuclear basket protein Nup, TPR, was upregulated upon NL43GFP infection (Dataset MSV000086616, Figure 2.9B), supporting earlier findings (233). TPR facilitates HIV-1 integration into the human genome, and its absence leads to random integration, sometimes in heterochromatic regions (233). Furthermore, *in silico* analysis of HIV-1 protein and cellular protein interactions suggests that HIV-1 proteins manipulate a wide array of cellular proteins to facilitate its life cycle, particularly proteins involved in nuclear transport such as Nup153 and TPR.

HIV-1 infection altered host-virus protein interactions and increased the localization of HIV-1 proteins at the nuclear envelope in cells treated with IFN-β.

We also identified that several ISGs were modulated by HIV-1 infection in the presence of IFN-β treatment. The presence of HIV-1 negatively modulated ISGs such as TRIM22 and MX2, while RPL36A was positively modulated (Figure 2.10). HIV-1 is known to bypass host antiviral defenses by inhibiting IFN-I induction through the action of the Vpu protein, which interferes with the cGAS DNA sensor (251). Our findings further support these mechanisms and highlight the interplay between HIV-1 infection and the host's innate immune response. Given the antiviral activity of IFN-β, we expected a reduction in the abundance of HIV-1 peptides in cells infected with NL43GFP in the presence of IFN-β. However, surprisingly, a higher abundance of HIV-1 peptides was detected in nuclear envelope-enriched fractions from IFN-β-treated and NL43GFP-infected cells. This may be due to the upregulation of MX2, which targets the HIV-1 CA protein during nuclear entry at the NPC.

3. **MX2, not alone but along with other ISGs alters IFN-β-mediated antiviral response against HIV-1.**

To explore the interrelationship between modulated proteins, we conducted experiments using MX2 knockdown cells. These cells displayed protein modulation patterns similar to wild-type cells

under different conditions (Figure 2.14A-B). For instance, in cells treated with HIV-1 and IFN-β, LGALS3BP was upregulated, while MX2 was downregulated in shMX2shTRIM5α cells compared to shLUCshTRIM5α cells. In wild-type cells treated with IFN-β, we identified 18 commonly upregulated ISGs, including CD209, IFI27, IFI44, IFI44L, IFIT1, IFIT3, IFITM3, ISG15, LGALS3BP, MX2, OAS1, OAS2, PARP14, SIGLEC1, SP110, and USP18 (Table available upon request). Although MX2 downregulation altered the expression of various ISGs, it did not show a significant change in HIV-1 CA peptide levels at the NPC (Figure 2.17). We believe that other ISGs may help mitigate the effects of MX2 depletion, suggesting that MX2 could work in concert with other ISGs or host factors to regulate the accumulation of HIV-1 peptides at the nuclear envelope. Future research aimed at identifying additional ISGs involved in this process could offer deeper insights into host defense mechanisms and open up new possibilities for antiviral therapeutic strategies.

In conclusion, this study demonstrates that IFN-β and HIV-1 infection modulate proteins in the nuclear envelope. It also suggests that other ISGs might be responsible for the increased detection of HIV-1 CA at the NPC in the presence of IFN-β treatment. Additionally, the dampening effect of HIV-1 on IFN-β was observed, supporting the idea that HIV-1 can escape innate immune responses. Although the essential ISG MX2 plays a significant role in restricting HIV-1 nuclear entry, its knockdown does not completely abolish IFN-β-mediated antiviral effects, indicating that a broader network of ISGs contributes to HIV-1 regulation. Building on these findings, the next chapter investigates how HIV-1 infection and IFN-β treatment influence viral replication when capsid assembly is disrupted using GS-CA1, a capsid-targeting inhibitor that interferes with CA-CA interactions.

Acknowledgement:

Data availability: Mass spectrometry raw data (Dataset MSV000086616) is available on the MassIVE website (https://massive.ucsd.edu/ProteoSAFe/static/massive.jsp).

Supplementary file: 1. table (excel file of MS raw data)

Chapter 3

Effects of GS-CA1 on nuclear envelope-associated early HIV-1 infection steps

Amita Singh[1], Victor Fourcassié[2], Karen Cristine Goncalves Dos Santos[3], Hocine Chelbi[1], Natacha Merindol[3], Arnaud Droit[2], Hugo Germain[3], Lionel Berthoux[1]

[1]Department of medical biology, Université du Québec à Trois-Rivières, Trois-Rivières, Québec, Canada

[2]Proteomics platform of the CHU de Québec, Québec, QC, Canada and Centre de recherche du CHU de Québec, Québec, Canada

[3]Department of chemistry, biochemistry and physics, Université du Québec à Trois-Rivières, Québec, Canada

*Corresponding author. Phone: +1 (819) 376-5011 x4466; Email: lionel.berthoux@uqtr.ca.

Address: Department of medical biology, Université du Québec à Trois-Rivières, 3351 Boulevard des Forges, Trois-Rivières, QC, G8Z 4M3, Canada

Running title: GS-CA1 and HIV-1 nuclear import

Abstract

The novel HIV-1 drugs GS-CA1 and the recently approved lenacapavir (GS-6207) target the viral structural protein capsid (CA). However, their multiple mechanisms of action have not been fully characterized. Here, we investigated the effects of GS-CA1 on the early stages of HIV-1 infection, specifically the steps involving the nuclear envelope, in comparison to the antiviral cytokine IFN-β. Mass spectrometry data indicated that nuclear envelope proteins were only modestly affected by either GS-CA1 treatment or HIV-1 infection, but combining the two had a more significant impact, altering the levels of many proteins including proteasomal components. GS-CA1 induced a small but significant accumulation of HIV-1 capsid cores at nuclear pores, as seen by microscopy, whereas IFN-β caused a strong accumulation of HIV-1 cores at the nuclear envelope but not specifically at nuclear pores. These observations are consistent with GS-CA1 inhibiting the nuclear translocation of HIV-1 capsid cores through nuclear pores.

Keywords: HIV-1; HIV-1 capsid; GS-CA1; mass spectrometry; NPC; nuclear envelope

Introduction

HIV-1 capsid (CA) proteins have a central role in several of early post-entry stages of infection, including retrograde transport, nuclear import and integration (252-256). In particular, CA is key to HIV-1 nuclear import through nuclear pore complexes (NPCs), which are large protein channels embedded in the nuclear envelope. Comprising multiple copies of Nups, NPCs facilitate the bidirectional transport of macromolecules such as proteins, RNA and ribonucleoprotein complexes (reviewed in (257)). About one-third of Nups contain phenylalanine-glycine-rich motifs (FG repeats) and are important for the selection of cargos to be transported through NPCs (258). Consistent with its central role in nuclear import, CA was found to interact with several FG-containing Nups, such as Nup88, Nup214, Nup358/RanBP2 (cytoplasmic side); Nup62, Nup98, Nup107 (central ring); and Nup153 (nuclear basket) (reviewed in (84)). These findings have led to a model whereby the capsid core interacts sequentially with various Nups present in NPCs, driving its import to the nucleus; according to this model, the capsid core would act as its own transporter for nuclear import (84). Interestingly, HIV-1 was also found to modulate the levels of Nup358 at NPCs , which opens the possibility that HIV-1 cores affect NPCs integrity instead of simply using them to achieve passage to the nucleus.

Current HIV pharmacological treatments rely largely on targeting the viral enzymes protease, reverse transcriptase and integrase. By contrast, GS-CA1 and the structurally close GS-6207 (lenacapavir) are CA inhibitors that disrupt viral capsid formation by interfering with CA-CA interactions (183). In clinical trials, GS-6207/lenacapavir has demonstrated efficacy against multidrug-resistant HIV-1 strains and was approved in 2022, first by the European Union and then in the United States and Canada, for the treatment of heavily treatment-experienced individuals (226). GS-CA1 has not been pursued in humans but showed a strong protective effect against HIV-1 in a primate model (181). Consistent with the important role for CA in both early and late stages of the virus life cycle, GS-CA1 and GS-6207 have pleiotropic effects on HIV-1 (183, 220). Their effects on early stages seem to stem from a stabilization of the viral capsid core, as seen in “fate-of-capsid assays” using cores isolated from acutely infected cells as well as virus core-like “tubes” assembled *in vitro* from recombinant CA (220). Quantitative analyses of reverse transcribed HIV-1 cDNA as well as its specifically nuclear species (2-LTR DNA and integrated DNA) suggest that

GS-CA1 and GS-6207 can inhibit several early HIV-1 replication steps. At relatively low doses, the HIV-1 cDNA is produced and imported to the nucleus, but integration is inhibited; at higher doses, nuclear import is affected as well; and at yet higher concentrations, reverse transcription is inhibited in addition to nuclear import (183, 220). Another group also proposed that GS-6207 inhibits nuclear import (259). Consistent with these observations, GS-6207 was found to decrease HIV-1 integrase punctate signal in the nucleus, reinforcing the notion that nuclear import was affected (220). However, discordant results were obtained from another team, who did not observe an effect of GS-CA1 on CA presence in the nucleus following infection (213). Whether GS-CA1 and GS-6207 cause HIV-1 to be specifically sequestered at NPCs is unknown. In addition, the combined effects of these CA-targeting drugs and of HIV-1 on the integrity of NPCs are also unknown. Here, using mass spectrometry and immunofluorescence microscopy, we evaluated the impact of HIV-1 infection and GS-CA1 treatment, as well as beta interferon (IFN-β) treatment, on the nuclear envelope and the localization of HIV-1 capsid cores at the nuclear envelope and nuclear pores.

Materials and methods

Cell culture

THP-1 monocytic cells were cultured in RPMI 1640 medium (HyClone, Thermo Scientific, USA) supplemented with 10% fetal bovine serum (FBS, HyClone) and antibiotics (Penicillin and Streptomycin, HyClone). Crandell-Rees Feline Kidney (CRFK) cells and human embryonic kidney 293T cells (HEK293T) were maintained in DMEM (HyClone) supplemented with 10% FBS and penicillin/streptomycin (HyClone).

HIV-1 vector production and titration

To produce the GFP-expressing HIV-1 vector $NL43_{GFP}$, HEK293T cells were transfected with 10 µg $pNL43_{GFPDEnvDNef\ (228,\ 260)}$ and 5 µg pMD2G (228) using polyethyleneimine (PEI, Polysciences, Niles, IL) (261) for 16 h, after which the supernatants were replaced with fresh medium (228). The supernatants were collected 24 and 48 h later. Cell debris were removed by low-speed centrifugation (3,000 rpm, 10 min at room temperature), followed by filtration through 0.45 µm filters (Millipore Sigma Durapore PVDF). Virus titrations were performed by infecting

CRFK cells with serial dilutions of the vector preparations. CRFK cells were fixed in PBS containing 4% formaldehyde, and the percentage of infected cells was assessed by flow cytometry using a Beckman Coulter FC500 instrument. CRFK viral titers were calculated by analyzing flow cytometry results using FCS Express 6 software (De Novo Software).

EC_{50} determination

THP-1 cells were seeded at a density of 20,000 cells/well in 96-well plates. Cells were then treated with 2-fold serial dilutions of GS-CA1 and 2 h later were infected with $NL43_{GFP}$ (CRFK MOI = 1). 48 h later, cells were fixed in 4% formaldehyde and the percentage of GFP-positive cells was determined using flow cytometry. GS-CA1 EC_{50} was calculated using an online tool available at https://www.aatbio.com/tools/ic50-calculator.

Large-scale infections and nuclear envelope purification

2 x 10^7 THP-1 cells cultured in flasks were treated or not with GS-CA1 (Gilead Sciences, Foster City, California, USA) for 2 h and then were infected or not with $NL43_{GFP}$ (MOI = 2) for 12 h. In a distinct experiment, cells were treated or not with IFN-b (10 ng/ml; PeproTech, Rocky Hill, NJ, USA) and were infected 12 h later with $NL43_{GFP}$ for 12 h. A small aliquot of the cells was preserved for flow cytometry analysis 36 h later. The remainder of the cells were processed for the extraction of nuclear envelope-enriched fractions using a Minute™ Nuclear Envelope Protein Extraction Kit (Invent Biotechnologies, Plymouth, MN, USA). Whole-cell lysates, cytoplasmic extracts, and nuclear extracts also prepared using the same kit were included in the purification validation experiments.

Western blotting

Protein concentrations in the nuclear envelope extracts were determined using the Bio-Rad Protein Assay kit and samples were normalized accordingly prior to SDS-polyacrylamide gel electrophoresis and transfer to polyvinylidene difluoride (PVDF) or nitrocellulose membranes. Blotted proteins were analyzed using the FG repeats-specific MAb414 mouse monoclonal antibody at 1:2,000 dilution (BioLegend, San Diego, CA), followed by detection with an HRP-conjugated anti-mouse secondary antibody (Cell Signaling Technology, Whitby, Ontario). Detection of glyceraldehyde phosphate dehydrogenase (GAPDH) using the 9484 mouse monoclonal antibody (Abcam, Toronto, ON) was used as a marker for cytosolic proteins. Blots

were visualized using the Thermo Scientific SuperSignal West Femto substrate, and images were recorded using the Bio-Rad ImageLab system.

Mass spectrometry

10 µg of protein from nuclear envelope-enriched fractions were reduced using 0.2 mM dithiothreitol, alkylated using 0.8 mM iodoacetamide and digested with 0.2 µg of trypsin (sequencing grade, Promega, Madison, WI). Samples were analysed by nano-LC/MSMS using a Dionex UltiMate 3000 nanoRSLC chromatography system (Thermo Fisher Scientific) interfaced to an Orbitrap Fusion mass spectrometer (Thermo Fisher Scientific, San Jose, CA, USA) equipped with a nanoelectrospray ion source. 1 µg of peptides were separated on a C18 Pepmap Acclaim column (50 cm length, 75 µm internal diameter) using a 90 min linear gradient at 300 nL/min with 5-40% solvent B (A: 0.1% formic acid, B: 80% acetonitrile, 0.1% formic acid). Mass spectra were obtained with a data-dependent acquisition method using the Thermo XCalibur software version 4.1.50. Full scan mass spectra (350–1800 m/z, 120,000 resolution) were acquired from Orbitrap using an AGC target of 4e5 with a maximum injection time of 50 ms. Precursors were filtered in the quadrupole analyzer with 1.6 m/z isolation windows and fragmented by higher-energy Collision-induced Dissociation (HCD) with 35% collision energy. The resulting fragments were detected using the linear ion trap at a rapid scan rate with an AGC target of 1e4 and a maximum injection time of 50 ms.

MS data analysis

For the IFN-β-treated THP-1 cells experiment, the acquired spectra were processed using the Minora feature detector algorithm in Proteome Discoverer 2.3 (Thermo Fisher Scientific). The resulting data were subjected to MASCOT searches against the UniProt *Homo sapiens* protein database (reference proteome UP000005640 with 74485 entries, downloaded on 2019-02-12) considering trypsin digestion. For protein validation, a false discovery rate (FDR) of ≤ 0.01 was allowed at peptide and protein levels based on a target/decoy search. Unique and razor peptides were considered for protein quantification, and normalization was performed based on the summed abundance of the peptides. The data were normalized using the intensity normalization factor, which was calculated by dividing the median intensity for each sample by the median intensity for all samples combined. The results were exported to an Excel file where samples were compared

to each other using absolute Z-score > 1.96, q-value < 0.05 and log2 ratio between the two conditions > 0, in order to determine the statistical significance of the observed variations. For the GS-CA1 experiments, spectra were analyzed in Maxquant using the Andromeda search engine (version 2.0.2.0) against a UniProt *Homo sapiens* protein database (reference proteome UP000005640 with 97094 entries, downloaded on 2020-09-24). Trypsin was set as the digestion parameter and a maximum FDR of 1% was set both at the peptide and protein level. The proteinGroups.txt output file was imported into R software and the LFQ normalized intensities were used to compare the groups considering the same z-score and q-value thresholds as above.

In silico analysis

UniProt was used as the main source for summarized information on protein names, gene names, protein localization and protein functions. Their putative interactions with HIV-1 proteins were compiled using the NCBI HIV-1 human interaction database available at the NCBI website.

Microscopy

THP-1 cells were infected with $NL43_{GFP}$ (MOI = 1) for 48 h in the presence or absence of IFN-β (added 12 h before infection) and GS-CA1 (added 2 h before infection) before fixation with 4% formaldehyde. The cells were permeabilized with Triton (0.2%) in 1x PBS for 10 min. Cells were then stained for HIV-1 CA protein using a mouse monoclonal antibody (Clone 183 diluted 1:5000, AIDS Research Reagents Program, contributed by Bruce Chesebro), co-stained for Nup TPR (rabbit antibody, 1:1000 dilution, Abcam), and for DNA using Hoeschst 333422 (262). Alexa Fluor 488 anti-mouse and 594 anti-rabbit secondary antibodies were used (1:5000 dilution, Molecular Probes). Images were acquired with a Leica TSC SP8 confocal microscope fitted with a 63×/1.40 oil objective using the optimal resolution for the wavelength (determined using the Leica software). CA signal dots were counted out of 19-20 slides for each condition, and CA dots that co-localized with the TPR signal were counted as well, allowing us to calculate the co-localization ratio. Counting was performed blindly, from anonymized pictures and by a student who was not involved in the “wet lab” phase of the experiment.

Results

GS-CA1 efficiently inhibits early stages of HIV-1 infection in THP-1 cells

THP-1 monocytic cells are representative of the monocyte-macrophage lineage, one of the main types of HIV-1 host cells *in vivo* (263). To assess the effects of GS-CA1 on the early steps of HIV-1 infection in these cells, we used an NL4-3-derived HIV-1 vector expressing GFP in place of Nef (260). THP-1 cells were challenged with $NL43_{GFP}$ in the presence of multiple drug concentrations, and the percentage of GFP-positive cells was determined using flow cytometry (Figure 3.1A). We found that GS-CA1 strongly inhibits THP-1 infection, with an EC_{50} of approximately 0.125 nM (Figure 3.1A), which is consistent with previous studies.

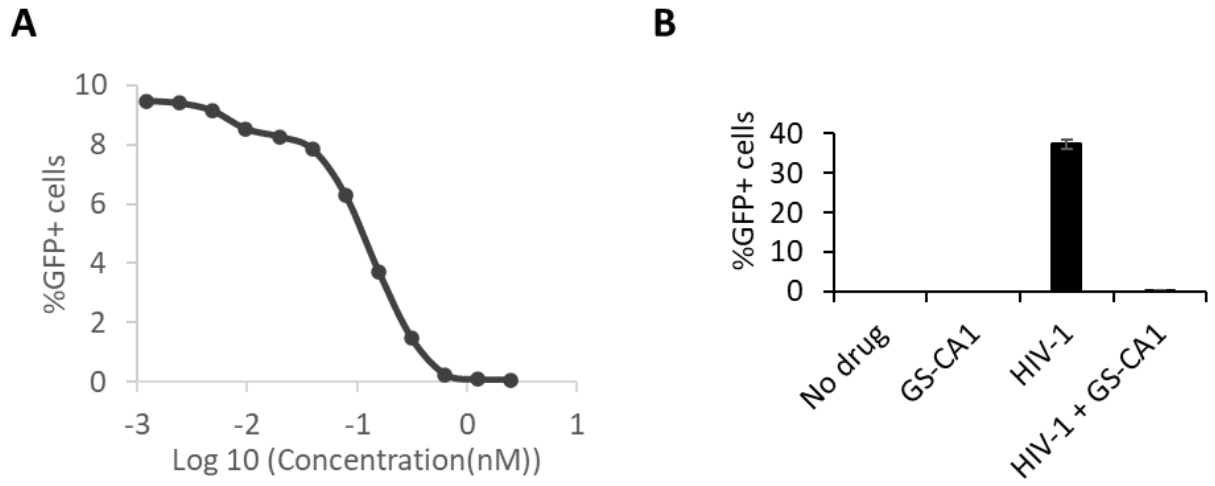

Figure 3.1: GS-CA1 efficiently inhibits HIV-1 early infection stages in THP-1 cells. (A) Dose-dependent inhibition of $NL43_{GFP}$. THP-1 cells were treated with multiple dilutions of GS-CA1 and infected with $NL43_{GFP}$ for 48 h. % GFP-positive cells were determined by FACS. (B) Infection control in mass spectrometry (MS) experiments. Cells were infected or not with $NL43_{GFP}$ (CRFK MOI = 2) and treated or not with 2 nM GS-CA1. 12 h later, cells were processed for MS but small aliquots were placed back in culture for one more day. % GFP-positive cells were determined by FACS. Shown are average data from 5 replicates, with standard deviations.

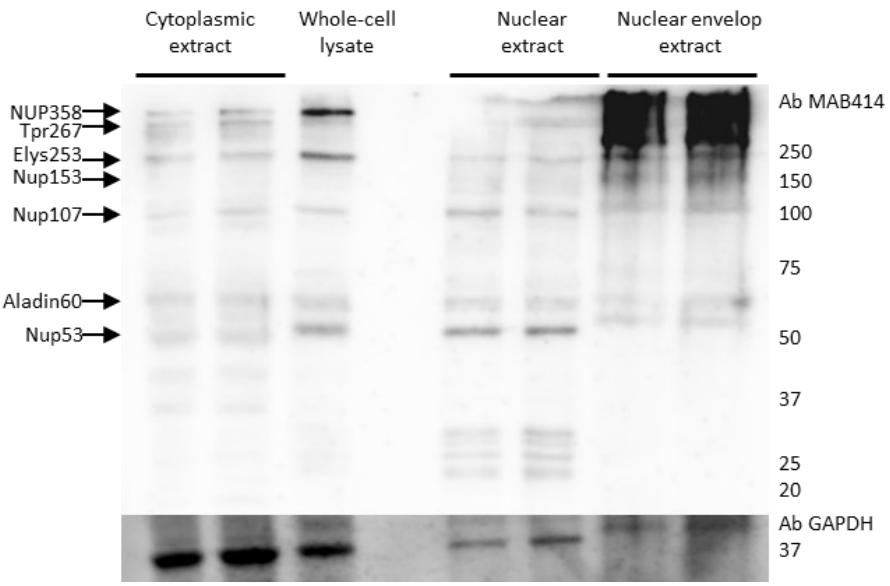

Figure S3.1: Western blot analysis of nuclear envelope-enriched fractions, using the Mab414 antibody specific for FG repeats and the GAPDH as a cytoplasmic control.

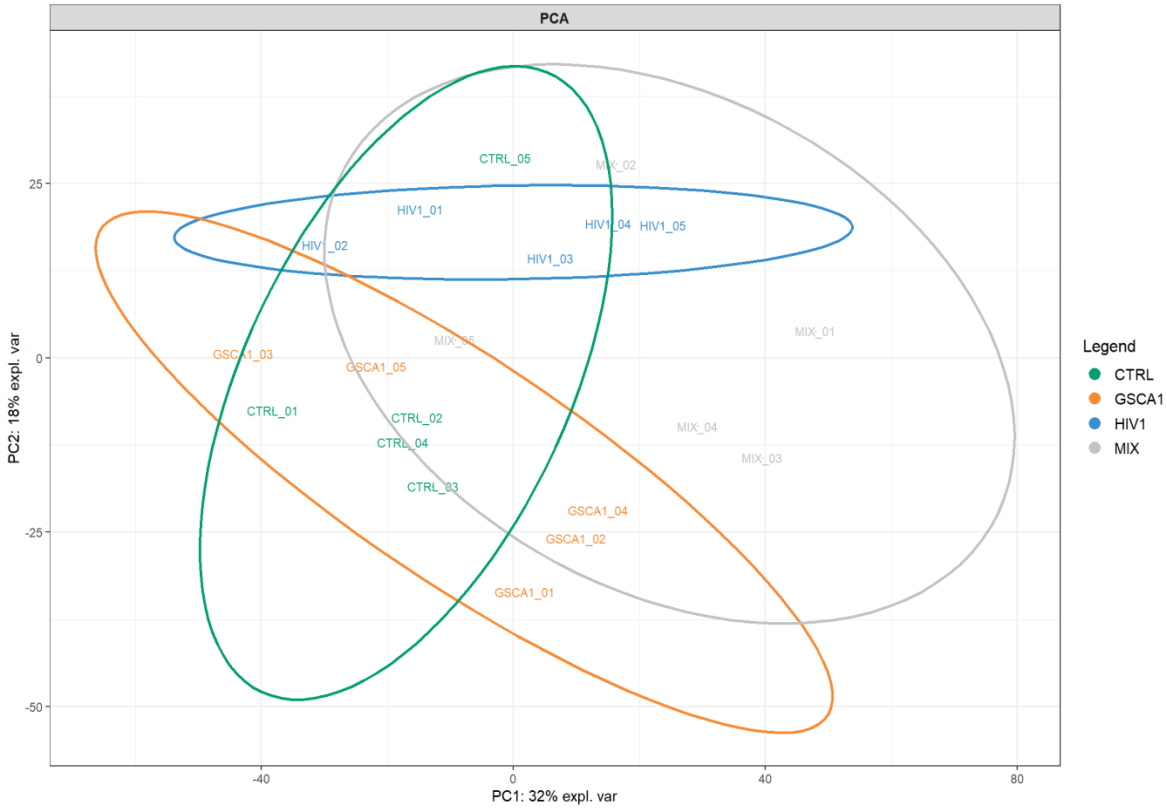

Figure S3.2: Principal component analysis (PCA) shows variability between samples. PC1 (x-axis) explained 32% of data variability, whereas PC2 (y-axis) explained 18%. The color code

is as follows: Control, light blue; GS-CA1 treatment, orange; HIV-1-infected, grey; MIX (HIV1 + GS-CA1), green. PCA was performed using the z-scores of all proteins in all samples. The distance between dots indicates the level of dissimilarity between replicates.

Isolation of nuclear envelopes for mass spectrometry analyses

To analyze the effects of HIV-1 vector infection and/or drug treatment on nuclear pore proteins, we produced nuclear envelope-enriched fractions. First, we performed a pilot experiment with uninfected/untreated cells, to assess nuclear envelope extracts extracted using a commercial kit (S3.1). Whole-cell, cytoplasmic, nuclear and nuclear envelope protein lysates were obtained. "Nuclear" fractions are supernatants of the nuclear envelope precipitation step. Fractions were analyzed by Western blotting with the monoclonal antibody MAb414 which recognizes several Nups through binding to the FG repeats (264). Using this antibody, we observed an enrichment in bands above 150 kDa in the nuclear envelope fractions, consistent with the high molecular weight of several FG-containing Nups. Some bands were specific to nuclear extracts (e.g., between 20 and 35 kDa), whereas others were specific to cytoplasmic extracts (around 40 kDa); it is unclear whether these are true Nups that did not co-purify with nuclear envelopes, or whether they are non-Nups recognized by the antibody in an unspecific fashion. As expected, the protein glyceraldehyde 3-phosphate dehydrogenase (GAPDH) was absent from the nuclear envelope fractions (Figure S3.1).

In the next experiment, THP-1 cells were infected or not with $NL43_{GFP}$ for 12 h, in the presence or absence of 2 nM GS-CA1. Quintuplicate infections were performed at a multiplicity of infection leading to about 40% infected cells in the absence of drug (Figure 3.1B). The GS-CA1 concentration used was 16-times higher than the observed EC_{50}. As expected, infection with the $NL43_{GFP}$ vector was completely abrogated at this concentration (Figure 3.1B). Nuclear envelope extracts were subjected to label-free mass spectrometry (MS). The principal component analysis (PCA) shown in Figure S3.2 demonstrates that the control and GS-CA1 treated cells show only minor differences (except for sample CTRL_5), whereas the $NL43_{GFP}$-infected ("HIV1") group and the $NL43_{GFP}$-infected + GS-CA1-treated ("MIX") group are clearly distinct. Figure S3.3 summarizes the number of proteins quantified for each condition, as well as the number of proteins found to be regulated in pairwise analyses, showing that the greatest number of dysregulated

proteins is found when comparing HIV-1 + GS-CA1 to either control samples or GS-CA1-treated ones.

Effect of HIV-1 and GS-CA1 on nuclear envelope-associated proteins as seen by mass spectrometry

Volcano plots were created based on the MS data in order to visually identify the most dysregulated proteins between two conditions (Figure. 3.2). With the threshold parameters used (z-score ≥ or ≤ 1.96; p-values and q-values ≤ 0.05), we found that HIV-1 vector infection alone and GS-CA1 treatment alone had little impact on nuclear envelope proteins, as previously observed in the PCA (Figure S3.2). HIV-1 ($NL43_{GFP}$) infection resulted in the reduced relative abundance of only 5 proteins, *i.e.* Lysozyme C (gene name: LYZ), pH domain leucine-rich repeat-containing protein phosphatase 1 (PHLPP1), NEPRO (Nucleolus and neural progenitor protein; C3orf17), DEAD/H-box helicase 12 pseudogene (DDX12P) and tetratricopeptide repeat protein 37 (TTC37). The abundance of two proteins was increased by HIV-1 infection, *i.e.* forkhead box protein K1 (FOXK1) and Syntaxin-11 (STX11). Treatment with GS-CA1 led to the downregulation of only one cellular protein, signal recognition particle 19 (SRP19). Of note, none of the proteins found to be regulated by HIV-1 or GS-CA1 is known as an integral protein of the nuclear envelope, raising the possibility that they are either transiently associating with the nuclear envelope, or possibly contaminants. In contrast, HIV-1 infection in the presence of GS-CA1 altered the levels of 84 proteins, with 71 upregulated and 13 downregulated proteins. A full list of proteins regulated by HIV-1 and/or GS-CA1 is made available (see supplementary material). Again, most of these 84 proteins are not known as permanent nuclear envelope residents. Interestingly, several of them are ISG products, according to the Interferome database (265), whereas others are involved in the ubiquitin/proteasome pathway, as detailed in the Discussion section. We also performed single-variable comparisons, i.e. HIV-1 + GS-CA1 vs HIV-1 and HIV-1 + GS-CA1 vs GS-CA1 (Figure S3.4), and interestingly, we observed that GS-CA1 treatment was a much greater inducer of variation than HIV-1.

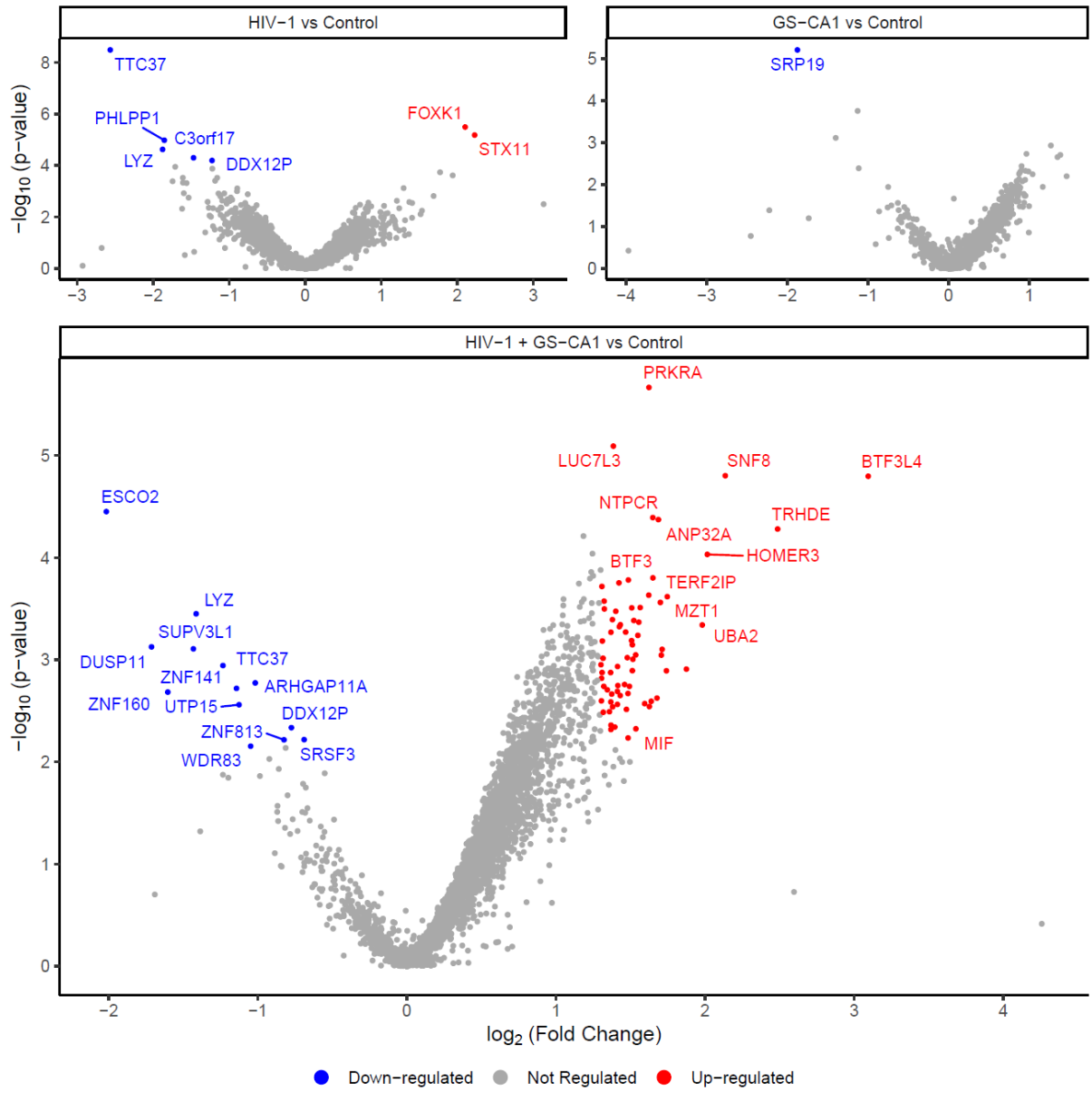

Figure 3.2: Modulation of proteins in nuclear envelope-enriched fractions by HIV-1 infection and GS-CA1 treatment. THP-1 cells were infected or not with $NL43_{GFP}$ (CRFK MOI = 2) and treated or not with 2 nM GS-CA1. Infections were done in quintuplicates. 12 h later, cells were processed for MS. Volcano plots show dysregulated proteins for $NL43_{GFP}$-infected cells compared to control (uninfected) cells (top left), GS-CA1-treated cells compared to control (untreated) cells (top right) and $NL43_{GFP}$-infected, GS-CA1-treated cells compared to control (uninfected, untreated) cells (bottom). Colored dots indicate proteins upregulated (red) or downregulated (blue). Grey dots indicate non-dysregulated proteins.

A

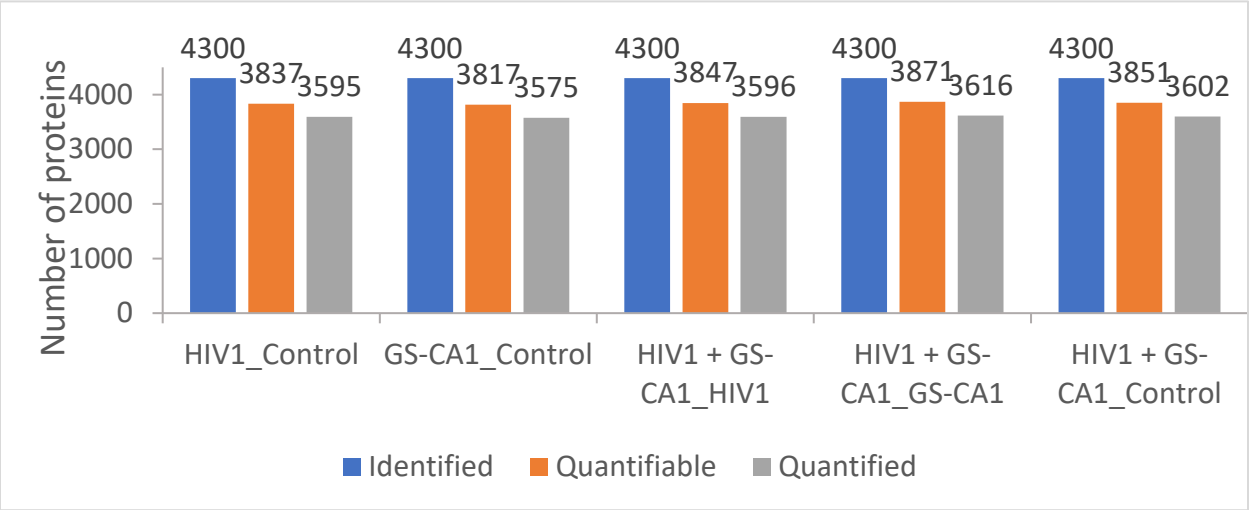

B

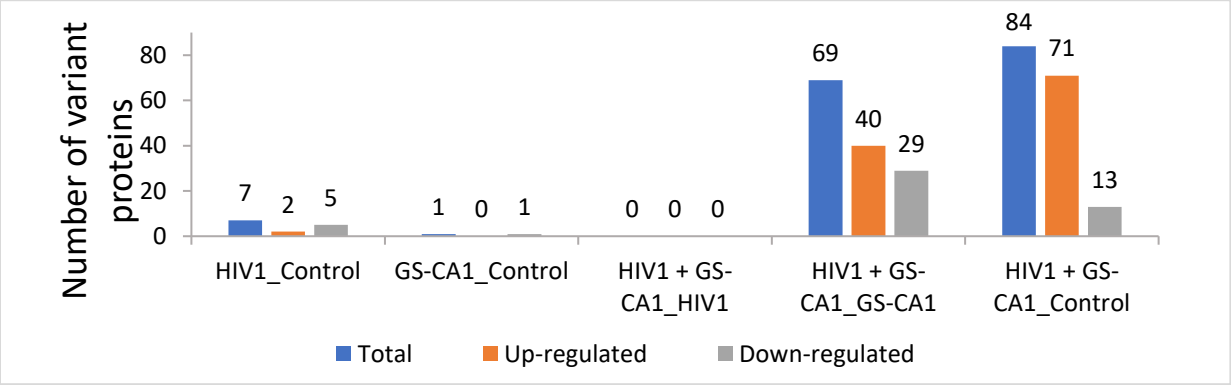

Figure S3.3: HIV-1 infection in the presence of GS-CA1 modulates many proteins. (A) Identified, quantifiable, and quantified proteins in comparison analyses. Identified proteins are total proteins identified in this analysis based on the presence of unique peptides; quantifiable proteins (orange) are proteins identified in all replicates of at least one of the two groups (4300 proteins were quantifiable on average for the whole analysis); quantified proteins (gray) are quantifiable proteins with at least two peptides. (B) Number of proteins found to be dysregulated. Blue bars show the total modulated proteins in each condition, orange bars indicate upregulated proteins, and gray bars represents downregulated proteins.

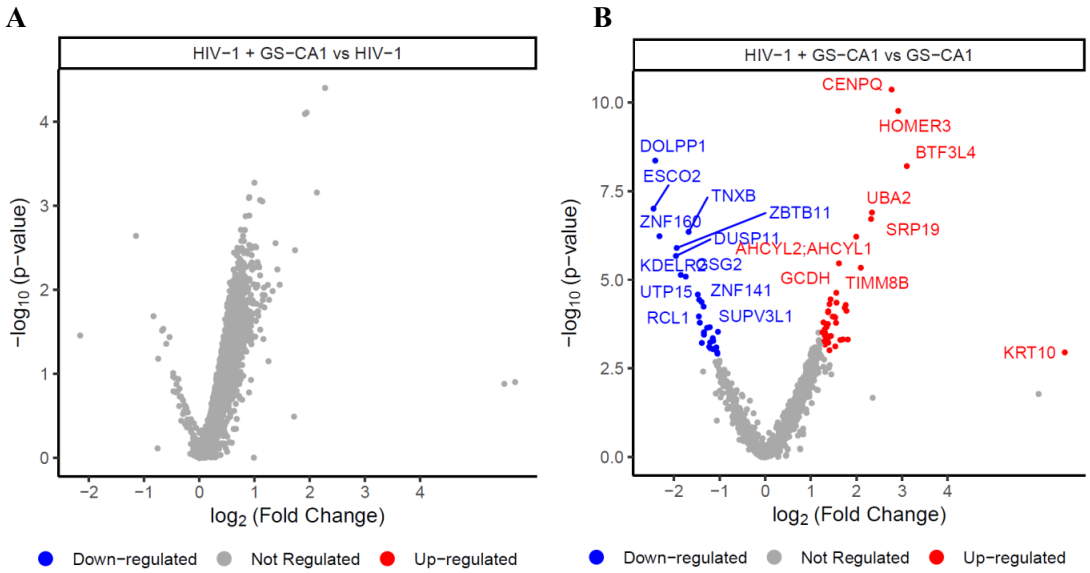

Figure S3.4: Effect of GS-CA1 on nuclear enriched fraction (in the presence of HIV-1 infection) MS analysis of nuclear envelope-enriched fractions from HIV-1 ($NL43_{GFP}$)-infected and GS-CA1-treated THP-1 cells, compared to HIV-1-infected cells (A) and compared to GS-CA1-treated cells (B). Colored dots indicate the upregulated (red) or downregulated (blue) proteins whereas gray dots indicate non-modulated proteins. The threshold parameters used are the same as in Figure. 2.

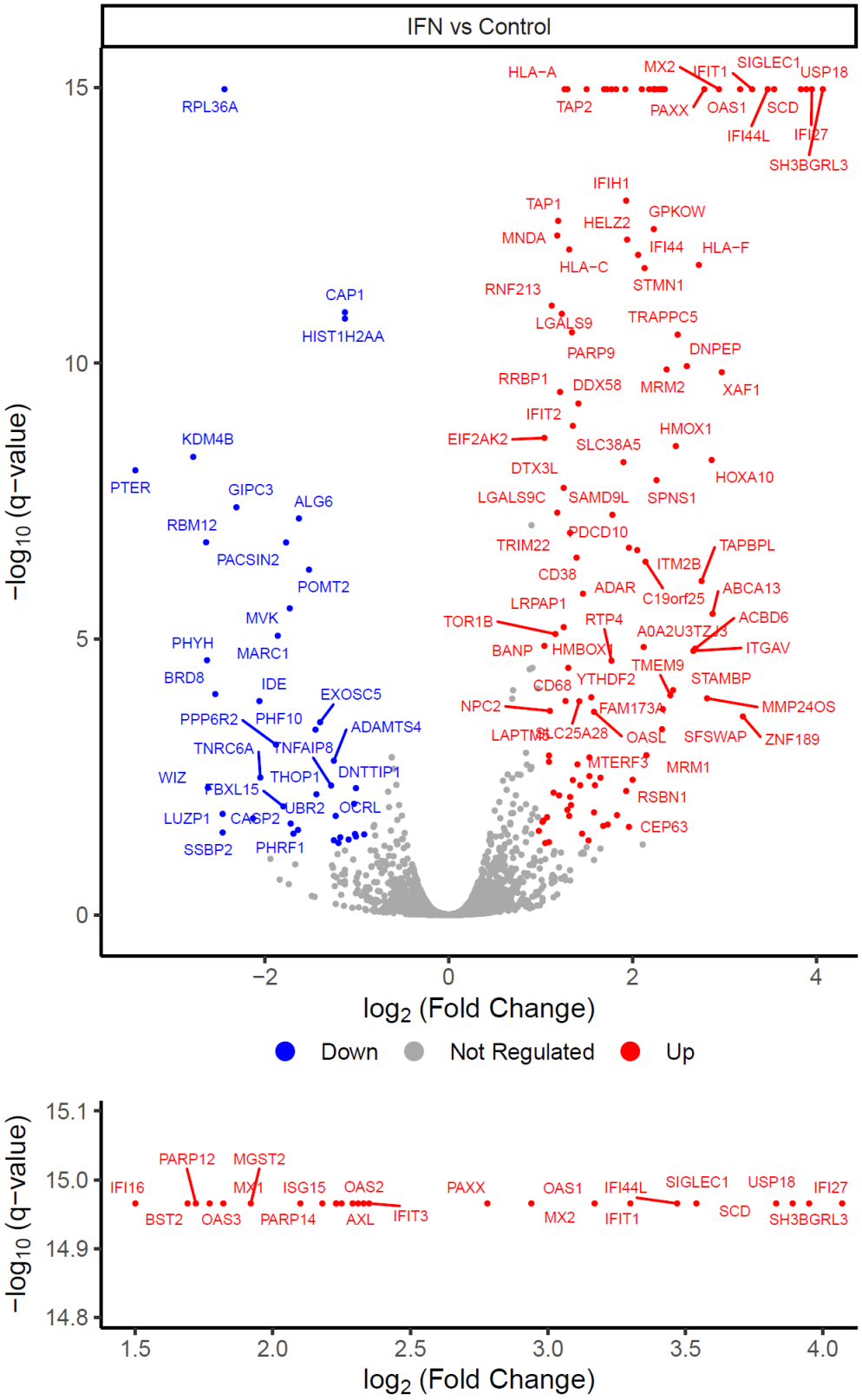
IFN vs Control
HLA−A
MX2
IFIT1
SIGLEC1
USP18
RPL36A
TAP2
PAXX
OAS1
SCD
IFI44L
IFI27
SH3BGRL3
IFIH1
TAP1
GPKOW
HELZ2
MNDA
IFI44
HLA−F
HLA−C
STMN1
CAP1
RNF213
HIST1H2AA
LGALS9
TRAPPC5
PARP9
DNPEP
RRBP1
DDX58
MRM2
XAF1
IFIT2
KDM4B
EIF2AK2
SLC38A5
HMOX1
DTX3L
HOXA10
PTER
GIPC3
LGALS9C
SAMD9L
SPNS1
ALG6
RBM12
PDCD10
TRIM22
TAPBPL
PACSIN2
ITM2B
CD38
ADAR
C19orf25
ABCA13
POMT2
LRPAP1
MVK
TOR1B
RTP4
ACBD6
A0A2U3TZJ3
PHYH
MARC1
BANP
HMBOX1
ITGAV
TMEM9
BRD8
IDE
CD68
YTHDF2
STAMBP
EXOSC5
NPC2
FAM173A
MMP24OS
PPP6R2
PHF10
ADAMTS4
LAPTM5
SLC25A28
OASL
SFSWAP
ZNF189
TNRC6A
TNFAIP8
MTERF3
MRM1
WIZ
THOP1
DNTTIP1
FBXL15
RSBN1
UBR2
OCRL
LUZP1
CASP2
CEP63
SSBP2
PHRF1
−log10 (q−value)
log2 (Fold Change)
Down
Not Regulated
Up
PARP12
MGST2
IFI16
MX1
ISG15
OAS2
PAXX
OAS1
IFI44L
SIGLEC1
USP18
IFI27
BST2
OAS3
PARP14
AXL
IFIT3
MX2
IFIT1
SCD
SH3BGRL3

Figure S3.5: Volcano plot showing proteins significantly modulated in an MS analysis of nuclear envelope-enriched fractions from THP-1 cells treated with IFN-β, compared with the untreated control. Colored dots indicate upregulated (red) or downregulated (blue) proteins whereas gray dots indicate non-modulated proteins. The plot at the bottom shows an enlargement for the highly upregulated proteins. The parameters used are the same as before.

Finally, in order to ascertain that the mass spectrometry approach chosen can detect an expected modulation pattern, we also treated THP-1 cells with IFN-β and then analyzed nuclear envelope-enriched fractions from treated and untreated cells (Figure S3.5). Results showed that 55 proteins were regulated, including 10 downregulated and 45 upregulated. As expected, most upregulated proteins were ISGs, including known antiviral factors such as MX2 and ISG15.

IFN-β but not GS-CA1 causes the accumulation of HIV-1 at the nuclear envelope

GS-CA1 was proposed to induce a block to nuclear import, though this is still disputed. Thus, we analyzed the presence in the nuclear envelope-enriched fractions of HIV-1 proteins-derived peptides, which were not included in the results shown in Figure 3.2. We performed an identical analysis in cells treated or not with IFN-β, as this drug promotes the expression of ISGs, including MX2 which was proposed to interfere with HIV-1 nuclear import by binding CA proteins (144). All the peptides detected were from the structural proteins matrix (MA) and capsid (CA). GS-CA1 did not result in any noticeable modulation in the relative abundance of these peptides in $NL43_{GFP}$-infected cells (Figure 3.3A). Remarkably, in the presence of IFN-β, a substantial increase in several of the HIV-1 peptides in the nuclear envelope extracts was evident (Figure 3.3B). These results point to differences in the mechanisms of action of GS-CA1 and IFN-β , with the latter promoting the significant accumulation of HIV-1 proteins in nuclear envelope-associated fractions.

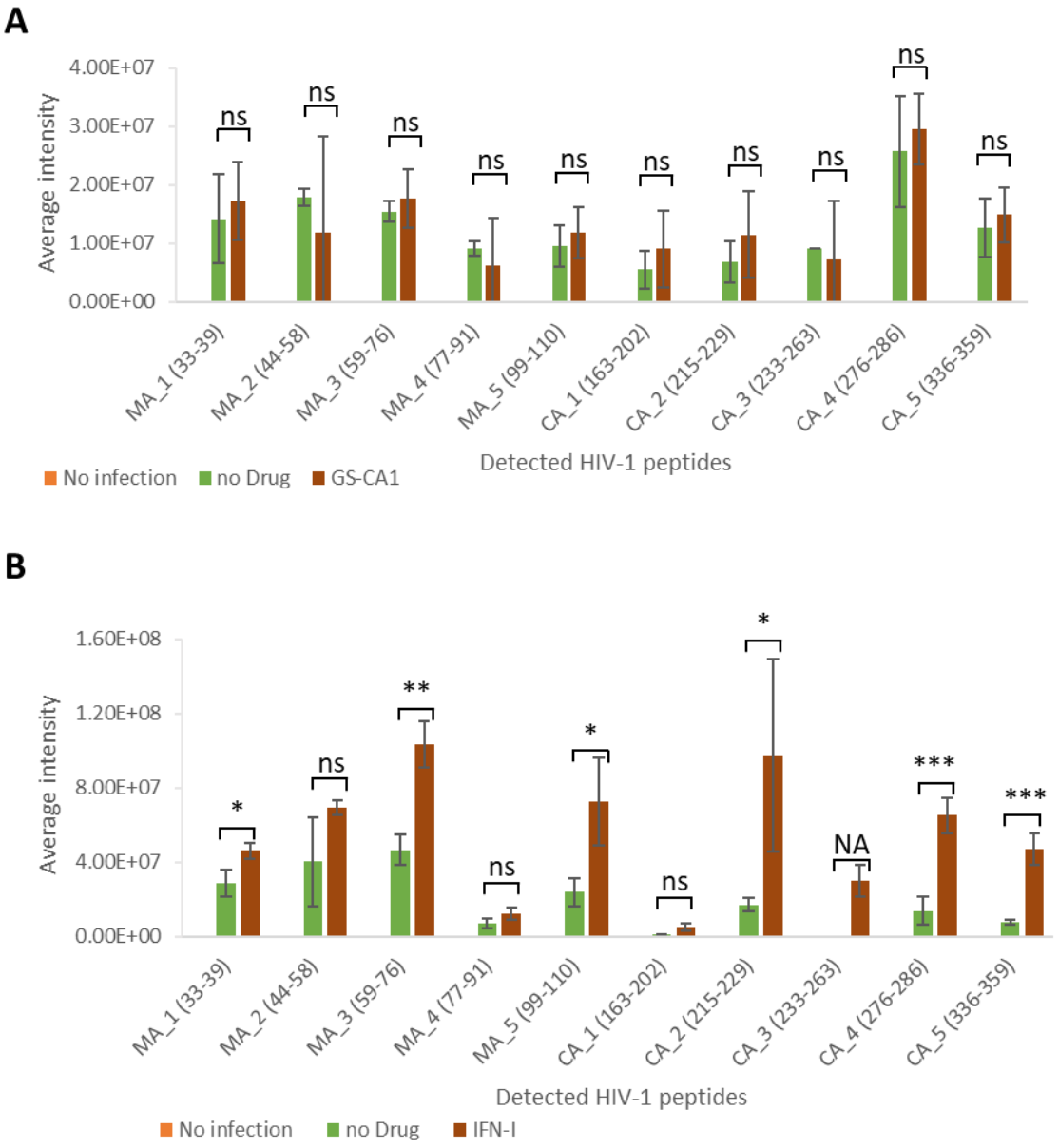

Figure 3.3: HIV-1 protein levels in nuclear envelope fractions are modulated by IFN-β but not GS-CA1. (A) Intensity of HIV-1 protein-associated peptides detected by MS in nuclear envelope-enriched fractions following infection with the $NL43_{GFP}$ vector in absence or presence of GS-CA1, or in uninfected, untreated cells as a control. Bars represent the average values from 5 replicates, with standard deviations. (B) Intensity of HIV-1 peptides in nuclear envelope-enriched fractions from cells infected with $NL43_{GFP}$ and treated or not with IFN-β. Bars represent the average values from 3 replicates, with standard deviations. In both (A) and (B), only peptides with intensity levels significantly above background were included. Statistical significance was determined using the one-tailed t-test. * $p < 0.05$; ** $p < 0.005$; *** $p < 0.0005$.

HIV-1 significantly colocalizes with TPR in the presence of GS-CA1

To evaluate the impact of GS-CA1 on HIV-1 cellular distribution in the early stages of the infection, we conducted immunofluorescence microscopy experiments, staining for HIV-1 CA as well as the Nup TPR as a nucleopore marker. As shown Figure 3.4A, HIV-1 CA signal was present mostly as small "dots" which were found throughout the cells in the conditions used. Based on previous work from our team and others, those dots are expected to represent mostly individual HIV-1 cores/replication complexes (266-268). TPR was found almost entirely at the nuclear envelope and was partially found in the form of punctate signal consistent with NPCs. In a blinded analysis, we quantified the percentage of CA "dots" colocalizing with TPR, in absence or presence of GS-CA1 and IFN-β. Colocalization examples are shown by white arrows in Figure 3.4A, whereas the quantification analysis is shown in Figure 3.4B. We found that in the presence of GS-CA1, the relative number of HIV-1 CA signal colocalizing with TPR significantly increased, by about 8-fold. Treatment with IFN-β also resulted in an increase in CA-TPR colocalization, but this phenotype was significantly smaller compared with GS-CA1 (Figure 3.4B). However, IFN-β induced a distinct CA distribution, *i.e.* its accumulation in the immediate vicinity of the nuclear envelope, but not particularly at TPR-positive nuclear pore (see blue arrows in Figure 3.4A). These results again point to differences in the effects of GS-CA1 and IFN-β on HIV-1 early stages and are consistent with GS-CA1 causing the sequestration of HIV-1 at NPCs, albeit this concerns a very small proportion of detectable HIV-1 in the infected cells.

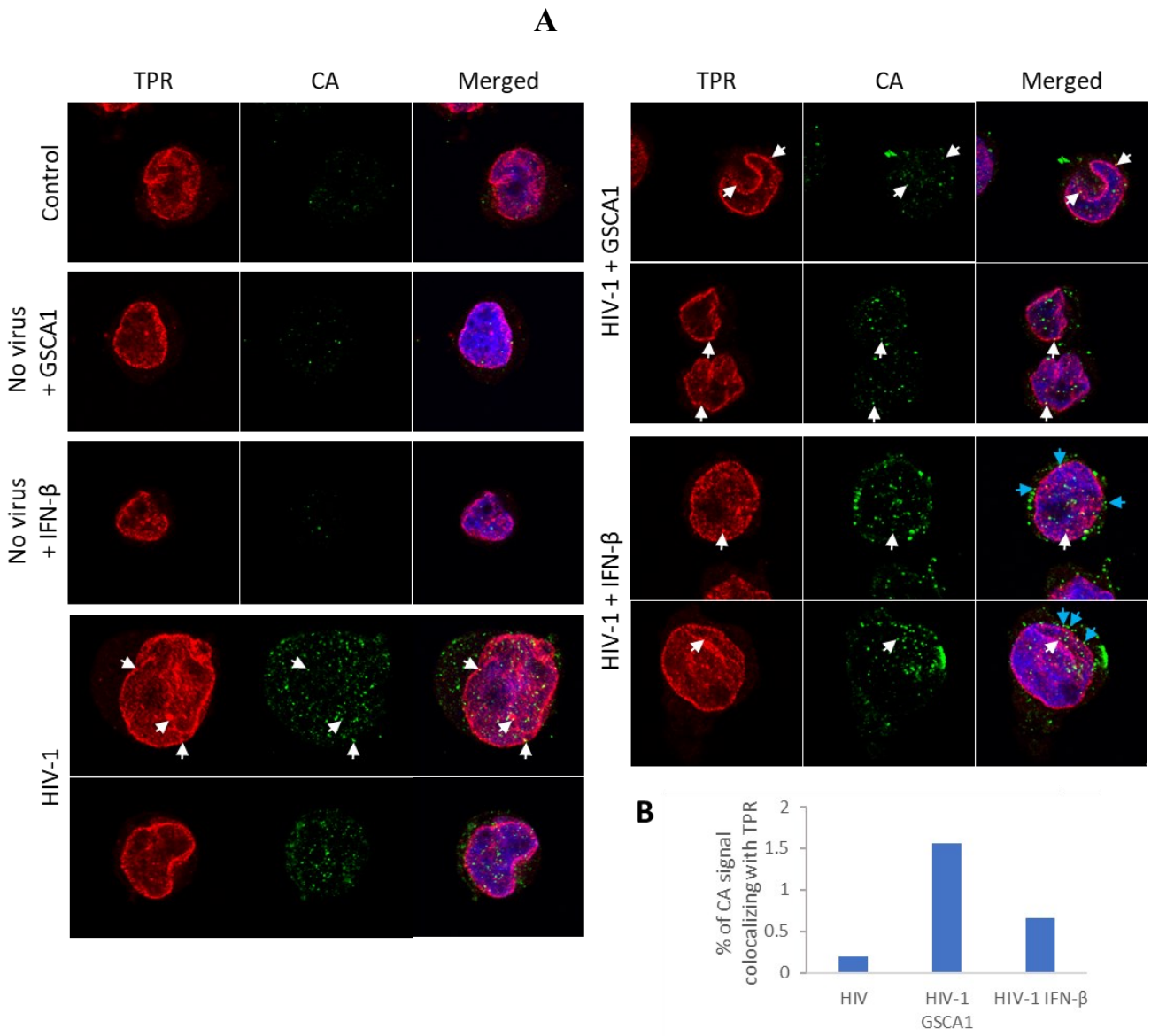

Figure 3.4. Effect of GS-CA1 and IFN-β on HIV-1 subcellular distribution. (A) THP-1 cells were infected with $NL43_{GFP}$ (CRFK MOI = 2) for 12 h in the presence or absence of either IFN-β added 12 h before infection) or GS-CA1 (added 2 h prior to infection). Cells were then fixed and stained with a CA antibody (green) and a TPR antibody (red). Hoeschst 33342 was used to reveal DNA (blue). White arrows show examples of the CA-TPR co-localization whereas cyan arrows point to examples of CA signal accumulating in the vicinity of the nuclear envelope. (B) 20 randomly selected fields for each condition were used to count the percentage of CA signal "dots" colocalizaing with TPR, relative to the total number of CA signal dots.

Discussion

Considering its very low effective concentrations and advantageous pharmacodynamic properties, it is likely that usage of GS-6207 will expand in the future, as indicated by clinical trials under way (216). Thus, the mechanisms of action for this new class of HIV drugs need to be established more thoroughly. When this project was initiated, GS-6207 was not approved yet, and the compound was not made available to us, but GS-CA1 was. We focused on the effect of GS-CA1 on HIV-1 functional interactions with the nuclear envelope. Mass spectrometry on nuclear envelope-enriched fractions had been done in the context of late stages of HIV-1 replication (269). To the best of our knowledge, no similar investigation had been conducted focusing on the early stages of the infection. We found that few proteins were modulated by either HIV-1 infection or GS-CA1 treatment alone, though of course, a different conclusion may be reached by using less stringent threshold parameters. Although SRP19 (downmodulated by GS-CA1) has been linked to the antiviral effect of APOBEC3G , none of the proteins found to be modulated are known to be involved in the early stages of HIV-1, and none are *bona fide* NPC components. The results obtained were strikingly different in cells that were both infected and GS-CA1-treated, since we found 71 upregulated and 13 downregulated proteins, upon comparison with the control cells. It is unlikely that the difference in phenotype between, on one hand, HIV-1 alone or GS-CA1 alone, and on the other hand, the HIV-1 + GS-CA1 combination, is due to cytotoxicity. The concentration of GS-CA1 used in this experiment, 2 nM, is well below the cytotoxic concentrations for this drug (CC50 > 30 μM (183)). Also, less than half of the cells were infected in the control without drug in this experiment (Figure 3.1B), making it unlikely that the dose of virus used would have cytotoxic effects after 16 h of infection. Thus, we conclude that the modulation of nuclear envelope proteins in these conditions stems from the inhibition of the virus by GS-CA1. One possibility is that GS-CA1 causes HIV-1 cores to be sequestered at nuclear pores, leading to the increased presence of proteins interacting with them and/or proteins that are specialized sensors of viral pathogens. Another possibility is that HIV-1 may obstruct nuclear pores, leading to an accumulation of HIV-1-irrelevant proteins that normally transit through these pores. In the Excel file named “Singh et al – modulated proteins” shared as supporting information, we include the information available at the HIV-1 Human Interactions Database compiled by the National Center

for Biotechnology Information (https://www.ncbi.nlm.nih.gov/genome/viruses/retroviruses/hiv-1/interactions/), regarding human interactors of HIV-1 proteins with accompanying references. This analysis indicates that 29 of the 84 modulated proteins were previously found to interact with at least one HIV-1 protein. For instance, two proteins that are part of the 20S proteasome complex, proteasome subunit beta type-6 (PSMB6) and the immunoproteasome-specific proteasome subunit beta type-10 (PSMB10), which is known to functionally interact with HIV-1 CA , were upregulated. Similarly upregulated was Proteasome activator complex subunit 3 (PSME3, also called proteasome activator 28 gamma, PA28-γ), which is predicted to interact with HIV-1 Vif and Vpr (270). Other ubiquitin/proteasome-relevant proteins were found to be upregulated in this experiment, specifically UBE2L3, an E2 ubiquitin conjugase that is involved in the control of viruses and is itself targeted by viral proteins , and MGRN1, an E3 ubiquitin ligase that targets human papillomavirus (HPV) proteins (271). These observations hint at an increased association with the nuclear envelope of the ubiquitin-proteasome pathway, which has a central role in the control of retroviral infections by interferon-stimulated restriction factors (68). Thus, the results obtained open a series of doors to possible interactions between HIV-1 and host factors at the nuclear envelope. However, we did not observe modulation of Nups, a finding that we confirmed in a "manual" analysis of the peptide-level data (not shown).

Using MS, we were able to detect the presence of HIV-1 peptides in nuclear envelope-enriched fractions. Interestingly, all of the peptides that could be quantified belonged to MA or CA. Early work had involved MA as important for HIV-1 nuclear import, due to the presence of nuclear localization signals in this protein (272). Accordingly, MA was found long ago to co-purify with HIV-1 complexes present in the nucleus of acutely infected cells (273, 274). As detailed in the introduction, the modern view of HIV-1 nuclear import is that an intact or nearly intact capsid core transits through the NPCs, which implies that MA proteins are totally dissociated from the HIV-1 complex that gains access to the nucleus; perhaps this new model over-simplifies HIV-1 nuclear import. HIV-1 MA and CA peptides were present in significantly higher amounts in nuclear envelope fractions in the presence of IFN-β. This effect might be explained by the IFN-induced overexpression of MX2, a well-investigated host factor that stabilizes HIV-1 cores and inhibits their nuclear import (144). Upon immunofluorescence observation of acutely infected cells, we

did observe an increase in the relative co-localization of HIV-1 cores (as detected with a CA antibody) and NPCs stained with a TPR antibody, in presence of IFN-β. However, a more striking phenotype associated with IFN-β treatment was the accumulation of apparent HIV-1 capsid cores in close vicinity to the nucleus without a strong pattern of colocalization with TPR. By contrast, GS-CA1 caused a more pronounced phenotype of association with NPCs. Why, then, did we not see an increase in the relative amounts of HIV-1 peptides in nuclear envelope fractions upon GS-CA1 treatment? A simple explanation is that even in the presence of the drug, we only detected a small fraction of total cellular CA signal as colocalizing with TPR in the microscopy experiment (1.5%), and thus modulation of this specifically NPC-associated population probably could not have been detected in the nuclear envelope-enriched fractions that were used for MS.

Conclusions

Taken together, our MS and microscopy data suggest that GS-CA1 causes a block to nuclear import by sequestration of HIV-1 capsid cores at nuclear pores, whereas IFN-β causes their retention at the nuclear envelope or in an as-yet-undefined cellular compartment that associates and co-purifies with the nuclear envelope. In addition, GS-CA1 causes the dysregulation of nuclear envelope fraction proteins in acutely HIV-1-infected cells, an effect that is not predicted by the analysis of drug toxicity in the absence of viral infection.

Data availability statement

The research data supporting this publication are available from the Figshare database (https://figshare.com/account/home#/projects/194951).

Author disclosure statement

The authors declare that they have no competing interests.

Authors' Contributions

A.S.: Methodology, Investigation, Formal analysis, Visualization, Writing – Original Draft. V.F.: Methodology, Investigation, Formal analysis, Visualization, Writing – Review and Editing. K.C.G.D.S.: Methodology, Formal analysis, Visualization, Writing – Review and Editing. H.C.: Methodology, Investigation. N.M.: Writing – Review and Editing, Supervision. A.D.: Resources, Supervision, Funding acquisition. H.G.: Conceptualization, Writing – Review and Editing,

Supervision, Funding acquisition. L.B.: Conceptualization, Methodology, Formal analysis, Writing – Original Draft, Writing – Review and Editing, Supervision, Project administration, Funding acquisition.

Funding Information

This study was funded by the Canadian Foundation for AIDS Research (CANFAR) as well as a Queen Elizabeth Scholarship to AS, and FRQNT and MITACS Globalink Scholarships to KCGS.

Chapter 4
Discussion

4.1 Summary

The nuclear transport of the HIV-1 genome across the nuclear envelope is a critical step in the viral infection cycle. However, the role of the nuclear envelope and NPC proteins in HIV-1 infection remains poorly understood. This study investigates alterations in the nuclear envelope proteome during the early stages of HIV-1 infection. While previous studies have investigated HIV-1 nuclear import and capsid interactions with nucleoporins, few have specifically examined the host proteomic landscape at the nuclear envelope during early infection. Most work, such as that by Bejarano et al. and Zila et al. (82, 213, 275), focused on mechanistic or imaging-based analyses of capsid transit, without profiling nuclear envelope–enriched fractions. This study fills that gap by applying LC/MS/MS to nuclear envelope–enriched samples from HIV-1–infected THP-1 cells, revealing distinct host protein modulation under IFN-β and GS-CA1 treatment. These findings offer new insight into early host-virus interactions at the nuclear periphery.

This study reveals that HIV-1 infection modulates the expression of ISGs at the nuclear envelope, including MX2. However, knockdown experiments indicate that MX2 alone is not sufficient to regulate HIV-1 nuclear entry, suggesting the involvement of additional ISGs. This is further supported by the observation that IFN-β pretreatment leads to an accumulation of HIV-1 peptides at the nuclear envelope.

Additionally, this study explores the impact of the FDA-approved capsid inhibitor GS-CA1 on HIV-1 nuclear entry. Unlike IFN-β, which results in peptide accumulation at the nuclear envelope, GS-CA1 blocks HIV-1 entry at the NPC. These findings highlight the nuclear envelope as a key regulatory site in HIV-1 infection, influenced by both viral mechanisms and the host immune response. This underscores the need for further research into strategies that simultaneously inhibit HIV-1 nuclear entry and enhance IFN-mediated antiviral defense at the nuclear envelope.

4.2 Effect of IFN on proteins from nuclear envelope enriched fraction

4.2.1 IFN-stimulated genes in nuclear envelope enriched fractions

This study shows the effect of IFN on the nuclear envelope enriched fraction in different THP-1 cell conditions. In one condition, we administered IFN-β and compared it to THP-1 cells without

IFN-β, observing many modulated proteins (Chapter 2). We also assessed IFN in shLUCshTRIM5α HIV-1 infection with and without IFN-β. Additionally, the study showed IFN's effect on shMX2shTRIM5α infected with HIV-1 with and without IFN-β. Many proteins are ISGs upregulated by IFN-I signaling. IFIT1, IFIT3, IFITM3, ISG15, MX2, OAS1, OAS2, and USP18 are key ISGs in the innate immune response against viral infections (276). These proteins are components of the cellular antiviral defense induced by interferons, with several exhibiting direct antiviral activity. The reduced infection observed in IFN-treated cells supports their functional role in restricting HIV-1.. IFITM3 inhibits viral entry for multiple enveloped viruses by restricting fusion from late endosomes, in our study, IFITM3 was upregulated in IFN-β–treated THP-1 cells, consistent with its known antiviral role. (277). Both IFIT1 and IFIT3 were upregulated in IFN-treated conditions, supporting their role in amplifying antiviral signaling(278). ISG15, MX2, and OAS proteins also have well-characterized antiviral functions and as expected, these proteins were upregulated (276). While IFITM proteins influence CD4+ T cell differentiation (influencing Th1/Th2 polarization), in THP-1 cells their antiviral role is more prominent. (279). SIGLEC1 and CD209 are involved in immune cell interactions and pathogen recognition (280-282). In our dataset, several of these ISGs were enriched in the nuclear envelope fraction, suggesting potential trafficking or NPC association. Their presence in the nuclear envelope enriched fraction may reflect transient localization, trafficking through nuclear pore complexes, or proximity during active signaling. This interpretation is supported by known interactions of some ISGs with NPC components, such as MX2 and ISG15.

Similarly, shMX2shTRIM5α infection with HIV-1 with IFN-β presence and absence has revealed differential accumulation of ISGs such as MX2, ISG15, and OAS2, consistent with their roles in nuclear import restriction. Diotallevi et al., mention that Glutathione (GSH) depletion affects the expression of several ISGs, including OAS2, OAS3, MX2, IRF7, IRF9, and STAT1 (283). These genes are part of innate immunity and antiviral response, requiring GSH for optimal induction (283). Although GSH levels were not directly measured in our study, the modulation of OAS2, MX2, and STAT1 aligns with their GSH-sensitive expression. This suggests glutathione plays a role in fine-tuning the innate immune response to infection, rather than limiting inflammation. Oguejiofor et al. discuss the endometrial immune response to bacterial

lipopolysaccharide (LPS) and identify several up-regulated ISGs, including RSAD2, MX2, OAS1, ISG15, and BST2 (284). This indicates their importance in the innate immune response to viral and bacterial infections. Painter and his team describe a transgenic mouse model expressing a picornavirus RNA-dependent RNA polymerase (RdRP) that leads to upregulation of 80 ISGs, resulting in profound resistance to viral challenge (285). This supports the broader concept that sustained ISG expression, as observed in our IFN-treated THP-1 cells, can confer antiviral protection. This study demonstrates that sustained activation of the innate immune system through ISG upregulation can provide broad-spectrum antiviral protection without causing harmful autoimmunity or chronic inflammation. Examining common metabolic pathways, STAT1 and STAT2 are transcription factors shuttling between cytoplasm and nucleus upon interferon stimulation (286). Their presence in the nuclear envelope–enriched fraction may reflect active IFN signaling. They play crucial roles in interferon signaling and gene expression regulation. EIF2AK2 (PKR) shuttles between cytoplasm and nucleus, with nuclear localization mediated by a bipartite nuclear localization signal (NLS) (287). IFI16, primarily nuclear, can shuttle to the cytoplasm upon viral infection (286). It acts as a DNA sensor in innate immune responses. Some proteins interact with nuclear transport pathways or NPC components. ISG15, a ubiquitin-like protein, modifies RanGAP1, involved in nucleocytoplasmic transport (288). MX1 and MX2 are GTPases localized to different cellular compartments. MX2 associates with NPCs and inhibits HIV-1 nuclear import (289). In our study, MX2 was consistently enriched in IFN-treated conditions, reinforcing its role in NPC-mediated restriction.

Given the nuclear envelope enrichment strategy used in this study, it is possible that some proteins detected are not permanent residents but transiently associated or in transit. This is a known limitation of subcellular fractionation and should be considered when interpreting the proteomic data.

In conclusion, these genes are involved in various aspects of the immune response, including viral recognition, signaling, and effector functions. The studies highlight their importance in mounting an effective defense against viral infections and show how their expression can be modulated by factors like glutathione levels or genetic modifications. Future studies incorporating cytosolic and nuclear fraction comparisons, as well as imaging-based

localization, will help refine these interpretations and validate the spatial distribution of ISGs during infection.

4.2.2 MX2 knockdown modulated various proteins related to different metabolic pathways

Based on previous studies, proteins like PNKP, UBTF, and GTF3C2 play critical roles in DNA repair, transcription, and genome stability (290-292). Their downregulation upon HIV-1 infection in your experiments may reflect a viral strategy to suppress host processes that could hinder its replication. Similar to the observed response with CDK13, HIV-1 might target these proteins to weaken cellular defenses, such as DNA repair pathways or transcription-coupled mechanisms, thereby creating a favorable environment for its replication.

The downregulation of PNKP might compromise the cell's ability to repair HIV-induced DNA damage, contributing to genomic instability, a hallmark of viral infections. Similarly, suppressing UBTF and GTF3C2 could interfere with transcription and gene expression, potentially enhancing the virus's ability to hijack host machinery for viral production.

Future studies could explore the specific viral factors responsible for this suppression and identify therapeutic approaches to counteract these effects. These findings may open new avenues for understanding how HIV-1 manipulates host proteins and pathways for its survival and replication.

The proteins identified are VIM (related to cell structure), LYZ (linked to immune function), NIPSNAP1 (involved in vesicle movement), CTDNEP1 (helps form the nuclear envelope), DRAM2 (related to autophagy), CCBL2 (breaks down amino acids), and EXOG (repairs DNA)(293-295). These proteins warrant further investigation to better understand their roles in innate immunity and HIV-1 regulation at the nuclear pore complex (NPC). For instance, CTDNEP1, involved in nuclear envelope formation, may influence NPC architecture during IFN-β treatment and viral infection. Likewise, examining the relationship between LYZ and innate immune signaling at the NPC could provide additional insights..

There were common proteins modulated by IFN in wild-type and knockdown cells. CD209, ISG15, LGALS3BP, and OAS2 are involved in antiviral immunity, particularly in relation to HIV-1 infection and the interferon (IFN) response pathway. ISG15 and OAS2 are ISGs crucial in the innate immune response against viral infections, including HIV-1 (296, 297). ISG15 negatively regulates the IFN-I signaling cascade and confers broad-spectrum resistance to viral infections when deficient in humans (297). OAS2, part of the oligoadenylate synthetase (OAS) family,

produces 2'-5'-linked second messenger molecules that activate RNase L, leading to viral RNA degradation (296). CD209 (DC-SIGN) and LGALS3BP are also involved in antiviral immunity (298-300). CD209 recognizes and binds to HIV-1, potentially facilitating viral entry into cells. LGALS3BP (Galectin-3-binding protein) is an ISG implicated in the antiviral response against HIV-1. These proteins are part of the antiviral state induced by IFN-I. The IFN-I response leads to the expression of numerous ISGs, including ISG15 and OAS2, which contribute to establishing an antiviral state in cells (297, 301). This antiviral state is characterized by the upregulation of proteins that target different stages of the viral life cycle.

In the context of MX2 downregulation, the continued modulation of CD209, ISG15, LGALS3BP, and OAS2 suggests that IFN-induced antiviral activity is maintained through MX2-independent mechanisms. While MX2 is known to inhibit HIV-1 nuclear import, our data show that HIV-1 capsid peptides still accumulate at the nuclear envelope in MX2 knockdown cells, indicating that other ISGs may compensate for its absence. This highlights the redundancy and robustness of the IFN-I response, where multiple effectors contribute to viral restriction at the nuclear envelope. In summary, CD209, ISG15, LGALS3BP, and OAS2 are part of the innate immune response against viral infections, particularly HIV-1. They are either directly induced by interferons or modulate the interferon response, contributing to the overall antiviral state of the cell.

4.2.3 ISGs trap the HIV-1 peptides on the nuclear envelope

As mentioned in Chapter 2, IFN-β presence has led to increased HIV-1 peptides at the nuclear envelope. The observation that IFN-beta leads to increased HIV-1 capsid (CA) peptides at the nuclear envelope, even when MX2 is knocked down, suggests a complex interplay between interferon-induced antiviral mechanisms and HIV-1 infection. Several factors could explain this result:

Firstly, IFN-I, such as IFN-β, induces a broad range of antiviral genes beyond MX2. While MX2 is known to inhibit HIV-1 nuclear import (134), other ISGs may also contribute to the accumulation of CA peptides at the nuclear envelope. For instance, Bulli et al. (2016) indicate that HIV-1 CA mutations that escape MX2 inhibition still show increased sensitivity to IFN-α, suggesting the involvement of additional antiviral factors (149). In our study, the persistence of CA accumulation at the nuclear envelope despite MX2 knockdown suggests that other ISGs, such

as ISG15, OAS2, and LGALS3BP, may compensate for the absence of MX2 and contribute to nuclear import restriction.

Interestingly, the HIV-1 capsid protein itself plays a crucial role in protecting the virus from IFN-induced inhibitors during early post-entry steps (149). This suggests that the increased presence of CA peptides at the nuclear envelope might be a viral strategy to shield against antiviral effectors, rather than solely a result of host restriction factors. This observation reinforces the idea that MX2 is not the sole effector in IFN-mediated nuclear import inhibition. The redundancy of ISG functions, and their coordinated action at the nuclear envelope, likely underpins the robustness of the antiviral state.

In conclusion, the lack of significant change upon MX2 knockdown implies that multiple IFN-induced factors likely contribute to the observed phenotype. The complex interactions between HIV-1 capsid, cellular cyclophilins, and various ISGs (149) underscore the need for further investigation to fully understand the mechanisms governing HIV-1's interaction with the interferon response at the nuclear envelope. Some futuristic experiments could be to analyze all the CA-binding ISGs and their effect at the nuclear envelope. Future experiments could systematically analyze CA-binding ISGs and their spatial localization during infection to identify which factors directly contribute to capsid retention or nuclear import blockade. This would help clarify the hierarchy and interplay of ISGs in HIV-1 restriction.

4.3 GS-CA1 effect on nuclear envelope proteins and its parallel comparison with ISGs

This study includes the capsid inhibitor and precursor of Lenacapvir, GS-CA1. This drug inhibits HIV-1 at the nuclear envelope by stabilising the capsid prohibiting viral capsid uncoating. Interestingly, the mechanism of action for GS-CA1 appears to be different from some other CA inhibitors. While compounds like PF-3450074 (PF74) promote premature uncoating of the HIV-1 capsid (217), the specific effect of GS-CA1 on capsid disassembly is not explicitly stated in the provided context. However, the general mechanism of CA inhibitors suggests that they can impact the highly regulated activity of CA, potentially affecting both the early and late stages of the viral lifecycle (215). Mass spectrometry data on THP-1 cells infected with HIV-1 in the presence and absence of GS-CA1 or IFN has provided many proteins that could be of future interest.

4.3.1 Effect of HIV-1 and GS-CA1 on nuclear envelope-associated proteins as seen by mass spectrometry

The study shows that while HIV-1 infection or GS-CA1 treatment alone minimally affects nuclear envelope proteins, their combination significantly alters 84 proteins (Chapter 2, Figure 2). Many are ISG products or part of the ubiquitin/proteasome pathway, indicating a complex interplay between HIV-1, GS-CA1, and cellular responses. This finding is partially supported by previous studies. The minimal effect of HIV-1 alone on nuclear envelope proteins aligns with earlier work. However, the dramatic effect of combined HIV-1 and GS-CA1 treatment is novel. Previous studies showed GS-CA1 inhibits HIV-1 infection (183), but its effect on nuclear envelope proteins was not explored in detail.

Modulated proteins in HIV-1 infection in the presence of GS-CA1 fall into several processes: Transcription and RNA processing: SRSF3, ZNF141, ZNF813, UTP15, GTF2H3, MED21, PAPOLA, LUC7L3, POLR2D, KDM4A, TADA3, PCF11, BTF3, PURA, DR1, TFCP2, SF3A2, EZH2, IRF2BP1, MED10, and HMG20A are involved in transcription regulation and RNA processing (302). Protein degradation and modification: PSMB6, PSMB10, PSME3, UBE2L3, and UBA2 are part of the ubiquitin-proteasome system (302). Cell signaling and regulation: ARHGAP11A, GPSM3, PLEK, MIF, INPP5B, and CAPRIN1 play roles in signaling pathways (303). DNA replication and repair: ESCO2, SUPV3L1, and NSMCE4A are involved in DNA processes (302). Metabolism: GCDH and GBE1 are involved in metabolic processes (302). TRHDE is a potential target gene in the sensory neuronal specification and pain perception (304), associated with growth traits in sheep (305), and implicated in glioma tumorigenesis (306). These proteins cover a range of cellular and metabolic processes, with many involved in transcription, RNA processing, and protein degradation. TRHDE highlights the diverse roles of these proteins across biological systems and disease states.

The modulation of these proteins in our study of HIV-1 infection highlights the virus's ability to manipulate diverse cellular processes to establish and maintain infection. Proteins involved in transcription and RNA processing, such as POLR2D, SF3A2, and EZH2, are critical for both host and viral gene expression. Their modulation may reflect how HIV-1 hijacks the host transcription machinery to prioritize its gene expression while potentially suppressing host antiviral responses.

However, in the presence of GS-CA1, which blocks HIV-1 nuclear import, the continued modulation of these proteins suggests that either early post-entry events (such as capsid recognition or partial uncoating) still trigger host responses, or that GS-CA1 itself induces cellular stress or signaling changes that impact transcriptional regulation. Similarly, proteins linked to the ubiquitin-proteasome system, including PSMB6, PSMB10, and PSME3, are often exploited by HIV-1 for the degradation of host restriction factors or viral protein processing. The modulation of these pathways underscores the virus's strategy to optimize its replication and evade immune detection. These findings suggest that even in the absence of productive infection, host cells may respond to viral components or drug-induced perturbations, highlighting the need to disentangle direct antiviral effects from host-driven responses in future studies.

Furthermore, the impact on DNA repair proteins, such as ESCO2 and NSMCE4A, suggests that HIV-1 might suppress cellular DNA repair processes to facilitate its integration into the host genome, contributing to genomic instability commonly observed during infection. Proteins like MIF and CAPRIN1, which play roles in cell signaling and regulation, may be targeted to disrupt host immune responses or to influence RNA granule dynamics that are essential during viral infections. Metabolic proteins, such as GCDH and GBE1, highlight the virus's demand for altering energy and biosynthetic pathways to support its replication. The modulation of TRHDE, with its diverse roles in sensory neuronal functions and tumorigenesis, could also reflect unexplored neuroimmune aspects of HIV-1 pathogenesis.

These findings emphasize the extensive host-pathogen interactions during HIV-1 infection, where the virus manipulates a broad range of cellular processes to enhance its survival and replication. Understanding the roles of these modulated proteins offers valuable insights into viral strategies and presents potential therapeutic targets for intervention.

When comparing HIV-1 infected cells (with GS-CA1 treatment) to uninfected cells with GS-CA1 treatment, many proteins were modulated, particularly transport-related ones: SLC35B1 and SLC9A1 are solute carrier (SLC) family members, membrane-bound transporters moving substrates across cellular membranes (307). SLC transporters play crucial roles in cellular processes, including drug disposition and response (308, 309). TRAM1 is involved in protein translocation across the endoplasmic reticulum membrane (310). TIMM17A and TIMM8B are

part of the translocase of the inner mitochondrial membrane (TIM) complex, facilitating protein import into mitochondria (310). KDELR2 retrieves endoplasmic reticulum proteins from the Golgi apparatus. SRP19 targets secretory proteins to the endoplasmic reticulum membrane for translocation. These proteins relate to cellular transport, but may not all be directly involved in the transmembrane transport of small molecules like SLC and ABC transporters (308, 309, 311, 312).

A few proteins were particularly interesting: LYZ is an important innate immune system component with antimicrobial properties, defending against bacterial infections (305, 313). CREB1 and CEBPB are transcription factors regulating immune responses, including innate immunity (305, 313). SLC9A1 is involved in ion transport and pH regulation, indirectly affecting immune responses and viral entry (305, 313). TRHDE has been mentioned in sensory neuronal specification and nociception, potentially affecting immune responses indirectly (304). Further research on each protein's function in immune responses and viral interactions is necessary.

This result highlights the complex interactions between HIV-1, antiviral compounds, and cellular proteins, suggesting GS-CA1's mechanism may involve more than direct HIV-1 inhibition, potentially affecting cellular pathways, particularly those related to interferon responses and protein degradation. This could impact understanding drug efficacy and side effects.

Future research could explore the specific roles of affected proteins in HIV-1 infection and GS-CA1 action, potentially uncovering new therapeutic targets. Investigating synergies between GS-CA1 and interferon-based therapies might lead to more effective treatments. Exploring how protein changes impact HIV-1 latency and reactivation could provide insights into viral persistence. These findings may guide the development of novel antiviral strategies targeting newly identified pathways, potentially revolutionizing HIV-1 treatment and improving patient outcomes.

4.3.2 IFN-β but not GS-CA1 causes the accumulation of HIV-1 at the nuclear envelope

IFN-β treatment, but not GS-CA1, causes a significant accumulation of HIV-1 peptides (specifically MA and CA) in nuclear envelope-enriched fractions. This suggests different mechanisms of action for IFN-β and GS-CA1 in inhibiting HIV-1 infection, with IFN-β potentially blocking the nuclear import of viral components.

This finding is partially supported by previous research. The role of IFN-β in inducing ISGs, including MX2, which interferes with HIV-1 nuclear import, has been established (134). Our data build on these findings by showing that IFN-β treatment leads to the accumulation of HIV-1 proteins at the nuclear envelope, which is a novel observation. Notably, GS-CA1 treatment did not prevent this accumulation, challenging earlier hypotheses that capsid disruption would block nuclear envelope localization (https://doi.org/10.1128/mbio.00348-24).

This result provides new insights into the mechanisms of IFN-β-mediated inhibition of HIV-1 infection. It suggests that IFN-β may act by trapping viral components at the nuclear envelope, preventing nuclear entry. The contrasting effect of GS-CA1 indicates a different mode of action, potentially acting at a different stage of the viral life cycle.

Future research could explore the specific mechanisms of IFN-β-induced HIV-1 peptide accumulation at the nuclear envelope, focusing on individual ISGs like MX2. Investigating potential synergies between IFN-β and other antivirals, such as GS-CA1, could lead to more effective combination therapies. Additionally, these findings may inspire the development of novel antiviral strategies targeting HIV-1 nuclear import. Such research could significantly advance our understanding of HIV-1 infection dynamics and potentially yield new classes of antiretroviral drugs, improving treatment outcomes for HIV-1 patients.

4.3.3 HIV-1 significantly colocalizes with TPR in the presence of GS-CA1

GS-CA1 significantly increases HIV-1 CA colocalization with TPR at nuclear pores, suggesting sequestration of HIV-1 at NPCs. IFN-β also increases CA-TPR colocalization, but to a lesser extent, and causes CA accumulation near the nuclear envelope without specific NPC association. This indicates different mechanisms of action for GS-CA1 and IFN-β in inhibiting HIV-1 infection during early stages.

This finding partially supports previous studies suggesting GS-CA1 inhibits HIV-1 nuclear import (220). However, it contradicts studies proposing no effect of GS-CA1 on CA presence in the nucleus (220). The IFN-β effect aligns with known antiviral mechanisms but provides new insights into its spatial impact on HIV-1 distribution.

This study provides visual evidence for GS-CA1's mechanism of action, suggesting it specifically targets the nuclear import stage of HIV-1 infection. It also highlights differences

between GS-CA1 and IFN-β in their antiviral effects, potentially informing more targeted therapeutic approaches. The quantitative analysis of CA-TPR colocalization offers a new method for assessing antiviral compound efficacy at the nuclear pore level.

Future research could focus on understanding the molecular mechanisms behind GS-CA1-induced HIV-1 sequestration at NPCs. Investigating potential synergies between GS-CA1 and IFN-β could lead to more effective combination therapies. Further studies on the role of TPR and other Nups in HIV-1 infection might reveal new therapeutic targets. Finally, this approach could be extended to evaluate other antiviral compounds targeting HIV-1 nuclear import.

4.4 The examination of implications arising from these findings

The research presented in this thesis encompasses two interconnected projects that explore the intricate interactions between HIV-1, host cell proteins, and antiviral treatments at the nuclear envelope.

Project 1, detailed in Chapter 2, investigated the effects of IFN-β on cellular proteins, particularly those associated with the nuclear envelope. This study revealed significant modulation of ISGs and, notably, an unexpected accumulation of HIV-1 peptides at the nuclear envelope following IFN-β treatment. Intriguingly, this accumulation persisted even in the absence of MX2, a key ISG, suggesting the involvement of other IFN-induced factors in this process.1

Project 2, presented in Chapter 3, built upon these findings by examining the effects of GS-CA1, a novel HIV-1 capsid inhibitor. Unlike IFN-β, which broadly activates antiviral pathways and retains HIV-1 peptides at the nuclear envelope, GS-CA1 directly blocks nuclear import by arresting the capsid at the pore, leading to focused CA-TPR colocalization. This reflects distinct mechanisms: host-driven retention versus drug-induced capsid trapping.. Although not analyzed in detail here, a direct comparison between HIV-1 alone and GS-CA1 alone would be valuable, especially since the combination treatment triggered more pronounced proteomic changes than either condition alone. This suggests potential synergy or additive effects worth exploring in future studies.

The connection between these projects lies in their complementary exploration of HIV-1 interactions with the nuclear envelope under different antiviral conditions. Both studies highlight the critical role of the nuclear envelope in HIV-1 infection and demonstrate how different antiviral

agents can disrupt this process, albeit through distinct mechanisms. The contrasting effects of IFN-β and GS-CA1 on HIV-1 localization provide valuable insights into the complexity of viral-host interactions and suggest multiple potential targets for therapeutic intervention.

Together, these projects advance our understanding of HIV-1 infection dynamics and open new avenues for antiviral strategy development, particularly those targeting nuclear import processes.

4.5 Significance of this study

The study presents several novel and original findings that significantly advance our understanding of HIV-1 infection and host-virus interactions. One of the most striking discoveries is the unexpected MX2-independent accumulation of HIV-1 peptides at the nuclear envelope following IFN-β treatment. While these findings challenge existing hypotheses about MX2's role, they are based on a subset of the nuclear envelope–enriched proteome and may not capture all relevant host factors. These findings challenge existing hypotheses about MX2's role and suggest the involvement of previously unrecognized factors in this process. However, further studies using broader proteomic or transcriptomic approaches will be necessary to fully elucidate the mechanisms.

Another significant contribution is the comparative analysis of how GS-CA1 and IFN-β affect HIV-1 localization at the nuclear envelope. While both treatments increase HIV-1 CA colocalization with TPR, GS-CA1 causes specific sequestration at nuclear pores, whereas IFN-β leads to a more general accumulation near the nuclear envelope. This distinction provides new insights into the mechanisms of action of these antiviral agents.

It is the first to conduct a comprehensive proteomic analysis of nuclear envelope-enriched samples from THP-1 cell lines using LC/MS/MS. This approach has yielded unprecedented insights into the dynamic changes occurring within the nuclear envelope in response to HIV-1 infection and IFN-β treatment. The identification of novel modulated proteins, including TPR and vimentin, opens new avenues for understanding HIV-1 pathogenesis and potential therapeutic targets.

Furthermore, the research reveals a complex interplay between HIV-1 and innate immunity, showing that the virus can dampen the effects of IFN-β on certain ISGs. This provides new insights into how HIV-1 evades host immune responses. The study also establishes a novel methodology

for assessing antiviral compound efficacy at the nuclear pore level through quantitative analysis of CA-TPR colocalization.

Collectively, these original findings challenge existing paradigms, provide new methodologies for studying HIV-1 infection, and open up new avenues for antiviral drug development and understanding of host-virus interactions. They set the stage for future research that could lead to more effective therapeutic strategies against HIV-1 and potentially other viral infections.

4.6 Comprehensive evaluation and future directions: analyzing HIV-1 interactions with the NPC

The study largely addresses the proposed hypotheses and objectives, providing valuable insights into the interactions between HIV-1, the NPC, and antiviral treatments. The study successfully investigates the impact of IFN-β on HIV-1 capsid peptide distribution in nuclear membrane-enriched samples and analyzes the role of MX2 in this process. Notably, the results challenge the initial hypothesis regarding MX2's role, revealing unexpected complexities in the interferon-mediated antiviral response.

Regarding the second hypothesis, the research effectively examines the effect of GS-CA1 on HIV-1 capsid peptide accumulation in nuclear membrane-enriched samples. The study also provides a comparative analysis of the mechanisms by which IFN-β and GS-CA1 block HIV-1 capsid at the NPC, revealing distinct patterns of viral capsid localization under these treatments. However, the study is limited by its focus on nuclear envelope–enriched proteomes, which may exclude key cytoplasmic or nuclear factors involved in HIV-1 restriction. Additionally, the absence of gene ontology or pathway enrichment analysis restricts broader biological interpretation of the proteomic shifts.

However, to fully meet the objectives and provide a more comprehensive understanding of HIV-1 interactions with the NPC, several additional experiments could be considered. These include investigating other ISGs given the unexpected results with MX2, conducting time-course analyses to understand the dynamics of HIV-1 capsid accumulation, and exploring combination treatments of IFN-β and GS-CA1 to assess potential synergistic or antagonistic effects.

Furthermore, structural studies using high-resolution imaging techniques could provide valuable insights into the interactions between HIV-1 capsid, NPC components, and antiviral

factors. In vivo studies in animal models would help validate the findings in a more physiologically relevant context. Lastly, more in-depth mechanistic studies could further elucidate the molecular processes by which IFN-β and GS-CA1 affect HIV-1 capsid accumulation at the NPC.

By incorporating these additional experiments, the research would provide an even more comprehensive understanding of HIV-1 interactions with the NPC and the mechanisms of action of both host immune responses and synthetic drugs in combating HIV-1 infection. This expanded knowledge could potentially pave the way for developing more effective and synergistic treatment strategies against HIV-1.

4.7 Conclusion

In conclusion, this study advances our understanding of HIV-1 interactions with the nuclear envelope and the host cell's innate immune response. It challenges existing paradigms, particularly regarding MX2's role, and opens new avenues for future research. The findings suggest that HIV-1 nuclear entry mechanisms and the host cell's attempts to block this entry are more complex than previously thought, involving multiple proteins and pathways. This research sets the stage for developing novel therapeutic strategies targeting nuclear import processes and exploiting the interplay between antiviral compounds and cellular responses.

Bibliography

1. Gelderblom HR. Structure and Classification of Viruses. In: Baron S, editor. Medical Microbiology. 4th ed. Galveston (TX)1996.
2. Scholthof KB, Adkins S, Czosnek H, Palukaitis P, Jacquot E, Hohn T, et al. Top 10 plant viruses in molecular plant pathology. Mol Plant Pathol. 2011;12(9):938-54.
3. Taubenberger JK, Morens DM. 1918 Influenza: the mother of all pandemics. Emerg Infect Dis. 2006;12(1):15-22.
4. Al Hajjar S, McIntosh K. The first influenza pandemic of the 21st century. Ann Saudi Med. 2010;30(1):1-10.
5. Harapan H, Itoh N, Yufika A, Winardi W, Keam S, Te H, et al. Coronavirus disease 2019 (COVID-19): A literature review. Journal of Infection and Public Health. 2020;13(5):667-73.
6. Gayle H. An overview of the global HIV/AIDS epidemic, with a focus on the United States. AIDS. 2000;14 Suppl 2:S8-17.
7. Centers for Disease C. Kaposi's sarcoma and Pneumocystis pneumonia among homosexual men--New York City and California. MMWR Morb Mortal Wkly Rep. 1981;30(25):305-8.
8. Barre-Sinoussi F, Chermann JC, Rey F, Nugeyre MT, Chamaret S, Gruest J, et al. Isolation of a T-lymphotropic retrovirus from a patient at risk for acquired immune deficiency syndrome (AIDS). Science. 1983;220(4599):868-71.
9. Gallo RC, Salahuddin SZ, Popovic M, Shearer GM, Kaplan M, Haynes BF, et al. Frequent detection and isolation of cytopathic retroviruses (HTLV-III) from patients with AIDS and at risk for AIDS. Science. 1984;224(4648):500-3.
10. German Advisory Committee Blood SAoPTbB. Human Immunodeficiency Virus (HIV). Transfus Med Hemother. 2016;43(3):203-22.
11. Simmonds P, Balfe P, Peutherer JF, Ludlam CA, Bishop JO, Brown AJ. Human immunodeficiency virus-infected individuals contain provirus in small numbers of peripheral mononuclear cells and at low copy numbers. J Virol. 1990;64(2):864-72.
12. Vodicka MA. Determinants for lentiviral infection of non-dividing cells. Somat Cell Mol Genet. 2001;26(1-6):35-49.
13. Jill Seladi-Schulman AT, Joseph Vinetz, MD, Nastassja Myer. How Many HIV Strains, Types, and Subtypes Are There? Healthline. 2021.
14. Taxon Details: History of the taxon. Taxon Details ICTV. 2022.
15. Meissner ME, Talledge N, Mansky LM. Molecular Biology and Diversification of Human Retroviruses. Front Virol. 2022;2.
16. Fischl MA, Richman DD, Grieco MH, Gottlieb MS, Volberding PA, Laskin OL, et al. The efficacy of azidothymidine (AZT) in the treatment of patients with AIDS and AIDS-related complex. A double-blind, placebo-controlled trial. N Engl J Med. 1987;317(4):185-91.
17. Temesgen Z, Siraj DS. Raltegravir: first in class HIV integrase inhibitor. Ther Clin Risk Manag. 2008;4(2):493-500.

18. Prather C, Lee A, Yen C. Lenacapavir: A first-in-class capsid inhibitor for the treatment of highly treatment-resistant HIV. Am J Health Syst Pharm. 2023;80(24):1774-80.
19. Briggs JAG, Wilk T, Welker R, Kräusslich HG, Fuller SD. Structural organization of authentic, mature HIV-1 virions and cores. The EMBO Journal. 2003;22(7):1707-15.
20. Sakuragi J-I. Morphogenesis of the Infectious HIV-1 Virion. Frontiers in Microbiology. 2011;volume 2 - 2011.
21. Mueller N, Klaver B, Berkhout B, Das AT. Human immunodeficiency virus type 1 splicing at the major splice donor site is controlled by highly conserved RNA sequence and structural elements. J Gen Virol. 2015;96(11):3389-95.
22. Jane Flint VRR, Glenn F. Rall, Theodora Hatziioannou, Anna Marie Skalka. Principles of Virology Google Books.
23. Das AT, Harwig A, Berkhout B. The HIV-1 Tat protein has a versatile role in activating viral transcription. J Virol. 2011;85(18):9506-16.
24. Tae-Wook Chun; Anthony S. Fauci MAOSJJACCAHLAESBMPNKJAM. Expression of Chemokine Receptors CXCR4 and CCR5 in HIV-1-Infected and Uninfected Individuals. J Immunol. 1998;161(6):3195–201.
25. Tang X, Lu H, Ramratnam B. Neurotoxicity of HIV-1 Tat is attributed to its penetrating property. Sci Rep. 2020;10(1):14002.
26. Brandt S, Blissenbach M, Grewe B, Konietzny R, Grunwald T, Uberla K. Rev proteins of human and simian immunodeficiency virus enhance RNA encapsidation. PLoS Pathog. 2007;3(4):e54.
27. Fischer U, Pollard VW, Luhrmann R, Teufel M, Michael MW, Dreyfuss G, et al. Rev-mediated nuclear export of RNA is dominant over nuclear retention and is coupled to the Ran-GTPase cycle. Nucleic Acids Res. 1999;27(21):4128-34.
28. Vercruysse T, Daelemans D. HIV-1 Rev multimerization: mechanism and insights. Curr HIV Res. 2013;11(8):623-34.
29. Fankhauser C, Izaurralde E, Adachi Y, Wingfield P, Laemmli UK. Specific complex of human immunodeficiency virus type 1 rev and nucleolar B23 proteins: dissociation by the Rev response element. Mol Cell Biol. 1991;11(5):2567-75.
30. Goncalves J, Silva F, Freitas-Vieira A, Santa-Marta M, Malho R, Yang X, et al. Functional neutralization of HIV-1 Vif protein by intracellular immunization inhibits reverse transcription and viral replication. J Biol Chem. 2002;277(35):32036-45.
31. Batisse J, Guerrero SX, Bernacchi S, Richert L, Godet J, Goldschmidt V, et al. APOBEC3G impairs the multimerization of the HIV-1 Vif protein in living cells. J Virol. 2013;87(11):6492-506.
32. Batisse J, Guerrero S, Bernacchi S, Sleiman D, Gabus C, Darlix JL, et al. The role of Vif oligomerization and RNA chaperone activity in HIV-1 replication. Virus Res. 2012;169(2):361-76.
33. Alteri C, Surdo M, Bellocchi MC, Saccomandi P, Continenza F, Armenia D, et al. Incomplete APOBEC3G/F Neutralization by HIV-1 Vif Mutants Facilitates the Genetic Evolution from CCR5 to CXCR4 Usage. Antimicrob Agents Chemother. 2015;59(8):4870-81.
34. Zhao RY, Bukrinsky MI. HIV-1 accessory proteins: VpR. Methods Mol Biol. 2014;1087:125-34.

35. Le Rouzic E, Benichou S. The Vpr protein from HIV-1: distinct roles along the viral life cycle. Retrovirology. 2005;2:11.
36. Jacquot G, Le Rouzic E, David A, Mazzolini J, Bouchet J, Bouaziz S, et al. Localization of HIV-1 Vpr to the nuclear envelope: impact on Vpr functions and virus replication in macrophages. Retrovirology. 2007;4:84.
37. Khan N, Geiger JD. Role of Viral Protein U (Vpu) in HIV-1 Infection and Pathogenesis. Viruses. 2021;13(8).
38. Bour S, Schubert U, Strebel K. The human immunodeficiency virus type 1 Vpu protein specifically binds to the cytoplasmic domain of CD4: implications for the mechanism of degradation. J Virol. 1995;69(3):1510-20.
39. Neil SJ, Zang T, Bieniasz PD. Tetherin inhibits retrovirus release and is antagonized by HIV-1 Vpu. Nature. 2008;451(7177):425-30.
40. Madhavi V, Wines BD, Amin J, Emery S, Lopez E, Kelleher A, et al. HIV-1 Env- and Vpu-Specific Antibody-Dependent Cellular Cytotoxicity Responses Associated with Elite Control of HIV. Journal of Virology. 2017;91(18):10.1128/jvi.00700-17.
41. Khan N, Geiger JD. Role of Viral Protein U (Vpu) in HIV-1 Infection and Pathogenesis. Viruses. 2021;13(8):1466.
42. Tokarev AA, Munguia J, Guatelli JC. Serine-threonine ubiquitination mediates downregulation of BST-2/tetherin and relief of restricted virion release by HIV-1 Vpu. J Virol. 2011;85(1):51-63.
43. Magadan JG, Perez-Victoria FJ, Sougrat R, Ye Y, Strebel K, Bonifacino JS. Multilayered mechanism of CD4 downregulation by HIV-1 Vpu involving distinct ER retention and ERAD targeting steps. PLoS Pathog. 2010;6(4):e1000869.
44. Dube M, Roy BB, Guiot-Guillain P, Binette J, Mercier J, Chiasson A, et al. Antagonism of tetherin restriction of HIV-1 release by Vpu involves binding and sequestration of the restriction factor in a perinuclear compartment. PLoS Pathog. 2010;6(4):e1000856.
45. Basmaciogullari S, Pizzato M. The activity of Nef on HIV-1 infectivity. Front Microbiol. 2014;5:232.
46. Gluck JM, Hoffmann S, Koenig BW, Willbold D. Single vector system for efficient N-myristoylation of recombinant proteins in E. coli. PLoS One. 2010;5(4):e10081.
47. Wang B, Dai T, Sun W, Wei Y, Ren J, Zhang L, et al. Protein N-myristoylation: functions and mechanisms in control of innate immunity. Cell Mol Immunol. 2021;18(4):878-88.
48. Pene-Dumitrescu T, Shu ST, Wales TE, Alvarado JJ, Shi H, Narute P, et al. HIV-1 Nef interaction influences the ATP-binding site of the Src-family kinase, Hck. BMC Chem Biol. 2012;12:1.
49. Pereira EA, daSilva LL. HIV-1 Nef: Taking Control of Protein Trafficking. Traffic. 2016;17(9):976-96.
50. Lundquist CA, Tobiume M, Zhou J, Unutmaz D, Aiken C. Nef-mediated downregulation of CD4 enhances human immunodeficiency virus type 1 replication in primary T lymphocytes. J Virol. 2002;76(9):4625-33.
51. Gelderblom HR. Assembly and morphology of HIV: potential effect of structure on viral function. AIDS. 1991;5(6):617-37.
52. AlBurtamani N, Paul A, Fassati A. The Role of Capsid in the Early Steps of HIV-1 Infection: New Insights into the Core of the Matter. Viruses. 2021;13(6).

53. Jiang J, Ablan SD, Derebail S, Hercik K, Soheilian F, Thomas JA, et al. The interdomain linker region of HIV-1 capsid protein is a critical determinant of proper core assembly and stability. Virology. 2011;421(2):253-65.
54. Novikova M, Zhang Y, Freed EO, Peng K. Multiple Roles of HIV-1 Capsid during the Virus Replication Cycle. Virol Sin. 2019;34(2):119-34.
55. Rossi E, Meuser ME, Cunanan CJ, Cocklin S. Structure, Function, and Interactions of the HIV-1 Capsid Protein. Life (Basel). 2021;11(2).
56. De Iaco A, Luban J. Cyclophilin A promotes HIV-1 reverse transcription but its effect on transduction correlates best with its effect on nuclear entry of viral cDNA. Retrovirology. 2014;11:11.
57. Mateu MG. The capsid protein of human immunodeficiency virus: intersubunit interactions during virus assembly. FEBS J. 2009;276(21):6098-109.
58. Accola MA, Strack B, Gottlinger HG. Efficient particle production by minimal Gag constructs which retain the carboxy-terminal domain of human immunodeficiency virus type 1 capsid-p2 and a late assembly domain. J Virol. 2000;74(12):5395-402.
59. Guirakhoo F, Weltzin R, Chambers TJ, Zhang ZX, Soike K, Ratterree M, et al. Recombinant chimeric yellow fever-dengue type 2 virus is immunogenic and protective in nonhuman primates. J Virol. 2000;74(12):5477-85.
60. Gross I, Hohenberg H, Krausslich HG. In vitro assembly properties of purified bacterially expressed capsid proteins of human immunodeficiency virus. Eur J Biochem. 1997;249(2):592-600.
61. Li S, Hill CP, Sundquist WI, Finch JT. Image reconstructions of helical assemblies of the HIV-1 CA protein. Nature. 2000;407(6802):409-13.
62. Ganser BK, Li S, Klishko VY, Finch JT, Sundquist WI. Assembly and analysis of conical models for the HIV-1 core. Science. 1999;283(5398):80-3.
63. Martinez-Costas J, Gonzalez-Lopez C, Vakharia VN, Benavente J. Possible involvement of the double-stranded RNA-binding core protein sigmaA in the resistance of avian reovirus to interferon. J Virol. 2000;74(3):1124-31.
64. Wilson W, Braddock M, Adams SE, Rathjen PD, Kingsman SM, Kingsman AJ. HIV expression strategies: ribosomal frameshifting is directed by a short sequence in both mammalian and yeast systems. Cell. 1988;55(6):1159-69.
65. Hill M, Tachedjian G, Mak J. The packaging and maturation of the HIV-1 Pol proteins. Curr HIV Res. 2005;3(1):73-85.
66. Tran EE, Borgnia MJ, Kuybeda O, Schauder DM, Bartesaghi A, Frank GA, et al. Structural mechanism of trimeric HIV-1 envelope glycoprotein activation. PLoS Pathog. 2012;8(7):e1002797.
67. Li Y, Deng L, Liang J, Dong GH, Xia YL, Fu YX, et al. Molecular dynamics simulations reveal distinct differences in conformational dynamics and thermodynamics between the unliganded and CD4-bound states of HIV-1 gp120. Phys Chem Chem Phys. 2020;22(10):5548-60.
68. Seissler T, Marquet R, Paillart JC. Hijacking of the Ubiquitin/Proteasome Pathway by the HIV Auxiliary Proteins. Viruses. 2017;9(11).

69. Zaitseva M, Peden K, Golding H. HIV coreceptors: role of structure, posttranslational modifications, and internalization in viral-cell fusion and as targets for entry inhibitors. Biochim Biophys Acta. 2003;1614(1):51-61.
70. David SA, Smith MS, Lopez GJ, Adany I, Mukherjee S, Buch S, et al. Selective transmission of R5-tropic HIV type 1 from dendritic cells to resting CD4+ T cells. AIDS Res Hum Retroviruses. 2001;17(1):59-68.
71. Waters L, Mandalia S, Randell P, Wildfire A, Gazzard B, Moyle G. The impact of HIV tropism on decreases in CD4 cell count, clinical progression, and subsequent response to a first antiretroviral therapy regimen. Clin Infect Dis. 2008;46(10):1617-23.
72. Grivel JC, Shattock RJ, Margolis LB. Selective transmission of R5 HIV-1 variants: where is the gatekeeper? J Transl Med. 2011;9 Suppl 1(Suppl 1):S6.
73. Perez-Alvarez L, Delgado E, Vega Y, Montero V, Cuevas T, Fernandez-Garcia A, et al. Predominance of CXCR4 tropism in HIV-1 CRF14_BG strains from newly diagnosed infections. J Antimicrob Chemother. 2014;69(1):246-53.
74. Lopalco L. CCR5: From Natural Resistance to a New Anti-HIV Strategy. Viruses. 2010;2(2):574-600.
75. Doranz BJ, Berson JF, Rucker J, Doms RW. Chemokine receptors as fusion cofactors for human immunodeficiency virus type 1 (HIV-1). Immunol Res. 1997;16(1):15-28.
76. Zhao SF, Li W, Dornadula G, Dicker D, Hoxie J, Peiper SC, et al. Chemokine receptors and the molecular basis for human immunodeficiency virus type 1 entry into peripheral hematopoietic stem cells and their progeny. J Infect Dis. 1998;178(6):1623-34.
77. Gabuzda D, Wang J. Chemokine receptors and virus entry in the central nervous system. J Neurovirol. 1999;5(6):643-58.
78. Finkel TH, Tudor-Williams G, Banda NK, Cotton MF, Curiel T, Monks C, et al. Apoptosis occurs predominantly in bystander cells and not in productively infected cells of HIV- and SIV-infected lymph nodes. Nat Med. 1995;1(2):129-34.
79. Garg H, Joshi A. Host and Viral Factors in HIV-Mediated Bystander Apoptosis. Viruses. 2017;9(8).
80. Zurcher T, Pavlovic J, Staeheli P. Mouse Mx2 protein inhibits vesicular stomatitis virus but not influenza virus. Virology. 1992;187(2):796-800.
81. Wilen CB, Tilton JC, Doms RW. Molecular mechanisms of HIV entry. Adv Exp Med Biol. 2012;726:223-42.
82. Zila V, Margiotta E, Turonova B, Muller TG, Zimmerli CE, Mattei S, et al. Cone-shaped HIV-1 capsids are transported through intact nuclear pores. Cell. 2021;184(4):1032-46 e18.
83. Xue G, Yu HJ, Buffone C, Huang SW, Lee K, Goh SL, et al. The HIV-1 capsid core is an opportunistic nuclear import receptor. Nat Commun. 2023;14(1):3782.
84. Muller TG, Zila V, Muller B, Krausslich HG. Nuclear Capsid Uncoating and Reverse Transcription of HIV-1. Annu Rev Virol. 2022;9(1):261-84.
85. Dwivedi R, Prakash P, Kumbhar BV, Balasubramaniam M, Dash C. HIV-1 capsid and viral DNA integration. mBio. 2024;15(1):e00212-22.
86. Mouzakis A, Petrakis V, Tryfonopoulou E, Panopoulou M, Panagopoulos P, Chlichlia K. Mechanisms of Immune Evasion in HIV-1: The Role of Virus-Host Protein Interactions. Current Issues in Molecular Biology. 2025;47(5):367.

87. Di Nunzio F, Danckaert A, Fricke T, Perez P, Fernandez J, Perret E, et al. Human nucleoporins promote HIV-1 docking at the nuclear pore, nuclear import and integration. PLoS One. 2012;7(9):e46037.
88. Bernad R, van der Velde H, Fornerod M, Pickersgill H. Nup358/RanBP2 attaches to the nuclear pore complex via association with Nup88 and Nup214/CAN and plays a supporting role in CRM1-mediated nuclear protein export. Mol Cell Biol. 2004;24(6):2373-84.
89. Matreyek KA, Engelman A. The requirement for nucleoporin NUP153 during human immunodeficiency virus type 1 infection is determined by the viral capsid. J Virol. 2011;85(15):7818-27.
90. RivièRe L, Cimarelli A, Darlix J-L. Analysis of the Viral Elements Required in the Nuclear Import of HIV-1 DNA. Journal of Virology. 2009;84(2):729-39.
91. Bukrinsky MI, Haffar OK. HIV-1 nuclear import: in search of a leader. Front Biosci. 1999;4:D772-81.
92. Wang Z. Regulation of Cell Cycle Progression by Growth Factor-Induced Cell Signaling. Cells. 2021;10(12).
93. Dultz E, Wojtynek M, Medalia O, Onischenko E. The Nuclear Pore Complex: Birth, Life, and Death of a Cellular Behemoth. Cells. 2022;11(9).
94. Beck M, Hurt E. The nuclear pore complex: understanding its function through structural insight. Nat Rev Mol Cell Biol. 2017;18(2):73-89.
95. Bley CJ, Nie S, Mobbs GW, Petrovic S, Gres AT, Liu X, et al. 2021.
96. Kelley K, Knockenhauer KE, Kabachinski G, Schwartz TU. Atomic structure of the Y complex of the nuclear pore. Nat Struct Mol Biol. 2015;22(5):425-31.
97. Mendes A, Fahrenkrog B. NUP214 in Leukemia: It's More than Transport. Cells. 2019;8(1):76.
98. Chug H, Trakhanov S, Hülsmann BB, Pleiner T, Görlich D. Crystal structure of the metazoan Nup62•Nup58•Nup54 nucleoporin complex. Science. 2015;350(6256):106-10.
99. Aksenova V, Smith A, Lee H, Bhat P, Esnault C, Chen S, et al. Nucleoporin TPR is an integral component of the TREX-2 mRNA export pathway. Nat Commun. 2020;11(1):4577.
100. Zaitsava H, Gachowska M, Bartoszewska E, Kmiecik A, Kulbacka J. The Potential of Nuclear Pore Complexes in Cancer Therapy. Molecules. 2024;29(20).
101. Light WH, Brickner JH. Nuclear pore proteins regulate chromatin structure and transcriptional memory by a conserved mechanism. Nucleus. 2013;4(5):357-60.
102. Zuleger N, Robson MI, Schirmer EC. The nuclear envelope as a chromatin organizer. Nucleus. 2011;2(5):339-49.
103. Ma J, Kelich JM, Junod SL, Yang W. Super-resolution mapping of scaffold nucleoporins in the nuclear pore complex. Journal of Cell Science. 2017;130(7):1299-306.
104. Kosinski J, Mosalaganti S, von Appen A, Teimer R, DiGuilio AL, Wan W, et al. Molecular architecture of the inner ring scaffold of the human nuclear pore complex. Science. 2016;352(6283):363-5.
105. Onischenko E, Tang JH, Andersen KR, Knockenhauer KE, Vallotton P, Derrer CP, et al. Natively Unfolded FG Repeats Stabilize the Structure of the Nuclear Pore Complex. Cell. 2017;171(4):904-17.e19.

106. Amlacher S, Sarges P, Flemming D, van Noort V, Kunze R, Devos DP, et al. Insight into structure and assembly of the nuclear pore complex by utilizing the genome of a eukaryotic thermophile. Cell. 2011;146(2):277-89.
107. Frey S, Richter RP, Gorlich D. FG-rich repeats of nuclear pore proteins form a three-dimensional meshwork with hydrogel-like properties. Science. 2006;314(5800):815-7.
108. Yoshida K, Seo HS, Debler EW, Blobel G, Hoelz A. Structural and functional analysis of an essential nucleoporin heterotrimer on the cytoplasmic face of the nuclear pore complex. Proc Natl Acad Sci U S A. 2011;108(40):16571-6.
109. Moroianu J. Distinct nuclear import and export pathways mediated by members of the karyopherin beta family. J Cell Biochem. 1998;70(2):231-9.
110. Yoneda Y, Nagoshi E, Miyamoto Y, Hieda M. Nucleocytoplasmic Protein Transport and Recycling of Ran. Cell Structure and Function. 1999;24(6):425-33.
111. Gorlich D, Pante N, Kutay U, Aebi U, Bischoff FR. Identification of different roles for RanGDP and RanGTP in nuclear protein import. EMBO J. 1996;15(20):5584-94.
112. Nachury MV, Weis K. The direction of transport through the nuclear pore can be inverted. Proc Natl Acad Sci U S A. 1999;96(17):9622-7.
113. Dong X, Biswas A, Chook YM. Structural basis for assembly and disassembly of the CRM1 nuclear export complex. Nat Struct Mol Biol. 2009;16(5):558-60.
114. Wagner RS, Kapinos LE, Marshall NJ, Stewart M, Lim RYH. Promiscuous Binding of Karyopherinβ1 Modulates FG Nucleoporin Barrier Function and Expedites NTF2 Transport Kinetics. Biophysical Journal. 2015;108(4):918-27.
115. Ben-Efraim I, Gerace L. Gradient of increasing affinity of importin beta for nucleoporins along the pathway of nuclear import. J Cell Biol. 2001;152(2):411-7.
116. von Appen A, Kosinski J, Sparks L, Ori A, DiGuilio AL, Vollmer B, et al. In situ structural analysis of the human nuclear pore complex. Nature. 2015;526(7571):140-3.
117. Brohawn SG, Partridge JR, Whittle JR, Schwartz TU. The nuclear pore complex has entered the atomic age. Structure. 2009;17(9):1156-68.
118. Bilokapic S, Schwartz TU. Molecular basis for Nup37 and ELY5/ELYS recruitment to the nuclear pore complex. Proc Natl Acad Sci U S A. 2012;109(38):15241-6.
119. Bastos R, Ribas de Pouplana L, Enarson M, Bodoor K, Burke B. Nup84, a novel nucleoporin that is associated with CAN/Nup214 on the cytoplasmic face of the nuclear pore complex. J Cell Biol. 1997;137(5):989-1000.
120. Hawryluk-Gara LA, Shibuya EK, Wozniak RW. Vertebrate Nup53 interacts with the nuclear lamina and is required for the assembly of a Nup93-containing complex. Mol Biol Cell. 2005;16(5):2382-94.
121. Lutzmann M, Kunze R, Stangl K, Stelter P, Toth KF, Bottcher B, et al. Reconstitution of Nup157 and Nup145N into the Nup84 complex. J Biol Chem. 2005;280(18):18442-51.
122. Fischer J, Hurt E, Teimer R, Kunze R, Amlacher S. Linker Nups connect the nuclear pore complex inner ring with the outer ring and transport channel. Nature Structural & Molecular Biology. 2015;22(10):774-81.
123. Raices M, D'Angelo MA. Nuclear pore complex composition: a new regulator of tissue-specific and developmental functions. Nature Reviews Molecular Cell Biology. 2012;13(11):687-99.

124. Capelson M, Hetzer MW. The role of nuclear pores in gene regulation, development and disease. EMBO Rep. 2009;10(7):697-705.
125. Capelson M, Hetzer MW, Doucet C. Nuclear Pore Complexes: Guardians of the Nuclear Genome. Cold Spring Harbor Symposia on Quantitative Biology. 2010;75(0):585-97.
126. Ibarra A, Hetzer MW. Nuclear pore proteins and the control of genome functions. Genes Dev. 2015;29(4):337-49.
127. Stanley GJ, Fassati A, Hoogenboom BW. Atomic force microscopy reveals structural variability amongst nuclear pore complexes. Life Science Alliance. 2018;1(4):e201800142.
128. Veldsink AC, Veenhoff LM. How to unravel a basket: NPC reorganization during meiosis. J Cell Biol. 2023;222(2).
129. Li Y, Zhu J, Zhai F, Kong L, Li H, Jin X. Advances in the understanding of nuclear pore complexes in human diseases. Journal of Cancer Research and Clinical Oncology. 2024;150(7):374.
130. Teer E, Mukonowenzou NC, Essop MF. The Role of Sustained Type I Interferon Secretion in Chronic HIV Pathogenicity: Implications for Viral Persistence, Immune Activation, and Immunometabolism. Viruses. 2025;17(2).
131. Bosinger SE, Utay NS. Type I interferon: understanding its role in HIV pathogenesis and therapy. Curr HIV/AIDS Rep. 2015;12(1):41-53.
132. Raftery N, Stevenson NJ. Advances in anti-viral immune defence: revealing the importance of the IFN JAK/STAT pathway. Cell Mol Life Sci. 2017;74(14):2525-35.
133. Soper A, Konno Y, Nagaoka S, Koyanagi Y, Yamamoto K, Sato K, et al. Type I Interferon Responses by HIV-1 Infection: Association with Disease Progression and Control. Frontiers in Immunology. 2018;8(1):1823.
134. Kane M, Wilson SJ, Yamashita M, Rice CM, Zang T, Bitzegeio J, et al. MX2 is an interferon-induced inhibitor of HIV-1 infection. Nature. 2013;502(7472):563-6.
135. Schoggins JW, Wilson SJ, Panis M, Murphy MY, Jones CT, Bieniasz P, et al. A diverse range of gene products are effectors of the type I interferon antiviral response. Nature. 2011;472(7344):481-5.
136. Chintala K, Mohareer K, Banerjee S. Dodging the Host Interferon-Stimulated Gene Mediated Innate Immunity by HIV-1: A Brief Update on Intrinsic Mechanisms and Counter-Mechanisms. Front Immunol. 2021;12:716927.
137. D`Urbano V, De Crignis E, Re MC. Host Restriction Factors and Human Immunodeficiency Virus (HIV-1): A Dynamic Interplay Involving All Phases of the Viral Life Cycle. Current HIV Research. 2018;16(3):184-207.
138. Hou Z, Shen Y, Fronik S, Shen J, Shi J, Xu J, et al. HIV-1 nuclear import is selective and depends on both capsid elasticity and nuclear pore adaptability. Nature Microbiology. 2025;10(8):1868-85.
139. Dharan A, Campbell EM. HIV-1 capsid found guilty of breaking and entering. Nature Microbiology. 2025;10(8):1800-1.
140. Altfeld M, Gale Jr M. Innate immunity against HIV-1 infection. Nature Immunology. 2015;16(6):554-62.
141. Wang A, Li MY. Viral dynamics of HIV-1 with CTL immune response. Discrete and Continuous Dynamical Systems - B. 2021;26(4):2257-72.

142. Betancor G. You Shall Not Pass: MX2 Proteins Are Versatile Viral Inhibitors. Vaccines (Basel). 2023;11(5).
143. Fribourgh JL, Nguyen HC, Matreyek KA, Alvarez FJD, Summers BJ, Dewdney TG, et al. Structural insight into HIV-1 restriction by MxB. Cell Host Microbe. 2014;16(5):627-38.
144. Dicks MDJ, Goujon C, Jimenez-Guardeño JM, Apolonia L, Pessel-Vivares L, Malim MH, et al. Multiple components of the nuclear pore complex interact with the amino-terminus of MX2 to facilitate HIV-1 restriction. PLOS Pathogens. 2018;14(11):e1007408.
145. Goujon C, Moncorge O, Bauby H, Doyle T, Ward CC, Schaller T, et al. Human MX2 is an interferon-induced post-entry inhibitor of HIV-1 infection. Nature. 2013;502(7472):559-62.
146. Layish B, Kvaratskhelia M, Flick H, Kane M, Huang S-W, Goli R, et al. Virus specificity and nucleoporin requirements for MX2 activity are affected by GTPase function and capsid-CypA interactions. PLoS pathogens. 2024;20(3):e1011830.
147. Busnadiego I, Willett BJ, Kane M, Zang TM, Wilson SJ, Strouvelle VP, et al. Host and viral determinants of Mx2 antiretroviral activity. Journal of Virology. 2014;88(14):7738-52.
148. Jackson-Jones KA, McKnight Á, Sloan RD. The innate immune factor RPRD2/REAF and its role in the Lv2 restriction of HIV. mBio. 2023;14(6):e0257221.
149. Bulli L, Apolonia L, Kutzner J, Pollpeter D, Goujon C, Herold N, et al. Complex Interplay between HIV-1 Capsid and MX2-Independent Alpha Interferon-Induced Antiviral Factors. J Virol. 2016;90(16):7469-80.
150. Dicks MDJ, Goujon C, Malim MH, Pollpeter D, Apolonia L, Bergeron JRC, et al. Oligomerization Requirements for MX2-Mediated Suppression of HIV-1 Infection. Journal of Virology. 2015;90(1):22-32.
151. Yang H, Ji X, Gronenborn AM, Zhao Q, Aiken C, Zhao G, et al. Structural insight into HIV-1 capsid recognition by rhesus TRIM5α. Proceedings of the National Academy of Sciences. 2012;109(45):18372-7.
152. Nakayama EE, Shioda T. Role of Human TRIM5alpha in Intrinsic Immunity. Front Microbiol. 2012;3:97.
153. Yu A, Skorupka KA, Pak AJ, Ganser-Pornillos BK, Pornillos O, Voth GA. TRIM5alpha self-assembly and compartmentalization of the HIV-1 viral capsid. Nat Commun. 2020;11(1):1307.
154. Pertel T, Uchil PD, Grütter MG, Mothes W, Guerra J, Morger D, et al. TRIM5 is an innate immune sensor for the retrovirus capsid lattice. Nature. 2011;472(7343):361-5.
155. Stremlau M, Perron M, Lee M, Li Y, Song B, Javanbakht H, et al. Specific recognition and accelerated uncoating of retroviral capsids by the TRIM5alpha restriction factor. Proc Natl Acad Sci U S A. 2006;103(14):5514-9.
156. Imam S, Hope TJ, Dharan A, Talley S, O'Connor C, Nelson RS, et al. TRIM5α Degradation via Autophagy Is Not Required for Retroviral Restriction. Journal of Virology. 2016;90(7):3400-10.
157. Merindol N, Berthoux L. Restriction Factors in HIV-1 Disease Progression. Current HIV Research. 2015;13(6):448-61.
158. Matreyek K, Engelman A. Viral and Cellular Requirements for the Nuclear Entry of Retroviral Preintegration Nucleoprotein Complexes. Viruses. 2013;5(10):2483-511.
159. Jang S, Engelman AN. Capsid-host interactions for HIV-1 ingress. Microbiology and molecular biology reviews : MMBR. 2023;87(4):e0004822.

160. Rebensburg SV, Morrison J, Wei G, Kewalramani V, Lindenberger J, Huang S-W, et al. Sec24C is an HIV-1 host dependency factor crucial for virus replication. Nature microbiology. 2021;6(4):435-44.
161. Dickson CF, Tuckwell AJ, Sierecki E, Ariotti N, Böcking T, Morris RG, et al. The HIV capsid mimics karyopherin engagement of FG-nucleoporins. Nature. 2024;626(8000):836-42.
162. Hudait A, Voth GA. HIV-1 capsid shape, orientation, and entropic elasticity regulate translocation into the nuclear pore complex. Proc Natl Acad Sci U S A. 2024;121(4):e2313737121.
163. Zila V, Kräusslich H-G, Müller B, Laketa V, Müller TG. Analysis of CA Content and CPSF6 Dependence of Early HIV-1 Replication Complexes in SupT1-R5 Cells. mBio. 2019;10(6).
164. Deshpande A, Bryer AJ, Andino-Moncada JR, Shi J, Hong J, Torres C, et al. Elasticity of the HIV-1 core facilitates nuclear entry and infection. PLoS pathogens. 2024;20(9):e1012537.
165. Zhuang S, Torbett BE. Interactions of HIV-1 Capsid with Host Factors and Their Implications for Developing Novel Therapeutics. Viruses. 2021;13(3):417.
166. Baggaley RF, Boily MC, White RG, Alary M. Risk of HIV-1 transmission for parenteral exposure and blood transfusion: a systematic review and meta-analysis. Aids. 2006;20(6):805-12.
167. Boily M-C, Baggaley RF, Wang L, Masse B, White RG, Hayes RJ, et al. Heterosexual risk of HIV-1 infection per sexual act: systematic review and meta-analysis of observational studies. The Lancet Infectious Diseases. 2009;9(2):118-29.
168. Amin O, Powers J, Bricker KM, Chahroudi A. Understanding Viral and Immune Interplay During Vertical Transmission of HIV: Implications for Cure. Frontiers in Immunology. 2021;Volume 12 - 2021.
169. Naidu RT, Toal P, Mishra SC, Nair B, Shejul YK. Incidence of needlestick injury among healthcare workers in western India. Indian Journal of Medical Research. 2023;158(5&6):552-8.
170. Berhanu Elfu F. Prevalence and Determinant Factors for Sharp Injuries among Addis Ababa Hospitals Health Professionals. Science Journal of Public Health. 2013;1(5):189-93.
171. Lefrère J-J, Dahourouh H, Dokekias AE, Kouao MD, Diarra A, Diop S, et al. Estimate of the residual risk of transfusion-transmitted human immunodeficiency virus infection in sub-Saharan Africa: a multinational collaborative study. Transfusion. 2011;51(3):486-92.
172. Ribeiro RM, Qin L, Chavez LL, Li D, Self SG, Perelson AS. Estimation of the initial viral growth rate and basic reproductive number during acute HIV-1 infection. J Virol. 2010;84(12):6096-102.
173. Fidler S, Fraser C, Fox J, Tamm N, Griffin JT, Weber J. Comparative potency of three antiretroviral therapy regimes in primary HIV infection. AIDS. 2006;20(2):247-52.
174. Khan S, Telwatte S, Trapecar M, Yukl S, Sanjabi S. Differentiating Immune Cell Targets in Gut-Associated Lymphoid Tissue for HIV Cure. AIDS Res Hum Retroviruses. 2017;33(S1):S40-S58.
175. Chvatal-Medina M, Lopez-Guzman C, Diaz FJ, Gallego S, Rugeles MT, Taborda NA. Molecular mechanisms by which the HIV-1 latent reservoir is established and therapeutic strategies for its elimination. Arch Virol. 2023;168(8):218.
176. Khanal S, Schank M, El Gazzar M, Moorman JP, Yao ZQ. HIV-1 Latency and Viral Reservoirs: Existing Reversal Approaches and Potential Technologies, Targets, and Pathways Involved in HIV Latency Studies. Cells. 2021;10(2).
177. Geskus RB, Prins M, Hubert JB, Miedema F, Berkhout B, Rouzioux C, et al. The HIV RNA setpoint theory revisited. Retrovirology. 2007;4:65.

178. Schellekens PT, Tersmette M, Roos MT, Keet RP, de Wolf F, Coutinho RA, et al. Biphasic rate of CD4+ cell count decline during progression to AIDS correlates with HIV-1 phenotype. AIDS. 1992;6(7):665-9.
179. Kaseke C, Tano-Menka R, Senjobe F, Gaiha GD. The Emerging Role for CTL Epitope Specificity in HIV Cure Efforts. J Infect Dis. 2021;223(12 Suppl 2):32-7.
180. Marquis KA, Bushman FD, Cantu A, Gillis E, Krystal M, McFarland A, et al. The HIV-1 Capsid-Targeted Inhibitor GSK878 Alters Selection of Target Sites for HIV DNA Integration. AIDS research and human retroviruses. 2023;40(2):114-26.
181. Vidal SJ, Bekerman E, Hansen D, Lu B, Wang K, Mwangi J, et al. Long-acting capsid inhibitor protects macaques from repeat SHIV challenges. Nature. 2022;601(7894):612-6.
182. Tuan J, Ogbuagu O. Lenacapavir: a twice-yearly treatment for adults with multidrug-resistant HIV infection and limited treatment options. Expert Rev Anti Infect Ther. 2023;21(6):565-70.
183. Yant SR, Mulato A, Hansen D, Tse WC, Niedziela-Majka A, Zhang JR, et al. A highly potent long-acting small-molecule HIV-1 capsid inhibitor with efficacy in a humanized mouse model. Nat Med. 2019;25(9):1377-84.
184. HIV Overview: FDA-Approved HIV Medicines. HIVinfo@NIHgov. July 31, 2024.
185. Shin YH, Park CM, Yoon C-H. An Overview of Human Immunodeficiency Virus-1 Antiretroviral Drugs: General Principles and Current Status. Infection & Chemotherapy. 2021;53(1):29-45.
186. Temereanca A, Ruta S. Strategies to overcome HIV drug resistance-current and future perspectives. Frontiers in Microbiology. 2023;14:1133407.
187. Puertas MC, Ploumidis G, Ploumidis M, Fumero E, Clotet B, Walworth CM, et al. Pan-resistant HIV-1 emergence in the era of integrase strand-transfer inhibitors: a case report. Lancet Microbe. 2020;1(3):e130-e5.
188. Hue S, Gifford RJ, Dunn D, Fernhill E, Pillay D, Resistance UKCGoHD. Demonstration of sustained drug-resistant human immunodeficiency virus type 1 lineages circulating among treatment-naive individuals. J Virol. 2009;83(6):2645-54.
189. Barbaro G, Scozzafava A, Mastrolorenzo A, Supuran CT. Highly active antiretroviral therapy: current state of the art, new agents and their pharmacological interactions useful for improving therapeutic outcome. Curr Pharm Des. 2005;11(14):1805-43.
190. Sluis-Cremer N, Wainberg MA, Schinazi RF. Resistance to reverse transcriptase inhibitors used in the treatment and prevention of HIV-1 infection. Future Microbiol. 2015;10(11):1773-82.
191. Asahchop EL, Wainberg MA, Sloan RD, Tremblay CL. Antiviral drug resistance and the need for development of new HIV-1 reverse transcriptase inhibitors. Antimicrob Agents Chemother. 2012;56(10):5000-8.
192. Joly V, Jidar K, Tatay M, Yeni P. Enfuvirtide: from basic investigations to current clinical use. Expert Opin Pharmacother. 2010;11(16):2701-13.
193. Este JA. Virus entry as a target for anti-HIV intervention. Curr Med Chem. 2003;10(17):1617-32.
194. Ghosh RK, Ghosh SM, Chawla S. Recent advances in antiretroviral drugs. Expert Opin Pharmacother. 2011;12(1):31-46.
195. Quashie PK, Sloan RD, Wainberg MA. Novel therapeutic strategies targeting HIV integrase. BMC Med. 2012;10:34.

196. Anstett K, Brenner B, Mesplede T, Wainberg MA. HIV drug resistance against strand transfer integrase inhibitors. Retrovirology. 2017;14(1):36.
197. Karmon SL, Markowitz M. Next-generation integrase inhibitors : where to after raltegravir? Drugs. 2013;73(3):213-28.
198. Chahine EB, Durham SH. Ibalizumab: The First Monoclonal Antibody for the Treatment of HIV-1 Infection. Ann Pharmacother. 2021;55(2):230-9.
199. Siliciano RF, Greene WC. HIV latency. Cold Spring Harb Perspect Med. 2011;1(1):a007096.
200. Mbonye U, Karn J. The cell biology of HIV-1 latency and rebound. Retrovirology. 2024;21(1):6.
201. Sadowski I, Hashemi FB. Strategies to eradicate HIV from infected patients: elimination of latent provirus reservoirs. Cell Mol Life Sci. 2019;76(18):3583-600.
202. Palermo E, Acchioni C, Di Carlo D, Zevini A, Muscolini M, Ferrari M, et al. Activation of Latent HIV-1 T Cell Reservoirs with a Combination of Innate Immune and Epigenetic Regulators. J Virol. 2019;93(21).
203. Ciccullo A, Iannone V, Farinacci D, Steiner RJ, Lombardi F, Carbone A, et al. Cardiovascular Safety of Doravirine/Lamivudine/Tenofovir Disoproxil Fumarate in Virologically Suppressed PLWHIV: A Comparative Analysis of CVD Scores. AIDS Res Hum Retroviruses. 2025;41(2):87-9.
204. Lanting VR, Oosterhof P, Ait Moha D, van Heerde R, Kleene MJT, Stalenhoef JE, et al. Switching to Doravirine in cART-Experienced Patients: An Effective and Highly Tolerated Option With Substantial Cost Savings. J Acquir Immune Defic Syndr. 2024;95(2):190-6.
205. Markham A. Fostemsavir: First Approval. Drugs. 2020;80(14):1485-90.
206. Heidary M, Shariati S, Nourigheimasi S, Khorami M, Moradi M, Motahar M, et al. Mechanism of action, resistance, interaction, pharmacokinetics, pharmacodynamics, and safety of fostemsavir. BMC Infect Dis. 2024;24(1):250.
207. Diamond TL, Goh SL, Ngo W, Rodriguez S, Xu M, Klein DJ, et al. No antagonism or cross-resistance and a high barrier to the emergence of resistance in vitro for the combination of islatravir and lenacapavir. Antimicrob Agents Chemother. 2024;68(7):e0033424.
208. Bekker LG, Das M, Abdool Karim Q, Ahmed K, Batting J, Brumskine W, et al. Twice-Yearly Lenacapavir or Daily F/TAF for HIV Prevention in Cisgender Women. N Engl J Med. 2024;391(13):1179-92.
209. Henning MS, Dubose BN, Burse MJ, Aiken C, Yamashita M. In Vivo Functions of CPSF6 for HIV-1 as Revealed by HIV-1 Capsid Evolution in HLA-B27-Positive Subjects. PLOS Pathogens. 2014;10(1):e1003868.
210. Zhou J, Price AJ, Halambage UD, James LC, Aiken C. HIV-1 Resistance to the Capsid-Targeting Inhibitor PF74 Results in Altered Dependence on Host Factors Required for Virus Nuclear Entry. Journal of Virology. 2015;89(17):9068-79.
211. Singh K, Lange MJ, Sönnerborg A, Burke DH, Neogi U, Gallazzi F, et al. GS-CA Compounds: First-In-Class HIV-1 Capsid Inhibitors Covering Multiple Grounds. Frontiers in Microbiology. 2019;10(Suppl 3):1227.
212. Tailor MW, Chahine EB, Koren D, Sherman EM. Lenacapavir: A Novel Long-Acting Capsid Inhibitor for HIV. Ann Pharmacother. 2024;58(2):185-95.

213. Selyutina A, Hu P, Miller S, Simons LM, Yu HJ, Hultquist JF, et al. GS-CA1 and lenacapavir stabilize the HIV-1 core and modulate the core interaction with cellular factors. iScience. 2022;25(1):103593.
214. Dvory-Sobol H, Shaik N, Callebaut C, Rhee MS. Lenacapavir: a first-in-class HIV-1 capsid inhibitor. Curr Opin HIV AIDS. 2022;17(1):15-21.
215. McArthur C, Gallazzi F, Quinn TP, Singh K. HIV Capsid Inhibitors Beyond PF74. Diseases. 2019;7(4).
216. Eron JJ, Little SJ, Crofoot G, Cook P, Ruane PJ, Jayaweera D, et al. Safety of teropavimab and zinlirvimab with lenacapavir once every 6 months for HIV treatment: a phase 1b, randomised, proof-of-concept study. Lancet HIV. 2024;11(3):e146-e55.
217. Shi J, Whitby K, Aiken C, Shah VB, Zhou J. Small-Molecule Inhibition of Human Immunodeficiency Virus Type 1 Infection by Virus Capsid Destabilization. Journal of Virology. 2010;85(1):542-9.
218. Guedan A, Donaldson CD, Caroe ER, Cosnefroy O, Taylor IA, Bishop KN. HIV-1 requires capsid remodelling at the nuclear pore for nuclear entry and integration. PLoS Pathog. 2021;17(9):e1009484.
219. Wei G, Iqbal N, Courouble VV, Francis AC, Singh PK, Hudait A, et al. Prion-like low complexity regions enable avid virus-host interactions during HIV-1 infection. Nat Commun. 2022;13(1):5879.
220. Bester SM, Wei G, Zhao H, Adu-Ampratwum D, Iqbal N, Courouble VV, et al. Structural and mechanistic bases for a potent HIV-1 capsid inhibitor. Science. 2020;370(6514):360-4.
221. Simon Collins Hi-B. Pipeline report 2021: HIV drugs in development. HIV i-Base. 2021;22(1).
222. Simon Collins Hi-B. CROI 2023: Pipeline HIV drugs and formulations for treatment and PrEP. i-base. 2023.
223. Ramdas P, Sahu AK, Mishra T, Bhardwaj V, Chande A. From Entry to Egress: Strategic Exploitation of the Cellular Processes by HIV-1. Front Microbiol. 2020;11:559792.
224. Sun L, Dick A, Meuser ME, Huang T, Zalloum WA, Chen CH, et al. Design, Synthesis, and Mechanism Study of Benzenesulfonamide-Containing Phenylalanine Derivatives as Novel HIV-1 Capsid Inhibitors with Improved Antiviral Activities. J Med Chem. 2020;63(9):4790-810.
225. Tuckwell AJ, Márquez CL, Jacques DA, Towers GJ, Walsh JC, Faysal KMR, et al. Pharmacologic hyperstabilisation of the HIV-1 capsid lattice induces capsid failure. eLife. 2024;13.
226. Paik J. Lenacapavir: First Approval. Drugs. 2022;82(14):1499-504.
227. Merindol N, El-Far M, Sylla M, Masroori N, Dufour C, Li JX, et al. HIV-1 capsids from B27/B57+ elite controllers escape Mx2 but are targeted by TRIM5alpha, leading to the induction of an antiviral state. PLoS pathogens. 2018;14(11):e1007398.
228. Merindol N, El-Far M, Sylla M, Masroori N, Dufour C, Li JX, et al. HIV-1 capsids from B27/B57+ elite controllers escape Mx2 but are targeted by TRIM5α, leading to the induction of an antiviral state. PLoS Pathog. 2018;14(11):e1007398.
229. Yao B, Xu Y, Wang J, Qiao Y, Zhang Y, Zhang X, et al. Reciprocal regulation between O-GlcNAcylation and tribbles pseudokinase 2 (TRIB2) maintains transformative phenotypes in liver cancer cells. Cell Signal. 2016;28(11):1703-12.

230. Cao W, Cao J, Huang J, Yao J, Yan G, Xu H, et al. Discovery and confirmation of O-GlcNAcylated proteins in rat liver mitochondria by combination of mass spectrometry and immunological methods. PLoS One. 2013;8(10):e76399.
231. Cronshaw JM, Krutchinsky AN, Zhang W, Chait BT, Matunis MJ. Proteomic analysis of the mammalian nuclear pore complex. J Cell Biol. 2002;158(5):915-27.
232. Davis LI, Blobel G. Identification and characterization of a nuclear pore complex protein. Cell. 1986;45(5):699-709.
233. Lelek M, Casartelli N, Pellin D, Rizzi E, Souque P, Severgnini M, et al. Chromatin organization at the nuclear pore favours HIV replication. Nat Commun. 2015;6:6483.
234. Gautier VW, Gu L, O'Donoghue N, Pennington S, Sheehy N, Hall WW. In vitro nuclear interactome of the HIV-1 Tat protein. Retrovirology. 2009;6:47.
235. Chandrasekar AP, Cummins NW, Badley AD. The Role of the BCL-2 Family of Proteins in HIV-1 Pathogenesis and Persistence. Clinical Microbiology Reviews. 2019;33(1):e00107-19.
236. Mbita Z, Hull R, Dlamini Z. Human immunodeficiency virus-1 (HIV-1)-mediated apoptosis: new therapeutic targets. Viruses. 2014;6(8):3181-227.
237. Jarboui MA, Bidoia C, Woods E, Roe B, Wynne K, Elia G, et al. Nucleolar protein trafficking in response to HIV-1 Tat: rewiring the nucleolus. PloS one. 2012;7(11):e48702-e.
238. Betancor G, Dicks MDJ, Jimenez-Guardeño JM, Ali NH, Apolonia L, Malim MH. The GTPase Domain of MX2 Interacts with the HIV-1 Capsid, Enabling Its Short Isoform to Moderate Antiviral Restriction. Cell Rep. 2019;29(7):1923-33.e3.
239. Bailey CC, Zhong G, Huang IC, Farzan M. IFITM-Family Proteins: The Cell's First Line of Antiviral Defense. Annu Rev Virol. 2014;1:261-83.
240. Wang Q, Zhang X, Han Y, Wang X, Gao G. M2BP inhibits HIV-1 virion production in a vimentin filaments-dependent manner. Sci Rep. 2016;6:32736.
241. Kretzschmar G, Paez LP, Tan Z, Wang J, Gonzalez L, Mugabo CH, et al. Normalized Interferon Signatures and Clinical Improvements by IFNAR1 Blocking Antibody (Anifrolumab) in Patients with Type I Interferonopathies. J Clin Immunol. 2024;45(1):31.
242. Gobin SJP, Zutphen Mv, Woltman AM, Elsen PJvd. Transactivation of Classical and Nonclassical HLA Class I Genes Through the IFN-Stimulated Response Element. The Journal of Immunology. 1999;163(3):1428-34.
243. Pozniak A. Quality of life in chronic HIV infection. Lancet HIV. 2014;1(1):e6-7.
244. Basavaraj KH, Navya MA, Rashmi R. Quality of life in HIV/AIDS. Indian J Sex Transm Dis AIDS. 2010;31(2):75-80.
245. Blair HA. Ibalizumab: A Review in Multidrug-Resistant HIV-1 Infection. Drugs. 2020;80(2):189-96.
246. Jakobsen MR, Olagnier D, Hiscott J. Innate immune sensing of HIV-1 infection. Curr Opin HIV AIDS. 2015;10(2):96-102.
247. Kajaste-Rudnitski A, Marelli SS, Pultrone C, Pertel T, Uchil PD, Mechti N, et al. TRIM22 inhibits HIV-1 transcription independently of its E3 ubiquitin ligase activity, Tat, and NF-kappaB-responsive long terminal repeat elements. J Virol. 2011;85(10):5183-96.
248. Luo Y, Jacobs EY, Greco TM, Mohammed KD, Tong T, Keegan S, et al. HIV-host interactome revealed directly from infected cells. Nat Microbiol. 2016;1(7):16068-.
249. Le Sage V, Cinti A, Valiente-Echeverría F, Mouland AJ. Proteomic analysis of HIV-1 Gag interacting partners using proximity-dependent biotinylation. Virol J. 2015;12:138.

250. Renga B, Francisci D, Carino A, Marchianò S, Cipriani S, Chiara Monti M, et al. The HIV matrix protein p17 induces hepatic lipid accumulation via modulation of nuclear receptor transcriptoma. Sci Rep. 2015;5:15403.
251. He B, Tran JT, Sanchez DJ. Manipulation of Type I Interferon Signaling by HIV and AIDS-Associated Viruses. J Immunol Res. 2019;2019:8685312-.
252. Carnes SK, Zhou J, Aiken C. HIV-1 Engages a Dynein-Dynactin-BICD2 Complex for Infection and Transport to the Nucleus. J Virol. 2018;92(20).
253. Malikov V, da Silva ES, Jovasevic V, Bennett G, de Souza Aranha Vieira DA, Schulte B, et al. HIV-1 capsids bind and exploit the kinesin-1 adaptor FEZ1 for inward movement to the nucleus. Nat Commun. 2015;6:6660.
254. Forshey BM, von Schwedler U, Sundquist WI, Aiken C. Formation of a human immunodeficiency virus type 1 core of optimal stability is crucial for viral replication. J Virol. 2002;76(11):5667-77.
255. Lee K, Ambrose Z, Martin TD, Oztop I, Mulky A, Julias JG, et al. Flexible use of nuclear import pathways by HIV-1. Cell Host Microbe. 2010;7(3):221-33.
256. Engelman AN. HIV Capsid and Integration Targeting. Viruses. 2021;13(1).
257. Petrovic S, Mobbs GW, Bley CJ, Nie S, Patke A, Hoelz A. Structure and Function of the Nuclear Pore Complex. Cold Spring Harb Perspect Biol. 2022;14(12).
258. Aramburu IV, Lemke EA. Floppy but not sloppy: Interaction mechanism of FG-nucleoporins and nuclear transport receptors. Semin Cell Dev Biol. 2017;68:34-41.
259. Link JO, Rhee MS, Tse WC, Zheng J, Somoza JR, Rowe W, et al. Clinical targeting of HIV capsid protein with a long-acting small molecule. Nature. 2020;584(7822):614-8.
260. He J, Chen Y, Farzan M, Choe H, Ohagen A, Gartner S, et al. CCR3 and CCR5 are co-receptors for HIV-1 infection of microglia. Nature. 1997;385(6617):645-9.
261. Masroori N, Cherry P, Merindol N, Li JX, Dufour C, Poulain L, et al. Gene Knockout Shows That PML (TRIM19) Does Not Restrict the Early Stages of HIV-1 Infection in Human Cell Lines. mSphere. 2017;2(3).
262. Pawlica P, Dufour C, Berthoux L. Inhibition of microtubules and dynein rescues human immunodeficiency virus type 1 from owl monkey TRIMCyp-mediated restriction in a cellular context-specific fashion. J Gen Virol. 2015;96(Pt 4):874-86.
263. Kedzierska K, Crowe SM. The role of monocytes and macrophages in the pathogenesis of HIV-1 infection. Curr Med Chem. 2002;9(21):1893-903.
264. Davis LI, Blobel G. Nuclear pore complex contains a family of glycoproteins that includes p62: glycosylation through a previously unidentified cellular pathway. Proc Natl Acad Sci U S A. 1987;84(21):7552-6.
265. Rusinova I, Forster S, Yu S, Kannan A, Masse M, Cumming H, et al. Interferome v2.0: an updated database of annotated interferon-regulated genes. Nucleic Acids Res. 2013;41(Database issue):D1040-6.
266. McDonald D, Vodicka MA, Lucero G, Svitkina TM, Borisy GG, Emerman M, et al. Visualization of the intracellular behavior of HIV in living cells. J Cell Biol. 2002;159(3):441-52.
267. Nepveu-Traversy ME, Demogines A, Fricke T, Plourde MB, Riopel K, Veillette M, et al. A putative SUMO interacting motif in the B30.2/SPRY domain of rhesus macaque TRIM5alpha important for NF-kappaB/AP-1 signaling and HIV-1 restriction. Heliyon. 2016;2(1):e00056.

268. Pawlica P, Berthoux L. Cytoplasmic Dynein Promotes HIV-1 Uncoating. Viruses. 2014;6(11):4195-211.
269. Monette A, Pante N, Mouland AJ. HIV-1 remodels the nuclear pore complex. J Cell Biol. 2011;193(4):619-31.
270. Jager S, Cimermancic P, Gulbahce N, Johnson JR, McGovern KE, Clarke SC, et al. Global landscape of HIV-human protein complexes. Nature. 2011;481(7381):365-70.
271. Poirson J, Biquand E, Straub ML, Cassonnet P, Nomine Y, Jones L, et al. Mapping the interactome of HPV E6 and E7 oncoproteins with the ubiquitin-proteasome system. FEBS J. 2017;284(19):3171-201.
272. Haffar OK, Popov S, Dubrovsky L, Agostini I, Tang H, Pushkarsky T, et al. Two nuclear localization signals in the HIV-1 matrix protein regulate nuclear import of the HIV-1 pre-integration complex. J Mol Biol. 2000;299(2):359-68.
273. Bukrinsky MI, Sharova N, McDonald TL, Pushkarskaya T, Tarpley WG, Stevenson M. Association of integrase, matrix, and reverse transcriptase antigens of human immunodeficiency virus type 1 with viral nucleic acids following acute infection. Proc Natl Acad Sci U S A. 1993;90(13):6125-9.
274. Miller MD, Farnet CM, Bushman FD. Human immunodeficiency virus type 1 preintegration complexes: studies of organization and composition. J Virol. 1997;71(7):5382-90.
275. Bejarano DA, Peng K, Laketa V, Börner K, Jost KL, Lucic B, et al. HIV-1 nuclear import in macrophages is regulated by CPSF6-capsid interactions at the nuclear pore complex. Elife. 2019;8.
276. Matreyek KA, Engelman A. Viral and cellular requirements for the nuclear entry of retroviral preintegration nucleoprotein complexes. Viruses. 2013;5(10):2483-511.
277. Desai TM, Marin M, Chin CR, Savidis G, Brass AL, Melikyan GB. IFITM3 restricts influenza A virus entry by blocking the formation of fusion pores following virus-endosome hemifusion. PLoS Pathog. 2014;10(4):e1004048.
278. Mears HV, Sweeney TR. Better together: the role of IFIT protein-protein interactions in the antiviral response. J Gen Virol. 2018;99(11):1463-77.
279. Yánez DC, Powell R, Furmanski AL, Lau CI, Ross S, Solanki A, et al. IFITM proteins drive type 2 T helper cell differentiation and exacerbate allergic airway inflammation. European Journal of Immunology. 2018;49(1):66-78.
280. Duan S, Paulson JC. Siglecs as Immune Cell Checkpoints in Disease. Annu Rev Immunol. 2020;38:365-95.
281. Rahimi N. C-type Lectin CD209L/L-SIGN and CD209/DC-SIGN: Cell Adhesion Molecules Turned to Pathogen Recognition Receptors. Biology (Basel). 2020;10(1).
282. van Kooyk Y, Geijtenbeek TB. A novel adhesion pathway that regulates dendritic cell trafficking and T cell interactions. Immunol Rev. 2002;186:47-56.
283. Diotallevi M, Peyrot F, Coppo L, Celestino I, Holmgren A, Palamara AT, et al. Glutathione Fine-Tunes the Innate Immune Response toward Antiviral Pathways in a Macrophage Cell Line Independently of Its Antioxidant Properties. Frontiers in Immunology. 2017;8(12):1239.
284. Oguejiofor CF, Wathes DC, Abudureyimu A, Cheng Z, Fouladi-Nashta AA. Global transcriptomic profiling of bovine endometrial immune response in vitro. I. Effect of lipopolysaccharide on innate immunity. Biology of Reproduction. 2015;93(4):100.

285. Painter MM, Morrison JH, Turkowski KL, Bieber AJ, Warrington AE, Rinkoski TA, et al. Antiviral Protection via RdRP-Mediated Stable Activation of Innate Immunity. PLOS Pathogens. 2015;11(12):e1005311.
286. Fontoura BM, Faria PA, Nussenzveig DR. Viral Interactions with the Nuclear Transport Machinery: Discovering and Disrupting Pathways. IUBMB Life. 2005;57(2):65-72.
287. Roth P, Uv A, Fornerod M, Sabri N, Samakovlis C, Xylourgidis N. The Drosophila nucleoporin DNup88 localizes DNup214 and CRM1 on the nuclear envelope and attenuates NES-mediated nuclear export. The Journal of Cell Biology. 2003;163(4):701-6.
288. Mavlyutov TA, Ferreira PA, Cai Y. Identification of RanBP2- and kinesin-mediated transport pathways with restricted neuronal and subcellular localization. Traffic. 2002;3(9):630-40.
289. Tijms MA, Snijder EJ, Van Der Meer Y. Nuclear localization of non-structural protein 1 and nucleocapsid protein of equine arteritis virus. Journal of General Virology. 2002;83(4):795-800.
290. Islam A, Aryal UK, Boldogh I, Sarker AH, Sharma G, Hazra T, et al. Site-specific acetylation of polynucleotide kinase 3'-phosphatase regulates its distinct role in DNA repair pathways. Nucleic Acids Research. 2024;52(5):2416-33.
291. Chakraborty A, Venkova T, Ghosh G, Mitra J, Ashizawa T, Maciel P, et al. Deficiency in classical nonhomologous end-joining–mediated repair of transcribed genes is linked to SCA3 pathogenesis. Proceedings of the National Academy of Sciences. 2020;117(14):8154-65.
292. Berro R, Pedati C, Kehn-Hall K, Wu W, Klase Z, Even Y, et al. CDK13, a new potential human immunodeficiency virus type 1 inhibitory factor regulating viral mRNA splicing. J Virol. 2008;82(14):7155-66.
293. Labarre A, Tétreault M, Labrecque M, Forest A, Ruiz M, Bareke E, et al. Fatty acids derived from the probiotic Lacticaseibacillus rhamnosus HA-114 suppress age-dependent neurodegeneration. Communications Biology. 2022;5(1):1340.
294. Liu Z, Wang J, Liu G, Zhu R, Cui X, Wang K, et al. Multiomics analyses of Jining Grey goat and Boer goat reveal genomic regions associated with fatty acid and amino acid metabolism and muscle development. Animal bioscience. 2023;37(6):982-92.
295. Tozlu S, Cohen P, Spyratos F, Andrieu C, Vacher S, Girault I, et al. Identification of novel genes that co-cluster with estrogen receptor alpha in breast tumor biopsy specimens, using a large-scale real-time reverse transcription-PCR approach. Endocrine-Related Cancer. 2006;13(4):1109-20.
296. Hornung V, Hartmann R, Ablasser A, Hopfner K-P. OAS proteins and cGAS: unifying concepts in sensing and responding to cytosolic nucleic acids. Nature Reviews Immunology. 2014;14(8):521-8.
297. Jurczyszak D, Bogunovic D, Simon V, Sachidanandam R, Manganaro L, Cipolla M, et al. ISG15 deficiency restricts HIV-1 infection. PLOS Pathogens. 2022;18(3):e1010405.
298. Granelli-Piperno A, Pritsker A, Pack M, Shimeliovich I, Arrighi JF, Park CG, et al. Dendritic cell-specific intercellular adhesion molecule 3-grabbing nonintegrin/CD209 is abundant on macrophages in the normal human lymph node and is not required for dendritic cell stimulation of the mixed leukocyte reaction. J Immunol. 2005;175(7):4265-73.

299. Schetters STT, Kruijssen LJW, Crommentuijn MHW, Kalay H, Ochando J, den Haan JMM, et al. Mouse DC-SIGN/CD209a as Target for Antigen Delivery and Adaptive Immunity. Front Immunol. 2018;9:990.
300. Xu G, Xia Z, Deng F, Liu L, Wang Q, Yu Y, et al. Inducible LGALS3BP/90K activates antiviral innate immune responses by targeting TRAF6 and TRAF3 complex. PLoS Pathog. 2019;15(8):e1008002.
301. Philips RL, Wang Y, Cheon H, Kanno Y, Gadina M, Sartorelli V, et al. The JAK-STAT pathway at 30: Much learned, much more to do. Cell. 2022;185(21):3857-76.
302. Kinterova V, Toralova T, Petruskova V, Kanka J. Inhibition of Skp1-Cullin-F-box complexes during bovine oocyte maturation and preimplantation development leads to delayed development of embryos†. Biology of Reproduction. 2018;100(4):896-906.
303. Liu L, Jiang W, Xie D, Xie H, Zhang J, Xie D, et al. ARHGAP10 Inhibits the Proliferation and Metastasis of CRC Cells via Blocking the Activity of RhoA/AKT Signaling Pathway. OncoTargets and Therapy. 2019;12(6):11507-16.
304. Nagy V, Cole T, Van Campenhout C, Khoung TM, Leung C, Vermeiren S, et al. The evolutionarily conserved transcription factor PRDM12 controls sensory neuron development and pain perception. Cell Cycle. 2015;14(12):1799-808.
305. Zhang L, Yuan Z, Zhao F, Ma X, Zhu C, Xuan J, et al. Identification of MEF2B and TRHDE Gene Polymorphisms Related to Growth Traits in a New Ujumqin Sheep Population. PLOS ONE. 2016;11(7):e0159504.
306. Liang A, Sun W, Zhou B. Integrated genomic characterization of cancer genes in glioma. Cancer Cell International. 2017;17(1):90.
307. He L, Vasiliou K, Nebert DW. Analysis and update of the human solute carrier (SLC) gene superfamily. Human Genomics. 2009;3(2):195.
308. Franke R, Gardner E, Sparreboom A. Pharmacogenetics of Drug Transporters. Current Pharmaceutical Design. 2010;16(2):220-30.
309. De Mattia E, Corona G, Dreussi E, Polesel J, D'Andrea M, Toffoli G, et al. Pharmacogenetics of ABC and SLC transporters in metastatic colorectal cancer patients receiving first-line FOLFIRI treatment. Pharmacogenetics and Genomics. 2013;23(10):549-57.
310. Gyimesi G, Pujol-Gimenez J, Kanai Y, Hediger MA. Sodium-coupled glucose transport, the SLC5 family, and therapeutically relevant inhibitors: from molecular discovery to clinical application. Pflugers Arch. 2020;472(9):1177-206.
311. Droździk M, Lapczuk-Romanska J, Wenzel C, Skalski Ł, Szeląg-Pieniek S, Post M, et al. Protein Abundance of Drug Transporters in Human Hepatitis C Livers. International journal of molecular sciences. 2022;23(14):7947.
312. Huang Y. Pharmacogenetics/genomics of membrane transporters in cancer chemotherapy. Cancer and Metastasis Reviews. 2007;26(1):183-201.
313. Katoh M, Katoh M. Human FOX gene family (Review). Int J Oncol. 2004;25(5):1495-500.

Appendix

Effects of GS-CA1 on nuclear envelope-associated early HIV-1 infection steps

Amita Singh, Victor Fourcassié, Karen Cristine Gonalves Dos Santos, Hocine Chelbi, Natacha Merindol, Arnaud Droit,Arnaud Droit, Hugo Germain, Lionel Berthoux

Published: Front. Virol., 02 February 2025

Sec. Antivirals and Vaccines

Volume 5 - 2025 | https://doi.org/10.3389/fviro.2025.1547176

Abstract

The novel HIV-1 drugs GS-CA1 and the recently approved lenacapavir (GS-6207) target the viral structural protein capsid (CA). However, their multiple mechanisms of action have not been fully characterized. Here, we investigated the effects of GS-CA1 on the early stages of HIV-1 infection, specifically the steps involving the nuclear envelope, in comparison to the antiviral cytokine IFN-β. Mass spectrometry data indicated that nuclear envelope proteins were only modestly affected by either GS-CA1 treatment or HIV-1 infection, but combining the two had a more significant impact, altering the levels of many proteins including proteasomal components. GS-CA1 induced a small but clear accumulation of HIV-1 capsid cores at nuclear pores, as seen by microscopy, whereas IFN-β caused a strong accumulation of HIV-1 cores at the nuclear envelope but not specifically at nuclear pores. These observations are consistent with GS-CA1 inhibiting the nuclear translocation of HIV-1 capsid cores through nuclear pores.

frontiers | Frontiers in Virology

TYPE Brief Research Report
PUBLISHED 03 February 2025
DOI 10.3389/fviro.2025.1547176

OPEN ACCESS

EDITED BY
Tsutomu Murakami,
National Institute of Infectious Diseases (NIID), Japan

REVIEWED BY
Akatsuki Saito,
University of Miyazaki, Japan
Kazuaki Monde,
Kumamoto University, Japan

*CORRESPONDENCE
Lionel Berthoux
lionel.berthoux@uqtr.ca

RECEIVED 17 December 2024
ACCEPTED 15 January 2025
PUBLISHED 03 February 2025

CITATION
Singh A, Fourcassié V, Gonçalves Dos Santos KC, Chelbi H, Merindol N, Droit A, Germain H and Berthoux L (2025) Effects of GS-CA1 on nuclear envelope-associated early HIV-1 infection steps. *Front. Virol.* 5:1547176. doi: 10.3389/fviro.2025.1547176

Effects of GS-CA1 on nuclear envelope-associated early HIV-1 infection steps

Amita Singh[1], Victor Fourcassié[2,3], Karen Cristine Gonçalves Dos Santos[4], Hocine Chelbi[1], Natacha Merindol[3], Arnaud Droit[2,3], Hugo Germain[4] and Lionel Berthoux[1]*

[1]Department of Medical Biology, Université du Québec à Trois-Rivières, Trois-Rivières, QC, Canada, [2]Proteomics Platform of the Centre Hospitalier Universitaire de Québec - Université Laval, Québec, QC, Canada, [3]Centre de recherche du Centre Hospitalier Universitaire de Québec - Université Laval, Québec, QC, Canada, [4]Department of Chemistry, Biochemistry and Physics, Université du Québec à Trois-Rivières, Trois-Rivières, QC, Canada

The novel HIV-1 drugs GS-CA1 and the recently approved lenacapavir (GS-6207) target the viral structural protein capsid (CA). However, their multiple mechanisms of action have not been fully characterized. Here, we investigated the effects of GS-CA1 on the early stages of HIV-1 infection, specifically the steps involving the nuclear envelope, in comparison to the antiviral cytokine IFN-β. Mass spectrometry data indicated that nuclear envelope proteins were only modestly affected by either GS-CA1 treatment or HIV-1 infection, but combining the two had a more significant impact, altering the levels of many proteins including proteasomal components. GS-CA1 induced a small but clear accumulation of HIV-1 capsid cores at nuclear pores, as seen by microscopy, whereas IFN-β caused a strong accumulation of HIV-1 cores at the nuclear envelope but not specifically at nuclear pores. These observations are consistent with GS-CA1 inhibiting the nuclear translocation of HIV-1 capsid cores through nuclear pores.

KEYWORDS

HIV-1, HIV-1 capsid, GS-CA1, mass spectrometry, nuclear pore complex, nuclear envelope, interferon

Introduction

HIV-1 capsid (CA) proteins have a central role in several early post-entry stages of infection, including retrograde transport, nuclear import and integration (1–5). In particular, CA is key to HIV-1 nuclear import through nuclear pore complexes (NPCs), which are large protein channels embedded in the nuclear envelope. Comprising multiple

copies of nucleoporins (Nups), NPCs facilitate the bidirectional transport of macromolecules such as proteins, RNA and ribonucleoprotein complexes [reviewed in (6)]. About one-third of Nups contain phenylalanine-glycine-rich motifs (FG repeats) and are important for the selection of cargos to be transported through NPCs (7). Consistent with its central role in nuclear import, CA was found to interact with several FG-containing Nups, such as Nup88, Nup214, Nup358/RanBP2 (cytoplasmic side); Nup62, Nup98, Nup107 (central ring); and Nup153 (nuclear basket) (8–10) [reviewed in (11)]. These findings have led to a model whereby the capsid core interacts sequentially with various Nups present in NPCs, driving its import to the nucleus (11). Interestingly, HIV-1 was also found to modulate the levels of Nup358 at NPCs (12, 13), which opens the possibility that HIV-1 cores affect NPCs integrity instead of simply using them to achieve passage to the nucleus. In addition to being relevant to HIV-1 nuclear import, NPCs are key to antiviral responses triggered by type I interferons (IFN-I), including IFN-β. For instance, IFN-I-induced antiviral protein Mx2 (MxB) interactions with multiple nucleoporins is required for its inhibitory activity against HIV-1 at the nuclear import step (14). Interestingly, CA is the target of Mx2, and their interaction results in a block to HIV-1 nuclear transport (15, 16). Furthermore, NPCs play a central role in the signaling cascades that form the basis of the IFN-I pathway, and as a result, viruses are known to interfere with the nuclear-cytoplasmic transport of IFN-I signaling components (17).

Current HIV pharmacological treatments rely largely on targeting the viral enzymes protease, reverse transcriptase and integrase. By contrast, GS-CA1 and the structurally close GS-6207 (lenacapavir) are CA inhibitors that disrupt viral capsid formation by interfering with CA-CA interactions (18). In clinical trials, GS-6207/lenacapavir has demonstrated efficacy against multidrug-resistant HIV-1 strains (19) and was approved in 2022 for the treatment of heavily treatment-experienced individuals (20). GS-CA1 has not been pursued in humans but showed a strong protective effect against HIV-1 in a primate model (21). Consistent with the important role for CA in both early and late stages of the virus life cycle, GS-CA1 and GS-6207 have pleiotropic effects on HIV-1 (18, 22, 23). Their effects on early stages seem to stem from a stabilization of the viral capsid core, as seen in "fate-of-capsid assays" (22, 24). Quantitative analyses of reverse transcribed HIV-1 cDNA as well as its specifically nuclear species (2-LTR DNA and integrated DNA) suggest that GS-CA1 and GS-6207 can inhibit several early HIV-1 replication steps, including nuclear import (18, 22, 23). However, discordant results were obtained from another team, who did not observe an effect of GS-CA1 on CA presence in the nucleus following infection (24). Whether GS-CA1 and GS-6207 cause HIV-1 to be specifically sequestered at NPCs is unknown. The effects of these novel CA-targeting drugs and of HIV-1 on the composition of NPCs in the early stages of the virus life cycle have never been investigated by mass spectrometry (MS). Here, using MS and immunofluorescence microscopy, we evaluated the impact of HIV-1 infection and GS-CA1 treatment, in comparison to IFN-β treatment, on the nuclear envelope and the localization of HIV-1 capsid cores at the nuclear envelope and nuclear pores.

Materials and methods

Cell culture

THP-1 monocytic cells were cultured in Cytiva HyClone RPMI 1640 medium containing L-glutamine (SH3002701) supplemented with 10% Cytiva HyClone fetal bovine serum (FBS, SH3039603) and penicillin-streptomycin (Cytiva HyClone, SV30010). Crandell-Rees Feline Kidney (CRFK) cells and human embryonic kidney 293T cells (HEK293T) were maintained in high glucose Cytiva HyClone Dulbecco's Modified Eagle's Medium (DMEM) containing L-glutamine and sodium pyruvate (SH3024301) supplemented with 10% FBS and penicillin-streptomycin. All cell culture reagents were purchased through Fisher Scientific, Ottawa, Canada.

HIV-1 vector production and titration

To produce the GFP-expressing, vesicular stomatitis virus protein G (VSV-G)-pseudotyped HIV-1 vector $NL43_{GFP}$, HEK293T cells were transfected with 10 µg $pNL43_{GFP\Delta Env\Delta Nef}$ (25, 26) and 5 µg pMD2.G (26) using polyethyleneimine (PEI, Polysciences, Niles, IL) (27) for 16 h, after which the supernatants were replaced with fresh medium (26). The supernatants were collected 24 and 48 h later. Cell debris were removed by low-speed centrifugation (3,000 rpm, 10 min at room temperature), followed by filtration through 0.45 µm filters (Millipore Sigma Durapore PVDF). Virus titrations were performed by infecting CRFK cells with serial dilutions of the vector preparations. CRFK cells were fixed in Cytiva HyClone Dulbecco's phosphate buffer saline (PBS; #SH30028LS) containing 4% formaldehyde (37% solution, BioBasic, Quebec, Canada), and the percentage of infected cells was assessed by flow cytometry using a Beckman Coulter FC500 instrument. CRFK viral titers were calculated by analyzing flow cytometry results using FCS Express 6 software (*De Novo* Software).

EC_{50} determination

THP-1 cells were seeded at a density of 20,000 cells/well in 96-well plates. Cells were then treated with 2-fold serial dilutions of GS-CA1 (Gilead Sciences, Foster City, California, USA) and 2 h later were infected with $NL43_{GFP}$ (CRFK MOI = 1). 48 h later, cells were fixed in 4% formaldehyde and the percentage of GFP-positive cells was determined using flow cytometry. GS-CA1 EC_{50} was calculated using an online tool available at https://www.aatbio.com/tools/ic50-calculator (accessed 2021-02-08).

Large-scale infections and nuclear envelope purification

2 x 10^7 THP-1 cells cultured in flasks were treated or not with 2 nM GS-CA1 for 2 h and then were infected or not with $NL43_{GFP}$ using a viral dose (MOI = 2) leading to about 40% productively infected THP-1 cells, for 12 h. In a distinct experiment, cells were treated or not with 10 ng/ml IFN-β (PeproTech, Rocky Hill, NJ, USA) and were infected 12 h later with $NL43_{GFP}$ for 12 h. A small aliquot of the cells was preserved for flow cytometry analysis 36 h later. The remainder of the cells were processed for the extraction of nuclear envelope-enriched fractions using a Minute™ Nuclear Envelope Protein Extraction Kit (Invent Biotechnologies, Plymouth, MN, USA). Whole-cell lysates, cytoplasmic extracts, and nuclear extracts also prepared using the same kit were included in the purification validation experiments.

Western blotting

Protein concentrations in the nuclear envelope extracts were determined using the Bio-Rad Protein Assay kit and samples were normalized accordingly prior to SDS-polyacrylamide gel electrophoresis and transfer to polyvinylidene difluoride (PVDF) or nitrocellulose membranes. Blotted proteins were analyzed using the FG repeats-specific MAb414 mouse monoclonal antibody at 1:2,000 dilution (#902907, BioLegend, San Diego, CA), followed by detection with an HRP-conjugated anti-mouse secondary antibody (#7076S, New England Biolabs, Whitby, Ontario). Detection of glyceraldehyde 3-phosphate dehydrogenase (GAPDH) using the #9484 mouse monoclonal antibody (Abcam, Toronto, ON) was used as a marker for cytosolic proteins. Blots were visualized using the Thermo Scientific SuperSignal West Femto substrate, and images were recorded using the Bio-Rad ImageLab system.

Mass spectrometry

10 µg of protein from nuclear envelope-enriched fractions were reduced using 0.2 mM dithiothreitol, alkylated using 0.8 mM iodoacetamide and digested with 0.2 µg of trypsin (sequencing grade, Promega, Madison, WI). Samples were analyzed by nano-LC/MSMS using a Dionex UltiMate 3000 nanoRSLC chromatography system (Thermo Fisher Scientific) interfaced to an Orbitrap Fusion mass spectrometer (Thermo Fisher Scientific, San Jose, CA, USA) equipped with a nanoelectrospray ion source. 1 µg of peptides were separated on a C18 Pepmap Acclaim column (50 cm length, 75 µm internal diameter) using a 90 min linear gradient at 300 nL/min with 5-40% solvent B (A: 0.1% formic acid, B: 80% acetonitrile, 0.1% formic acid). Mass spectra were obtained with a data-dependent acquisition method using the Thermo XCalibur software version 4.1.50. Full scan mass spectra (350–1800 m/z, 120,000 resolution) were acquired from Orbitrap using an AGC target of 4e5 with a maximum injection time of 50 ms. Precursors were filtered in the quadrupole analyzer with 1.6 m/z isolation windows and fragmented by higher-energy Collision-induced Dissociation (HCD) with 35% collision energy. The resulting fragments were detected using the linear ion trap at a rapid scan rate with an AGC target of 1e4 and a maximum injection time of 50 ms.

MS data analysis

For the IFN-β-treated THP-1 cells experiment, the acquired spectra were processed using the Minora feature detector algorithm in Proteome Discoverer 2.3 (Thermo Fisher Scientific). The resulting data were subjected to MASCOT searches against the UniProt *Homo sapiens* protein database (reference proteome UP000005640 with 74485 entries, downloaded on 2019-02-12) considering trypsin digestion. For protein validation, a false discovery rate (FDR) of ≤ 0.01 was allowed at peptide and protein levels based on a target/decoy search. Unique and razor peptides were considered for protein quantification, and normalization was performed based on the summed abundance of the peptides. The data were normalized using the intensity normalization factor, which was calculated by dividing the median intensity for each sample by the median intensity for all samples combined. The results were exported to an Excel file where samples were compared to each other using absolute Z-score > 1.96, q-value < 0.05 and log2 ratio between the two conditions > 0, in order to determine the statistical significance of the observed variations. For the GS-CA1 experiments, spectra were analyzed in Maxquant using the Andromeda search engine (version 2.0.2.0) against a UniProt *Homo sapiens* protein database (reference proteome UP000005640 with 97094 entries, downloaded on 2020-09-24). Trypsin was set as the digestion parameter and a maximum FDR of 1% was set both at the peptide and protein level. The proteinGroups.txt output file was imported into R software and the LFQ normalized intensities were used to compare the groups considering the same Z-score and q-value thresholds as above.

Microscopy

Cells were fixed in 4% formaldehyde and permeabilized with Triton X-100 (0.2%) in 1x PBS for 10 min. Cells were then stained for HIV-1 CA protein using a mouse monoclonal antibody (Clone 183 diluted 1:5000, AIDS Research Reagents Program, contributed by Bruce Chesebro), co-stained for nucleoporin TPR (rabbit antibody, 1:1000 dilution, Abcam #84516), and for DNA using Hoechst 33342 (Invitrogen #3570, through Fisher Scientific Canada) (28). Alexa Fluor 488 anti-mouse and 594 anti-rabbit secondary antibodies were used (1:5000 dilution, Molecular Probes). Images were acquired with a Leica TSC SP8 confocal microscope fitted with a 63×/1.40 oil objective using the optimal resolution for the wavelength (determined using the Leica software). CA signal dots were counted out of 19-20 slides for each condition (26 to 28 cells), and CA dots that co-localized with the TPR signal were counted as well (as seen by the presence of orange color), allowing us to calculate the colocalization ratio. Counting was performed blindly, from anonymized pictures and

by a student who was not involved in the "wet lab" phase of the experiment.

Results

GS-CA1 efficiently inhibits early stages of HIV-1 infection in THP-1 cells

THP-1 monocytic cells are representative of the monocyte-macrophage lineage, one of the main types of HIV-1 host cells *in vivo* (29). To assess the effects of GS-CA1 on the early steps of HIV-1 infection in these cells, we used an NL4-3-derived, VSV-G-pseudotyped HIV-1 vector expressing GFP in place of Nef (25). VSV-G pseudotyping greatly increases virus entry efficiency, allowing for detection of HIV-1 cores in cells by MS and by microscopy, and is not believed to alter post-fusion steps of the infection process (30). THP-1 cells were challenged with $NL43_{GFP}$ in the presence of multiple drug concentrations, and the percentage of GFP-positive cells was determined using flow cytometry (Figure 1A). We found that GS-CA1 strongly inhibits THP-1 infection, with an EC_{50} of approximately 0.125 nM (Figure 1A), which is consistent with previous studies (18).

Isolation of nuclear envelopes for mass spectrometry analyses

To analyze the effects of HIV-1 vector infection and/or drug treatment on nuclear pore proteins, we produced nuclear envelope-enriched fractions. First, we performed a pilot experiment with uninfected/untreated cells, to assess nuclear envelope fractions extracted using a commercial kit (Supplementary Figure S1). Whole-cell, cytoplasmic, nuclear and nuclear envelope protein lysates were obtained. "Nuclear" fractions are supernatants of the nuclear envelope precipitation step. Fractions were analyzed by Western blotting with the monoclonal antibody MAb414 which recognizes several Nups through binding to the FG repeats (31). Using this antibody, we observed an enrichment in bands above 150 kDa in the nuclear envelope fractions, consistent with the high molecular weight of several FG-containing Nups. As expected, GAPDH was absent from the nuclear envelope fractions (Supplementary Figure S1).

In the next experiment, THP-1 cells were infected or not with $NL43_{GFP}$ for 12 h, in the presence or absence of 2 nM GS-CA1, which was the lowest concentration at which no infection could be detected (Figure 1A). Quintuplicate infections were performed at a multiplicity of infection leading to about 40% infected cells in the absence of drug (Figure 1B). The GS-CA1 concentration used was 16-times higher than the observed EC_{50}. As expected, infection with the $NL43_{GFP}$ vector was completely abrogated at this concentration (Figure 1B). Nuclear envelope extracts were subjected to label-free mass spectrometry (MS). The principal component analysis (PCA) shown in Supplementary Figure S2 demonstrates that the control and GS-CA1 treated cells show only minor differences (except for sample CTRL_5), whereas the $NL43_{GFP}$-infected ("HIV-1") group and the $NL43_{GFP}$-infected + GS-CA1-treated group are clearly distinct. Supplementary Figure S3 summarizes the number of proteins quantified for each condition, as well as the number of proteins found to be regulated in pairwise analyses, showing that the greatest number of dysregulated proteins is found when comparing HIV-1 + GS-CA1 to either control samples or GS-CA1-treated ones.

Effect of HIV-1 and GS-CA1 on nuclear envelope-associated proteins as seen by mass spectrometry

Volcano plots were created based on the MS data in order to visually identify the most dysregulated proteins between two conditions (Figure 2). With the threshold parameters used (z-score ≥ or ≤ 1.96; p-values and q-values ≤ 0.05), we found that HIV-1 vector infection alone and GS-CA1 treatment alone had little impact on nuclear envelope proteins, as previously observed in the PCA (Supplementary Figure S2). HIV-1 ($NL43_{GFP}$) infection resulted in the reduced relative abundance of only 5 proteins, *i.e.* Lysozyme C (LYZ), pH domain leucine-rich repeat-containing

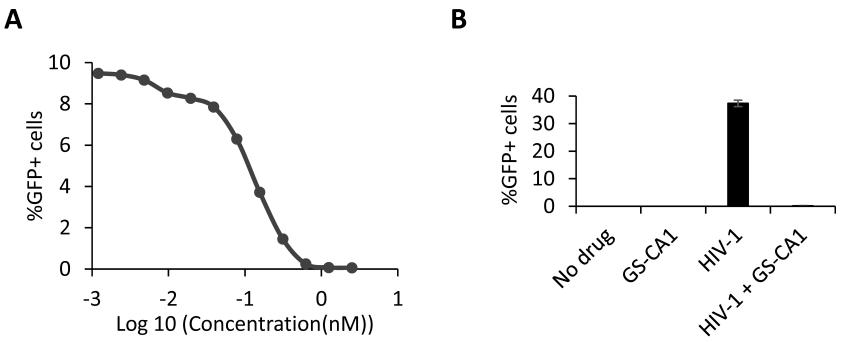

FIGURE 1
GS-CA1 efficiently inhibits HIV-1 early infection stages in THP-1 cells. **(A)** Dose-dependent inhibition of $NL43_{GFP}$. THP-1 cells were treated with multiple dilutions of GS-CA1 and infected with $NL43_{GFP}$ for 48 h, at which point, % GFP-positive cells were determined by FACS. **(B)** Infection control in mass spectrometry (MS) experiments. Cells were infected or not with $NL43_{GFP}$ (CRFK MOI = 2) and treated or not with 2 nM GS-CA1. 12 h later, cells were processed for MS but small aliquots were placed back in culture for one more day. % GFP-positive cells were determined by FACS. Shown are average data from 5 replicates, with standard deviations.

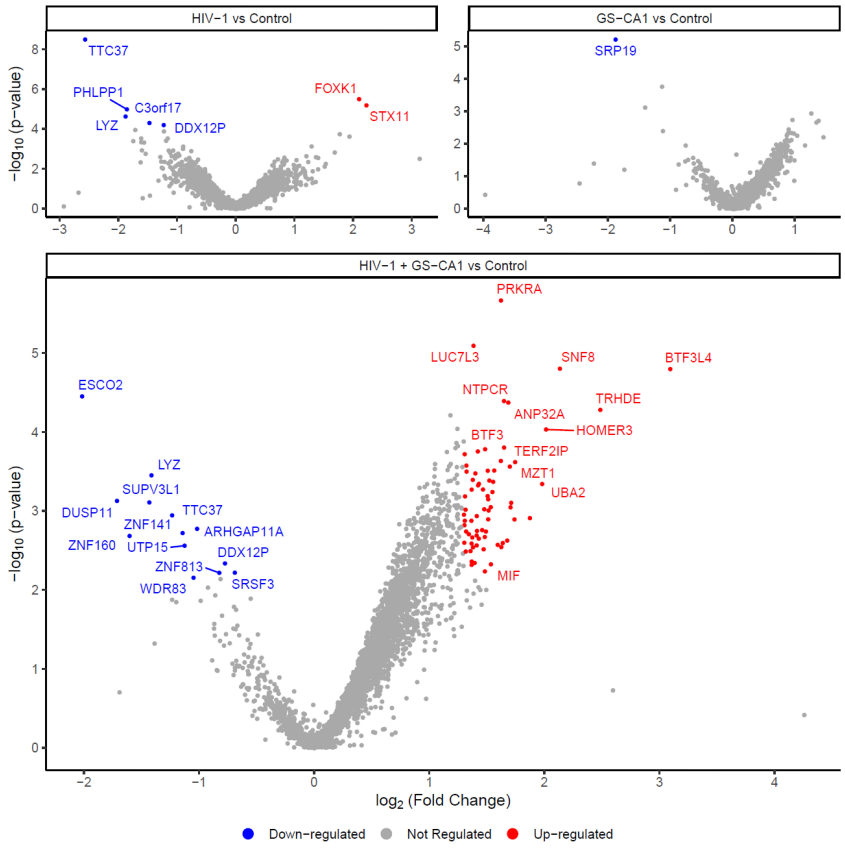

FIGURE 2
Modulation of proteins in nuclear envelope-enriched fractions by HIV-1 infection and GS-CA1 treatment. THP-1 cells were infected or not with $NL43_{GFP}$ (CRFK MOI = 2) and treated or not with 2 nM GS-CA1. Infections were done in quintuplicates. 12 h later, cells were processed for MS. Volcano plots show dysregulated proteins for $NL43_{GFP}$-infected cells compared to control (uninfected) cells (top left), GS-CA1-treated cells compared to control (untreated) cells (top right) and $NL43_{GFP}$-infected, GS-CA1-treated cells compared to control (uninfected, untreated) cells (bottom). Colored dots indicate proteins upregulated (red) or downregulated (blue). Grey dots indicate non-dysregulated proteins.

protein phosphatase 1 (PHLPP1), NEPRO (Nucleolus and neural progenitor protein; C3orf17), DEAD/H-box helicase 12 pseudogene (DDX12P) and tetratricopeptide repeat protein 37 (TTC37). The abundance of two proteins was increased by HIV-1 infection, *i.e.* forkhead box protein K1 (FOXK1) and Syntaxin-11 (STX11). Treatment with GS-CA1 led to the downregulation of only one cellular protein, signal recognition particle 19 (SRP19). Of note, none of the proteins found to be regulated by HIV-1 or GS-CA1 is known as an integral protein of the nuclear envelope, raising the possibility that they are transiently associating with the nuclear envelope. In contrast, HIV-1 infection in the presence of GS-CA1 altered the levels of 84 proteins, with 71 upregulated and 13 downregulated proteins. A full list of proteins regulated by HIV-1 and/or GS-CA1 is made available (see Supplementary Material). Again, most of these 84 proteins are not known as permanent nuclear envelope residents. Interestingly, several of them are interferon-stimulated gene products, according to the Interferome database (32). We also performed single-variable comparisons, i.e. HIV-1 + GS-CA1 vs HIV-1 and HIV-1 + GS-CA1 vs GS-CA1 (Supplementary Figure S4), and interestingly, we observed that HIV-1 was a much greater inducer of variation than GS-CA1 treatment.

Finally, in order to ascertain that the mass spectrometry approach chosen can detect an expected modulation pattern, we also treated THP-1 cells with IFN-β and then analyzed nuclear envelope-enriched fractions from treated and untreated cells (Supplementary Figure S5). Results showed that nearly 120 proteins were either downregulated or upregulated. As expected, most upregulated proteins were ISGs, including known antiviral factors such as Mx2 and ISG15 (33, 34). Interestingly, when we compared the proteins regulated by HIV-1 or HIV-1 + GS-CA1 treatment, on one hand, to the proteins regulated by IFN-I treatment, on the other hand, we found that SH3 domain-binding glutamic acid-rich-like protein 3 (SH3BGRL3) was upregulated in both conditions.

IFN-β but not GS-CA1 causes the accumulation of HIV-1 at the nuclear envelope

GS-CA1 was proposed to induce a block to nuclear import, though this is still disputed. Thus, we analyzed the presence in the nuclear envelope-enriched fractions of HIV-1 proteins-derived

peptides, which were not included in the results shown in Figure 2. We performed an identical analysis in cells treated or not with IFN-β, as this drug promotes the expression of ISGs, including Mx2 which was proposed to interfere with HIV-1 nuclear import by binding CA proteins (14). All the peptides detected were from the structural proteins matrix (MA) and capsid (CA). GS-CA1 did not result in any noticeable modulation in the relative abundance of these peptides in $NL43_{GFP}$-infected cells (Figure 3A). Remarkably, in the presence of IFN-β, a substantial increase in several of the HIV-1 peptides in the nuclear envelope extracts was evident (Figure 3B).

HIV-1 colocalizes with TPR in the presence of GS-CA1

To evaluate the impact of GS-CA1 on HIV-1 cellular distribution in the early stages of the infection, we conducted immunofluorescence microscopy experiments, staining for HIV-1 CA as well as the Nup TPR as a nucleopore marker. As shown Figure 4A, HIV-1 CA signal was present mostly as small "dots" which were found throughout the cells in the conditions used. Based on previous work from our team and others, those dots are expected to represent mostly individual HIV-1 cores/replication complexes (30, 35, 36). TPR was found almost entirely at the nuclear envelope and was partially found in the form of punctate signal consistent with NPCs. In a blinded analysis, we quantified the percentage of CA "dots" colocalizing with TPR, in absence or presence of GS-CA1 and IFN-β. Colocalization was rare, but examples are shown by white arrows in Figure 4A, whereas the quantification analysis is shown in Figure 4B. We found that in the presence of GS-CA1, the relative number of HIV-1 CA signal colocalizing with TPR increased by about 8-fold. Treatment with IFN-β also resulted in an increase in CA-TPR colocalization, but this phenotype was smaller compared with GS-CA1 (Figure 4B). However, IFN-β induced a distinct CA distribution, *i.e.* its accumulation in the immediate vicinity of the nuclear envelope, but not particularly at TPR-positive nuclear pore (see blue arrows in Figure 4A).

Discussion

The mechanisms of action for GS-6207 and related antiviral compounds need to be established more thoroughly. When this

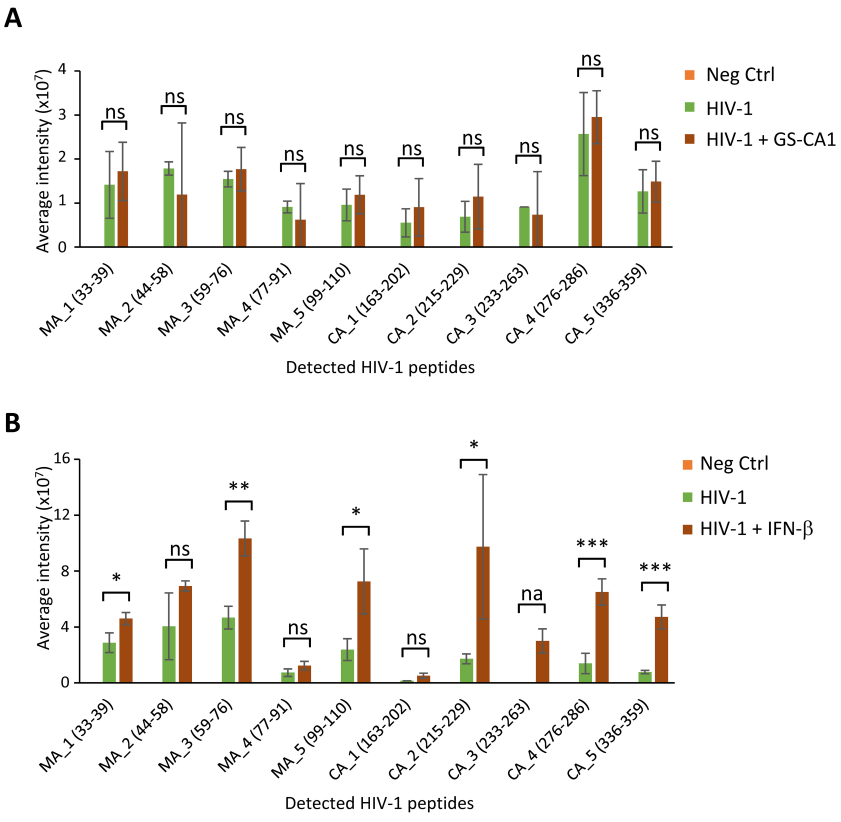

FIGURE 3
HIV-1 protein levels in nuclear envelope fractions are modulated by IFN-β but not GS-CA1. **(A)** Intensity of HIV-1 protein-associated peptides detected by MS in nuclear envelope-enriched fractions following infection with the $NL43_{GFP}$ vector in absence or presence of GS-CA1 (2nM), or in uninfected, untreated cells as a control (Neg Ctrl). Bars represent the average values from 5 replicates, with standard deviations. **(B)** Intensity of HIV-1 peptides in nuclear envelope-enriched fractions from cells infected with $NL43_{GFP}$ and treated or not with IFN-β (10 ng/ml) or in uninfected, untreated cells as a control (Neg Ctrl). Bars represent the average values from 3 replicates, with standard deviations. In both **(A, B)**, only peptides with intensity levels significantly above background were included. Statistical significance was determined using the one-tailed t-test. *$p < 0.05$; **$p < 0.005$; ***$p < 0.0005$; ns, not significant; na, not applicable due to a lack of detectable peptide in absence of GS-CA1.

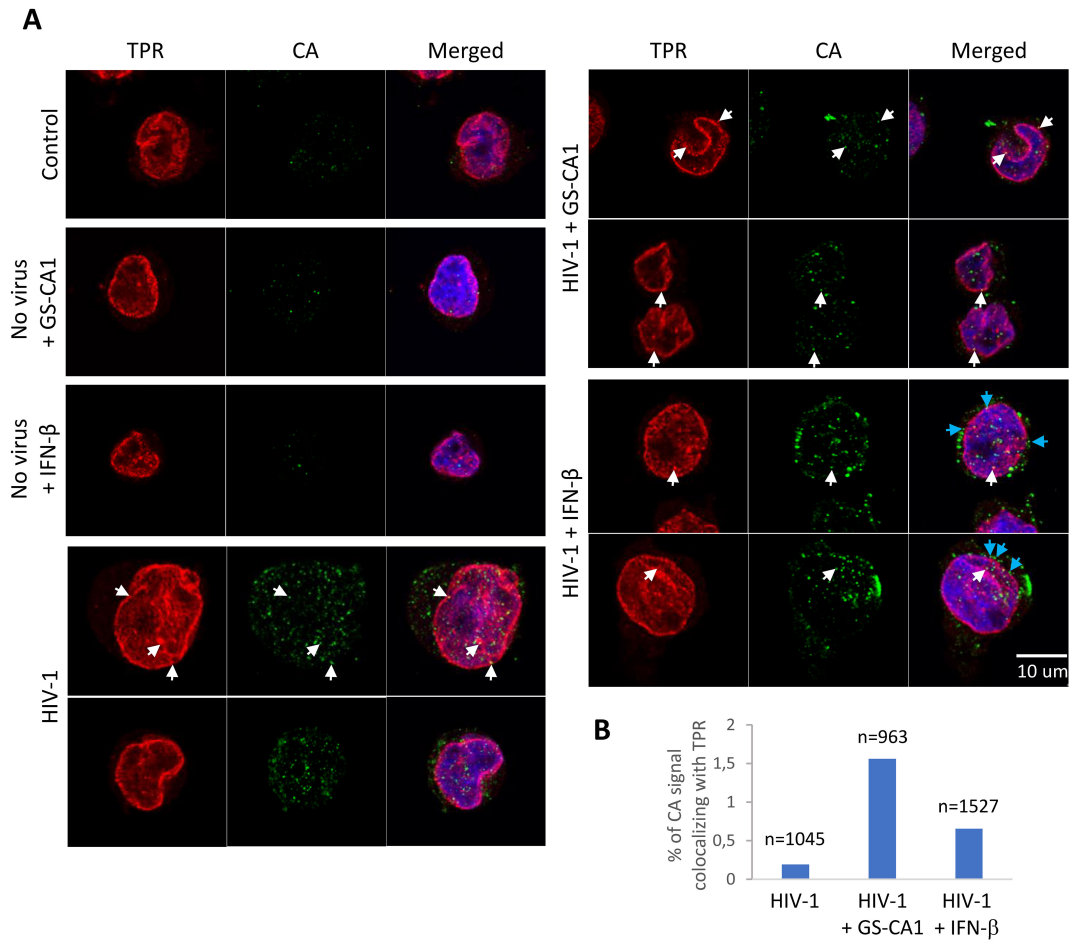

FIGURE 4
Effect of GS-CA1 and IFN-β on HIV-1 subcellular distribution. **(A)** THP-1 cells were infected with $NL43_{GFP}$ (CRFK MOI = 2) for 12 h in the presence or absence of either IFN-β added 12 h before infection) or GS-CA1 (added 2 h prior to infection). Cells were then fixed and stained with a CA antibody (green) and a TPR antibody (red). Hoechst 33342 was used to reveal DNA (blue). White arrows show examples of the CA-TPR colocalization whereas cyan arrows point to examples of CA signal accumulating in the vicinity of the nuclear envelope. **(B)** 20 randomly selected fields for each condition were used to count the percentage of CA signal "dots" colocalizing with TPR, relative to the total number of CA signal dots (see Methods). The total number of CA dots analyzed is shown on top of each bar.

project was initiated, GS-6207 was not approved yet, and the compound was not made available to us, but GS-CA1 was. We focused on the effect of GS-CA1 on HIV-1 functional interactions with the nuclear envelope. Mass spectrometry on nuclear envelope-enriched fractions had been done in the context of late stages of HIV-1 replication (37). To the best of our knowledge, no similar investigation had been conducted focusing on the early stages of the infection. We found that few proteins were modulated by either HIV-1 infection or GS-CA1 treatment alone (Figure 2), though of course, a different conclusion may be reached by using less stringent threshold parameters. Although SRP19 (downmodulated by GS-CA1) has been linked to the antiviral effect of APOBEC3G (38), none of the proteins found to be modulated are known to be involved in the early stages of HIV-1, and none are *bona fide* NPC components. The results obtained were strikingly different in cells that were both infected and GS-CA1-treated, since we found 71 upregulated and 13 downregulated proteins, upon comparison with the control cells (Figure 2). It is unlikely that the difference in phenotype between, on one hand, HIV-1 alone or GS-CA1 alone, and on the other hand, the HIV-1 + GS-CA1 combination, is due to cytotoxicity. The concentration of GS-CA1 used in this experiment, 2 nM, is well below the cytotoxic concentrations for this drug [CC50 > 30 μM (18)]. Also, less than half of the cells were infected in the control without drug in this experiment (Figure 1B), making it unlikely that the dose of virus used would have cytotoxic effects after 16 h of infection. Thus, we conclude that the modulation of nuclear envelope proteins in these conditions stems from the inhibition of the virus by GS-CA1. One possibility is that GS-CA1 causes HIV-1 cores to be sequestered at nuclear pores, leading to the increased presence of proteins interacting with them and/or proteins that are specialized sensors of viral pathogens. Along these lines, we found that SH3BGRL3, an IFN-β-stimulated protein in these cells, was also upregulated by HIV-1. Though no functional interactions between HIV-1 and SH3BGRL3 have been described so far, the

latter may be part of an antiviral response targeting the former. Another possibility is that HIV-1 may obstruct nuclear pores, leading to an accumulation of HIV-1-irrelevant proteins that normally transit through these pores. However, we did not observe modulation of Nups. It should be reminded that the HIV-1 vector used in this study was VSV-G-pseudotyped; the possibility that this affects the results obtained cannot be excluded.

Using MS, we were able to detect the presence of HIV-1 peptides in nuclear envelope-enriched fractions (Figure 3). Interestingly, all of the peptides that could be quantified belonged to MA or CA. Early work had involved MA as important for HIV-1 nuclear import, due to the presence of nuclear localization signals in this protein (39). Accordingly, MA was found long ago to co-purify with HIV-1 complexes present in the nucleus of acutely infected cells (40, 41). As stated in the introduction, the modern view of HIV-1 nuclear import is that an intact or nearly intact capsid core transits through the NPCs, which implies that MA proteins are totally dissociated from the HIV-1 complex that gains access to the nucleus; perhaps this new model over-simplifies HIV-1 nuclear import. HIV-1 MA and CA peptides were present in significantly higher amounts in nuclear envelope fractions in the presence of IFN-β. This effect might be explained by the IFN-induced overexpression of Mx2, a well-investigated host factor that stabilizes HIV-1 cores and inhibits their nuclear import (14). Upon immunofluorescence analysis of acutely infected cells (Figure 4), we did observe an increase in the relative colocalization of HIV-1 cores (as detected with a CA antibody) and NPCs stained with a TPR antibody, in presence of IFN-β. However, a more striking phenotype associated with IFN-β treatment was the accumulation of apparent HIV-1 capsid cores in close vicinity to the nucleus without a strong pattern of colocalization with TPR. By contrast, GS-CA1 caused a more pronounced phenotype of association with NPCs. Why, then, did we not see an increase in the relative amounts of HIV-1 peptides in nuclear envelope fractions upon GS-CA1 treatment (Figure 3)? A simple explanation is that even in the presence of the drug, we only detected a small fraction of total cellular CA signal as colocalizing with TPR in the microscopy experiment (1.5%), and thus modulation of this specifically NPC-associated population probably could not have been detected in the nuclear envelope-enriched fractions that were used for MS.

Taken together, our MS and microscopy data suggest that GS-CA1 causes a block to nuclear import in THP-1 cells by sequestration of HIV-1 capsid cores at nuclear pores, whereas IFN-β causes their retention at the nuclear envelope or in an as-yet-undefined cellular compartment that associates and co-purifies with the nuclear envelope. In addition, GS-CA1 causes the dysregulation of nuclear envelope fraction proteins in acutely HIV-1-infected cells, an effect that is not predicted by the analysis of drug toxicity in the absence of viral infection. Limitations to this study, however, include (i) the focus on a single monocytic cell line and the absence of data from cells of the lymphoid lineage; (ii) the use of VSV-G pseudotyping, as mentioned before; (iii) the use of a single inhibitor concentration and a single MOI. Future studies will need to include a more diverse set of conditions in order to more fully characterize the relevance of nuclear membranes to the mechanism of action of GS-CA1 or IFN-I.

Data availability statement

The original contributions presented in the study are included in the article/Supplementary Material and were previously uploaded here: https://figshare.com/projects/Singh_et_al_2025/194951. Further inquiries can be directed to the corresponding author/s.

Ethics statement

Ethical approval was not required for the studies on humans in accordance with the local legislation and institutional requirements because only commercially available established cell lines were used.

Author contributions

AS: Formal analysis, Investigation, Methodology, Visualization, Writing – original draft. VF: Formal analysis, Investigation, Methodology, Visualization, Writing – original draft. KS: Formal analysis, Methodology, Visualization, Writing – review & editing. HC: Investigation, Methodology, Writing – original draft. NM: Supervision, Writing – review & editing. AD: Funding acquisition, Resources, Supervision, Writing – review & editing. HG: Conceptualization, Funding acquisition, Supervision, Writing – review & editing. LB: Conceptualization, Formal analysis, Funding acquisition, Methodology, Project administration, Supervision, Writing – original draft, Writing – review & editing.

Funding

The author(s) declare that financial support was received for the research, authorship, and/or publication of this article. This study was funded by a grant (30-117) from the Canadian Foundation for AIDS Research (CANFAR) to LB, as well as a Queen Elizabeth Scholarship to AS, and FRQNT and MITACS Globalink Scholarships to KS.

Conflict of interest

The authors declare that the research was conducted in the absence of any commercial or financial relationships that could be construed as a potential conflict of interest.

The author(s) declared that they were an editorial board member of Frontiers, at the time of submission. This had no impact on the peer review process and the final decision.

Generative AI statement

The author(s) declare that no Generative AI was used in the creation of this manuscript.

Publisher's note

All claims expressed in this article are solely those of the authors and do not necessarily represent those of their affiliated organizations, or those of the publisher, the editors and the reviewers. Any product that may be evaluated in this article, or claim that may be made by its manufacturer, is not guaranteed or endorsed by the publisher.

Supplementary material

The Supplementary Material for this article can be found online at: https://www.frontiersin.org/articles/10.3389/fviro.2025.1547176/full#supplementary-material

References

1. Forshey BM, Von Schwedler U, Sundquist WI, Aiken C. Formation of a human immunodeficiency virus type 1 core of optimal stability is crucial for viral replication. *J Virol*. (2002) 76:5667–77. doi: 10.1128/JVI.76.11.5667-5677.2002

2. Lee K, Ambrose Z, Martin TD, Oztop I, Mulky A, Julias JG, et al. Flexible use of nuclear import pathways by HIV-1. *Cell Host Microbe*. (2010) 7:221–33. doi: 10.1016/j.chom.2010.02.007

3. Malikov V, Da Silva ES, Jovasevic V, Bennett G, De Souza Aranha Vieira DA, Schulte B, et al. HIV-1 capsids bind and exploit the kinesin-1 adaptor FEZ1 for inward movement to the nucleus. *Nat Commun*. (2015) 6:6660. doi: 10.1038/ncomms7660

4. Carnes SK, Zhou J, Aiken C. HIV-1 engages a dynein-dynactin-BICD2 complex for infection and transport to the nucleus. *J Virol*. (2018) 92. doi: 10.1128/JVI.00358-18

5. Engelman AN. HIV capsid and integration targeting. *Viruses*. (2021) 13. doi: 10.3390/v13010125

6. Petrovic S, Mobbs GW, Bley CJ, Nie S, Patke A, Hoelz A. Structure and function of the nuclear pore complex. *Cold Spring Harb Perspect Biol*. (2022) 14. doi: 10.1101/cshperspect.a041264

7. Aramburu IV, Lemke EA. Floppy but not sloppy: Interaction mechanism of FG-nucleoporins and nuclear transport receptors. *Semin Cell Dev Biol*. (2017) 68:34–41. doi: 10.1016/j.semcdb.2017.06.026

8. Schaller T, Ocwieja KE, Rasaiyaah J, Price AJ, Brady TL, Roth SL, et al. HIV-1 capsid-cyclophilin interactions determine nuclear import pathway, integration targeting and replication efficiency. *PloS Pathog*. (2011) 7:e1002439. doi: 10.1371/journal.ppat.1002439

9. Matreyek KA, Yucel SS, Li X, Engelman A. Nucleoporin NUP153 phenylalanine-glycine motifs engage a common binding pocket within the HIV-1 capsid protein to mediate lentiviral infectivity. *PloS Pathog*. (2013) 9:e1003693. doi: 10.1371/journal.ppat.1003693

10. Xue G, Yu HJ, Buffone C, Huang SW, Lee K, Goh SL, et al. The HIV-1 capsid core is an opportunistic nuclear import receptor. *Nat Commun*. (2023) 14:3782. doi: 10.1038/s41467-023-39146-5

11. Muller TG, Zila V, Muller B, Krausslich HG. Nuclear capsid uncoating and reverse transcription of HIV-1. *Annu Rev Virol*. (2022) 9:261–84. doi: 10.1146/annurev-virology-020922-110929

12. Dharan A, Talley S, Tripathi A, Mamede JI, Majetschak M, Hope TJ, et al. KIF5B and nup358 cooperatively mediate the nuclear import of HIV-1 during infection. *PloS Pathog*. (2016) 12:e1005700. doi: 10.1371/journal.ppat.1005700

13. Dharan A, Bachmann N, Talley S, Zwikelmaier V, Campbell EM. Nuclear pore blockade reveals that HIV-1 completes reverse transcription and uncoating in the nucleus. *Nat Microbiol*. (2020) 5:1088–95. doi: 10.1038/s41564-020-0735-8

14. Dicks MDJ, Betancor G, Jimenez-Guardeno JM, Pessel-Vivares L, Apolonia L, Goujon C, et al. Multiple components of the nuclear pore complex interact with the amino-terminus of MX2 to facilitate HIV-1 restriction. *PloS Pathog*. (2018) 14:e1007408. doi: 10.1371/journal.ppat.1007408

15. Merindol N, Berthoux L. Restriction factors in HIV-1 disease progression. *Curr HIV Res*. (2015) 13:448–61. doi: 10.2174/1570162X13666150608104412

16. Zhuang S, Torbett BE. Interactions of HIV-1 capsid with host factors and their implications for developing novel therapeutics. *Viruses*. (2021) 13. doi: 10.3390/v13030417

17. Shen Q, Wang YE, Palazzo AF. Crosstalk between nucleocytoplasmic trafficking and the innate immune response to viral infection. *J Biol Chem*. (2021) 297:100856. doi: 10.1016/j.jbc.2021.100856

18. Yant SR, Mulato A, Hansen D, Tse WC, Niedziela-Majka A, Zhang JR, et al. A highly potent long-acting small-molecule HIV-1 capsid inhibitor with efficacy in a humanized mouse model. *Nat Med*. (2019) 25:1377–84. doi: 10.1038/s41591-019-0560-x

19. Ogbuagu O, Segal-Maurer S, Ratanasuwan W, Avihingsanon A, Brinson C, Workowski K, et al. Efficacy and safety of the novel capsid inhibitor lenacapavir to treat multidrug-resistant HIV: week 52 results of a phase 2/3 trial. *Lancet HIV*. (2023) 10:e497–505. doi: 10.1016/S2352-3018(23)00113-3

20. Paik J. Lenacapavir: first approval. *Drugs*. (2022) 82:1499–504. doi: 10.1007/s40265-022-01786-0

21. Vidal SJ, Bekerman E, Hansen D, Lu B, Wang K, Mwangi J, et al. Long-acting capsid inhibitor protects macaques from repeat SHIV challenges. *Nature*. (2022) 601:612–6. doi: 10.1038/s41586-021-04279-4

22. Bester SM, Wei G, Zhao H, Adu-Ampratwum D, Iqbal N, Courouble VV, et al. Structural and mechanistic bases for a potent HIV-1 capsid inhibitor. *Science*. (2020) 370:360–4. doi: 10.1126/science.abb4808

23. Link JO, Rhee MS, Tse WC, Zheng J, Somoza JR, Rowe W, et al. Clinical targeting of HIV capsid protein with a long-acting small molecule. *Nature*. (2020) 584:614–8. doi: 10.1038/s41586-020-2443-1

24. Selyutina A, Hu P, Miller S, Simons LM, Yu HJ, Hultquist JF, et al. GS-CA1 and lenacapavir stabilize the HIV-1 core and modulate the core interaction with cellular factors. *iScience*. (2022) 25:103593. doi: 10.1016/j.isci.2021.103593

25. He J, Chen Y, Farzan M, Choe H, Ohagen A, Gartner S, et al. CCR3 and CCR5 are co-receptors for HIV-1 infection of microglia. *Nature*. (1997) 385:645–9. doi: 10.1038/385645a0

26. Merindol N, El-Far M, Sylla M, Masroori N, Dufour C, Li JX, et al. HIV-1 capsids from B27/B57+ elite controllers escape Mx2 but are targeted by TRIM5alpha, leading to the induction of an antiviral state. *PloS Pathog*. (2018) 14:e1007398. doi: 10.1371/journal.ppat.1007398

27. Masroori N, Cherry P, Merindol N, Li JX, Dufour C, Poulain L, et al. Gene knockout shows that PML (TRIM19) does not restrict the early stages of HIV-1 infection in human cell lines. *mSphere*. (2017) 2. doi: 10.1128/mSphereDirect.00233-17

28. Pawlica P, Dufour C, Berthoux L. Inhibition of microtubules and dynein rescues human immunodeficiency virus type 1 from owl monkey TRIMCyp-mediated restriction in a cellular context-specific fashion. *J Gen Virol*. (2015) 96:874–86. doi: 10.1099/jgv.0.000018

29. Kedzierska K, Crowe SM. The role of monocytes and macrophages in the pathogenesis of HIV-1 infection. *Curr Med Chem*. (2002) 9:1893–903. doi: 10.2174/0929867023368935

30. Mcdonald D, Vodicka MA, Lucero G, Svitkina TM, Borisy GG, Emerman M, et al. Visualization of the intracellular behavior of HIV in living cells. *J Cell Biol*. (2002) 159:441–52. doi: 10.1083/jcb.200203150

31. Davis LI, Blobel G. Nuclear pore complex contains a family of glycoproteins that includes p62: glycosylation through a previously unidentified cellular pathway. *Proc Natl Acad Sci U.S.A*. (1987) 84:7552–6. doi: 10.1073/pnas.84.21.7552

32. Rusinova I, Forster S, Yu S, Kannan A, Masse M, Cumming H, et al. Interferome v2.0: an updated database of annotated interferon-regulated genes. *Nucleic Acids Res*. (2013) 41:D1040–1046. doi: 10.1093/nar/gks1215

33. Morales DJ, Lenschow DJ. The antiviral activities of ISG15. *J Mol Biol*. (2013) 425:4995–5008. doi: 10.1016/j.jmb.2013.09.041

34. Betancor G, Jimenez-Guardeno JM, Lynham S, Antrobus R, Khan H, Sobala A, et al. MX2-mediated innate immunity against HIV-1 is regulated by serine phosphorylation. *Nat Microbiol*. (2021) 6:1031–42. doi: 10.1038/s41564-021-00937-5

35. Pawlica P, Berthoux L. Cytoplasmic dynein promotes HIV-1 uncoating. *Viruses*. (2014) 6:4195–211. doi: 10.3390/v6114195

36. Nepveu-Traversy ME, Demogines A, Fricke T, Plourde MB, Riopel K, Veillette M, et al. A putative SUMO interacting motif in the B30.2/SPRY domain of rhesus macaque TRIM5alpha important for NF-kappaB/AP-1 signaling and HIV-1 restriction. *Heliyon*. (2016) 2:e00056. doi: 10.1016/j.heliyon.2015.e00056

37. Monette A, Pante N, Mouland AJ. HIV-1 remodels the nuclear pore complex. *J Cell Biol*. (2011) 193:619–31. doi: 10.1083/jcb.201008064

38. Wang T, Tian C, Zhang W, Luo K, Sarkis PT, Yu L, et al. 7SL RNA mediates virion packaging of the antiviral cytidine deaminase APOBEC3G. *J Virol*. (2007) 81:13112–24. doi: 10.1128/JVI.00892-07

39. Haffar OK, Popov S, Dubrovsky L, Agostini I, Tang H, Pushkarsky T, et al. Two nuclear localization signals in the HIV-1 matrix protein regulate nuclear import of the HIV-1 pre-integration complex. *J Mol Biol*. (2000) 299:359–68. doi: 10.1006/jmbi.2000.3768

40. Bukrinsky MI, Sharova N, Mcdonald TL, Pushkarskaya T, Tarpley WG, Stevenson M. Association of integrase, matrix, and reverse transcriptase antigens of human immunodeficiency virus type 1 with viral nucleic acids following acute infection. *Proc Natl Acad Sci U.S.A*. (1993) 90:6125–9. doi: 10.1073/pnas.90.13.6125

41. Miller MD, Farnet CM, Bushman FD. Human immunodeficiency virus type 1 preintegration complexes: studies of organization and composition. *J Virol*. (1997) 71:5382–90. doi: 10.1128/jvi.71.7.5382-5390.1997